Thomas Michel
Hugo Fournier

Editors

Coal Geology
Research Progress

NOVA

COAL GEOLOGY RESEARCH PROGRESS

https://telegram.me/Geologybooks

COAL GEOLOGY RESEARCH PROGRESS

THOMAS MICHEL
AND
HUGO FOURNIER
EDITORS

Nova Science Publishers, Inc.
New York

https://telegram.me/Geologybooks

Nova Science Publishers, Inc.; New York

https://telegram.me/Geologybooks

CONTENTS

between 1 and 4. These values allow the dimensioning of the works and the exposed structures and the evaluation of the structures damage.

The empirical methods allow the prediction of total and residual subsidence of abandoned mines subject to potential subsidence. This prediction is necessary to determine the amplitude and the extension of the subsidence of the already subsided zones. It is also useful to estimate the amplitude and the duration of residual subsidence and to predict the characteristics of progressive subsidence due to a failure of the pillars of the partial exploitations. We will describe the relations established by feedback experience for the exploitations of French coal and iron mines. The coalmines are deeper (>400 m) than iron mines (<200 m).

4.4. The case of French coalmines

The exploitation of coalmines in France was stopped in 2004. There are no more movements induced by the production run. The establishment of administration stop folders includes the estimation of the movements previously induced by the exploitation and calculation of the amplitude and the extension of residual subsidence.

In the coal basins of Nord and Pas-de-Calais and Lorraine, the method of Proust was used (Proust, 1964) to estimate the subsidence for exploitations by caving and backfilling for a depth higher than 500 m. In Provence coalmine (southern of France), the method of NCB was employed thanks to an empirical profile function (figure 7) established by Arcamone (1980) and checked by Aissaoui (1999). The prediction obtained with this curve is generally in conformity with *in-situ* measurements.

Figure 7. Curves of the forecast of subsidence in the center of the panels according to the geometrical parameters (Width, Depth, Open or Thickness of extraction area), Provence coalmines.

PREFACE

Coal geology is the study of a field that concentrates on the origin, occurring relationships and geological characteristics of coal and similarly traited rocks. This field is also involved in the study of coal-derived gases, fluids, both naturally occurring and man-made solid coal by-products. This new book presents state-of-the art research from around the world.

Chapter 1 - Coal is still the main energy source of China, the annual production of coal was up to 2.3 billion tons in 2006. With increasing use of coal, the growing impact on the environment from the potentially hazardous trace elements (PHTEs) becomes a serious concern. The information about the concentration, distribution, occurrence, emission, and control of the PHTEs in coals are of great importance.

More than 3000 coal samples were collected in different coalfields around China, and the concentration and distribution of the PHTEs were determined and evaluated. The results show that the average concentrations of most PHTEs in Chinese coals are close to, but As, Cl, Tl, Zn, and Sb are lower than and Mn, V, F, and U are higher than that in U.S. coals. Moreover, the distributions of the PHTEs in coals from Shanxi Province which is the biggest coal production province in China，Shenfu coalfield which is the biggest coal exportation base, and another typical coalfield - western Guizhou coalfield in China - have been analyzed respectively. Most of Shanxi coals and Shenfu coals contain low concentrations of the PHTEs, but the concentrations of the PHTEs in some western Guizhou coals are higher.

The distribution and the occurrence of some PHTEs in typical Chinese coal samples have been studied. The average values of Hg, F, As, and Cr in Chinese coals are 0.19, 131, 3.8, and 15 µg/g, respectively. The content of arsenic varies from 0.3 µg/g to 3.2 wt.% in Chinese coals, only a few samples have an arsenic content of more than 1000 µg/g, which are very restricted and the coal seams are generally not economically minable. The contents of chromium range from 0.1 µg/g to 943 µg/g in Chinese coals and are strongly enriched in the Shenbei lignite, in which the average content is up to 79 µg/g. Arsenic and Cr are mainly associated with organic components in the typical high-arsenic coal and high-chromium lignite. The concentration of mercury in Chinese coals has a range from 0.003 µg/g to 10.5 µg/g, and Hg mainly occurs in the sulfides of coal. The content of fluorine varies from 8 µg/g to 4000 µg/g in Chinese coals.

Emissions of Hg during combustion, pyrolysis and gasification processes have been studied, and the results show that the emission of mercury is influenced by the coal types and operational conditions. Distribution and occurrence of fluorine in coal and the combustion

products in typical endemic fluorosis area in southwestern China has been evaluated, the results show that the endemic fluorosis is likely caused by the combination of high fluorine coals and high-fluorine clays. Emissions of arsenic and chromium during combustion of typical high-arsenic coal and high chromium lignite were investigated through drop tube furnace experiments. Their emissions are influenced by their occurrence modes in the coals and the conditions during coal combustion. Sorbent injection is an effective method to reduce the emission of the PHTEs during coal combustion.

Chapter 2 - Coal Clarke values are the average trace element contents in the World coals. The modern table of coal Clarkes is presented, based on new calculations using a very large source of information (thousands of analyses of coal and coal ashes for trace elements). For each trace element seven figures were calculated: average content in hard coals and their ashes; average content in brown coals and their ashes; average content in all coals and their ashes; coal affinity index (or "coalphile index") = average content in all ashes/Clarke values of sedimentary rocks. The coal Clarkes presented are the scientific base for many geochemical comparisons and issues.

Chapter 3 - The World average F content in coals (coal Clarke of F) for the hard and brown coals are, respectively, 82±6 and 90±7 ppm. On an ash basis, these contents are greatly increased and are 580±20 and 630±50 ppm, respectively. As an average, F content in ash is 605 ppm (lower than the Clarke value for sedimentary rocks, 650 ppm). F is, on average, *not a coalphile element.*

Nevertheless, some coals are known to have an F content one order of magnitude more than the coal Clarke level. In general, these are either high-ash or high-phosphorus coals, with both features often combined. This (and some other) features show some similarity between F and P geochemistry in coal. In particular, F, like P, seems to be depleted from the buried peat during diagenesis toward hosting rocks.

No less than three F-forms (modes of occurrence) may be present in coal: phosphatic (F_{phosph}), silicatic (mostly F_{clay}), and organic (F_{org}). It can be suggested that F_{clay} dominates in high-ash coals, F_{phosph} in high-P coals, and in ordinary coals with moderate ash yield and near-Clarke P and F contents, F_{org} may be dominant. There is no information concerning chemical species of the F_{org} form. However, by an analogy with P, it seems to exist as an F compound with Ca_{org}, not with organics itself.

It is yet not clear, if F is in authigenic CaF_2 and what could be a contribution of such a form to total F content. It seems not to be excluded that such form may have genetic relation with F_{org} (diagenetic or catagenetic transformation, $F_{org} \Rightarrow F_{min}$?).

There are no clear relationships concerning F enrichment in coals. Plausible hypothesis is that F might be syngenetically enriched in coals (a) in paralic (near-marine) coals, and (b) in coals formed with a volcanic activity background. On the other hand, some F anomalies (like that in some Alabama coals) may have resulted from epigenetic hydrothermal F-input, during (or after) coal metamorphism.

Chapter 4 - Rhenium is a very rare element with Clarke value (average content in the Earth's crust) about 0.001 ppm (= 1 ppb). Geochemistry of Re in coal is poor known up to day because of analytical problems. Special analytical methods are needed for reliable Re determination in coal. Some coals are known, with Re contents 2–3 orders-of-magnitude higher than Re Clarke value in the Earth's crust, in the range from 0.n ppm up to a few ppm.

In Re-bearing coals, it is no doubt that Re_{org} form exists. Perhaps, Re is sorbed on coal organics by weak, ion-exchange bonds. This is accounted for the Re leachability from coals

by surface and ground waters. Some analogues with Re state in black shales indicate that some part of Re may be present in bituminous components of coal (liptinite). The other authigenic Re form may be its sulfide, ReS_2. However, Re sites in coal (modes of occurrence) are now only hypothetic; a microprobe study is needed for more knowledge.

There are at least three genetic types of Re-concentrations in coal: Uzbek, Spanish and Kazakh. In *Uzbek* type, Re is probably syngenetic. Its accumulation is due to enhanced Re contents in source rocks. Rhenium leached from terrigenic material may further be captured on reducing peatbog barrier – in organic or sulfide form. In *Spanish* type Re is also mostly syngenetic. Its accumulation is due to considerable contribution of the bituminous organics (like black shale) having extremely high affinity to Re. In *Kazakh* type Re is closely associated with U and its companions, in the infiltration epigenetic deposits of the "*bed oxidation*" type. Re dissolved in oxidized waters as perrhenate ion ReO_4^-, may be captured in brown-coal beds on the reducing barrier, in organic or sulfide forms.

Recently Re-bearing fumaroles were described in the Kurily Islands. Therefore, some Re accumulations may occur in peatbogs of the volcanic areas, or in young lignites – in orogenic depressions with synchronous volcanism. Such Re accumulations may be associated with In, Ge, Mo, Bi and some other elements enriching the volcanic exhalations.

Because Re is a very valuable metal, Re-bearing coals may serve as an Re industrial resource. The most promising are epigenetic uranium-coal deposits. In addition, some intermountain trough brown-coal fields must be studied for Re, if these coals are associated with volcanics.

Chapter 5 - The objective of this chapter is to review the methods (often used or currently under development) that use to predict ground movements (subsidence and sinkhole) in France at the time of the exploitation of the underground resources and those induced surface movements after the closure and abandonment mines.

Chapter 6 - About 400 coal samples from coal mines and 100 fly ash and cinder samples from power stations were collected to study the amount of total annual nitrogen emissions as well as emission ratio from steam coal combustion in China. The results show that burning 1t coal (nitrogen content is about 1.14%) in the high-temperature power stations emits about 11.35kg nitrogen into the atmosphere, in the mid-low temperature the fluid bed furnace, chain-grate furnace and boil furnace emit about 12.28kg, 6.45kg and 6.72kg nitrogen, respectively. The nitrogen emission ratio of coal combustion in the high-temperature power stations is about 99.56%, in the mid-low temperature the nitrogen emission ratios of coal combustion of the fluid bed furnace, chain-grate furnace and boil furnace are about 91.64%, 65.16% and 73.82% respectively. The annual total nitrogen emissions from steam coal combustion into the atmosphere in China is estimated to be 18.20 Mt now.

Chapter 7 - In the Lower Paleozoic strata in South Qinling Mountain in the middle of China, there are a lot of thin bed of stone-like coal - applied here to a burnable black shale that is nearly 40% ash, is very heavy and hard, looks like stone, is generally called stone coal, and is enwrapped in the lumpish trachytic or interbedded in the fault zone or in the axis of fold of the Lower Paleozoic strata. The stone-like coal has high stages of coal development and in general is high-stage anthracite coal. About 260 samples of stone-like coal were collected from southwest China to determine the arsenic (As), selenium (Se), mercury (Hg), fluorine (F) content and other element content, and study their distribution pattern and source in this area. The stone-like coal is very rich in sulfur and heavy metals. The sulfur content is about 1.5 to 3%, mercury from 0.3 mg/kg to 2.6 mg/kg, arsenic from 15 to 534 mg/kg, mostly

x Thomas Michel and Hugo Fournier

from 50 mg/kg to 150 mg/kg, much higher than the average arsenic content of Chinese coals 4.5 mg/kg and the average world coal of 6.1 mg/kg. Selenium ranged from 10 mg/kg to 42 mg/kg, cadmium from 0.2 mg/kg to 36 mg/kg. Fluorine content is from 600 to 3400 mg/kg. The Se, F,Hg, Cd content enrichment in the stone-like coal and is higher than the average content of Chinese coals and the average of world coal, and higher than the typical Permo-Carboniferous or later coal deposits.

Use of the stone-like coal for heating and cooking by local residents has caused serious health problems --endemic fluorosis and arsenic poisoning in this area.

Chapter 8 - Minerals are important components in coals. The transformations of mineral matter during coal combustion are a key factor in clean utilization of coal. The mineralogical characteristics in coals and their products have been investigated broadly and there are various tasks to be carried out. Some of these are outlined below.

1. Heavy minerals in coal. Use the low temperature ashing (LTA) and the float-sinking methods to separate heavy minerals in coals, and combine X-ray diffraction (XRD) and scanning electron microscopy with energy dispersive X-ray analysis (SEM-EDX) to describe the mineralogical characteristics of heavy minerals. Reveal the mother-rock properties of the sediment-source region, the coal-forming environments and hydrodynamic conditions.
2. Interaction and redistribution of single minerals during coal combustion. Speculate on the complex mineral combination evolution during coal combustion and elucidate the interaction mechanism of various minerals combination through a simple monomineral partitioning mechanism.
3. Relationship between typical minerals (Fe-bearing minerals, Ca-bearing minerals, and Al-bearing minerals) in coal and the formation of particulate matter (PM). The minerals are the main source of PM during coal combustion, however, the detailed relation between the minerals and PM is unknown. Systematic drop tube furnace experiments should be conducted to elucidate the contribution of typical minerals to PM formation during coal combustion.
4. Mineralogy of ash deposits of coal-fired boilers. The vaporization of minerals in coal is the main source of deposition in coal-fired boilers. Combine muti-discipline theories to investigate the mineralogy of slag and fouling, and interpret the formation mechanisms of boiler slagging, fouling and ash deposit.

In summary, the integrated theory of physicochemical transformation and interaction of mineral components during coal combustion should be constructed, which would be helpful to operating the coal combustion equipments safely and controlling the pollution emissions.

Chapter 9 - The identification and quantification of minerals contained in coals are very important in a) elucidating the environmental conditions established during peat accumulation in the palaeomires, b) assessing the behavior of coals during combustion for power generation, c) evaluating the potential for various industrial applications, and d) determining the mode of occurrence of potential toxic and hazardous trace elements.

X-ray diffraction (XRD) is the most frequently applied method in determining the mineralogical composition of coal samples. The inherent limitation to the quantitative identification, when bulk sample is used, is the low signal to noise ratio of the diffractogramme due to the interference of the organic matter. In order to increase the

sensitivity of X-ray diffraction, 'coal products' obtained after low-temperature (using oxygen-plasma) or high-temperature ashing or even oxidation using chemical agents, are used. Nevertheless, the composition of these 'products' might significantly differ from the original on the bulk coal samples as a result of the treatment.

Quantification of mineral matter based on XRD patterns also exhibits inaccuracies due to certain effects such as the preferred orientation of the mineral grains in the sample holder and the variation in absorption of X-rays by the minerals and the organic matter. Various quantification methods for the study of minerals in coals have been developed, which mainly operate on a semi-quantitative basis. Among the most known and promising quantitative methods are the analyses using an external standard (spike) such as corundum and the Rietveld-based method (integrated intensities of the main diffractogramme peaks), as well as a combination of Rietveld technique and full pattern fitting.

By using curved position-sensitive detectors (PSD) that enable the rapid (5 min) acquisition of diffraction patterns in the angular range 3-120° 2θ, a quantification method of minerals in bulk low-rank coals was developed. This was worked out in a series of published and unpublished studies, which are reviewed in this communication. The method is based on full mineral pattern fitting techniques, also incorporating the fitting of pure organic phases in order to simulate the whole coalified sample. Fresh to slightly humified (recent) plant material, in the case of peat samples, and heavy-media separated organic material in the case of lignites, have been used as standards after determining their mass absorption coefficients experimentally. The procedure, as well as the advantages and limitations of the method are described in detail.

Chapter 10 - Although coal geology study evolves slowly, in the 80's and 90's of the last century, there has been a great progress. Examples include a study on peatland, coal petrology, coal geochemistry, coal measures deposits and its sedimentary environment, especially on coalbed gas and environmental protection from coal combustion in the recent year. This article's aim is to put forward a new study method to solve some problems in coal geology study. Through summarizing the former study, consulting the petroleum system's concept and method, and integrating coal geology and systematology, the authors put forward the concept of a coal system. Coal system is an integrated system that includes coalbed, coal measures, depositional facies and all kinds of geological actions relating to coal forming. As a system, the Coal system has its own factors, actions, hierarchy and study content. Its basic factors are substance sources (paleobotanic and peat), coal-accumulation environment and underground thermal stream. And its geologic actions include: Peat original and allochthonous accumulation; burying action caused by diastrophism and geothermal metamorphism. The rational collocation of these basic factors and coal-forming actions in dimensional-temporal domain conduce the forming of valuable coalbed. In hierarchy, a coal system can be divided into substance source subsystem, accumulation subsystem and metamorphism subsystem in temporal domain. In dimensional domain, it may fall into lower class subsystems resembling upper systems. And the study contents include every aspect of coal system factors, actions and hierarchy. At last, the authors take Fuxin basin as an example to explain how to start a coal system study. And discuss the problem that should be focused on in a study process.

Chapter 11 - Decision by the Czech Government that the increase in proportion of energy production from nuclear sources is the only possible solution in the long-term perspective. In 2005, about 65 % of the electric energy was based on burning coal, mostly lignite, which is

actually the worst alternative for the use of this raw material in the new millennium. It is also to be borne in mind that Czech reserves of coal will be exhausted by about 2040, at the latest. Moreover, we burn raw material which even nowadays serves for the manufacture of plastics, pharmaceutical products and other chemicals. Although all large power plants burning coal are desulphurized, they still exhale a number of toxic elements such as As, Be, F, Se and heavy metals. The idea that a part of the electric energy may be generated from alternative sources is correct, but its advocates are usually silent about the very high price of this energy. Currently, only about 3.5 % of electricity is generated from these sources.

Chapter 12 - The chapter describes the C_7 light hydrocarbons technique to oil and condensate from Type III organic matter in Northwestern Taiwan, and discusses the potential of C_7 light hydrocarbons as markers for petroleum exploration. Their bulk geochemical features include the whole oil $\delta^{13}C‰$ values, Pristane/ Phytane ratio and C_7 compounds parameters. With relatively limited coverage of oil samples, this detailed C_7 compounds geochemical study on a large set of condensate and oil samples collected from major fields across the basin has provided significant insights into the biodegradation evaporative fractionation maturation depositional environment and oil system in petroleum generation in northwestern Taiwan.

Chapter 1

DISTRIBUTION, OCCURRENCE, EMISSION AND CONTROL OF TRACE ELEMENTS IN TYPICAL CHINESE COALS

Junying Zhang[*], Yongchun Zhao, Deyi Ren and Chuguang Zheng

State Key Laboratory of Coal Combustion,
Huazhong University of Science and Technology, Wuhan 430074 China
China University of Mining and Technology,
D11, Xueyuan Road, Haidian District, Beijing 100083, China

ABSTRACT

Coal is still the main energy source of China, the annual production of coal was up to 2.3 billion tons in 2006. With increasing use of coal, the growing impact on the environment from the potentially hazardous trace elements (PHTEs) becomes a serious concern. The information about the concentration, distribution, occurrence, emission, and control of the PHTEs in coals are of great importance.

More than 3000 coal samples were collected in different coalfields around China, and the concentration and distribution of the PHTEs were determined and evaluated. The results show that the average concentrations of most PHTEs in Chinese coals are close to, but As, Cl, Tl, Zn, and Sb are lower than and Mn, V, F, and U are higher than that of in US coals. Moreover, the distributions of the PHTEs in coals from Shanxi Province which is the biggest coal production province in China，Shenfu coalfield which is the biggest coal exportation base, and another typical coalfield - western Guizhou coalfield in China have been analyzed respectively. Most of Shanxi coals and Shenfu coals contain low concentrations of the PHTEs, but the concentrations of the PHTEs in some western Guizhou coals are higher.

[*] Email: jyzhang@hust.edu.cn

The distribution and the occurrence of some PHTEs in typical Chinese coal samples have been studied. The average values of Hg, F, As, and Cr in Chinese coals are 0.19, 131, 3.8, and 15 μg/g, respectively. The content of arsenic varies from 0.3 μg/g to 3.2 wt.% in Chinese coals, only a few samples have the arsenic content more than 1000 μg/g, which are very restricted and the coal seams are generally not economically minable. The contents of chromium range from 0.1 μg/g to 943 μg/g in Chinese coals and are strongly enriched in the Shenbei lignite, in which the average content is up to 79 μg/g. Arsenic and Cr are mainly associated with organic components in the typical high-arsenic coal

Keywords: distribution, occurrence, emission, control, trace elements, coal

1. INTRODUCTION

With increasing use of coal, the growing impact on the environment of the potentially hazardous trace elements (PHTEs) has become a serious problem [1-4]. China is the largest coal producer and consumer in the world. The emission of the PHTEs has caused serious problems in several areas. Southwestern Guizhou province is the area of endemic arseniasis and fluorosis related to coal combustion [5]. The use of locally mined, high-arsenic coals has caused in excess of 3000 cases of arseniasis in several villages [3, 6]. Zheng et al., (1992) reported nearly 500 cases of human selenosis in southwestern China, which were attributed to the use of selenium-rich carbonaceous shales known locally as "stone coal". Many researchers investigated the distribution and origin of the PHTEs in Chinese coals from different districts [2, 5, 7-15]. However, most of them were focus on the several coalfields or coal mines in China. Thus, one of the purposes of this paper is to elucidate the distribution and occurrence of trace elements especially for some PHTEs in Chinese coals. To better understand the distribution of the PHTEs in Chinese coals in details, we summarized the distribution of the PHTEs in the coals from the biggest coal production province - Shanxi Province, the biggest coal exportation base - Shenhua, and an important coal base - western Guizhou.

Among the PHTEs, Hg, F, As, and Cr attracted many researchers' attention because of their high toxicity. Huang and Yang (2002) investigated the distribution of mercury in Chinese coals.[16]. Streets et al., (2005) analyzed the anthropogenic mercury emissions in China.[17]. Chen and Tang (2002) investigated the distribution of fluorine in Chinese coals.[18], Dai and Ren (2006) and Luo et al., (2004) investigated and analyzed the fluorine concentration and distribution in Chinese coals based on the reserves of coal [5, 19]. Ren et al., (2004) reported the concentration and distribution of chromium in the Shenbei lignite [8]. There are many references about the distributions and occurrences of arsenic in western Guizhou and Chinese coals [2, 6, 9, 11]. Another important purpose of present study is to summarize and describe the distribution and concentration of these four important PHTEs in coals.

Control of the PHTEs emissions from coal combustion has been regulated in many countries. However, the emission of the PHTEs has not got enough attention in China. At the same time, there are rare references about the emission and partition of the PHTEs during

coal combustion in China [7, 20]. The final aim of this paper is to understand the partition, emission, and control of the PHTEs during coal combustion, especially for the combustion of some typical high PHTEs coals.

2. DISTRIBUTION OF PHTES IN CHINESE COALS

In the literature, more than 3000 coal samples were collected from different coalfields in China, and the concentrations and distributions of the PHTEs from different coal-forming periods were determined and evaluated (Table 1).

Table 1. Contents of PHTEs in coals from different coal-forming periods ° in China (in μg/g)

PHTEs	Northern China C-P	Southern China P₂	T₃	J₁₋₂	J₃-K₁	E-N	Average contents in Chinese coals
Be	1.92	2.42	2.67	2.41	1.88	0.93	2.13
F	148.4	206.5	84.1	82.8	134.2	352.8	131.3
Cl	389	255	193	215	75	74	264
V	39.59	94.69	74.89	14.37	43.08	62.85	35.05
Cr	15.81	29.02	50.40	11.40	11.89	43.33	15.35
Mn	56.8	166.2	77.1	171.1	180.6	42.7	125
Co	4.24	10.24	7.72	8.59	8.09	11.75	7.05
Ni	11.75	24.11	28.14	11.97	10.56	56.46	13.71
Cu	21.97	40.51	34.21	10.55	13.57	45.18	18.35
Zn	48.99	41.69	80.21	32.22	48.54	59.36	42.18
Ga	9.88	8.27	9.48	2.77	7.48	4.77	6.52
Ge	3.35	2.95	0.74	2.46	3.90	0.96	2.97
As	2.57	6.37	10.01	3.23	6.04	12.16	3.80
Se	4.84	4.71	1.47	0.43	0.63	1.01	2.47
Mo	3.47	8.40	3.14	1.92	2.55	3.44	3.11
Cd	0.30	0.62	0.99	0.13	0.16	0.44	0.24
Sb	0.68	1.67	3.62	0.61	1.37	1.03	0.83
Hg	0.22	0.42	0.45	0.11	0.19	0.06	0.19
Tl	0.35	0.42	0.67	0.55	0.44	1.29	0.48
Pb	20.34	26.95	20.38	8.76	12.29	26.21	15.55
Th	8.71	7.81	9.07	3.01	4.91	3.72	5.81
U	2.60	4.29	3.90	1.24	1.72	3.93	2.41
Reserve ratio of coal forming period /%	38.1	7.5	0.4	39.6	12.1	2.3	100

When the PHTEs contents of coals from different coal-forming periods in China are compared to each other, Early and Middle Jurassic coals have the lowest concentration of the PHTEs. For the Carboniferous-Permian coal, the content of As, Co, and Tl is the lowest, and

---

° Carboniferous and Early Permian (C–P1), Late Permian (P2), Late Triassic (T3), Early and Middle Jurassic (J1-2), Late Jurassic and Early Cretaceous (J3–K1), and Eogene and Neogene (E–N)

only the content of Se is the highest. For the Late Jurassic- Early Cretaceous coal, the content of Ni is the lowest, and only the content of Mn is the highest. The resources and reserves of these three age coals occupy 89.8% of the total coal reserves in China, so the emission of PHTEs from most of Chinese coals are low, and the impact of PHTEs on the environment is minimal during coal combustion.

However, for the Late Permian coal, the contents of V, Mo, Pb, and U are the highest in all coal-forming periods, the contents of Hg, Cd, and F are also higher, more than one time of the arithmetic mean value of Chinese coals. The amount of the Paleogene and Neogene coal and the Late Triassic coal are limited, but it is necessary to pay more attention to them because of their higher PHTEs contents.

The average contents of the PHTEs in Chinese coals，American coals, world coals, and the earth's crust (Clarke value) are compared in Table 2. Comparing with the Clarke value, Se, Sb, Hg, F, Cl, Mo, and As are enriched in Chinese coals. Most of the PHTEs contents in Chinese coals are close to that in American coals, the differences of Hg, Cr, and Ni contents in two countries coals are less than 10%, for Mo, Se, Cu, and Co, are less than 20%. The contents of Sb, Zn, Cd, Cl, and As in Chinese coals only occupy 67%, 66%, 56%, 42%, and 15% of their contents in American coals, respectively. However, the contents of Mn and Th in Chinese coals are much higher about three and twice times than that in American coals, respectively. The contents of V, F, U, and Pb in Chinese coals are also higher than in American coals.

Table 2. Average contents of the PHTEs in Chinese, American, and world coals (in μg/g)

PHTEs	Chinese coals	Sample number	American coals [21, 22]	World coals [22, 23]	Clarke values [24]
F	131.3	729	96	80	62.5
Cl	264	721	628	1000	130
V	35.05	1266	22.2	25	135
Cr	15.35	1592	14.1	10	100
Mn	125	1269	43	50	950
Co	7.05	1488	6.1	5	25
Ni	13.71	1335	14	15	75
Cu	18.35	1296	16	15	55
Zn	42.18	1394	53	50	70
As	3.80	3386	24	5	1.8
Se	2.47	1536	2.8	3	0.05
Mo	3.11	679	3.3	5	1.5
Cd	0.24	1317	0.47	0.3	0.2
Sb	0.83	537	1.2	3	0.2
Hg	0.19	1413	0.17	0.012	0.08
Pb	15.55	1387	11	25	12.5
Th	5.81	1011	3.2	2	7.2
U	2.41	1317	2.1	1-3	1.8

In all the PHTEs investigated, the arithmetic mean value of As content in Chinese coals is much less than that in U.S. coals, only about 15% of the latter. It should be pointed out that there were some differences in the calculation of the arithmetic mean values between ours and American. We calculated the values by reserves weight methods, whereas, they got the values based on random arithmetic mean methods. For example, most of coal samples (about 55.6%)

were collected from Appalachian coalfield which has a high arsenic concentration with the arithmetic mean value of 34 µg/g, but the coal production of Appalachian is only 33% of the total production of the country (2004-2005). In contrast, only 26% samples were collected from the Rocky Mountain and northern plain which is the largest coal production base in America. The coal production of this coalfield is about 51% of the total U.S. production in 2004-2005. So this may have significant effect on the calculation of the arithmetic mean value of As concentration in American coal. In accordance with this, Finkelman (1993) suggested that the arithmetic mean value of As in American coal is 6.5 µg/g may be a better value [21].

3. DISTRIBUTION OF THE PHTES IN SHANXI COALS

As the biggest coal production base in China, the annual production of raw coal from Shanxi province is up to 550 million tons (in 2005), which is more than a quarter of the annual total production of raw coal in China [25]. The information about the concentration and distribution of the PHTEs in Shanxi coals is of great importance.

There are coals with all kinds of coalification ranks in the province. The five coal-forming periods are Late Carboniferous (Taiyuan Formation), Early Permian (Shanxi Formation), Middle Jurassic (Datong Formation), Tertiary (Taxigou Formation), and Quaternary (peat). There are six major coalfields in Shanxi province, which include Hedong (A), Datong (B), Ningwu (C), Xishan (D), Qinshui (E), and Huoxi (F) (Fig.1)[26].
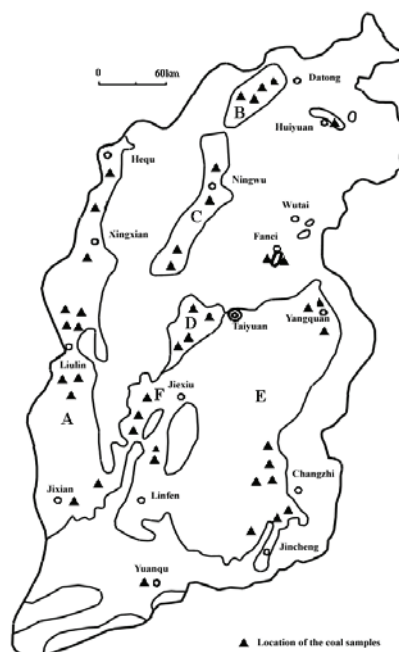
A. Hedong Coalfield; B. Datong Coalfield; C. Ningwu Coalfield; D. Xishan Coalfield; E. Qinshui Coalfield; F. Huoxi Coalfield.

Figure 1. Major coalfields in Shanxi province and locations of coal samples analyzed [26].

The Upper Carboniferous Taiyuan Formation and Lower Permian Shanxi Formation are terrestrial–marine alternating coal-bearing strata, the predominant sedimentary environment is tidal flat and delta, the palaeo-plants of coal-forming are Cordaitopsida, Lepidophyta, and so on. Middle Jurassic Datong Formation is mostly terrestrial coal-bearing strata, their main sedimentary environments are river, lake-delta, and lake, the palaeo-plants of coal-formation consist mainly of Gymnosperm and Pteridophyta. Tertiary brown coal and Quaternary peat are formed in small intermountain fault basins

Sampling program was designed according to the coal resources distribution and the coal production. 110 coal samples and a peat sample were collected from the main coal mines, small coal mines, and drilling cores in Shanxi province, China. The distributions and contents of more than 20 PHTEs (As, B, Ba, Cd, Cl, Co, Cr, Cu, F, Hg, Mn, Mo, Ni, Pb, Sb, Se, Th, U, V, and Zn) in these samples were determined. Ranges and arithmetic means of concentrations for 20 PHTEs in Shanxi coals are listed in Table 3.

Table 3. Contents of the PHTEs in coals from Shanxi province, China (in μg/g)

Element	Range	Average	Number of samples
As	bdl-82.4	4.1	110
B	bdl-45.0	6.1	24
Ba	<10-493	102.9	110
Cd	bdl-2.5	1.1	92
Cl	bdl -1865	466	93
Co	0.41-25.0	4.1	110
Cr	1.63-53.1	11.3	79
Cu	bdl-264.0	18.6	92
F	bdl-3600	186	87
Hg	bdl-2.89	0.40	92
Mn	bdl-215	38	22
Mo	bdl-56.9	5.9	104
Ni	1.8-46.0	15.6	25
Pb	bdl-88.0	24.7	91
Sb	0.1-11.3	0.5	110
Se	bdl-12.6	4.9	110
Th	0.5-20.6	7.2	110
U	0.2-49.9	3.6	110
V	bdl-84.1	18.2	22
Zn	bdl-193.0	45.9	99

bdl: below detection limit.

By comparison with the crustal abundances (Table 2), the Shanxi coals are highly enriched in Cd (5.5×) and Se (up to 98×), and are moderately enriched in As, Cl, Hg, Mo, Pb, Sb, and U (2-5×). The arithmetic means of concentrations of Cd, F, and Hg in Shanxi coals are higher than the world coal averages, concentrations of As, Ba, Co, Cr, Cu, Mn, Mo, Ni, Pb, Se, Th, U, V, and Zn are about equal to, and B, Cl, and Sb are lower than world arithmetic means. A comparison with the United States coals indicates that the arithmetic

means of concentrations of Cd, Hg, Pb, Se, and Th in Shanxi coals are higher than, Ba, Cl, Co, Cr, Cu, F, Mn, Mo, Ni, U, V, and Zn are about equal to, and As, B, and Sb are lower than American arithmetic means.

3.1 PHTEs in Quaternary peat

Quaternary peat occurs in Fanci County in northeastern Shanxi province, China. Only one sample of Quaternary peat in Shanxi province was collected and analyzed by instrumental neutron activation analysis (INAA). The contents of the PHTEs in the Quaternary peat are shown in Table 4.

Table 4. Contents of the PHTEs in Quaternary peat from Shanxi province (in μg/g)

Element	Content
As	32.3
Ba	240
Cd	bdl
Co	12.6
Cr	48.1
Mo	135.0
Sb	0.8
Se	2.5
Th	6.6
U	2.3

bdl: below detection limit.

The average contents of the PHTEs in China coals, U.S. coals, and world coals are listed in Table 2. Comparing the PHTEs contents of the Fanci peat with the crustal abundances (Clarke value), we conclude that As, Mo, and Se are strongly enriched, and Sb shows a moderate enrichment in the peat. Comparing with world averages of trace elements, the Fanci peat is highly enriched in As and Mo, whereas Co, Cr, and Th show a moderate enrichment. The contents of As and Mo are high, up to 32.3 and 135 μg/g, because there are areas of gold mineralization in the northwestern part of the basin and these areas may provide source materials for trace metal deposition.

3.2 PHTEs in Tertiary brown coals

Tertiary brown coals occur simultaneously in Fanci County in northeastern Shanxi province and in Yuanqu County of the southeastern Shanxi province. The coal beds were deposited in small intermountain fault basins. Four samples of Tertiary brown coals from Shanxi province were collected and analyzed, and the results are listed in Table 5.

Table 5. Contents of the PHTEs in Tertiary brown coals from Shanxi province (in μg/g)

Element	Range	Average	Number of samples
As	7.6-18.4	13.5	4
Ba	52.6-493.0	303.9	4
Cd	2.1-2.5	2.2	3
Cl	bdl-100	60	3
Co	4.3-9.9	7.4	4
Cr	26.2	26.2	1
Cu	21-108	53	3
F	259-393	313	3
Hg	0.03-0.05	0.04	3
Mo	3.8-37.9	9.4	4
Pb	29.0-38.0	33.5	2
Sb	0.4-0.7	0.5	4
Se	bdl-12.6	4.5	4
Th	2.9-7.1	4.8	4
U	2.2-20.2	8.2	4
Zn	58.4-106	83.4	3

bdl: below detection limit.

A comparison of the PHTEs contents of the Tertiary brown coals in Shanxi province with the crustal abundances (Clarke values) indicates that As (up to 7.5×), Cd (up to 11×), Mo (up to 6.3×), and Se (up to 90×) are highly enriched, whereas Hg, Pb, Sb, Se, and U (2–5×) show a moderate enrichment in the Tertiary brown coals. Comparing with world averages of trace elements in coals, the Tertiary brown coals are only highly enriched in Cd (more than 7×), and As, Ba, Cr, Cu, F, Hg, Th, and U (2–5×) show a moderate enrichments in the Tertiary brown coals. Basalt occurs in broad areas of the basins and may be considered as a source for some PHTEs in Tertiary brown coals during coal deposition.

3.3 PHTEs in Middle Jurassic coals

The Middle Jurassic coals in Shanxi province occur only in Datong Coalfield in the northeast of Shanxi province. It is the biggest coal base for power generation. Seventeen samples of Middle Jurassic coals were collected and analyzed. The contents of PHTEs are shown in Table 6.

Comparing the PHTEs contents with the crustal abundances, only As and Se (>5×) show a moderate enrichment, cadmium and Sb (3×) show a slight enrichment in the Middle Jurassic coals. A comparison with world averages of trace elements indicates that most PHTEs in the Middle Jurassic coals from Shanxi province are lower than world averages. However, Hg

Table 6. Contents of the PHTEs in Middle Jurassic coals from Shanxi province (in µg/g)

Element	Range	Average	Number of samples
As	0.1-82.4	12.3	17
Ba	<15-200	71	17
Cd	bdl-1.1	0.6	11
Cl	bdl-260	116	11
Co	1.6-25.0	7.4	17
Cr	2.2-19.4	7.2	11
Cu	bdl-264	29.8	11
F	bdl-117.6	35.2	11
Hg	bdl-0.28	0.10	11
Mo	bdl-6.4	2.3	11
Ni	11.1-17.0	13.1	3
Pb	bdl—30.0	9.4	11
Sb	0.1-1.7	0.6	17
Se	0.1-1.9	0.6	17
Th	0.5-8.0	1.5	17
U	0.22-3.4	0.8	17
Zn	bdl-64.1	23.7	17

bdl: below detection limit.

(8×) shows a high enrichment, Arsenic and Cd (2–2.5×) show a slight enrichment. There are magmatic lamprophyre intrusions in the area which may be a cause of increasing arsenic content in some Middle Jurassic coals of Datong Coalfield.

It is also found that the concentrations of As and Cu are higher in the Middle Jurassic coals than in the Early Permian and the Late Carboniferous coals of Shanxi province (Table 6-8).

3.4 PHTEs in Early Permian coals

The Early Permian coals of Shanxi province occur in Hedong Coalfield (A), Datong Coalfield (B), Ningwu Coalfield (C), Xishan Coalfield (D), Qinshui Coalfield (E), and Huoxi Coalfield (F) (Fig..1). The production of Early Permian coal is more than that of any other coal-forming ages. Fifty-two samples of Early Permian coals were collected and analyzed, and the results are shown in Table 7.

A comparison of the PHTEs contents with the crustal abundances indicates that only Se (up to 108×) are highly enriched, and Cd, Cl, Hg, Pb, and Sb (2–5×) show lower enrichment factors in the Early Permian coals. Comparing with world averages of trace elements in coals indicates that the Early Permian coals of Shanxi province are only highly enriched in Hg (more than 29×), and a moderate enrichment in Cd and Th (2–5×). Occurrence of coalbed methane in several coalfields (such as Hedong Coalfield and Qinshui Coalfield) may be related to the sources of mercury in coals, because the content of mercury is high in coalbed methane and the thermal release mercury is used to explore for coalbed methane in northern China.

The concentrations of Ba, Sb, and Th are higher in the Early Permian coals than that in the Middle Jurassic and the Late Carboniferous coals of Shanxi province (Table 6-8).

Table 7. Contents of the PHTEs in Early Permian coals from Shanxi province (in µg/g)

Element	Range	Average	Number of samples
As	bdl-17.5	1.7	52
B	bdl-3.3	1.4	10
Ba	31-427	103	52
Cd	bdl-2.4	1.0	44
Cl	100-1865	366	45
Co	0.4-22.5	4.8	52
Cr	2.5-32.8	11.0	52
Cu	bdl-48	15.7	44
F	bdl-1900	157	43
Hg	bdl-2.89	0.35	44
Mo	bdl-24.1	5.0	52
Ni	2.7-46.0	11.2	10
Pb	bdl-66	25.0	44
Sb	0.1-11.3	0.7	52
Se	0.1-12.2	5.4	52
Th	0.5-20.6	9.4	52
U	0.2-5.9	2.7	52
V	bdl-25.8	9.2	10
Zn	bdl-149	38.6	45

bdl: below detection limit.

3.5 PHTEs in Late Carboniferous coals

Similar to the Early Permian coals, the Late Carboniferous coals of Shanxi province occur also in Hedong Coalfield (A), Datong Coalfield (B), Ningwu Coalfield (C), Xishan Coalfield (D), Qinshui Coalfield (E) and Huoxi Coalfield (F) (Fig.1). Thirty-seven samples of Late Carboniferous coals were collected and analyzed, and the results are shown in Table 8.

A comparison of the PHTEs contents of the Late Carboniferous coals of Shanxi province with the crustal abundances indicates that the former are highly enriched in Cd (up to 6×), Hg (up to 7.3×), Mo (up to 5.3×), and Se (more than 30×), and are moderately enriched in Pb, Cl, and U (2–5×). Comparing with world averages of trace elements in coals, the Late Carboniferous coals of Shanxi province are only highly enriched in Hg (more than 49×), and are slightly enriched in Cd, F, Se, and Th (2–5×). The Late Carboniferous coals of Shanxi province have high content of sulfur (pyrite) which may be related to the enrichment of chalcophile trace elements Cd, Hg, Mo, and Pb.

The concentrations of Cd, Cl, Cr, F, Hg, Mo, Se, and Zn are relatively higher in the Late Carboniferous coals than in the Middle Jurassic and the Early Permian coals of Shanxi province (Table 6-8).

**Table 8. Contents of the PHTEs in Late Carboniferous coals
from Shanxi province (in µg/g)**

Element	Range	Average	Number of samples
As	<0.4-4.8	2.6	37
B	bdl-45	12	11
Ba	<10-244	96	37
Cd	bdl-2.0	1.2	34
Cl	bdl-940	557	34
Co	0.7-10.0	1.2	37
Cr	1.6-53.1	14.4	15
Cu	bdl-60.9	15.8	34
F	bdl-3600	270	30
Hg	bdl-2.67	0.59	34
Mo	bdl-56.9	7.8	37
Ni	2.7-46.0	19.8	12
Pb	bdl-88.0	28.7	34
Sb	0.1-0.7	0.3	37
Se	bdl-12.1	6.1	37
Th	0.7-17.1	7.3	37
U	0.9-49.9	5.7	37
V	bdl-84.1	25.7	12
Zn	bdl-193.0	63.3	34

bdl: below detection limit.

4. DISTRIBUTION OF THE PHTES IN SHENFU COALS

Shenhua Ltd. is one of the largest coal companies in the world. In the mean time, it is the largest coal producer and export coal producer in China. The discovered reserve of Shenfu coalfield is up to 239 billions tons, and the annual coal production capacity is going to reach 200 million tons by 2010. The study of distribution of the PHTEs is of great importance to the utilization of Shenfu coals.

More than 800 coal samples were collected, and the content of PHTEs were determined. The results are listed in Table 9.

Compared to the average content of the PHTEs in Chinese coals, most of Shenfu coals contain low concentrations of the PHTEs, which maybe related to their lower ash and sulfur contents. However, Mn, Co, Be, and Tl in the Shenfu coals are higher than the average values in Chinese coals. The enrichment of Mn may derive from the high content of calcite and other carbonate minerals in the coal.

The As content in Shenfu coals is 1.8 µg/g, only half of the arithmetic mean value of Chinese coals, and the content range is 0.1-6 µg/g, only 4% of the samples has an As content more than 6 µg/g. It can be concluded that the As content of Shenfu coals is low and it will not cause harm to the environment.

The fluorine content of Shenfu coals is 78.7 µg/g, lower than the arithmetic mean value of Chinese coals (130 µg/g). The F content of coals from different coal beds is consistent with

variation of ash content, which indicates that the F content may be related to the clay minerals.

Table 9. Content of the PHTEs in Shenfu Coals

Element	Number of samples	Range (μg/g)	Average content (μg/g)
As	752	0.04-78.0	1.88
Hg	737	0.006-1.71	0.08
F	9	8-208	78.7
Se	712	0.02-13.2	0.27
Sb	3	0.13-0.60	0.52
Mo	6	0.47-4.9	0.92
Pb	732	0.3-790	8.41
Zn	732	3.0-584	35.25
Cd	713	0.01-1.18	0.057
Cu	741	0.90-560.6	10.40
Cr	756	0.10-127.6	12.23
Co	732	2.0-30.0	10.19
Ni	732	0.50-35.0	10.64
Tl	664	0.05-3.50	0.51
Be	732	0.10-72.8	2.73
Cl	185	10-855	208
Mn	758	5.2-2622	174
U	15	0.09-6.40	1.13
Th	15	0.28-14.40	3.81
V	738	1.70-150.90	11.51

Generally, the content of the PHTEs in Shenfu coals is not high and the environment impact is minimal. However, considering the varied distribution of some PHTEs, we still need to pay more attention, especially to the enrichment of the PHTEs in typical coal mines.

5. DISTRIBUTION OF THE PHTES IN WESTERN GUIZHOU COALS

Guizhou province, located in southwestern China, contains a major coal resource. Western Guizhou is an important coal base of China, some endemic diseases, such as arsenism and fluorosis, may be related to coal utilization in this area.

Tectonically, western Guizhou Province has a complicated geological setting because of extensive faulting [11]. The geological evolution is characterized by frequent volcanic activities during the Late Permian and epigenetic low-temperature hydrothermal fluid alteration of coal seams, which could account for some of the geochemical and mineralogical anomalies of coals from western Guizhou Province [27,28]. There are more than 50 coal seams in total, including both workable and unworkable seams within the coal-bearing strata in the study area. The Late Permian paleogeography in the area varied from alluvial and fluvial plains through paralic deltas and tidal flats, and shallow marine to abyssal basins. Western Guizhou Province contains Late Permian coal-bearing strata. Permian coal-bearing strata in the area include the Upper Permian Emeishan Formation, the Late Permian Longtan

Formation, the Late Permian Changxin Formation, and the Late Permian Dalong Formation. The Emeishan Formation mainly consists of tholeiite, volcanic breccia, and tuff, and, in places, marine limestone layers. The Longtan Formation is the major coal-bearing formation and consists of sandstone, siltstone, mudstone, over 10 limestone layers, and over 30 coal seams, with a total thickness of about 300 m. The sedimentary environment of the Longtan Formation varied from lagoons and tidal flats through lower delta plains to tidal flats and carbonate subtidal flats. The thickness of the Changxin Formation is 130 m on average and represents shallow marine and paralic delta sedimentary environments. The Dalong Formation, with a thickness of about 51 m, mainly consists of intercalated silica rocks and mudstones, and its sedimentary environment is subtidal facies [11].

The contents of the PHTEs in 71 Late Permian whole-seam coal channel samples from western Guizhou Province were investigated. The results are shown in Table 10. Compare with the Clarke value of the earth's crust (Table 2), the results show that in the Late Permian coal from western Guizhou Province the contents of As, Cd, Mo, Sb, Se, and U are higher. The enrichment factor (EF: the ratio between the content of some element in coal and the Clarke value of the earth's crust) of these elements are more than or equal to two times. Compare with the element content of America coals, the contents of Co, Cr, Cu, Ga, Mo, Ni, Th, U, and V are higher, but the content of As, F, Hg, Se, and Tl are less, the other element content are similar. The arithmetic means of concentrations for Co, Cr, Cu, Ga, Mo, Ni, U, V, and Zn in western Guizhou coals are higher than those in Chinese coals, F and Hg are lower than.

Table 10. Contents of the PHTEs in Late Permian coals of western Guizhou

PHTEs	Range (µg/g)	Arithmetic mean value (µg/g)	Enrichment Factor
Be	0.21-12.47	2.19	0.78
F	16.6-500	83.1	1.3
V	18.01-574.4	123.42	0.91
Cr	0.02-139.3	31.91	0.32
Co	0.39-118.6	13.59	0.54
Ni	4-160	36.74	0.49
Cu	7.23-369.9	61.12	1.11
Zn	2.01-561.4	55.1	0.79
Ga	0.38-99.5	13.05	0.87
As	0.30-10.45	3.9	2.15
Se	0.10-6.02	1.65	33.04
Mo	0.10-76.58	8.24	5.50
Cd	0.02-8.19	0.40	2
Sb	0.05-6.06	0.97	4.85
Hg	0.031-0.217	0.09	1.11
Tl	0.01-0.51	0.11	0.25
Pb	1.26-184.7	14.73	1.18
Th	1.99-47.5	6.52	0.68
U	0.10-176.2	13.65	5.05

(EF: the ratio between the content of some elements in coal and the Clarke value of the earth's crust)

Because arseniasis and fluorosis is prevalent in this area, we should pay more attention on the content of As and F in the Late Permian coals from western Guizhou Province. Although, as reported by some authors, western Guizhou Province is the area of endemic arseniasis related to coal combustion, it is worth pointing out that the arithmetic mean of As (3.9 μg/g) from western Guizhou Province is similar to and lower than that of in Chinese coals and US coals, 3.8 and 24 μg/g, respectively. Belkin et al., (1997) found the highest arsenic-bearing sample (up to 3.2%) in Haizhi Township from Xingren County, southwestern Guizhou Province [6]. However, such high-As coal samples are not whole-seam channel, but lump samples, and the coal seams are unworkable. In addition, the occurrence of the high As coal is restricted to an outcrop area (including the mouth of the well) of only about 100 m^2, although it has led to the serious endemic arseniasis. Unfortunately, now it is very difficult to collect the high-As coal samples because the mines that produced high-As coal had been closed for years.

The fluorine content in coals from western Guizhou Province ranges form 17 to 500 μg/g, with an average of 83 μg/g, which is lower than that of the Chinese coals (131 μg/g). The highest content of fluorine (500 μg/g) in the No. 9 coal seam from the Zhijin Coalfield of western Guizhou Province was attributed to the synsedimentary volcanic ash. During epidemiology investigations, Dai et al., (2004) found that the local residents from western Guizhou Province are accustomed to not only using furnaces without chimneys to dry corn, to cook, and to keep warm indoors, but also to using a yellow clay for a coal-burning additive in the furnace and as a binder in briquette-making. This clay contains high fluorine content with an average of 1028 μg/g. Almost every family in villages from western Guizhou Province uses the mixture of coal and clay (the ratio is from 4:1 to 2:1) as their daily primary fuel. Taking the ratio of coal to clay into account, the fluorine content in the mixture can be figured out as more than 300 μg/g, which is much higher than that in coals alone from the western Guizhou Province (83 μg/g). In the areas where unhealthy traditional coal-burning habits and customs are kept and furnaces without chimneys are used, the more clay used for a coal-burning additive and as a binder for briquettes, the more serious the fluorosis problem is. The endemic fluorosis in western Guizhou Province is likely attributed to the high content of fluorine in the clay, rather than to fluorine in coals alone [29].

6. DISTRIBUTION AND PARTITION OF MERCURY DURING COAL UTILIZATIONS

6.1. Content and distribution of mercury in coals from different provinces of China

Atmospheric mercury emission is an international problem as the troposphere provides effective global transport of mercury. China is estimated to be the largest producer of mercury emissions [30]. A recent comprehensive study of anthropogenic mercury emissions in China [17] yielded a figure of 536 t of mercury for the year 1999 from coal combustion (all types) accounting for 38% of the total. Although the estimates vary, China produces about three times more mercury per ton of coal burnt than the USA because of the lack of modern pollution technology and limited use of clean coal. Studies of the mercury distribution in

Chinese coal and the partition of mercury during coal combustion are vital to assess and retention the mercury pollution from Chinese coal combustion.

Table 11. Mercury content of raw coal as mined in China by province (µg/g)[17]

Province	Hg content	Province	Hg content
Anhui	0.26	Jiangxi	0.22
Beijing	0.44	Jilin	0.20
Fujian	0.08	Liaoning	0.17
Gansu	0.05	Nei Mongol	0.22
Guangdong	0.15	Ningxia	0.20
Guangxi	0.30	Qinghai	0.04
Guizhou	0.52	Shaanxi	0.11
Hainan	0.15	Shandong	0.18
Hebei	0.14	Shanxi	0.16
Heilongjiang	0.09	Sichuan	0.14
Henan	0.25	Xinjiang	0.02
Hubei	0.16	Yunnan	0.29
Hunan	0.10	Zhejiang	0.35
Jiangsu	0.16		

Streets et al., (2005) summarized studies about the Hg content of raw coal as mined in different provinces of China [17], among which significant differences are shown in Table 11. These differences can be attributed to the selection of coal mine, the location of sampling, test methodology, etc. The Hg content in most provinces is close to or less than the average content of Hg in Chinese coal (0.19 µg/g). Guizhou province has the highest Hg content coal mines, which also validated by Huang and Yang (2002) [16].

The content of mercury in Chinese coals from different coal-forming periods is listed in (Table 1). Mercury content in coals from Late Triassic and Late Permian is much higher than that of from other periods, while in coals from Paleogene-Neogene is lowest.

6.2. Partition of mercury during coal pyrolysis

Mercury is one of the most volatile elements in coal during coal utilization, especially for elemental mercury. Elemental mercury has a low boiling point (356℃) and has been shown to be released from coals at the lower temperatures during mild pyrolysis [31-33]. The chemical thermal dynamical equilibrium software F*A*C*T was used to predict the partition of mercury during coal pyrolysis. Calculation results show that mercury species at equilibrium are all distributed in gas phase. Hg^0 is the main species at temperature higher than 500K.

Two bituminous coals were chosen to determine the mercury behavior during coal pyrolysis. The experiments were carried out in a tube furnace with a nitrogen blanket at different residence times and different temperatures. The experimental data indicate that the percentage of mercury removed from coal increases with increasing temperature and

residence time, which also validated in low-ranked coal and high-volatile bituminous by other researchers [34,35].

Elemental mercury (Hg^0) is the dominant species of mercury presents in both coal pyrolysis gases, up to about 72% and 64% in the total mercury for Shenfu coal and Yongzhou coal, respectively. And the content of elemental mercury (Hg^0) decreases and the content of oxidation mercury increases with the increasing temperature (Fig.2), which indicates that the high temperature is helpful to for oxidation mercury formation during coal pyrolysis.
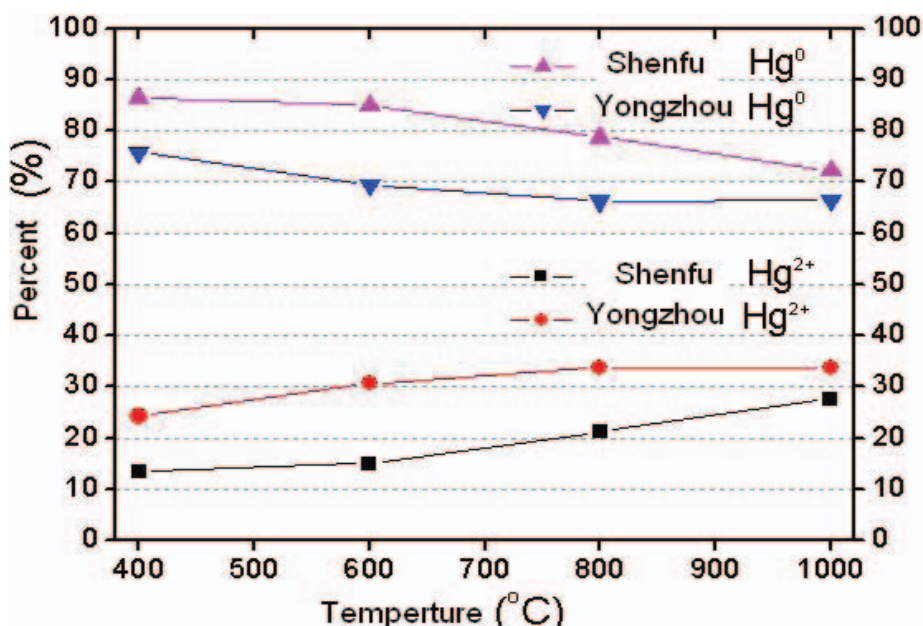
Figure 2. The impact of temperature on mercury speciation during coal pyrolysis

6.3. Partition of mercury during coal gasification

The results of thermodynamic calculation show that the elemental mercury is the mainly species in the coal gas, and the oxidized mercury increases with the increasing temperature and pressure of gasification.

The gasification experiments were also carried out in a tube furnace at deferent resident times and different temperatures. Carbon dioxide was used as the reaction gas. The results show that the release of mercury increases with the temperature increasing, most of mercury emission when the temperature reaches 1000℃, the release percent of Shenfu coal is up to 92%, and for Yongzhou coal is 95% (Fig.3).

The influence of temperature on mercury speciation in gasification of CO_2 is also the same with the condition in coal pyrolysis (Fig.4). The percent of oxidized mercury (Hg^{2+}) in total mercury increases with the temperature increasing. And more Hg^{2+} was produced during coal gasification of CO_2 than that during coal pyrolysis. It is uncertain for mercury speciation in gasification of H_2O.
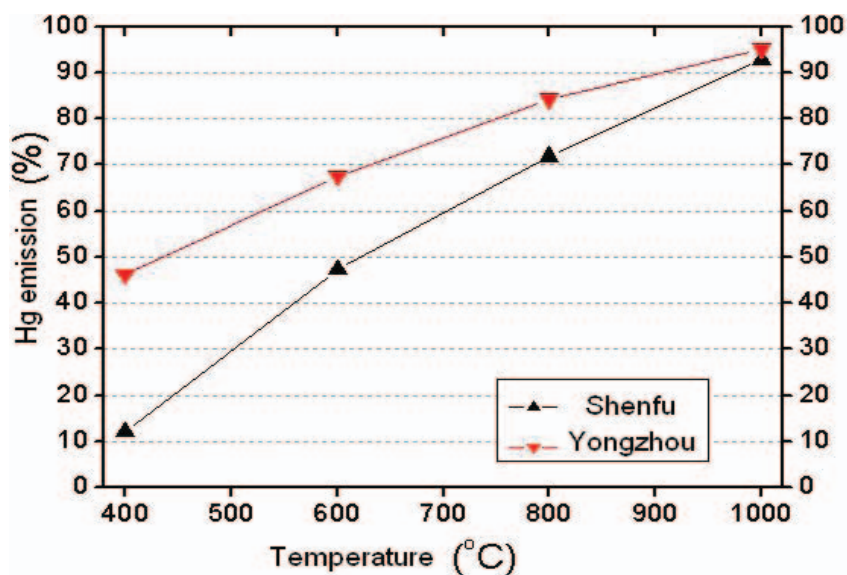
Figure 3. The impact of temperature on mercury emission during coal gasification
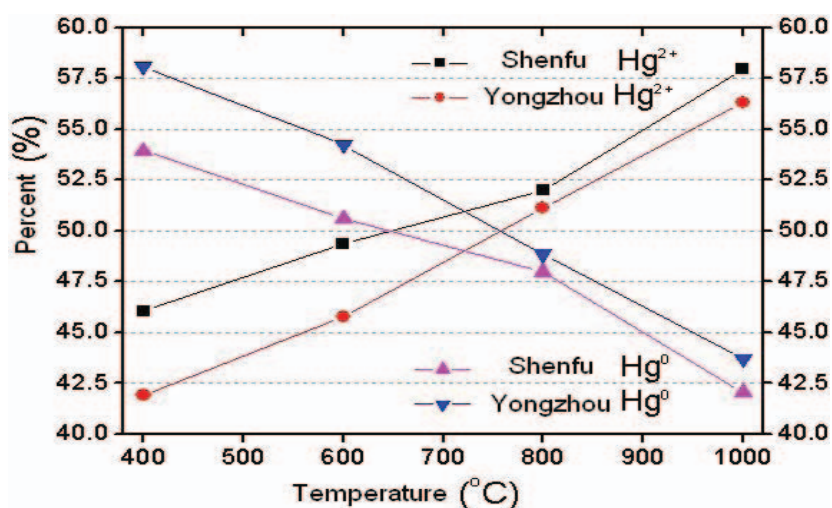
Figure 4. The impact of temperature on mercury speciation during coal gasification.

6.4. Mercury emissions from coal-fired power plants

To understand the fate of mercury in coal combustion, Guo et al., (2007) conducted experiments in a 300 MW coal-fired plant equipped with an electrostatic precipitator (ESP). The percentages of mercury in the slag, fly ash, and stack emissions are 1%, 13%, and 86%, respectively. This means that the high proportion of mercury would be emitted to the atmosphere after passing though the particulate controls. The vapor phase emissions of mercury vary over the range 13.65-21.15 $\mu g/Nm^3$. A total of 31-45% of the mercury that was

present in the stack gas was in the elemental form, and 55-69% of the mercury was in the oxidized form.

Mercury transformation across particulate control devices in six power plants of China was also studied by Chen et al, (2007) [37]. The measurements in this study show that 10% to 87% mercury was oxidized at the outlet of ESP/FF, where the flue gas temperature is about 160 ℃. The proportions of oxidized mercury in gas phase at the inlet of ESP/FF increase with the increasing of chlorine concentration in coal. Oxidized mercury in total gaseous mercury increases from about 10% to 60% as the chlorine content in coal increases from 150 µg/g to 350 µg/g. Coal characteristics, i.e., chlorine concentration and ash composition in coal, play a more important role in determining gas phase mercury speciation than any other practical conditions such as boiler capacity and particulate control device type. It is necessary to pay much more attention to the coal subcategories when estimating mercury emission and speciation. Chinese coals have a varied mercury concentration, chlorine concentration and ash compositions due to their origins and geological history. A more comprehensive mercury investigation on coal characteristics and power plant emission is needed to obtain more detailed information before estimating the overall mercury emission from Chinese power plants, and setting up the reasonable and reliable mercury control strategies for China.

Much work has shown that there is a degree of retention in the dust [38-40]. Ash plays a role in both the oxidation of elemental mercury and the adsorption of mercury in flue gas. It is this interaction of fly ash particles with mercury vapor that contributes to the final partitioning of mercury. Surprisingly good correlations of Hg content with loss of ignition (LOI) were observed Figure. 5, the mercury concentration in fly ash has a positive correlation with the LOI of fly ash and is independent of the particle size [36]. To elucidate the interaction mechanism of mercury and fly ash, Table 12 lists the results of fly ashes vacuumized at 100   for 10 h to remove gas in the fly ashes and then absorbed with mercury-free nitrogen gas, after which the fly ashes reanalyzed the mercury concentration. The concentration of mercury decreases for all fly ashes after desorption. The percentages of desorption of EF-1, EF-2, EF-3, EF-4, and PFA are 11%, 35.3%, 44.1%, 36.4%, and 32.6%, respectively (EF-1 is indicated for ash collected in hopper 1, EF-2 for ash collected in hopper 2, etc. whereas, PFA indicated for the ash carried away with the flue gases out of ESP). This reversible process indicates that physical adsorption does happen in some sense, which suggests that there may be more than one mechanism by which capture takes place at the post combustion zone in the case of fly ash, including chemisorption, chemical reaction, and physisorption.

Table 12. Comparison of the Mercury Concentration after Desorption [36]

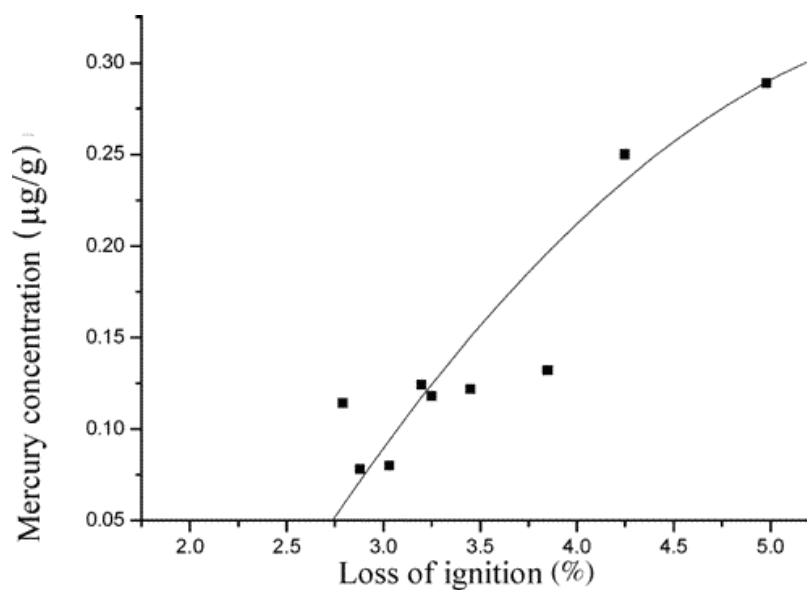| sample	mercury (µg/g)	after desorption of mercury (µg/g)	desorption (%)
EF-1	0.114	0.102	11
EF-1	0.122	0.079	35.3
EF-1	0.118	0.066	44.1
EF-1	0.132	0.084	36.4
PFA	0.086	0.058	32.6

Figure 5. Relationship between mercury retention and carbon-in-dust full scale [36]

7. DISTRIBUTION AND OCCURRENCE OF FLUORINE IN COALS AND THE COMBUSTION PRODUCTS

7.1. Fluorine in Chinese coals

Endemic fluorosis is prevalent in China covering 29 provinces, municipalities and autonomous regions, one of the important source of fluoride pollution is coal combustion. Several studies have determined the fluorine content and distribution pattern in Chinese coals. Zheng and Cai (1988) reported the average fluorine concentration in Chinese coals is 200 μg/g much higher than world mean value 80 μg/g [41]. Ren et al., (1999) studied trace element concentration of Chinese coals and thought that the arithmetic average fluorine concentration is 1200 μg/g [42], but the number of samples are so less. And all of the fluorine concentrations of coals from a certain region were generally given as arithmetic or geometric means of studied coal samples. Chen and Tang (2002) studied fluorine in Chinese coals, summarized fluorine concentration data of other researches, pointed out most Chinese coals fluorine concentration between 20-300 μg/g and the average concentration is 140 μg/g [18]. These results are helpful to understand the distribution of fluorine in China coals. However, the relative proportions of coal resources should be taken into account when average concentrations of trace elements in coals from a region are estimated to reflect their toxicity; otherwise, the estimated concentrations of trace elements in coals will not be representative for the certain region if coal samples were not evenly distributed either in space or in geologic ages [5,9]. Luo et, al., (2004) took into account many factors such as the different coal-forming basins, different coal-forming periods, different coal types, especially their different proportions to Chinese coal resource, give an average value of Chinese coals about 82 μg/g, close to that in the world average (80 μg/g), but the coal sample number is not enough [19].

Dai and Ren (2006) collected data for more than 2500 coal samples and analyzed the distribution and concentration of fluorine in coal systematically [5]. The overall average fluorine concentration of coals in China is 130 μg/g, which is approximately one third higher than the reported value of the U.S. coals [5]. At the same time, the statistics of arithmetic means of fluorine contents in different ages, different rank of coals, different districts, and different provinces were compared systematically.

Table 13 is the summary of the fluorine concentration of coals for the six geological ages, as well as the overall fluorine concentration of coals in China by Dai and Ren (2006) [5]. The fluorine concentration of E–N coals in China (352.8 μg/g) is higher than that of any other geological ages, and that of J_{1-2} age, which has the largest ensured coal reserves, is much lower (84.46 μg/g). The fluorine concentration of C–P_1 coals is 149.4 μg/g.

Table 13. Summary of fluorine concentration of each geological period and the overall fluorine concentration of coals in China [15]

Period	Number of Samples	Concentration (μg/g)	Reserve factor (%)	Sub value based on reserve (μg/g)
C–P_1	>273	149.4	38.1	56.9
P_2	>1609	200.9	7.5	15.1
T_3	>30	84.1	0.4	0.3
J_{1-2}	33	84.5	39.6	33.4
J_3–K_1	3	134.2	12.1	16.2
E–N	>23	352.8	2.3	8.1
Total	>1964		100	130

Carboniferous and Early Permian (C–P_1), Late Permian (P_2), Late Triassic (T_3), Early and Middle Jurassic (J_{1-2}), Late Jurassic and Early Cretaceous (J_3–K_1), and Paleogene and Neogene (E–N)

There are remarkable differences in the abundance of fluorine in coals from different areas of China (Table 14). The fluorine content in coals from South China is much higher than others, up to 323 μg/g, the reasons maybe related to the high sulfur content in the coals.

Table 14. The fluorine content in coals from different districts in China (arithmetic mean value, μg/g)

	Northern China	Northern China	Northeastern China	Northwestern China	Southern China
Content	144	128	198	135	323
Number of samples	378	83	134	63	357

7.2. Fluorine in ash water from coal-fired power plants

It is reported that there are 15% coal-fired power plants in China have problems with the pollution of fluorine in ash water. Lin et al., (1994) investigated the content of fluorine in the ash water of coal-fired power plants in Henan province (Table 15) [43]. The fluorine content in ash water at the wet scrubber outlet is highest in the product line, and decreases along with

the product line, because Ca^{2+} continuously is dissolved out and reacts with F^- that makes deposition of CaF_2. Xue et al., (1998) analyzed the content of fluorine in the ash water of Kaifeng coal-fired power plant in Henan province from April to July, 1998 (Table 16) [43]. They found that the concentration of fluorine in ash water exceeded the class Ⅱ of the national integrated wastewater discharge standard (GB 8978-1996) sometimes, and the pH of ash water always exceeded the class Ⅱ standard too. The conclusion they gained is the concentration of fluorine in ash water may exceed the class Ⅱ of the national integrated wastewater discharge standard when the content of fluorine in coal is more than 190 μg/g.

Table 15. Fluorine content in ash water from coal-fired power plants in Henan province

Sampling points	Yaomen (mg L^{-1})		Pingdingshan	Xinxiang	Shouyang	Zhengzhou
	1, 2 # units	3, 4 # units	(mg L^{-1})	(mg L^{-1})	(mg L^{-1})	(mg L^{-1})
Precipitator outlet	21.40	2.61	16.53	22.93	26.25	4.94
Slurry pump inlet			5.69			
Thickener inlet	21.24	2.14		19.29	15.00	5.38
Thickener overflow mouth		4.02		18.03	15.54	4.49
Ash pipeline inlet	17.96	6.92	5.88	17.43	15.10	4.94
Ash field clarified water			6.76	13.63		4.94

Table 16. Fluorine content in coal and ash water
from the Kaifeng coal-fired power plant

Date (1998)	Test item	Slurry water at 3# boiler	Slurry water at 4# boiler	Mixed slurry at slurry pump inlet	Backwater of thickener	Slurry at thickener outlet	Thick slurry at ash field inlet	Ash field waste water	F content in coal (ppm)
04-27	pH	3.41			9.19	10.96	12.42	12.32	190
	F^- /mg L^{-1}	31.10			11.88	8.48	8.35	8.23	
04-29	pH	5.67		7.68	8.67	11.39	12.71	12.25	210
	F^- /mg L^{-1}	32.11		24.15	16.65	13.45	12.27	11.02	
05-13	pH			8.25	8.72	12.13	12.51	10.73	270
	F^- /mg L^{-1}			25.13	21.80	15.78	13.67	12.54	
05-26	pH	4.52		8.65	8.46	10.72	12.31	10.66	220
	F^- /mg L^{-1}	31.82		25.00	17.00	14.01	13.15	11.20	
06-09	pH	6.04	5.71	6.45	8.64	10.74	11.80	11.66	190
	F^- /mg L^{-1}	28.18	28.92	17.10	15.69	14.35	13.42	8.25	

Table 16. Continued

Date (1998)	Test item	Slurry water at 3# boiler	Slurry water at 4# boiler	Mixed slurry at slurry pump inlet	Backwater of thickener	Slurry at thickener outlet	Thick slurry at ash field inlet	Ash field waste water	F content in coal (ppm)
06-22	pH	5.97	6.06	8.00	9.06	11.21	12.95	12.62	170
	F^-/mg L^{-1}	32.35	30.94	18.36	16.19	12.17	11.18	8.19	
06-29	pH	7.14	6.8	18.24	8.76	11.78	12.10	11.75	110
	F^-/mg L^{-1}	16.49	18.86	12.61	11.70	11.27	8.56	5.72	
07-06	pH		6.53	9.40	9.03	11.91	12.25	11.68	97
	F^-/mg L^{-1}		23.19	10.74	10.44	8.26	6.65	4.90	
07-15	pH	6.37	5.70		8.82	10.96	11.95	11.40	91
	F^-/mg L^{-1}	29.45	27.44		1.28	8.90	6.32	5.67	
07-27	pH	5.61	6.09		8.12	10.05	10.52	11.72	81
	F^-/mg L^{-1}	30.30	25.30		11.34	8.47	6.29	5.99	

7.3. Fluorine in flue gas

Xu et al., (2000) investigated the content of fluorine in flue gas of the No.1 and No.2 coal-fired power plants in Baotou, China (Table 17) [43]. In 1999, the average value of fluorine content in the flue gas of the No. 1 Power Plant in Baotou was 2.61 mg/m^3, and in 2000 the value was 1.80 mg/m^3. At the No. 2 power plant in Baotou, the arithmetic mean of fluorine content in the flue gas was 1.12 mg/m^3 and 2.71 mg/m^3 in 1999 and 2000, respectively.

7.4. The cause of endemic fluorosis in western Guizhou Province, Southwest China

The endemic fluorosis in western Guizhou Province, southwest China is usually attributed to the high-fluorine content in Late Permian coals [3,44]. Dai et al., (2004) investigated the fluorine in the typical coal channel samples, clay samples which used as an additive for coal-burning and as a binder in briquette-making, and the drinking water samples systematically, the average content of fluorine in these samples are listed in Table 18 [29].

Table 17. Fluorine concentration in flue gas at the
Baotou coal-fired power plants in (mg/m^3)

Power plant	Year	Testing item	Boiler number								Arithmetic mean value
			1	2	3	4	5	6	7	8	
The first thermal power plant	1999	Gas	0.279		0.227	0.182	0.282		0.222	0.325	
		Dust	0.878		0.665	2.461	4.124		3.016	3.005	
		Total	1.157		0.892	2.643	4.406		3.238	3.330	2.61
	2000	Gas		0.105			0.140		0.170		
		Dust		2.407			2.439		0.130		
		Total		2.513			2.580		0.301		1.80
The second thermal power plant	1999	Gas	0.045		0.072	0.0513	0.090		0.050		
		Dust	1.097		0.713	1.263	1.510		0.705		
		Total	1.142		0.785	1.314	1.600		0.755		1.12
	2000	Gas	0.065					0.065	0.125		
		Dust	2.451					2.737	2.681		
		Total	2.517					2.802	2.806		2.71

Table 18. The average content of fluorine in different samples of western Guizhou

	Coals in western Guizhou province (μg/g)	Coals in Zhijin county of Guizhou province (μg/g)	Clay (μg/g)	Drinking water (mg/L)
Content	83.1	89.3	1027	0.19

The regions of extreme fluorine enrichment in coals (>1000 ppm) in southwestern Guizhou, China are only Nibu area (A) and the Liuzhi well field (B) (Fig. 6). The fluorine concentration in coals from Nibu area is up to 2259 ppm. The fluorine concentration in coals from the Liuzhi well field is the highest in Guizhou province. The range of fluorine concentration is between 999 and 2544 ppm, and the average is surprisingly high, 1797 ppm, in the Liuzhi well field [45]. In these areas, the endemic fluorosis is likely caused by the combination of high fluorine coals and high-fluorine clays.

A. Nibu area; B. Liuzhi well field.

Figure 6. Locations of extreme high fluorine (>1000 ppm) coals in southwestern Guizhou, China.

8. Distribution, Occurrence and Emission of Arsenic in Typical High-Arsenic Coal in China

8.1. The distribution of arsenic in typical high-arsenic coals in China

On the basis of weighted coal resources of coal-forming periods and coal-forming areas, Ren et al., evaluated trace element concentration in a total of 3386 coal samples from China [9]. Arsenic content in coal ranges from 0.03 to 478.4 µg/g, with an average of 3.8 µg/g. Dai et al., (2005) studied arsenic contents in 71 Late Permian whole-seam coal channel samples from western Guizhou Province, and found that arsenic contents in most of samples were low, the average content of arsenic in these coal samples is 3.9 µg/g, which is close to the average value of arsenic concentration in whole country [11]. However, some typical high arsenic coals in southwestern Guizhou still need more attention. With the aim of better understanding distribution and occurrence of arsenic, 144 typical coal samples from southwestern Guizhou Province were collected and evaluated.

The coals are mainly Late Permian age and occur in the Longtan Formation and the Changxing Formation. Mineral matter showes moderate enrichment in some Late Permian coals in southwestern Guizhou Province, China, and the ash yield is up to 56.3%. The arsenic content varies from 0.3 µg/g to 3.2 wt.%. In most coal samples arsenic content was lower than 30 µg/g. The high arsenic coals which arsenic content are larger than 30 µg/g were listed in Table 19. Arsenic contents in 37 samples which were collected from several small coal mines were more than 30 µg/g, and their locations and regions have been mapped (Fig.7) [45]. They are distributed in areas of Xiongwu, Nibu, Dayakou, Getang, Longtoushan, Nanmuchang, and Dachang. Xiongwu area, Nibu area, Dayakou area, Getang area, and Nanmuchang area are the Late Permian coals; and Longtoushan area is the Late Triassic coals. More than 2000 cases of arseniasis have been documented in Jiaoluo Township in Getang area. Cases of arseniasis have been found in 85 villages in southwestern Guizhou, China. Among of them only 16 samples were more than 100µg/g.

Table 19. Arsenic content in high-arsenic coals studied

Location	Age	Rank	Content of As (µg/g)	Location	Age	Rank	Content of As (µg/g)
Anlong County	P2	A	39.2	Xingren County	P2	A	94.1
Anlong County	P2	A	52.6	Xingren County	P2	A	86.4
Anlong County	T3	H-B	34.9	Xingren County	P2	A	131.5
Anlong County	T3	H-B	49.6	Xingren County	P2	A	501
Qinglong County	P2	L-B	31.7	Xingren County	P2	A	1112
Qinglong County	P2	L-B	32.2	Zhenfeng County	P2	A	37.9
Qinglong County	P2	L-B	34.7	Zhenfeng County	P2	A	38.0
Qinglong County	P2	L-B	50.0	Zhenfeng County	P2	A	102.1

Location	Age	Rank	Content of As (µg/g)	Location	Age	Rank	Content of As (µg/g)
Qinglong County	P2	L-B	62.6	Zhenfeng County	P2	A	225.0
Qinglong County	P2	L-B	180.8	Zhenfeng County	T3	H-B	30.9
Xingren County	P2	A	56.3	Zhenfeng County	T3	H-B	36.1
Xingren County	P2	A	99.8	Zhenfeng County	T3	H-B	41.6
Xingren County	P2	A	127.2	Zhenfeng County	T3	H-B	45.3
Xingren County	P2	A	194.9	Zhenfeng County	T3	H-B	64.8
Xingren County♀	P2	A	230.4	Zhenfeng County	T3	H-B	207.0
Xingren County	P2	A	232.0	Zhenfeng County	T3	H-B	226.0
Xingren County	P2	A	3.2%	Zhenfeng County	T3	H-B	234.0
Xingren County	P2	A	33.1	Zhenfeng County	T3	H-B	238.0
Xingren County	P2	A	120				

A: anthracite; L-B: low-volatile bituminous coal; and H-B: high-volatile bituminous coal
♀: LT-K2 coal sample
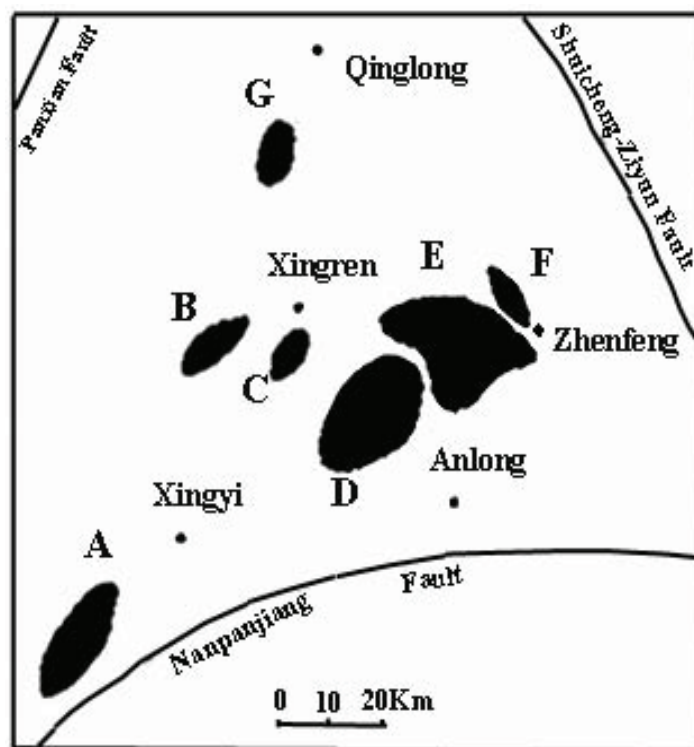
A. Xiongwu area; B. Nibu area; C. Dayakou area; D. Getang area; E. Longtoushan area; F. Nanmuchang area; G. Dachang area.

Figure 7. Locations of arsenic >30 µg/g in coals in QDFA, southwestern Guizhou, China.

8.2. The arsenic emission during coal combustion

To assess the environmental impact and determine the emission of arsenic during coal combustion, a typical high-arsenic coal (LT-K2) was chosen to conduct different experiments on a bench scale drop tube furnace.
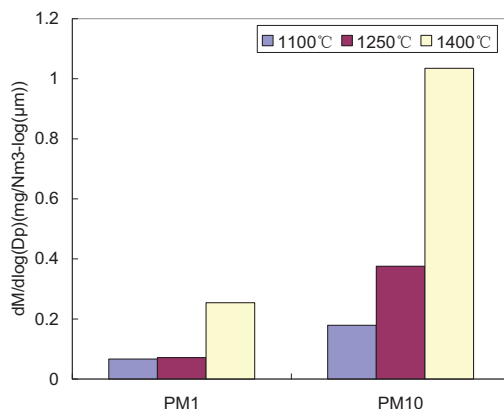
Figure 8. The emission of arsenic within PM at different temperatures.

The emission of arsenic in different temperature is shown in Figure. 8. Along with increasing temperature from $1100℃$ to $1400℃$, the emission of arsenic in PM_1 increases from 0.07 mg/Nm^3 to 0.25 mg/Nm^3 , the emission of arsenic in PM_{10} increases from 0.18 mg/Nm^3 to 1.03 mg/Nm^3. The results are caused by two reasons, one is the amount of total PM increased with increasing temperature, and the other is that much more arsenic vapor condensed and reacted on the PM surface at high temperature.

The emission of arsenic in different oxygen contents was shown in Fig. 9. In 20% oxygen content, almost each size stage has less arsenic concentration than in 50% oxygen content, the total arsenic emission in PM_{10} is 0.1 mg/Nm^3，which is only a tenth in high oxygen content. This results are due to the increase of particle temperature in 50% oxygen content.
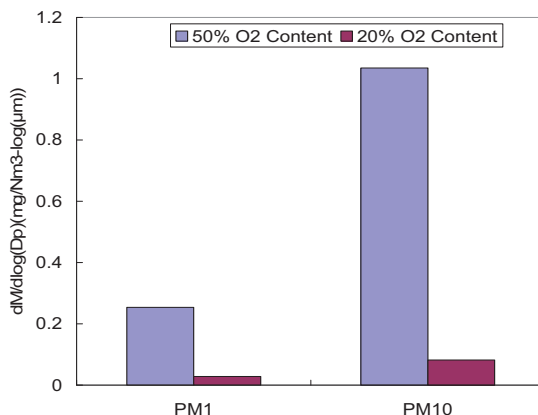
Figure 9. The emission of arsenic in different oxygen contents.

8.3. Arsenic emissions from coal-fired power plant

A study on arsenic emissions was conducted in a 300-MW coal-fired plant that was equipped with an electrostatic precipitator [46]. The input and output streams, such as coal, slag, ESP ash, and flue gas that contained the post-ESP particulates, were collected. Gaseous arsenic was sampled using United States Environmental Protection Agency (USEPA) Method 29, and the arsenic concentrations in the samples were measured using inductively coupled plasma-atomic emission spectrometry.

The mass balance recovery of arsenic estimated in this study was 87.2%. The arsenic concentration in the stack gas was 2.5 μg/Nm^3, which is below the China Pollution control standard for hazardous waste incineration ([As] + [Ni] =1 mg/Nm^3). Approximately 0.53% of the coal derived arsenic was incorporated into slag, 84.6% of the arsenic was found on the fly ash that was collected by the ESP, and 2.16% was found in the vapor phase. This means that fly ash is effective in capturing arsenic. The particulate loading after the ESP is 98 mg/Nm^3. Attention must be given to the enrichment of arsenic in these particulates, which may increase the risk of pollution after emission into the atmosphere [46].

Table 20 is the results of fly ashes vacuumized at 150 °C for 10 h and then absorbed with arsenic-free nitrogen gas, after which point the arsenic concentration in the fly ashes is analyzed. As can be observed, the concentration of arsenic decreases for the EF-1 and EF-2 fly ashes after desorption, suggesting that physical adsorption has happened, in some sense. A negligible loss of arsenic is observed for EF-3, EF-4, and the PFA. This irreversible process indicates that physical adsorption is not the mechanism between the fly ash and the arsenic at the post-combustion zone of 150 °C. The relationship between arsenic concentration and ash particle size was also assessed, and arsenic was significantly concentrated in the small-sized particles [46].

Table 20. Comparison of Arsenic Concentration after Desorption [46]

Sample	Arsenic Concentration (μg/g)	
	before desorption	after desorption
EF-1	6.03	4.81
EF-2	25.6	18.3
EF-3	37.7	36.6
EF-4	45.6	44.9
PFA	66.9	65.5

9. DISTRIBUTION, OCCURRENCE, AND EMISSION OF CHROUMIUM IN TYPICAL HIGH-CHROMIUM COAL IN CHINA

9.1. Distribution of chromium in Shenbei coalfield

On the basis of weighted coal resources of coal-forming periods and coal-forming areas, Ren et al., (2006) have evaluated trace element concentration in a total of 3386 coal samples from China [9]. They found that chromium content in coal ranges from 0.10 to 942.7 μg/g,

with an arithmetical average of 15 μg/g. With the aim of better understanding the distribution of chromium, more than 100 high-chromium coal samples were collected and analyzed. The concentration of chromium was determined by INAA. The average concentrations of chromium in coal from different ages are listed in Table 21. The results show that chromium content is low in J1-2, while it is much higher in E age coals. The chromium content varies from 0.46 μg/g to 145 μg/g. In most coal samples chromium content is lower than 15 μg/g which is close to a representative value of chromium concentration of coal in China. The arithmetic mean of chromium content in Shenbei lignite is 79 μg/g (Table 22), which is much higher than the average content in Chinese coals.

Table 21. The contents of chromium in coals from different ages (μg/g)

Ages	Cr content	Number of samples	Ages	Cr content	Number of samples
C2	13.9	23	J1-2	9.78	15
P1	13.2	22	J3-K1	14.3	4
P2	21.7	57	E	68.4	4
T3	35.8	5	N	22.4	5

Table 22. The mean concentrations of chromium in the Shenbei lignite (μg/g)

Element	AM[a]	STD1[b]	GM[c]	STD2[d]	Rang
Cr	79	50	55.3	31	0.46–145

a AM: arithmetic mean; b STD1: standard deviation for arithmetic mean; c GM: geometric mean; d STD2: standard deviation for geometric mean.

9.2. Occurrence of chromium in high-chromium coal

Sequential chemical extraction is an especially effective method for identifying the occurrence of trace elements in coal. Several typical coals were chose to conduct chemical extraction experiment. The experimental results show that, most of chromium in bituminous and anthracite is associated with aluminosilicate. Although the Cr in the studied Shenbei lignite samples has multiple modes of occurrences, it is mainly associated with fulvic acid and/or organic macromolecules fractions (Table 23). About 75–100% of Cr occurs in organic macromolecules.

9.3. Emission of chromium during high-chromium coal combustion

The emission of chromium in PM during different coals combustion has been assessed through systematic bench-scale drop tube furnace experiments (Figure 10). Although chromium content in two coals is approximately equal, the emission during coal combustion is obviously different. Some laboratory studies have suggested that the behavior of trace

Table 23. Percent leached data of chromium in different coal samples

Sample	LT01	QG04	XD05	ZM06	QS2	PH2	QT2-3
Coal ranks	Bituminous	Bituminous	Anthracite	Anthracite	Lignite	Lignite	Lignite
WS (%)	0	0	0	0	0	0	0
IE (%)	0	0	0	0	0	0	0
OB (%)	55.16	7.62	0	0	82.27	75.24	100
CB (%)	0	2.49	11.32	10.20	3.16	9.70	0
AS (%)	44.84	89.61	88.68	89.80	14.57	13.28	0
SF (%)	0	0.64	0	0	0	1.78	0
Total (%)	100	100	100	100	100	100	100

WS: in water-soluble state; IE: in ion-exchangeable state; OB: in organic macromolecular; CB: in carbonate; AS: in aluminosilicate; SF: in sulfide.

elements during combustion may be dominated by their occurrence mode in coal [48]. Chromium in SB (Shenbei) lignite mainly occurs in an organic form, while present as chromate in mixed PDS (Pingdingshan) bituminous coal [49]. The former mode might experience explosive volatilization, in which most of the chromium will be volatilized. So chromium emission in PM from the SB coal is higher than that from mixed PDS coal. The emission concentration of chromium in PM_1 from two coals is 4.8 mg/Nm^3 and 2.3 mg/Nm^3, respectively. Most of chromium concentrated in particles with diameter larger than 10 micrometers for PDS bituminous coal. Although the emission of chromium is not so high, the control is still important because of the toxicity of Cr (VI). Alumina, limestone and kaolinite have been documented that they are effective adsorbent for chromium during coal combustion in laboratory-scale fluidized-bed combustor [50].
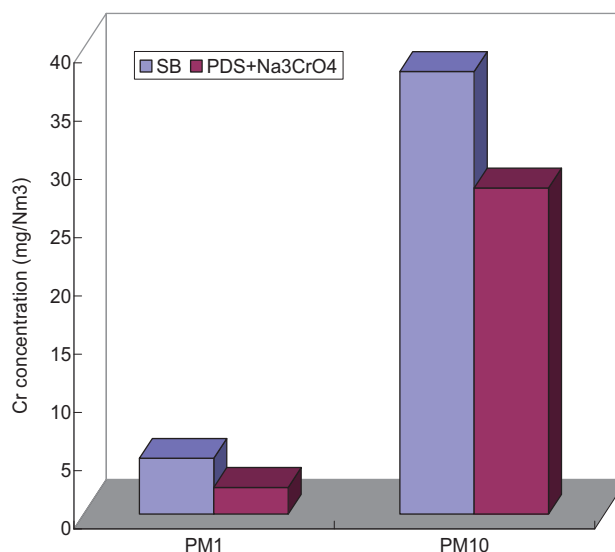
Figure 10. Emission of chromium during combustion of different coals.

10. SUMMARY

The concentration and distribution of PHTEs in Chinese coals were determined and evaluated. The average concentrations of most PHTEs in Chinese coals are close to that of U.S. coals. Most Shanxi coals and Shenfu coals contain low concentrations of PHTEs, but western Guizhou coals contain high contents of some PHTEs. The average values of Hg, F, As, and Cr in Chinese coals are 0.19, 131, 3.8, and 15 µg/g, respectively. The majority of mercury goes into flue gas during coal combustion and the emission of mercury from the coal-fired power plant is so high, up to 21.15 µg/Nm^3. The content of fluorine in flue gas of the coal-fired power plant is up to 2.7 mg/m^3. The concentration and distribution of fluorine in typical endemic fluorosis area in southwestern Guizhou has been evaluated and the fluorosis is likely caused by the combination of high fluorine coals and high-fluorine clays. The arsenic concentration in the stack gas from coal-fired power plant is low, only 2.5 µg/Nm^3, which is below the China Pollution control standard for hazardous waste incineration. Only few typical coal mines have the high content of arsenic and chromium. Emissions of arsenic and chromium during combustion of typical high-arsenic coal and high chromium lignite were investigated through drop tube furnace experiments. The emissions of the PHTEs are influenced by their occurrence modes in the coals and the conditions during coal combustion. Sorbents injection is an effective method to reduce the emission of the PHTEs during coal combustion.

ACKNOWLEDGMENT

REFERENCES

[1]   Swaine, D. J., Goodarzi, F. (1995). *Environmental Aspects of Trace Elements in Coal*. Kluwer Academic Publishing: Dordrecht, p 312.

[2]   Zhang, J., Ren, D., Zheng, C., Zeng, R., Chou, C.L., Liu, J. (2002). Trace element abundances in major minerals of Late Permian coals from southwestern Guizhou province, China. *International Journal of Coal Geology,* 53, (1), 55-64.

[3]   Finkelman, R. B., Orem, W., Castranova, V., Tatu, C. A., Belkin, H. E., Zheng, B., Lerch, H. E., Maharaj, S. V., Bates, A. L. (2002). Health impacts of coal and coal use: Possible solutions. *International Journal of Coal Geology,* 50, (1-4), 425-443.

[4]   Swaine, D. J. (2000). Why trace elements are important. *Fuel Processing Technology,* 65-66, 21-33.

[5]   Dai, S., Ren, D. (2006). Fluorine concentration of coals in China--An estimation considering coal reserves. *Fuel,* 85, (7-8), 929-935.

[6]   Belkin, H.E., Zheng, B.S., Zhou, D.X., Finkelman, R.B. (1997). In *Preliminary results on the geochemistry and mineralogy of arsenic in mineralized coals from endemic arsenosis areas in Guizhou province, P.R. China*, Fourteenth annual international Pittsburgh coal conference, Taiyuan, Shanxi, P.R. China, Taiyuan, Shanxi, P.R. China.

[7]   Yan, R., Lu, X., Zeng, H. (1999). Trace elements in Chinese coals and their partitioning during coal combustion. *Combustion Science and Technology,* 145, (1-6), 57-81.

[8]   Ren, D., Xu, D., Zhao, F. (2004). A preliminary study on the enrichment mechanism and occurrence of hazardous trace elements in the Tertiary lignite from the Shenbei coalfield, China. *International Journal of Coal Geology,* 57, (3-4), 187-196.

[9]   Ren, D., Zhao, F., Dai, S., Zhang, J., Luo, K. (2006). *Geochemistry of trace elements in coal*. Science Press: Beijing, China.

[10]   Querol, X., Alastuey, A., LopezSoler, A., Plana, F., FernandezTuriel, J. L., Zeng, R. S., Xu, W. D., Zhuang, X. G., Spiro, B. (1997). Geological controls on the mineral matter and trace elements of coals from the Fuxin basin, Liaoning Province, northeast China. *International Journal of Coal Geology,* 34, (1-2), 89-109.

[11]   Dai, S., Ren, D., Tang, Y., Yue, M., Hao, L. (2005). Concentration and distribution of elements in Late Permian coals from western Guizhou Province, China. *International Journal of Coal Geology,* 61, (1-2), 119-137.

[12]   Dai, S. F., Ren, D. Y., Zhang, J. Y., Hou, X. Q. (2003). Concentrations and origins of platinum group elements in Late Paleozoic coals of China. *International Journal of Coal Geology,* 55, (1), 59-70.

[13]   Song, D. Y., Qin, Y., Zhang, J. Y., Wang, W. F., Zhang, C. G. (2007). Concentration and distribution of trace elements in some coals from Northern China. *International Journal of Coal Geology,* 69, (3), 179-191.

[14]   Song, D. Y., Qin, Y., Wang, W. F., Zhang, J. Y., Zheng, C. G. (2007). Geochemistry and modes of occurrence of hazardous trace elements in the No. 11 coal seam, Antaibao surface mine, Shanxi Province. *Acta Geologica Sinica-English Edition,* 81, (1), 135-140.

[15]   Zeng, R. S., Zhuang, X. G., Koukouzas, N., Xu, W. D. (2005). Characterization of trace elements in sulphur-rich Late Permian coals in the Heshan coal field, Guangxi, South China. *International Journal of Coal Geology,* 61, (1-2), 87-95.

[16]   Huang, W., Yang, Y. (2002). Mercury in coal in China. *Coal Geology of China,* 14, (S), 37-40 (in Chinese with English abstract).

[17]   Streets, D. G., Hao, J., Wu, Y., Jiang, J., Chan, M., Tian, H., Feng, X. (2005). Anthropogenic mercury emissions in China. *Atmospheric Environment,* 39, (40), 7789-7806.

[18]   Chen, P., Tang, X. (2002). Fluorine in Coal of China. *Coal Geology of China,* 14, (z1), 25-28 (in Chinese with English abstract).

[19]   Luo, K., Ren, D., Xu, L., Dai, S., Cao, D., Feng, F., Tan, J. (2004). Fluorine content and distribution pattern in Chinese coals. *International Journal of Coal Geology,* 57, (2), 143-149.

[20]   Zhang, J., Zhao, Y., Ding, F., Zeng, H., Zheng, C. (2007). Preliminary study of trace element emissions and control during coal combustion. *Frontiers of Energy and Power Engineering in China,* 1, (3), 273-279.

[21]   Finkelman, R. B. (1993). Trace and minor elements in coal. In *Organic Geochemistry*, Engel, M. H.; Macko, S. A., Eds. Plenum Press: New York, USA, pp 593-607.

[22]   Swaine, D. J. (1990). *Trace elements in coal*. Butterworth Boston: London,UK, p 296.

[23]   Valkovic, V. V. (1985). *Trace elements in coal*. CRC Press, Boca Raton, IL, USA, p 520.

[24]   Mason, B. H., Moore, C. B. (1982). *Principles of geochemistry*. Wiley: New York, USA, p 344.

[25]   Zhao, Y., Zhang, J., Chou, C.L., Li, Y., Wang, Z., Ge, Y., Zheng, C. (2008). Trace element emissions from spontaneous combustion of gob piles in coal mines, Shanxi, China. *International Journal of Coal Geology,* 73, (1), 52-62.

[26]   Zhang, J. Y., Zheng, C. G., Ren, D. Y., Chou, C. L., Liu, J., Zeng, R. S., Wang, Z. P., Zhao, F. H., Ge, Y. T. (2004). Distribution of potentially hazardous trace elements in coals from Shanxi province, China. *Fuel,* 83, (1), 129-135.

[27]   Dai, S., Li, D., Ren, D., Tang, Y., Shao, L., Song, H. (2004), Geochemistry of the late Permian No. 30 coal seam, Zhijin Coalfield of Southwest China: influence of a siliceous low-temperature hydrothermal fluid. *Applied Geochemistry,* 19, (8), 1315-1330.

[28]   Dai, S., Ren, D., Hou, X., Shao, L. (2003). Geochemical and mineralogical anomalies of the late Permian coal in the Zhijin coalfield of southwest China and their volcanic origin. *International Journal of Coal Geology,* 55, (2-4), 117-138.

[29]   Dai, S., Ren, D., Ma, S. (2004). The cause of endemic fluorosis in western Guizhou Province, Southwest China. *Fuel,* 83, (14-15), 2095-2098.

[30]   Dastoor, A. P., Larocque, Y. (2004). Global circulation of atmospheric mercury: a modelling study. *Atmospheric Environment,* 38, (1), 147-161.

[31]   Merdes, A. C., Keener, T. C., Khang, S.J., Jenkins, R. G. (1998). Investigation into the fate of mercury in bituminous coal during mild pyrolysis. *Fuel,* 77, (15), 1783-1792.

[32]   Skodras, G., Natas, P., Basinas, P., Sakellaropoulos, G. P. (2006). Effects of pyrolysis temperature, residence time on the reactivity of clean coals produced from poor quality coals. *Global NEST Journal,* 8, (2), 89-94.

[33]   Iwashita, A., Tanamachi, S., Nakajima, T., Takanashi, H., Ohki, A. (2004). Removal of mercury from coal by mild pyrolysis and leaching behavior of mercury. *Fuel,* 83, (6), 631-638.

[34]   Guffey, F. D., Bland, A. E. (2004). Thermal pretreatment of low-ranked coal for control of mercury emissions. *Fuel Processing Technology,* 85, (6-7), 521-531.

[35]   Wang, M., Keener, T. C., Khang, S.J. (2000). The effect of coal volatility on mercury removal from bituminous coal during mild pyrolysis. *Fuel Processing Technology,* 67, (2), 147-161.

[36]   Guo, X., Zheng, C. G., Xu, M. H. (2007). Characterization of mercury emissions from a coal-fired power plant. *Energy and Fuels,* 21, (2), 898 -902.

[37]   Lei, C., Yufeng, D., Yuqun, Z., Liguo, Y., Liang, Z., Xianghua, Y., Qiang, Y., Yiman, J., Xuchang, X. (2007). Mercury transformation across particulate control devices in six power plants of China: The co-effect of chlorine and ash composition. *Fuel,* 86, (4), 603-610.

[38]   Hall, B., Schager, P., Weesmaa, J. (1995). The homogeneous gas phase reaction of mercury with oxygen, and the corresponding heterogeneous reactions in the presence of activated carbon and fly ash. *Chemosphere,* 30, (4), 611-627.

[39]   Norton, G. A., Yang, H., Brown, R. C., Laudal, D. L., Dunham, G. E., Erjavec, J. (2003). Heterogeneous oxidation of mercury in simulated post combustion conditions. *Fuel,* 82, (2), 107-116.

[40]   Dunham, G. E., DeWall, R. A., Senior, C. L. (2003). Fixed-bed studies of the interactions between mercury and coal combustion fly ash. *Fuel Processing Technology,* 82, (2-3), 197-213.

[41]   Zheng, B. S., Cai, R. G. (1988). Study of fluorine content in coal of China. *Chinese Journal of Control of Endemic Diseases,* 32, (21), 70-72.

[42]   Ren, D., Zhao, F., Wang, Y., Yang, S. (1999). Distributions of minor and trace elements in Chinese coals. *International Journal of Coal Geology,* 40, (2-3), 109-118.

[43]   Zheng, C., Xu, M., Zhang, J., Liu, J. (2002). *Emission and Control of trace elements during coal combustion.* Hubei Science and Technology Press: Wuhan, p 234.

[44]   Zheng, B., Ding, Z., Huang, R., Zhu, J., Yu, X., Wang, A., Zhou, D., Mao, D., Su, H. (1999). Issues of health and disease relating to coal use in southwestern China. *International Journal of Coal Geology,* 40, (2-3), 119-132.

[45]   Zhang, J. Y., Ren, D. Y., Zhu, Y. M., Chou, C. L., Zeng, R. S., Zheng, B. S. (2004). Mineral matter and potentially hazardous trace elements in coals from Qianxi Fault Depression Area in southwestern Guizhou, China. *International Journal of Coal Geology,* 57, (1), 49-61.

[46]   Guo, X., Zheng, C. G., Xu, M. H. (2004). Characterization of arsenic emissions from a coal-fired power plant. *Energy and Fuels,* 18, (6), 1822-1826.

[47]   Tessier, A., Campbell, P. G. C., Blsson, M. (1979). Sequential extraction procedure for the speciation of particulate trace metals. *Analytical Chemistry,* 51, (7), 844-851.

[48]   Querol, X., Juan, R., Lopez-Soler, A., Fernandez Turiel, J. L., Ruiz, C. R. (1996). Mobility of trace elements from coal and combustion wastes. *Fuel,* 75, (7), 821-838.

[49]   Wei, F. (2005). Study on sub-micron particle formation and agglomeration mechanism from coal combustion. Huazhong University of Science and Technology, Wuhan.

[50]   Lu, J.D., Yu, L.Y., Zhang, J. (2004). Study of control with adsorbents on trace elements during fluidized bed combustion. *Zhongguo Dianji Gongcheng Xuebao/Proceedings of the Chinese Society of Electrical Engineering,* 24, (3), 187-192.

Chapter 2

New Estimations of Coal Clarkes: World Averages for Trace Element Contents in Coal

M. P. Ketris and Ya. E. Yudovich

Institute of Geology, Komi Scientific Center, Ural Division of the
Russian Academy of Sciences, 167023 Syktyvkar, Morozova st., 100, ap. 49. Russia.
Corresponding author. Tel: + 7 821 2 31 19 24
E-mail address: yudovich@geo.komisc.ru (Y.E. Yudovich, office)
EYuYa@Yandex.ru (Y.E.Yudovich, home)

Abstract

Coal Clarke values are the average trace element contents in the World coals. The modern table of coal Clarkes is presented, based on new calculation using very large information (thousands analyses of coal and coal ashes for trace elements). For each trace element seven figures were calculated: average content in hard coals and their ashes; average content in brown coals and their ashes; average content in all coals and their ashes; coal affinity index (or "coalphile index") = average content in all ashes/Clarke values of sedimentary rocks. The coal Clarkes presented are the scientific base for many geochemical comparisons and issues.

Keywords: coal, geochemistry, trace elements, world average contents (coal Clarke values).

https://telegram.me/Geologybooks

1. INTRODUCTION

In 1923, the famous Russian geochemist A.E.Fersman[1] introduced the term "clark" (= Clarke, in English), in honor of the prominent American scientist, one of the founders of geochemistry, F.W. Clarke (who worked many years as Chief Chemist at U.S. Geol. Survey), who first calculated average composition of various rocks, and later, the earth's crust.

1.1. Meaning of the Russian Term "Clarke"

Fersman gave the name "Clarke" to the *average content of given chemical elements in the Earth's crust and also in the hydrosphere.* This term very soon took root in Russian literature, but, up to now, has been nearly unknown to Western researchers[2]. With time, however, a sense of the term was strongly extended: many other geochemical averages were named as "Clarkes", for example, "Clarkes of granites", "Clarkes of basalts", "Clarkes of sedimentary rocks", etc., including "coal Clarkes", i. e. *average trace element contents in the World coals.* For example, coal Clarke of Ge is 3.0 ± 0.3 ppm (hard coals) and 2.0 ± 0.2 ppm (brown coals) [Yudovich and Ketris, 2004].

1.2. Some history

Some attempts to calculate coal Clarkes for several trace elements are known. The first calculations were made by the famous Norwegian-German geochemist, another "father" of geochemistry[3], V.M. Goldschmidt, in the beginning of the 1930s. Goldschmidt firstly organized systematical analyses of some European coals for trace elements, using modern (for that time) analytical methods – emission spectrographic and X-ray fluorescence analyses [Goldschmidt, 1935]. Goldschmidt's estimations of trace element average contents for "ordinary" (common) and "enriched" *coal ashes* were, for many consequent years, the "compass" for geochemists dealing with coal[4].

At a later time, we can find some averages in studies by Krauskopf [1955] and Bethell [1962]. First more wide (including most trace elements and most World coals) calculation of coal Clarkes was performed in the USSR [Yudovich et al., 1972]. Later, Valkovič's estimations (based on U.S. figures but including some others) came into the world [Valcovič, 1983].

---

[1] Fersman was the first, who gave a lecture course "Geochemistry" (Moscow, 1912). Later, he created many fundamental proceedings on geochemistry, for example, "Pegmatites" (1931), "Geochemistry" (4 volumes, 1933–1939), etc.

[2] That is why, in our articles in As or Hg in coal [Yudovich and Ketris, 2005a, b], the terms like *"coal Clarke of As"* must have a special explanation for the Western reader!

[3] Two other "fathers" of geochemistry, new science of 20th century, were Russian scientists, V.I. Vernadski and his follower, A.E. Fersman.

[4] Only after World War II, when mass analyses of coal for trace elements started, it became clear that most of Goldschmidt's figures were not typical for the World coals but were strongly over-estimated [Yudovich et al., 1985].

It is of note, Valkovič [1983] used *frequency histograms* for statistical evaluations of averages. It is a very useful working procedure, and it was independently widely used in our new calculations, published by Yudovich et al., [1985]. The estimations based on thousands of analyses, were made as four figures for each trace element: (1, 2) for hard coals and their ashes, and (3,4) for brown coals and their ashes. These new coal Clarke figures (with detailed explanation of *stepped calculation procedure*), were cited in Russian, East European, Indian and Chinese studies for many years.

Unfortunately, it was in a Russian-language book, and for this reason, our figures remained practically unknown to most Western researchers. In 1990, D.Swaine published his excellent outline on trace elements in coal [Swaine, 1990]. He tried to embrace all the World coals, but his outline has very big omissions of the East (Soviet) Block coals. It is of note, Swaine's world estimation were, as a rule, rough interval values; for example, as 10–40 ppm (and not, say, as 16±5 ppm, where ±5 ppm means statistical standard deviation).

In the last decades of the 20th century, great changes appeared in coal geochemistry, due to environmental problems caused by wider consumption of coal in electric power plants. This enlarged demand for coal created abundant new geochemical studies, with analyses of coal on *toxic elements,* such as Be, Hg, Cd, Pb, As, Sb, Se, Cr, Mn, U and some others. Besides, coal mining was sharply increased in developing countries, such as Spain, Turkey, Greece, China, India, Brazil, and Peru, Nigeria, among others. These coals are analyzed using wide international cooperation, for example, with the U.S. Geological Survey, having modern analytical equipment.

Therefore, the amount of coal-trace-element figures has extremely increased. The U.S. Geological Survey created so called "Coal Quality (COALQUAL) Database" [Bragg et al.,, 1998], with more than 13,000 analyses for most trace elements. At last, in recent decades, due to mostly Russian researchers (V.V. Seredin, S.I. Arbuzov and some others), the old problem became again actual: coal as industrial resource of trace elements (Sc, Ge, REE, Nb, Ta, Re, Au and platinum group elements, PGE) [Arbuzov et al., 2000, 2003; Zharov et al., 1996; Seredin and Spirt, 1995].

All the latter work necessitated a new coal Clarkes calculation.

1.3. Coal-basis and ash-basis Clarkes

Up to 1970–1980, coal was mostly not directly analyzed for trace elements but through an analysis of coal ash. Standard coal ashing was performed at 750 $^{\circ}$C (in USA and many West countries), or at 850 $^{\circ}$C (in former USSR and now in Russia). It is well known that some elements may be almost fully (Hg, I, Br), or partly (Ge, Mo, etc.) volatilized by *high-temperature* ashing. Trace element loss may be minimized by *low-temperature* ashing (~130–150 $^{\circ}$C) by means of radio frequency exposure in oxygen plasma [Gluskoter, 1965]. This excellent method, is, however, time-consuming and for this reason is not widely acceptable.

So, up to the end of the 1980s, the content of trace element in coal (*coal-basis content*) was obtained by recalculation from the content in ash (*ash-basis content*). Such recalculation may lead to underestimation of coal-basis figures, and, as a result, to underestimation of coal-basis Clarkes.

During the last decades of the 20th century, several *direct methods* of coal analysis were introduced in coal geochemistry, and first of all – INAA, instrumental neutron activation

analysis. So, many directly obtained coal-basis figures appeared in the literature. Now a new opportunity appears – to recalculatie coal-basis figures to ash-basis ones.

If the analysis of coal ash was earlier simply "a technical tool" (because a direct analysis of coal was too hard and unreliable a procedure), have we any need for the "ash Clarkes" today? – Yes, we have such need: for the calculation of important geochemical values, "coal affinity indexes" (or "coalphile coefficients), as we will discuss below.

1. 4. "Coal-affinity" (coalphile) indexes

Goldschmidt [1935] first calculated the "enrichment coefficients" of coal ash, by comparison of element content in coal ash and Earth's crust Clarke value. For example: the Earth's crust As Clarke value was assumed as 5 ppm, and As content in As-rich ashes was determined as 500 ppm; so, enrichment coefficient was 500/5 = 100.

Later Yudovich [1978] used coal ash Clarke values (instead of "enriched ashes") and Clarkes of sedimentary rocks for such calculation. These figures (enrichment coefficients) were called *"typomorph coefficients"*, and were widely cited in Russian and Bulgarian literature[5]. At last, this poor term was substituted for *coalphile coefficient (index), or coal affinity index* [Yudovich and Ketris, 2002].

What does a coal affinity index mean? – *It shows, how efficiently coal acted as a geochemical barrier for trace elements, during all its geologic history.* The more coal concentrated trace elements from environment compared with sedimentary rocks, the greater would be the coal affinity index. A researcher could compare coal affinity indexes for different elements in given coal field, given coal basin, or province; for the coals of different rank; and for the same coal field (basin, province) but for different elements. For example, As coal affinity index is 50 ppm/11 ppm = about 5 [Yudovich and Ketris, 2005a], and Hg coal affinity index is 0.75 ppm /0.05 ppm = 15 [Yudovich and Ketris, 2005b]. So, Hg is threefold more coalphile element than As.

2. CALCULATION METHOD

All calculation procedures may be divided into several stages [Ketris and Yudovich, 2002]:

1) analytical data collection; 2) preliminary data processing and formation of basic tables; 3) using basic tables, formation of sufficiently homogeneous statistical data samples (data assemblages), and calculation of sample-averages; 4) using sample-averages, plotting of frequency histograms and evaluation of the Clarke value, as median.

---

[5] See numerous papers provided by Greta Eskenazy, Jordan Kortensky, Stanislav Vassilev and some others.

2.1. Analytical data collection

This is very time-consuming and the hardest part of all the work. We collected coal-analyses data nearly 45 years. From the literature, it is necessary to extract the following data: (a) coal locality (country, basin, coal field (deposit), coal seam; (b) coal rank and geological age; (c) ash yield on dry matter (Ad, %); (d) how units are used (%, ppm, mg/g etc.), and basis – coal or ash; (e) number of coal specimens (analyses). Unfortunately, only in a few instances could we obtain all the information! Often, a part of the information needed was lacking. For example, if the coal locality was lacking, such analytical data have to be rejected.

The stratigraphic data were needed in order to not include different-age coals within a united statistical sample. We need also to know: if the data collected belong to coal beds or *coal inclusions?* The latter may be extremely enriched in trace elements [Yudovich, 1972, 2003], and the use of such figures may sharply change the sample average. The other important question arises: was the given coal influenced by secondary processes? Such data may also distort a homogeneity of the statistical sample.

In literature prior to 1980, a simultaneous analysis presentation on an ash- and on a coal basis was rare; so, we needed to know an ash yield, in order to obtain the missing figure by recalculation. If an ash yield was lacking, we tried to evaluate it using all the available information sources (reference books, special monographs, etc.)

In many Soviet papers (where in fact, many thousand spectrographic analyses were averaged!), the number of analyses was lacking. In such instances, we needed to get only some "conditional" number of analyses. This means that our "number of analyses" was sometimes not enough accurate information (tends to be underestimated).

2.2. Preliminary data processing and formation of basic tables

Preliminary data processing may start even during data collection: the individual figures (belonging to each coal specimen) being averaged – if such average is lacking in original text. *As elemental information units we assumed a coal bed- or coal-field averages*. For example, if there were several figures for one coal bed, we calculated the coal-bed average and put it in the basic table. If there were the figures for three coal beds, these three figures were put in the basic table, etc. If the set of analyses had very sharp anomalies (for example, one-two order of magnitude more than coal geochemical background), such figures, as a rule, were not included in average calculation.

As a result, for each element we created two basic tables, for brown and hard coal, such as the following:

Hard (brown) coals

Country	Coal basin (province, region, area)	Coal field, bed	Geologic age	n	A^d	E, ppm on coal basis	E, ppm on ash basis	Reference (source of data)

In such a table, *n* means the number of analyses, A^d – ash yield, %, *E* – a chemical element.

2.3. Stepped averaging and final median calculation

After basic tables were formed, we could obtain the *assemblage of statistical samples (and their averages),* which would be used for the final Clarke calculation. Each statistical sample embraces the analyses of a coal basin or large coal area (region). All the analyses included are to be averaged. If the collected data allowed, we constructed two–four statistical samples for big coal basins (provinces) – for example, for some industrial regions (within Donetsk basin, Ukraine), coal fields, or other geographical units. The number of such "intra-basinal" statistical samples nearly corresponded with coal geological resources of the given basin.

The full concept involves stepped (successive) averaging, from minor to large: one coal bed $\Rightarrow$ several coal beds $\Rightarrow$ coal field (deposit) $\Rightarrow$ coal area (several coal fields) $\Rightarrow$ coal basin or province $\Rightarrow$ totality of the coal basins (= assemblage of statistical samples), i.e., Clarke value totality, comprising several dozen random (statistical) samples representing many thousands of analyses – Figure. 1.
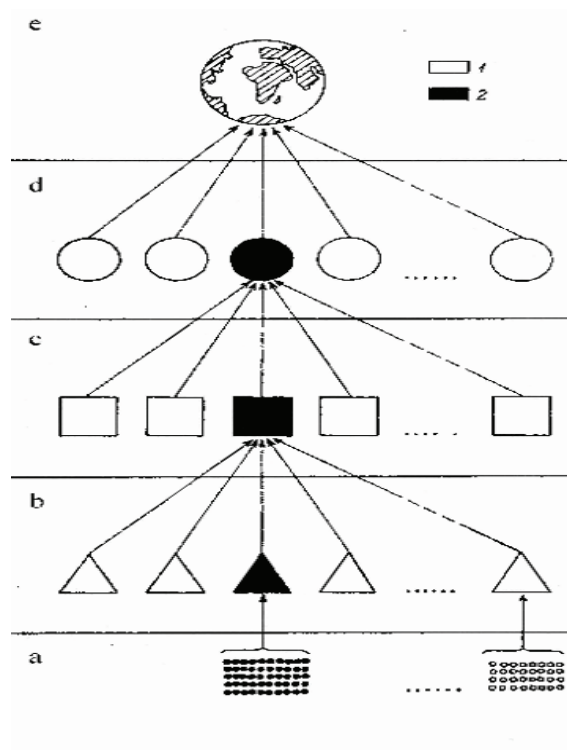
1 – any one object of the given step (level); 2 – specific object of this step (level), for which are shown its lower (composing) components.

Figure 1. A sketch showing a procedure of stepped averaging [Tkachev and Yudovich, 1975, p. 124]. The steps (levels): a – initial, the analyses of coal specimens; b – coal beds; c – coal fields; d – coal areas (basins, provinces), e – final totality of the areas (= global totality of statistical samples).

For example, As coal Clarke value was calculated using totality, consisting of 119 statistical samples (and about 21,000 analyses) – for hard coals, and 66 statistical samples (and about 21,000 analyses) – for brown coals [Yudovich and Ketris, 2005a]. On the steps, the averages were calculated as arithmetic mean (if the sample was more homogeneous), or as median (if the sample was less homogeneous).

Following our good experience in black shale geochemistry [Yudovich and Ketris, 1994], we use a sample totality median *(Me)* as a Clarke value estimation. As an estimation of the median accuracy (σ_{Me}) we use the value

$$\sigma_{Me} = (Q_3 - Q_1) / 2 \sqrt{n}, \tag{1}$$

where Q_1 and Q_3 – two distribution quartiles, corresponding ¼ and ¾ of the cumulative frequency.

Although a Clarke value (a median) is estimated analytically, it is very instructive to plot a frequency histogram. The distribution of trace element contents in coal is, as a rule, log-normal; that is why, for plotting the logarithmic scale is often used. The plot character could suggest: how "good" is the totality studied. If the histogram is "right" (for example – near to log-normal), the totality could be attested as a "good" one (Figure 2); in the opposite case, we can think the totality is too small and not representative enough for natural coals (Figure 3). In such a case, we need to get some new analyses for better Clarke estimation. In fact, the elements with "right" histograms nearly "do not react" upon new, supplementary analyses – their Clarke value could only vary little (as a rule – not more than within accuracy range of median, i.e. $\pm 1\sigma_{Me}$). On the contrary, some rare, poorly studied elements (such as Au, Pd, Tl, In, Ta, Te, Cl, I and some others) may in the future change their Clarkes more appreciably.
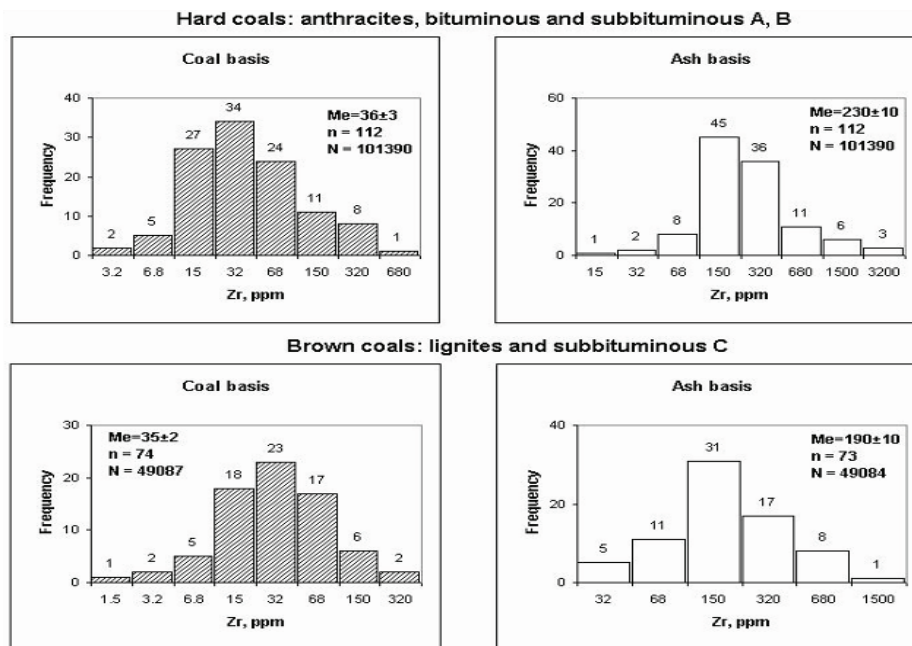
Figure 2. An example of the "appropriate" plot: zirconium. N – number of analyses, n – number of statistical samples, Me – the median of statistical samples.
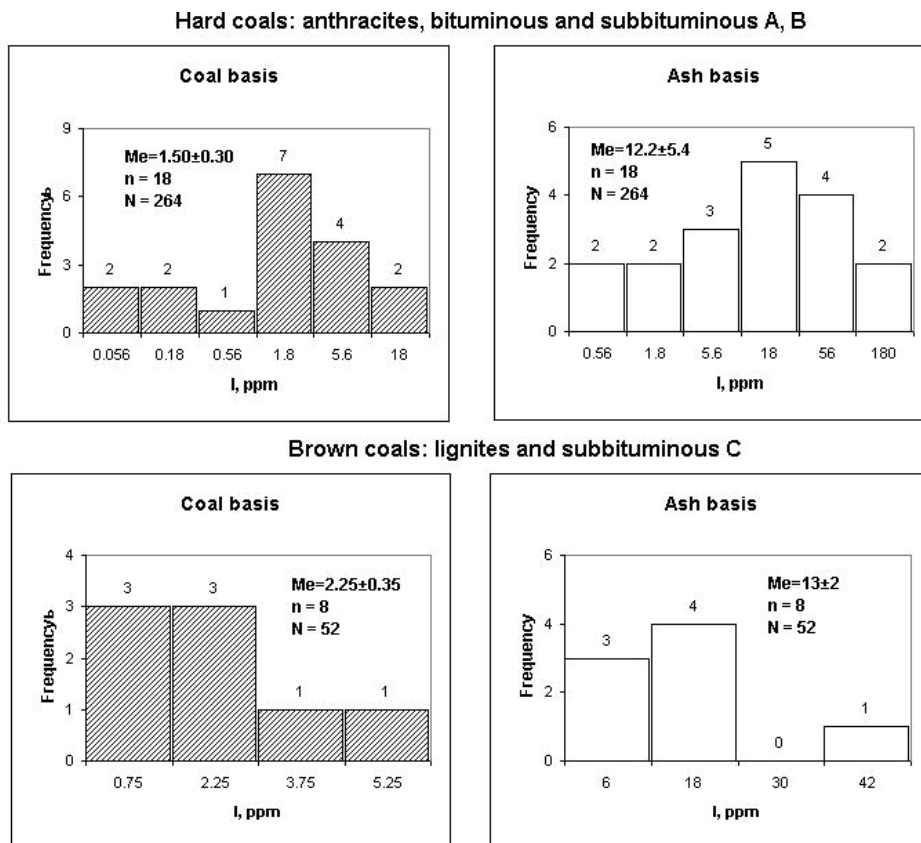
Figure 3. An example of the irregular plot: iodine.

The other (well known) histogram characteristic is its σ_{Me} value compared with *Me* value. If these figures are comparable (very large variance of the statistical distribution), the Clarke value is, of course, not very reliable if $\sigma_{Me} \ll Me$, the opposite is true. For example, average content of Pd in brown coal ashes was estimated only over eight statistical samples (nearly 50 analyses) as 0.066 ± 0.027 ppm. Such a figure appears to be too high and dubious, accounted for Chinese Pd-rich coals contribution. It is no doubt, as the sample assemblage is extended, the Pd Clarke in coal will be changed.

For the REE, one other criterion exists: the picture of the standardized (normalized) curve. As an example, Tm has some peak on such curve, that distinguishes Tm from the neighboring REE. It may mean that the Tm coal Clarke is now overestimated, and may be amended in the future, as more information becomes available.

3. CALCULATION RESULTS

The results of the calculations are shown in table 1.

https://telegram.me/Geologybooks

Table 1. New estimations (ppm) of the coal Clarke values for trace elements.
(Calculations by Marina P. Ketris, 2005)
CAI – coal affinity indexes ("coalphile indexes")
CAI = average element concentration in coal ash/Clarke value in sedimentary rocks

Elements	Coals			Coal ashes			Clarke value of sedimentary rocks	CAI
	Brown	**Hard**	**All**	**Brown**	**Hard**	**All**		
Typical cation-forming lithophile elements								
Li	10±1.0	14±1[6]	12	49±4	82±5	66	33	2.0
Rb	10±0.9	18±1	14	48±5	110±10	79	94	0.84
Cs	0.98±0.10	1.1±0.12	1.0	5.2±0.5	8.0±0.5	6.6	7.7	0.86
Tl	0.68±0.07	0.58±0.04	0.63	5.1±0.5	4.6±0.4	4.9	0.89	5.5
Sr	120±10	100±7	110	740±70	730±50	740	270	2.7
Ba	150±20	150±10	150	900±70	980±60	940	410	2.3
Cation- and anion-forming elements with stable valency								
Be	1.2±0.1	2.0±0.1	1.6	6.7±0.5	12±1	9.4	1.9	4.9
Sc	4.1±0.2	3.7±0.2	3.9	23±1	24±1	23	9.6	2.4
Y	8.6±0.4	8.2±0.5	8.4	44±3	57±2	51	29	1.8
La	10±0.5	11±1	11	61±3	76±3	69	32	2.2
Ce	22±1	23±1	23	120±10	140±10	130	52	2.5
Pr	3.5±0.3	3.4±0.2	3.5	13±2	26±3	20	6.8	2.9
Nd	11±1	12±1	12	58±5	75±4	67	24	2.8
Sm	1.9±0.1	2.2±0.1	2.0	11±1	14±1	13	5.5	2.4
Eu	0.50±0.02	0.43±0.02	0.47	2.3±0.2	2.6±0.1	2.5	0.94	2.7
Gd	2.6±0.2	2.7±0.2	2.7	16±1	16±1	16	4.0	4.0
Tb	0.32±0.03	0.31±0.02	0.32	2.0±0.1	2.1±0.1	2.1	0.69	3.0
Dy	2.0±0.1	2.1±0.1	2.1	12±1	15±1	14	3.6	3.9
Ho	0.50±0.05	0.57±0.04	0.54	3.1±0.3	4.8±0.2	4.0	0.92	4.3
Er	0.85±0.08	1.00±0.07	0.93	4.6±0.2	6.4±0.3	5.5	1.7	3.2
Tm	0.31±0.02	0.30±0.02	0.31	1.8±0.3	2.2±0.1	2.0	0.78	2.6
Yb	1.0±0.05	1.0±0.06	1.0	5.5±0.2	6.9±0.3	6.2	2.0	3.1
Lu	0.19±0.02	0.20±0.01	0.20	1.10±0.10	1.3±0.1	1.2	0.44	2.7
Ga	5.5±0.3	6.0±0.2	5.8	29±1	36±1	33	12	2.8
Ge	2.0±0.1	2.4±0.2	2.2	11±1	18±1	15	1.4	11

---

6 The ± figures mean ±1σMe, and numbers of analyses are omitted due to scarcity of the place. The reader can request these numbers.

Table 1. (continued)

Elements	Coals			Coal ashes			Clarke value of sedimentary rocks	CAI
	Brown	Hard	All	Brown	Hard	All		
Cation- and anion-forming elements with stable valency								
Ti	720±40	890±40	800	4000±200	5300±200	4650	3740	1.2
Zr	35±2	36±3	36	190±10	230±10	210	170	1.2
Hf	1.2±0.1	1.2±0.1	1.2	7.5±0.4	9.0±0.3	8.3	3.9	2.1
Th	3.3±0.2	3.2±0.1	3.3	19±1	23±1	21	7.7	2.7
Sn	0.79±0.09	1.4±0.1	1.1	4.7±0.4	8.0±0.4	6.4	2.9	2.2
V	22±2	28±1	25	140±10	170±10	155	91	1.7
Nb	3.3±0.3	4.0±0.4	3.7	18±1	22±1	20	7.6	2.6
Ta	0.26±0.03	0.30±0.02	0.28	1.4±0.1	2.0±0.1	1.7	1.0	1.7
Mo	2.2±0.2	2.1±0.1	2.2	15±1	14±1	14	1.5	9.3
W	1.2±0.2	0.99±0.11	1.1	6.0±1.7	7.8±0.6	6.9	2.0	3.5
U	2.9±0.3	1.9±0.1	2.4	16±2	15±1	16	3.4	4.7
Typical anion-forming lithophile elements								
B	56±3	47±3	52	410±30	260±20	335	72	4.7
P	200±30	250±10	230	1200±100	1500±100	1350	670	2.0
F	90±7	82±6	88	630±50	580±20	605	470	1.3
Cl	120±20	340±40	180	770±120	2100±300	1440	2700*	0.53
Br	4.4±0.8	6.0±0.8	5.2	32±5	32±9	32	44	0.73
I	2.3±0.4	1.5±0.3	1.9	13±2	12.2±5.4	12.6	1100	0.01
Metals-sulfophiles								
Cu	15±1	16±1	16	74±4	110±5	92	31	3.0
Ag	0.090±0.020	0.100±0.016	0.095	0.59±0.09	0.63±0.10	0.61	0.12	5.1
Au, ppb	3.0±0.6	4.4±1.4	3.7	20±5	24±10	22	6.0	3.7
Zn	18±1	28±2	23	110±10	170±10	140	43	3.3
Cd	0.24±0.04	0.20±0.04	0.22	1.10±0.17	1.20±0.30	1.2	0.80	1.5
Hg	0.10±0.01	0.10±0.01	0.10	0.62±0.06	0.87±0.07	0.75	0.068	11
In	0.021±0.002	0.040±0.020	0.031	0.11±0.01	0.21±0.18	0.16	0.043	3.7
Pb	6.6±0.4	9.0±0.7	7.8	38±2	55±6	47	12	3.9
Bi	0.84±0.09	1.1±0.1	0.97	4.3±0.8	7.5±0.4	5.9	0.26	23
Nonmetals-sulfophiles								
As	7.6±1.3	9.0±0.7	8.3	48±7	46±5	47	7.6	6.2
Sb	0.84±0.09	1.00±0.09	0.92	5.0±0.4	7.5±0.6	6.3	1.2	5.3
Se	1.0±0.15	1.6±0.1	1.3	7.6±0.6	10.0±0.7	8.8	0.27	33

Elements	Coals			Coal ashes			Clarke value of sedimentary rocks	CAI
	Brown	**Hard**	**All**	**Brown**	**Hard**	**All**		
Elements-siderophiles								
Cr	15±1	17±1	16	82±5	120±5	100	58	1.7
Mn	100±6	71±5	86	550±30	430±30	490	830	0.59
Co	4.2±0.3	6.0±0.2	5.1	26±1	37±2	32	14	2.3
Ni	9.0±0.9	17±1	13	52±5	100±5	76	37	2.1
Pd	0.013±0.006	0.001±0.002	0.0074	0.066±0.027	0.007±0.011	0.037		
Ir	0.002±0.006	0.001±0.0003	0.002	0.013±0.031	0.007±0.003	0.010		
Pt	0.065±0.018	0.005±0.003	0.035	0.22±0.04	0.038±0.018	0.13		

* Cl Clarke value in sedimentary rocks – according to (Ronov et al., 1980).

The last table column represents coal affinity indexes, calculated using our coal Clarkes and modern weighed Clarkes for sedimentary rocks [Grigoriev, 2003], calculated by Grigoriev using the Ronov's sedimentary shell model [Ronov, 1980; Ronov et al., 1990]. It is of note, the coal affinity indexes are calculated on the base of averaged ash Clarkes, i.e. (element Clarke in hard coal ash + element Clarke in brown coal ash)/2. For example, lithium: (49 ppm + 82 ppm)/2 ≈ 66 ppm; 66 ppm/33 ppm = 2 (coal affinity index).

4. DISCUSSION

The data in table 1 allow us to make some comparisons and to raise issues.

1. The values from 1985 and 2005: a comparison

Due to new analytical methods and the great information gain, the 2005 Clarke estimations for some elements were appreciable changed compared with 1985 estimations. Among these elements:

Li, Rb, Ag, Ti, Nb, As, Cl – for all the coals; Cu, Be, B, Sc, Th – for brown coals; Hg – for hard coals.

Other Clarke estimates also changed but less, only within 20–40 %: Ga, Y, Yb, P – for all the coals; Ba, B, Cd, Co – for brown coals; Zn, Sc, Mo, Mn – for hard coals.

Finally, many Clarke values have kept within the calculation accuracy range: Sr, Ge, Zr, Sn, V, F, Cr, Ni – for all the coals; Hg, Zn, Mo, Mn – for brown coals; Rb, Be, B, Cu, Th – for hard coals.

2. Comparison of brown and hard coal Clarkes

Such a comparison allows analysis of coal rank influence on coal geochemistry. Coal "metamorphism" is the thermal epigenetic process, involving hot brines and fluids influencing coal beds. These processes not only changed coal organic matter, but may greatly change the trace element contents by means of their input or output [Yudovich, 1978; Yudovich and Ketris, 2002]. However, this (obvious) issue is far from all. It is known that, *in general*, hard coals are Paleozoic, and brown ones – are Mesozoic and Cenozoic. This means that in some instances the geochemical difference "brown coals vs. hard coals" may be *primary,* accounted for the large initial difference of Paleozoic and Mesozoic-Cenozoic coal-forming flora!

As seen from the table 1, brown coals are enriched in B, U, and Mn. For all three elements, one can suggest their output during thermal metamorphism of the coal organic matter. More elements are enriched in hard coals compared with brown ones. Weak enrichments show Co, Ge, V, Pb, Se, and strong ones – Rb, Be, Zn and Ni. Only for the evident sulfophile elements (such as Pb, Se, Zn), such enrichments could be caused by hydrothermal input connected with coal metamorphism. However, for litho- and siderophile elements (such as Be, Cr, Co, Ni) such explanation appears to be dubious. It is not excluded that primary coal-formed flora acted here as actual factor of difference [Yudovich, 1978]. Such (non-trivial) conclusion could highlight some problems dealing with the biosphere evolution.

3. Coal affinity indexes

By analyzing ranges of the coalphile indexes (the latest column in the table 1), one can divide the elements in four groups:

(a) *non-coalphile elements* (coal affinity indexes are <1) : I, Cl, Mn, Br, Rb, Cs;

(b) *weakly or moderately coalphile elements* (coal affinity indexes range from 1 to 2): Ti, Zr, F, Cd, V, Ta, Cr, Y, Li, P;

(c) *coalphile elements* (coal affinity indexes range from 2 to 5): Ni, Hf, Sn, La, Co, Ba, Sc, Nb, Sr, Th, Ga, Cu, REE, Zn, W, Au, In, Pb, U, B, Be;

(d) *highly coalphile elements* (coal affinity indexes >5): Ag, Sb, Tl, As, Mo, Ge, Hg, Bi, Se.

The greater the coal affinity index, the greater the contribution of an *authigenic fraction* of given trace element (represented by organic or micro-mineral forms), and the less is one of a *clastogenic fraction* (represented by macro-mineral forms, for example, silicatic.

Due to the new (weighed) Clarkes of sedimentary rocks [Grigoriev, 2003], some earlier estimations of coal affinity have drastically changed. So, after the calculation of real evaporites contribution in sedimentary shell [Ronov, 1980; Ronov et al., 1990], the weighed Clarkes of halogens Cl, Br, and I in sedimentary rocks increased. This results in a corresponding sharp decrease in their coal affinity indexes: halogens "have transformed" from highly coalphile elements [Yudovich et al., 1985; Yudovich and Ketris, 2006b] to non-coalphile ones. Also, the coalphile indexes of Au, Cd, Y, V, U, Cr have unexpectedly lowered, and, in turn, ones of Tl, Zn, Hf and In have unexpectedly raised.

The extreme coalphile index of Bi appears to be very doubtful; the same could be said about Se. Such strange figures could be accounted for errors in the Clarke values for sedimentary rocks (and not for coal Clarkes errors?). It is of note, these elements are often not analyzed due to analytical difficulties; see, for example, for Se: [Yudovich and Ketris, 2006a]. This may be a factor.

5. CONCLUSION

Coal Clarke values are the average trace element contents in the World coals. The modern table of coal Clarkes is presented here, calculated by the authors (two preceding tables were published in 1972 and 1985), based on a very large amount of information (thousands analyses of coal and coal ashes for trace elements).

The coal Clarkes are the scientific tool for many geochemical comparisons and issues. First of all, coal Clarkes allow to compare given (studied) coal with World geochemical background, and to conclude: is the coal "normal" (near to the Clarke level), enriched or, in turn, impoverished in given trace element. Such comparisons are known of great importance *for toxic elements* (such as Hg, As, Se, Be etc.), as well *for valuable elements,* having industrial potential (such as Ge, Ga, Sc, Re, REE, PGE, etc.).

Other important values have the "coal affinity indexes" (coalphile indexes) of trace elements (average element content in coal ash/element Clarke in sedimentary rocks). These indexes show how efficiently coal acted as a geochemical barrier for trace elements, during all its geologic history. A comparison of coalphile indexes with each other allow to display a contribution of coal authigenic matter (organics, sulfides etc.) in coal inorganics. On the other hand, the comparison of the coalphile indexes of the same element but in different coals allow to see some non-obvious peculiarities of the coal fields or coal basins (see, for example, numerous Bulgarian papers for reference).

ACKNOWLEDGMENTS

REFERENCES

Arbuzov, S.I., Ershov, V.V., Potseluev, A.A., Rikhvanov, L.P. (2000). *Trace Elements in the Kuznetsk Basin Coals. Kemerovo*, 248 pp. (in Russian).

Arbuzov, S.I., Ershov, V.V., Rikhvanov, L.P., Usova, T.Yu., Kyargin, V.V., Bulatov, A.A., Dubovic, N.E. (2003). *Trace Element Potential of the Minusinsk Basin Coals*. Novosibirsk, 347 pp. (in Russian).

Bethell, F.V. (1962). The distribution and origin of minor elements in coal. Brit. Coal Util. *Res. Ass. Monthly Bull*. 26 (No. 12), 401–429.

Bragg, L.J., Oman, J.K., Tewalt, S.J. Oman, S.L., Rega, N.H., Washington, P.M., Finkelman, R.B. (1998). *Coal quality* (COALQUAL) database: version 2.0. Open-File Rep. (U.S. Geol. Surv). 97–134 (unpaginated CD-ROM).

Grigoriev, N.A. (2003). Average content of chemical elements in rocks composing the upper Earth's crust. *Geokhimiya [Geochemistry],* 7, 785–792 (in Russian).

Goldschmidt, V.M. (1935). Rare elements in coal ashes. *Ind. Eng. Chem.*, 27 (No. 9), 1100–1102.

Gluskoter, H.J. (1965). Electronic low-temperature ashing of bituminous coal. *Fuel*, 44 (No.4), 285–291.

Ketris, M.P., Yudovich, Ya. E. (2002). *Calculation procedure of the coal Clarkes*. Lithogenes i geochimiya osadochnykh formatsiy Timano-Ural'skogo regiona. Syktyvkar, 111–117. (Tr. In-ta geol. Komi nauch. tsentra UrO Ross. Acad. nauk, vyp. 111). [Proc. Inst. Geol. Komi Sci. Center, issue 111] (in Russian).

Krauskopf, K.B. (1955). *Sedimentary deposits of rare metals*. Econ. Geol., 50th ann. vol. Pt. 1, 411–463.

Ronov, A.B. (1980). *Sedimentary Shell of the Earth*. Moscow, Nauka ["Science" Pub. House], 80 pp. (in Russian).

Ronov, A.B., Yaroshevsky A.A., Migdisov A.A. (1990). *Chemical Composition of the Earth's Crust and Geochemical Balance of Main Elements*. Moscow, Nauka ["Science" Pub. House], 192 pp. (in Russian).

Seredin, V.V., Shpirt, M.Y. (1995). Metalliferous coals: a new potential source of valuable trace elements as by-products. *Coal Science*. (Eds. J.A.Pajares, J.M.D.Tascón). Amsterdam: Elsevier, 1649–1652. (8th ICCS Proc. Vol. II).

Swaine, D.J. (1990). *Trace Elements in Coal*. London, Butterworths, 278 pp.

Tkachev, Yu.A., Yudovich, Ya.E. (1975). *Statistical Processing of Geochemical Data: Methods and Problems. Leningrad,* Nauka ["Science" Publ. House], 233 pp. (in Russian).

Yudovich, Ya. E. (1978). *Geochemistry of Fossil Coals*. Leningrad, Nauka ["Science" Pub. House], 262 pp. (in Russian).

Yudovich, Ya. E. (1972). *Geochemistry of Coal Inclusions in Sedimentary Rocks*. Leningrad, Nauka ["Science" Pub. House], 84 pp. (in Russian).

Yudovich, Ya. E. (2003). Coal inclusions in sedimentary rocks: a geochemical phenomenon. A review. *Int. J. Coal. Geol.*, 56, 203–222.

Yudovich, Ya. E., Ketris, M.P. (2005a). Arsenic in coal: a review. *Int. J. Coal. Geol.*, 61, 141–196.

Yudovich Ya. E., Ketris M.P. (2004). Germanium in Coal. Syktyvkar, Komi Sci. Center Ural. *Div. Rus. Acad. Sci.*, 216 pp. (in Russian).

Yudovich, Ya. E., Ketris, M.P. (2006a). Chlorine in coal: a review. *Int. J. Coal. Geol.*, 67, 127–144.

Yudovich, Ya. E., Ketris, M.P. (2005b). Mercury in coal: a review. Pt. 1 and 2. *Int. J. Coal. Geol.*, 2005, 62, 107–134 and 135–165.

Yudovich, Ya.E., Ketris, M.P. (2002). *Inorganic Matter of Coals*. Ekaterinburg: URO RAN [Ural Division of the Russian Acad. Sci.], 422 pp. (in Russian).

Yudovich, Ya. E., Ketris, M.P. (2006b). Selenium in coal: a review. *Int. J. Coal. Geol.*, 67, 112–126.

Yudovich, Ya.E., Ketris, M.P. (1994). *Trace elements in Black Shales*. Ekaterinburg: Nauka ["Science" Pub. House], 304 pp. (in Russian).

Yudovich, Ya. E., Ketris, M.P., Merts, A.V. (1985). *Trace Elements in Fossil Coals*. Leningrad, Nauka ["Science" Pub. House], 239 pp. (in Russian).

Yudovich, Ya.E., Korycheva, A.A., Obruchnikov, A.S., Stepanov, Yu.V. (1972). Average contents of trace elements in fossil coals. *Geokhimiya [Geochemistry],* 8, 1023–1031. (in Russian)

Valkovič V. (1983). *Trace Elements in Coal*. Boca Raton, Fla. Chem. Rubber Co. Press. Vol. 1, 210 pp. Vol. 2, 281 pp.

Zharov, Yu.N., Meytov, E.S., Sharova, I.G. (compilers). (1996). Valuable *and Toxic Elements in Russian Raw Coals: a Reference Book*. Nedra ["Entrails" Publ. House], Moscow, 239 pp. (in Russian).

Chapter 3

FLUORINE IN COAL: A REVIEW

Ya. E. Yudovich and M.P. Ketris*

Institute of Geology, Komi Scientific Center,
Ural Division of the Russian Academy of Sciences,
167023 Syktyvkar, Morozova Street, 100, Ap. 49, Russia

ABSTRACT

The World average F content in coals (coal Clarke of F) for the hard and brown coals are, respectively, 82±6 and 90±7 ppm. On an ash basis, these contents are greatly increased and are 580±20 and 630±50 ppm, respectively. As an average, F content in ash is 605 ppm (lower than the Clarke value for sedimentary rocks, 650 ppm). F is, on average, not a coalphile element.

Nevertheless, some coals are known to have a F content one order of magnitude more than the coal Clarke level. In general, these are either high-ash or high-phosphorus coals, with both the features often combined. This (and some other) features show some similarity between F and P geochemistry in coal. In particular, F, like P, seems to be depleted from the buried peat during diagenesis toward hosting rocks.

No less than three F-forms (modes of occurrence) may be present in coal: phosphatic (F_{phosph}), silicatic (mostly F_{clay}), and organic (F_{org}). It can be suggested that F_{clay} dominates in high-ash coals, F_{phosph} in high-P coals, and in ordinary coals with moderate ash yield and near-Clarke P and F contents, F_{org} may be dominant. There is no information concerning chemical species of the F_{org} form. However, by an analogy with P, it seems to exist as an F compound with C_{aorg}, not with organics itself.

It is yet not clear, if F is in authigenic CaF_2 and what could be a contribution of such a form to total F content. It seems not to be excluded that such form may have genetic relation with F_{org} (diagenetic or catagenetic transformation, $F_{org} \Rightarrow F_{min}$?).

There are no clear relationships concerning F enrichment in coals. Plausible hypothesis is that F might be syngenetically enriched in coals (a) in paralic (near-marine) coals, and (b) in coals formed with a volcanic activity background. On the other hand,

---

* Corresponding author. Y.E.Yudovich
Tel.: + 7 821 31 19 24.
E-mail address: yudovich@geo.komisc.ru

some F anomalies (like that in some Alabama coals) may resulted from epigenetic hydrothermal F-input, during (or after) coal metamorphism.

Keywords: Fluorine; Coal; Geochemistry, Environmental impact.

1. INTRODUCTION

Some notes concerning F presence in coalified plant residues appeared in the middle of the 19th century (see references in Dässler et al., 1973). However, the first paper on F in coal was, probably, Lessing's (1934), in which he noticed a strong corrosion of the ceramic fillings in gas-generating installations. He supposed that it was due to fluorine and, in reality, he found nearly 80 ppm F in ammonium waters. He concluded that F could have originated only from coal. Qualitative analyses showed that F was contained in all the British coals studied; a coal dust enriched in fusain contained much more F than a lump coal. McIntyre et al.,'s (1985) microprobe study suggested F enrichment in fusinite. Fluorine was only weakly extracted by water but was appreciably extracted by 1 % NaOH. Lessing (1934) concluded that the main mode of F occurrence in coal is fluorspar, CaF_2. As the ratio F/Cl in one sample was the same as in sea water, he supposed that F entered coal from marine waters in the peat stage, in the same manner as $Cl^{1.}$

Unfortunately, due to analytical problems, we still know little about F geochemistry in coal. In ashing, much F may be volatilized as HF or SiF_4; the retention of F in ash needs much CaO, MgO, or K_2CO_3 in ash (either natural or added), at careful low-temperature ashing. In addition, the older analytical method of atomic emission spectral analysis does not work for F determination; however, F-analysis based on the CaF^+ molecular band is a rather new technique, although not in wide use. Besides, this procedure needs some CaO addition into ash. Many F-determinations made before end of 1980's by means of the ASTM method (bomb oxidation following ion-selective electrode [ISE] F-determination), resulted in appreciable underestimates due to incomplete decomposition of the F-bearing minerals. Godbeer and Swaine (1972) showed that such an underestimation ranged from 28 up to 72 %; in general, the error increased along with ash yield of coal analyzed (Godbeer, 1987; Martinez-Tarazona et al., 1994). So, for the reliable F-analysis, some intricate chemical procedures are needed (such as pyro-hydrolytic etc.), as discussed by Swaine (1990, p. 109, 112–113).

Coals can now be analyzed for F by means of PIGE method (proton-induced gamma-ray/X-ray emission analysis), described, for example, in Wong and Robertson (1993). This modern procedure gets good results (see, for example, some figures in Hower et al. (1997).

2. FLUORINE IN ENVIRONMENT

Fluorine has a high marine-affinity, with its Clarke value in sea water being as high as 1300 mg/L, much more than in fresh waters (100 mg/L). In the hypergene zone, F is mobile

in acid environments but can be trapped with pH increase on three geochemical barriers: Ca-bearing, phosphatic, and silicatic. Thus, in near-neutral and alkali milieus, dissolved F- may be extracted by carbonates (resulting in CaF2), phosphates (entering apatite structure), and clay (entering hydromica structure).

Fluorine has a high marine-affinity, with its Clarke value in sea water being as high as 1300 mg/L, much more than in fresh waters (100 mg/L). In the hypergene zone, F is mobile in acid environments but can be trapped with pH increase on three geochemical barriers: Ca-bearing, phosphatic, and silicatic. Thus, in near-neutral and alkali milieus, dissolved F- may be extracted by carbonates (resulting in CaF2), phosphates (entering apatite structure), and clay (entering hydromica structure).

Ivanov (1994, p. 274), based on more than 3000 analyses of sedimentary rocks from the Transbaikal region Russia, found the average F content in terrigenous continental strata to be 170 ppm, i.e. much less than in marine strata (300 ppm), reflecting the "marine-affinity" of fluorine. This has also been observed in pelitic fractions from the Mesozoic strata in the Tadzhik depression: 440 ppm (continental strata) versus 1200 ppm (marine strata) (Pachadzhanov, 1981)

In wet landscapes, F actively moves; its contents in surface and ground waters are related to the organic matter contents (Perel'man, 1972, p. 207), suggesting that F forms soluble complexes with organics. Waters in arid and volcanic landscapes are enriched in F. Arid-landscape waters concentrate F due to evaporation, and volcanic-derived waters concentrate F due to acid exhalations, such as HF. As important F source for water may be an erosion of the F-bearing sedimentary rocks, such as phosphates. However, not all volcanic waters are enriched in F; for example, in the Kamchatka peninsula (Russia), volcanic hydrotherms show near-background F contents in the range of 1.4–3.0 mg/L. Similar F concentrations are known in USA and New Zealand Cl-Na thermal waters (Trukhin, 2003) Although the data are scattered, Ivanov (1994, p. 278–279) noted a general regularity: F contents in water are positively correlated with a Na/Ca ratio.

Fluorine has a rather low bio-affinity: its bio-affinity index being lower than for chlorine. It is unclear what a biological role F plays in plants. However, in animals, such role is well known: F is an obligatory constituent of the bone skeletons, teeth, nails, plumes, hair and horns, entering biogenic F-OH-apatite.

It is worth noting, that according to Kowalevsky (1991 and others), an appreciable part of F in plants (up to 84 % on dry basis) is water-soluble; implying that such F may be leached in the peatbog.

There is an important question: may organics in marine or continental sediments scavenge F? Even in the modern Belorussian monograph (Evtukhovich and Lukashev, 2001) there are no figures on F content in peats. Only for the *peaty-soils* (horizons A_1 and B_{1-2}), some data are reported (p. 48): on average 63 ppm (the range 23–91 ppm) and 56 ppm (29–132 ppm). Pore waters of Recent carbonaceous sediments in the Black Sea contain more F than near-bottom sea water (Shishkina et al., 1969); indicating a F-input from the sediment, rather than an accumulation. Along with sediment diagenesis, F content in pore water (due to water metamorphization) decreases; however, F goes out as CaF2, not as Forg.

---

[1] There were romantic times of the geochemistry: the issues based on only one analysis were taken by the scientific community as quite valid data!

3. AN ESTIMATION OF COAL CLARKE VALUE OF F

In 1985, coal Clarke values (World averages) of F were calculated based only on 370 analyses, as follows (Yudovich et al., 1985, p. 133):

- 80±20 and 110±30 ppm for lignites and bituminous coals,
- 500–1000 ppm for their ashes.

In 2004, the Clarke value for F in coal was recalculated by Marina Ketris. The detailed calculation procedure was published elsewhere (Ketris and Yudovich, 2002), but the main idea is outlined here.

The concept involves *stepped (successive) averaging*, from minor to large: one coal bed ⇒ several coal beds ⇒ coal field (deposit) ⇒ coal area (several coal fields) ⇒ coal basin or province ⇒ totality of the coal basins, i. e. Clarke value totality, comprising several dozen random samples representing thousands of analyses. As a rule, the median is used for the Clarke estimation because it is very stable statistical parameter, only little influenced by large sample dispersion.

Modern estimations of F Clarke values are based on approximately 115 random samples, derived from nearly 11250 analyses (Figure 1):

- 90 ± 7and 82 ± 6 ppm for brown and hard coals,
- 630 ± 50 and 580 ± 20 ppm for their ashes

In comparison with the 1985 figures, the F Clarkes for some hard coals have been lowered (110 ⇒ 82 ppm) and for lignites (brown coals) – some increased (80 ⇒ 90 ppm). However, averages for ashes were estimated more correctly; though, they may be underestimated because of above-noted F loss in coal ashing.

In most coal basins, average F contents are rather near to the Clarke values. There is some relation between F content and ash yield of the coals, more correctly – with their hydromicas contribution, as main carriers (sites) of F in coal.

According to Swaine (1990, p. 109), world average F content is 150 ppm, ranging from 20 to 500 ppm. It is obvious now that this figure was overestimated. The background F estimation of Kler (1988, c. 68) for the former USSR coals was 100 ppm, much closer to our Clarke value. Based on 2469 analyses of World lignites, Bouška and Pešek (1999) calculated average content as 58 ppm F, and for Miocene lignites of the North Czech basin – 110 ppm (56 analyses).

Miocene lignites to the east of Elba River (Germany) contain 6–50 ppm F, and Eocene ones to the west – 2–178 ppm (Dässler et al., 1973). In the commercial bituminous coals of the Appalachian region, USA, the average F content is 80 ppm (Kopp et al., 1989). In Australian coals, average F contents strongly vary from 20 to 300 ppm, on average 110 ppm. In bituminous coals of New South Wales, F content ranged (over 90 % of the analyses) from 15 up to 458 ppm (on average 119 ppm). Queensland coals have an averageof 108 ppm (21–243 ppm). Brown coals contain on average in the range from 42–130 ppm but Victoria lignites are quite poor in F: on average 8–18 ppm, in the range from 4 up to 79 ppm (Godbeer and Swaine, 1987).
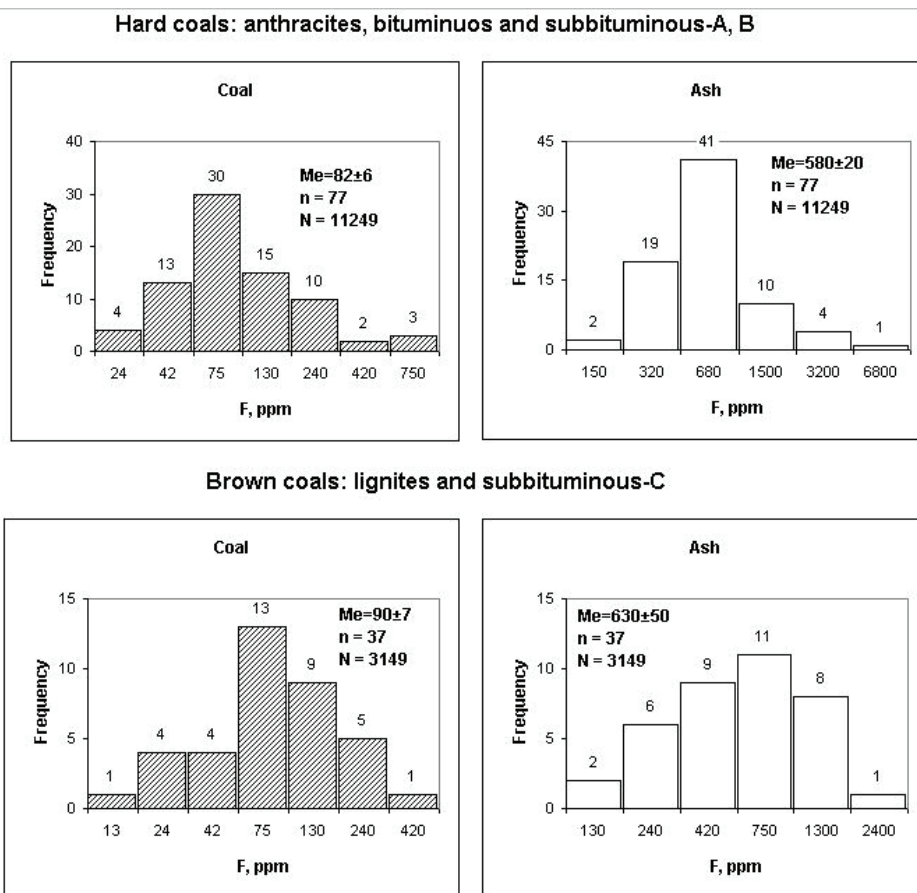
Figure 1. Frequency distribution of F in World coals. N – number of analysis, n – number of random samples, Me – a median content.

According to 448 analyses of some Chinese coals, the background A contents are from 20 up to 300 ppm, with arithmetic mean of 140 ppm (Huang, Che, Tang, 2003, p. 45).

4. "COAL AFFINITY" INDEX (COALPHILE INDEX) OF F

The Clarke value of concentration (the term of V.I.Vernadski) of F in coal ash (i.e. coalphile index or *"coal affinity index"* [2]) is 605 ppm (average F content in coal ash) / 650 ppm (F Clarke value in sedimentary rocks) = 0.93.

Therefore, according to modern F coal Clarke value, fluorine is *non-coalphile element* (see monograph by Yudovich and Ketris, 2002, for details).

---

[2] It is of note, that "coal affinity" is not the same thing as "organic affinity"! Coal affinity means an element affinity to all authigenic coal matter (organics and inorganics, including sulphides, carbonates, silicates etc., and excluding extraneous terrigenous or volcanogenic mineral clastics).

5. SOME COALS ENRICHED IN F

The coals notably enriched in F above the coal Clarke level are known in Russia, Greece, China, USA, and Canada. However, there is no doubt that such coals are widespread much more over the World, but were not analyzed up to date.

5.1. Russia: Various Coals

In the Jurassic Irkutsk basin coals, the highest F content is in the Cheremkhovo coal field: up to 1000 ppm in coal and up to 6000 ppm in coaly partings. Vyasova et al., (1989, p. 746) noted that Cheremkhovo and Voznesensk coals are much more enriched in F than many coals of the former USSR, USA, and former East Germany, and *"fit to the probably dangerous concentration level of 0.05 %"*

In drillholes penetrating coal beds of the east part of the Ulughem basin (Tyva Republic), F content reaches up to 300 ppm (and 54 ppm on average). In the Ulug seam, Mezhegeisk and Elegetsk coalfields, F content is up to 500 ppm (only 20 ppm on average) (Bykadorov et al.,, 2002).

Some F-anomalies reaching up 5500 ppm (ash basis) are found in Gusinoozersk Lower Cretaceous subbituminous coals, south Transbaikal region. F-enrichment seems to be related with "*known manifestations and deposits of fluorspar in near and distant bordering of the* (Gusinoozersk) *depression"* (Osokin, 1993, p. 117).

Some lignites of the Pacific Coast are enriched in F. For example, in the Shkotov deposit (Uglovsk basin), there are F-anomalies ranging from 300–600 ppm (Sedykh, 1997, c. 173). In the Ge-bearing Miocene Pavlovsk lignites (Khankaisk basin), some analyses showed up to 500 ppm F (Medvedev et al., 1997, c. 190). In the REE-bearing lignites, F contents may be as much as 1000–2000 ppm (Seredin et al., 1997, 1999; Seredin and Shpirt, 1995).

5.2. Greece: Neogene Lignites

F content in ash is negatively correlated with ash yield: $r(A^d – F_A{}^d) = – 0.95$. Such relation is explained as F bonding with coal organics (Iordanidis, 2002). At the same time, F is positively correlated with Sr; this may have two explanations: (a) Sr is also bonded with coal organics; (b) Sr and F enter apatite but the ashes of low-ash lignites contain more apatite than the ashes of high-ash lignites (?).

5.3. China: Various Coals

Some Chinese coals are F-bearing. For example, eight (typical?) coals have high geometric average: 729 ppm F (ranging from 100 up 3600 ppm) (Ren et al., 1999). Compared to the average F content for Chinese coals of 248 ppm (based on 328 analyses), coals from Fuling prefecture, Sichuan province have on average 866 ppm (up to 1488 ppm), and in Baoching, Xianxi prefecture – 1411 ppm (up to 2350 ppm) (Zheng et al., 1999).

Enhanced F contents in coals are found in Quanxi Fault Depression Area, SW Guizhou province, where Upper Permian coals (12 samples) have on average 693 ppm F (Zhang et.al., 2004, p. 55–56), or 2390 ppm F calculated on an ash basis[3]. Here, three areas are contoured with coals containing more than 1000 ppm F. In particular, in Liuzhi area, average F content is 1797 ppm, and the highest – 2544 ppm (Zhang et al., 2004, p. 58).

5.4. USA: Alabama Pennsylvanian Coals

The main part of coals enriched in F compared to US average level is in Warrior basin, in the marginal south of the Appalachian basin. The highest F content reaches here up to 4900 ppm and relates to later hydrothermal processes (Goldhaber et al., 1997; Oman et al., 1995).

5.5. Canada: Cretaceous coals

In British Columbia subbituminous coals, on average over 30 coal beds, F content is enhanced compared to coal Clarke level – 518 ppm (Grieve and Goodarzi, 1993).

6. MODE OF FLUORINE OCCURRENCE IN COAL

One can think that F modes of occurrence are different in coals with near-coal Clarke F-content level, and in coals enriched in F.

At near-Clarke F-contents, the contributions of various F-sites, such as phosphatic, silicatic, and organic, may be commensurable. By this, low values of the P/F ratio may indicate the F_{org} site, as well a dominant F_{sil} site in hydromicas (Beising and Kirsch, 1974), or in other clay minerals. Swaine hypothesizes even such exotic accessory F-carriers (contributors) as tourmaline and topaz (Godbeer and Swaine, 1987; Swaine, 1990).

For example, in Utah coals, the contents of P are 70–180 ppm and of F – from 53 up to 132 ppm, at a P/F ratio ranging from 0.7 up to 2.0 (Bradford, 1957). If F-apatite has the highest (as possible) F content, the contribution of such phosphatic F (F_{phosph}) will be 0.2xP. A contribution of terrigenous silicatic F (F_{clay}) can be estimated assuming that such fraction remains in ash, by high-temperature ashing (800 °C). At last, a contribution of organic F (F_{org}) can be calculated by the difference between total F and the sum of (F_{phosph} and F_{clay}).

The calculations show that F in Utah coal is a sum of three F-forms with F_{org} as a dominant form: F_{phosph} = 24–28 %, F_{clay} = 20–25 %, and F_{org} = 56–47 %. Note that such calculations are only very approximate because of a set of suggestions were made: a) all the P is in Ca-phosphate; b) Ca-phosphate is fluorapatite with maximal possible F-content; c) in the ash (800°C), only F_{clay} remains. Actually, there may be no Ca-phosphate at all, or it could have other F-content; the ash may capture a part of F_{org} or F_{phosph} (by reaction of F with CaO).

---

[3] Our calculation based on average ash yield of Permian (25 analyses) and Triassic (10 analyses) coals of 29.0 and 14. 5 %, respectively.

The suggestion (a) and (b) would overestimate F_{org} contribution, whereas the suggestion (c) would underestimate it.

Finkelman (1980) found fluorapatite in the majority of the 79 coal beds examined (from USA and other countries). However, the amount of fluorapatite is, in general, too minor to be a real F-contributor in coal. As a result, Finkelman concluded:

*"The problem of the mode of occurrence of F remains unresolved. It is possible that this element has a very complex mode, occurring in apatites, fluorites, amphiboles, clays and micas. In individual coals one form may dominate over the others" (*Finkelman, 1980, p. 154).

In two Kuzbas coals as much as 87 % F_{org} is estimated (Khrustaleva et al., 2001, p. 40), but this figure seems to be some questionable.

In general, one can suppose that a contribution of the silicatic F_{clay} must be the highest in high-ash coals with abundant hydromicas, F_{phosp} highest in high-ash phosphate-bearing coals, and F_{org} highest in low-phosphorus coals with low and moderate ash yield.

6.1. Silicate Form

Illites from German bituminous coals contain from 600 to 1600 ppm F. This means that 5 % of such illite in coal may result in, for example, 50 ppm F, that is rather near to the observed F contents in these coals (15–120 ppm). It is of note that some part of F (nearly 3 %) is water-leachable and can be attributed to a sorbed ion-exchange form, F_{sorb}. The water-extract becomes alkali (pH = 9) probably due to OH^- leaching from coal along with F (Beising and Kirsch, 1974).

In Rhine (German) lignites with 3–28 ppm F, most of the F is in illite; however, the regression line "F in coal – ash yield" does not start from zero ash and has an absolute term. This may indicate some F_{org} presence.

In "Vostochny" (East) brown coal open pit (East Siberia), average ash yield is 8.34 % with 550 ppm F (coal basis). The same F content is found in the overburden silty clays with nearly 5 % C_{org}. These rocks consist of quartz (32 %), mixed-layer clay minerals (27 %), kaolinite (21 %), feldspars (10 %), siderite (4.5 %), dolomite (2 %), calcite (1 %), and magnetite (2.5 %) (Shpirt et al., 1994). The carrier of F is likely to be only mixed-layer illite-montmorillonite minerals, of, possibly, pyroclastic origin. Equal F contents in coal and its roof means that coal has to contain a substantial part of F_{org} form.

Among the silicatic F-contributors may be also non-clay minerals. For example, in the non-magnetic fraction of the Pennsylvanian Waynesburg seam low-temperature ash (West Virginia), olive-green grains of hornblende with ~0.2 % F were found. Finkelman (1980, p. 42) argued that the F-contribution of hornblende is far more than that of the rarer apatite.

Some F-enrichment is found in the most heated (coked) contact coal in Colorado, USA (Finkelman et al., 1992). Here, F seems to be contained in silicatic form.

6.2. Phosphatic Form

A presence of F_{phosph} may be supposed by P/F ratio and some correlations, as well as estimated by means of stepped leaching.

https://telegram.me/Geologybooks

For example, in above mentioned relatively F-enriched low-ash Rhine lignites, fluorapatite may be the real F-contributor. The calculation shows that at 2 % P_2O_5 in ash, fluorapatite may result in up to 170 ppm F in ash (Beising and Kirsch, 1974).

The first studies of Australian coals (Phosphorus…, 1963) showed large variations of the P/F ratio (despite of general positive F-P correlation), which shifted from the 4.9 value (fluorapatite) to more (up to 6.6) or (rarer) lesser side (up to 4.6). The ratios more than 4.9 were explained by the contribution (along with fluorapatite) of hydroxyl-apatite. For the P/F <4.9 ratios no explanations have been offered. However, at least two explanations are possible: a presence of the part F as F_{sil} (in micas), or as F_{org}. In two high-ash coaly shales, much P (1.94–2.03 %) and F (3930–4860 ppm) were found. It is obviously, this is due to fluorapatite, because P/F ratios are 4.9 and 4.7.

The experiments with Australian F-bearing coals showed that Ca-phosphatic F may be fully extracted by the ion-exchange resin at heating up to 80 ^{o}C. From other phosphates (Fe, Al), fluorine can be extracted to a lesser extent, and F_{org} cannot be extracted. For example, from the low-ash Bulli coal seam, New South Wales (A^d = 6.7 %, P = 0.94%, F = 100 ppm), neither P nor F were extracted, and from other coals, no more than 30 % F were, on average, extracted (Phosphorus…, 1963).

6.3. Fluorite Form

Large excess F above P may imply fluorite presence, as proposed by Lessing (1934), and is assumed concerning some South African coals (Kunstmann et al., 1963).

Theoretically, CaF_2 may be formed during coal metamorphism due to Ca^{2+} and F^- interaction, both being liberated from the brown coal organics. Besides, in weathered coals, epigenetic fluorite may be, perhaps, present. If these processes operated, so a contribution of fluoritic F (F_{fl}) must be lesser in low-rank coals than in high-rank ones.

Besides, primary biogenic form, F_{bio}, may be, theoretically, also retained in coal. In ash of the so-called "phyto-schlichs" (the concentrate of the phytoliths, extracted from the living plants), containing 1–10 % F, very large fluorite particles, up to 0.2–0.5 mm, were found (Kowalevsky and Prokopchuk, 1999, p. 103).

6.4. Organic Form?

Finkelman (1980) considered only mineral forms of F in coals. F in natural environments has only anion F^- which appears to be not bonded with negatively-charged humic organics. However, it is well-known that peats and some coals may be enriched in P and Cl, which are also only anionic species. At least for P in peats, it is found that it bonds not with the peat-organics but with organic-peat Ca (i.e. Ca_{org}) (Ivanov, 1962). On the other hand, F may not be a "true" organic (F_{org}), not in F-organics chemical compounds but rather only sorbed on the organic matter surface (F_{sorb}). For example, in the fusain from a US coal, by means of XPS-method (X-ray photo-electronic spectroscopy), positive F–C correlation was found and was explained as an indication of F_{org} form (McIntyre et al., 1985). However, by analogy with results obtained for Cl (Huggins and Huffman, 1995), only organics-sorbed F (not firmly organic-bound) should be present.

An organic form of F always "appears" in our interpretations if the known (or supposed) mineral forms of F seem to be insufficient for the total F amount. For example, the F enrichment in low-ash coals may indicate organic F.

7. FACTORS AFFECTING FLUORINE DISTRIBUTION

The distribution of F in the given coal bed is influenced mostly by the ash yield, and in some high-F coals – also by P-content, due to appearance of the F_{phosph} form. Two other factors (coal petrographic composition and position of a bench within coal bed column) are usually masked by the two former factors.

7.1 Ash Yield

Fluorine entering clay matter depends on positive correlation «F in coal[4] – A^d". Such data are known for coals of Russia, Germany, Spain, and USA.

7.1.1. Russia: Eastern Donbas and Irkutsk Basin
In the statistical sample of the 65 Eastern Donbas bituminous coals, an exponential regression equation was obtained:

$$F\ (ppm) = 91.03\ A^d\ (\%)\ exp\ (0.01062\ A^d,\%)$$

Calculated average F content (107 ppm) very good matches to the analytically determined value of 109 ppm for the 240 samples (Kizilstein, 2002, p. 111–112).

In Jurassic Irkutsk basin coals, F content in high-ash tailings was 1.5–2 times than in raw coals. In the Voznesensk coalfield, F is enriched the 1.7–1.8 g/cm³ fraction, especially in high-ash raw coals. These relations, and a positive "F in coal – A^d" correlation in Cheremkhovsk and Voznesensk coals, allow the conclusion: "*in general, fluorine is bound with the mineral part of coal*" (Vyasova et al., 1989, p. 747).

7.1.2. Germany: Pennsylvanian Ruhr Coals
In bituminous coals containing from 15 to 120 ppm F, a strong positive correlation «F in coal – A^d» is found, as well as F–K_2O and F–Al_2O_3 correlations, resulting from F entering illite. In ash, F contents have a rather minor range of 600–900 ppm (Beising and Kirsch, 1974).

7.1.3. Spain: Pennsylvanian Asturian Coals
Study of 69 bituminous and anthracite coals showed strong positive correlation of «F in coal – A^d» in gross coal samples as well in sink-float fractions (Martinez-Tarazona et al., 1994). In low-ash fractions (A^d <3 %), F contents are <100 ppm, whereas in high-ash ones (A^d >60 %) they reach up to 800 ppm. Nearly the same F contents (700–800 ppm) are

---

[4] All the figures are on whole coal basis if other is not specified.

observed in coaly shales with an ash yield of more than 60 %. The ratio P/F is far less than for fluorapatite (4.9), sometimes it is as low as 0.5, therefore, it is obvious that apatite is not the primary F-carrier. The regression line «F in coal – A^d» goes to zero, therefore, F_{org} form seems to be absent. All these data suggest that illite is the main F-carrier.

7.1.4. USA: Pennsylvanian Central Appalachians Coals

Using the U.S. Geological Survey Database Bragg (et al., 1998), we examined the correlations «A^d, % – F, ppm in coal» and «A^d, % – F, ppm in ash (calculated)». Altogether, 63 coal beds and nearly 1300 F determinations (and approximately the same number of P determinations) were studied, for coal beds in Virginia, West Virginia, and Kentucky. For small-body statistical samples (5–15 analyses), the data were directly plotted; for more numerous (>20 analyses) – the data were previously grouped over 2-, 3-, 4- or 5 %- intervals of ash-yield, and the averaged data were plotted. In general, several types of plots were obtained – Figure 2 and Table 1.

Table 1. Typization of the "F–ash" correlations, for central Appalachian coals

Plot subtype	Description	Coal beds	Comment
Type I. F-contents (*ash basis*) of coals with the least ash yield are much more than of coals with the greatest ash yield[5]. F-contents (*coal basis*) do not correlate with an ash yield, or positively correlate. There are three subtypes:			
Subtype Ia	F-contents (*ash basis*) sharply monotone decrease along with ash yield increase; F-contents (*coal basis*) show no correlation with ash yield, or the correlation exists – linear or non-linear (with intermediate extremes)	Kentucky: Richardson and Peach Orchard.	No correlation "F–P" is observed
Subtype Ib	F-contents (*ash basis*) fast decrease along with ash yield increase from the beginning and further again increase but far not reaching the values of low-ash coals; F-contents (*coal basis*) show in general linear positive correlation (and rarer non-linear)	Tennessy: Big Mary; West Virginia: Beckley, Sewell (including Virginia); Kentucky: Fire Clay, Blue Gem, Jellico, Hazard.	More than 50 % beds show positive correlation "F–P"
Subtype Ic	F-contents (*ash basis*) show the same picture but **with intermediate maximum** *in rather ash-enriched coals*; F-contents (*coal basis*) show mostly non-linear positive correlation	Virginia: Upper Banner, Lowe; West Virginia: Stockton, Campbell Creek, Eagle, Winifrede, Bens Creek, Coalburg, Pocahontas-4 (including Virginia); Kentucky: Lily, Hazard-7, Unnamed, Alma (including West Virginia)	40 % beds show positive correlation "F–P"

---

[5] These terms are only relative because, in general, rather low ash yield of the Appalachian coals. For example, "low-ash" means there up to 6 %, "moderate-ash" – 6–12 % and "high-ash" – more than 12 % ash yield.

Table 1. Continued

Plot subtype	Description	Coal beds	Comment
Type II. F-contents (*ash basis*) of low-ash coals are some more (or even no more) than of high-ash coals but ***pass maxima*** on moderate- and/or high-ash coals. F-contents (*coal basis*) do not correlate with an ash yield, or positively non-linear correlate. There are five subtypes:			
Subtype IIa	F-contents (*ash basis*) weakly decrease along with ash yield increase and pass ***only one maximum*** on the middle-ash coals. F-contents (*coal basis*) show mostly non-linear positive correlation	Virginia: Lyons, Kennedy, Clintwood; West Virginia: Cedar Grove, Fire Creek; Kentucky: Hindman, Upper Elkhorn, Fire Clay Rider. 3.2 %.	Clintwood bed is included conditionally; it stands out by sharp F anomaly: 27500 ppm in ash (coal with an ash yield of 3.2 %). Only Fire Clay Rider bed shows positive correlation "F–P"
Subtype IIb	F-contents (*ash basis*) weakly decrease along with ash yield increase and pass ***two maxima on the middle- and high-ash coals, and the first maximum is more high than the second.*** F-contents (*coal basis*) show no correlation or non-linear positive correlation.	Virginia: Dorchester; West Virginia: Peerless; Kentucky: Skyline, Manchester, Amburgy, Princess 3-9, Upper Peach Orchard.	Two beds from seven studied show positive correlation "F–P"
Subtype IIc	F-contents (*ash basis*) show similar picture but ***the second maximum is more high than the first.*** F-contents (*coal basis*) show no correlation or non-linear positive correlation	Virginia: Jewel; West Virginia: Blair, Pocahontas-3 (including Virginia)	Two beds from tree studied show positive correlation "F–P"
Subtype IId	F-contents (*ash basis*) weakly decrease along with ash yield increase and pass ***absolute minimum on the low-ash coals.*** F-contents (*coal basis*) show no correlation with an ash yield.	The only example: Little Ralegh bed, West Virginia	
Subtype IIe	F-contents (*ash basis*) weakly decrease along with ash yield increase and pass ***absolute minimum on the high-ash coals.*** F-contents (*coal basis*) show no correlation with an ash yield.	The only example: Splashdam bed, Virginia	
Type III: F-contents (*coal basis*) increase along with ash increase (that is normal); F-contents (*ash basis*) also increase (that is very unusual). There are two subtipes:			
Subtype IIIa	F-contents (*ash basis*) droningly increase	The only example: Pocahontas-6 bed, West Virginia	
Subtype IIIb	F-contents (*ash basis*) increase with intermediate maximum	The only example: Broas bed, Kentucky	

It is evident that a plot type is due to the ratios of three main F-forms: Forg, Fclay, and F_{phosph}. If F_{org} predominates, the *plot types I* are observed; if F_{org} and F_{clay}, or F_{org} and F_{phosph} are similar, then the *plot types II* are the most characteristic. Only very rarely is the *plot type III*; in such coals, inorganic F seems to be dominant, and the more, the more an ash yield.
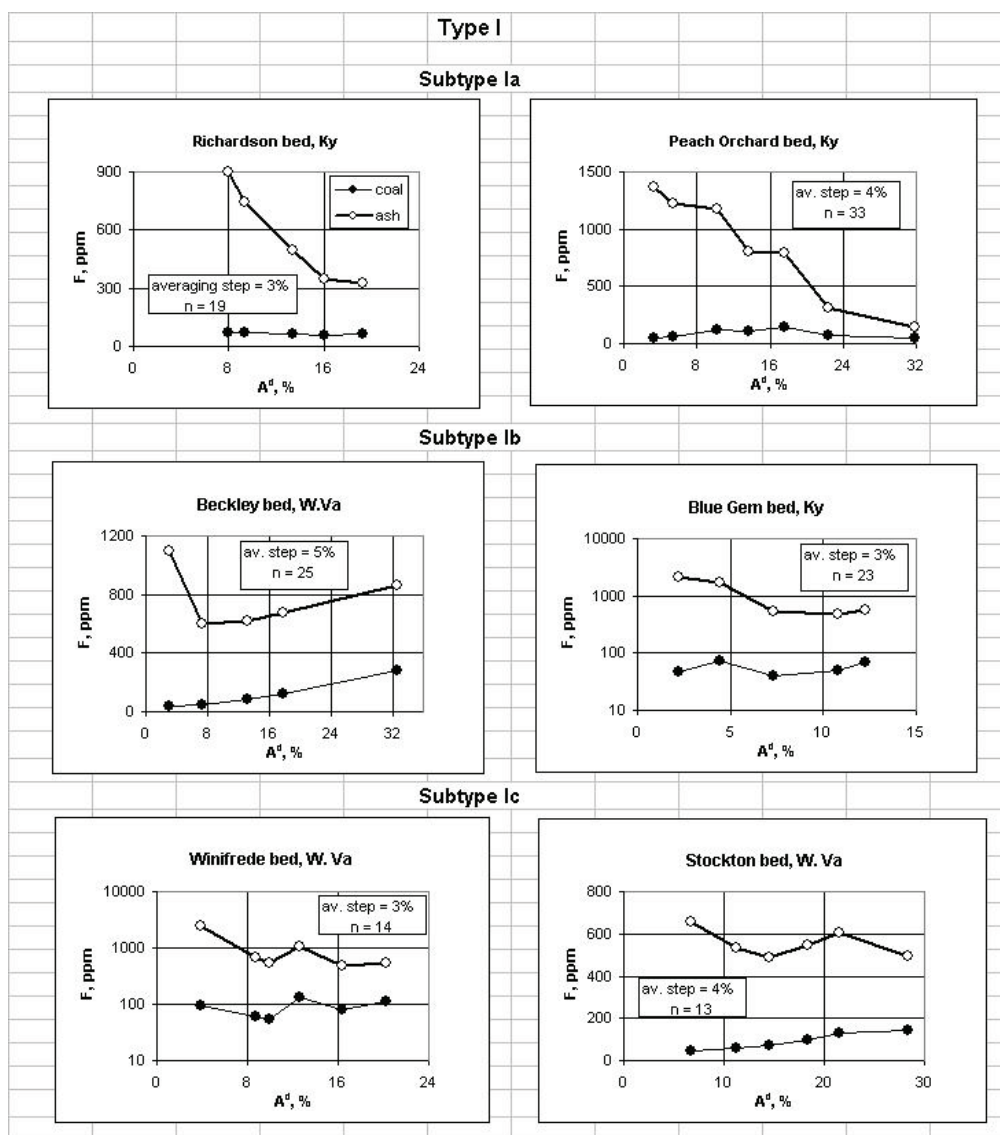
Figure 2. Type-I plot of F contents in coals of the central Appalachian basin. See table 1 for description.

7.1.5. USA: Pennsylvanian Illinois Basin Coals

In two Kentucky power plants, a blend of Pennsylvanian bituminous coals from western Kentucky and Indiana is burned. The data from Wong's dissertation (1994) show some correlation «F in coal – A^d» for feed coals collected in 1978 – Figure 5. Compared to the Appalachian plots (see Figure 3 for comparison), such a type of plot may be attested as *IIe type*.
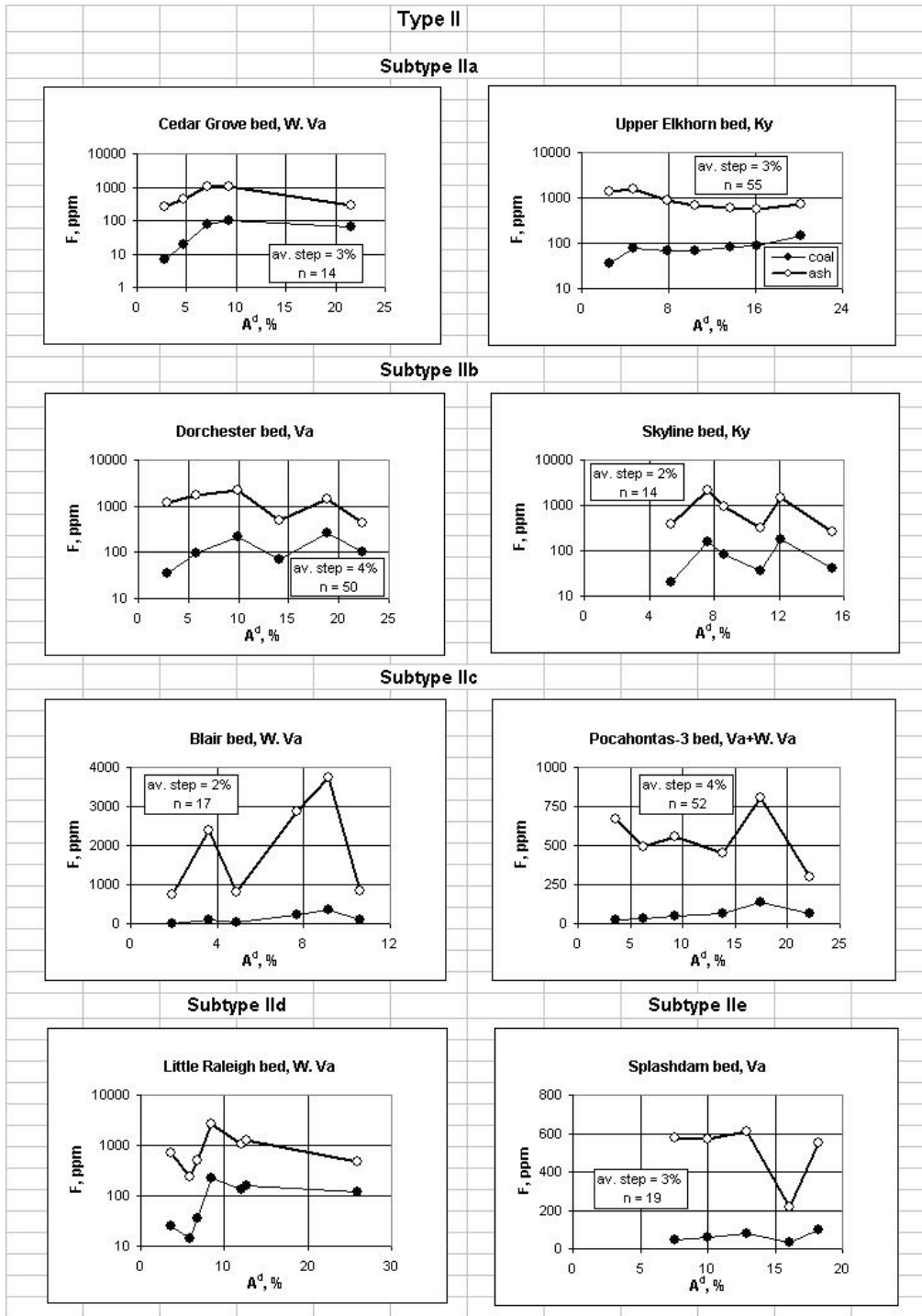
Figure 3. Type-II plot of F contents in coals of the central Appalachian basin. See Table 1 for description.
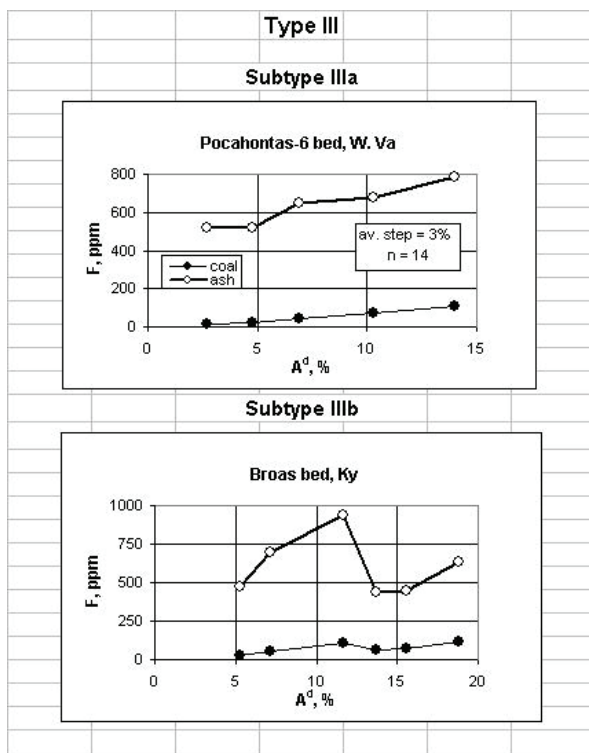
Fig. 4. Type-III plot of F contents in coals of the central Appalachian basin. See Table 1 for description.
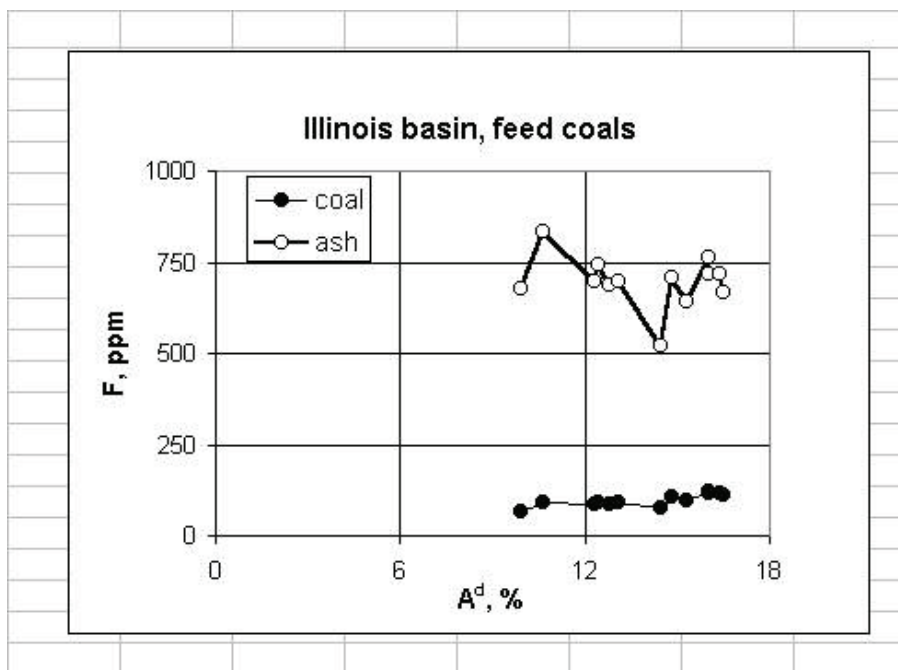
Plotted from the A.Wong's (1994) dissertation unpublished data

Fig. 5. Plot of F contents in coal and ash (calculated) of the Illinois basin**.**

7.1.6. USA: Eocene Green River Lignites

In the Vermillion Creek coalfield Wyoming (Green River basin), the relation of the F content with ash yield (Hatch, 1987) is complicated (Figure 6). It is of note, the highest F content is in coal with high, but not the highest, ash yield. Such a picture is typical for the most of *coalphile elements* and indicates several (two or more) elemental mode of occurrence (Yudovich, 1978; Yudovich and Ketris, 2002). Based on the Appalachian plots (see Figure 3 for comparison), such a type of plot may be described as the *IIc type*.
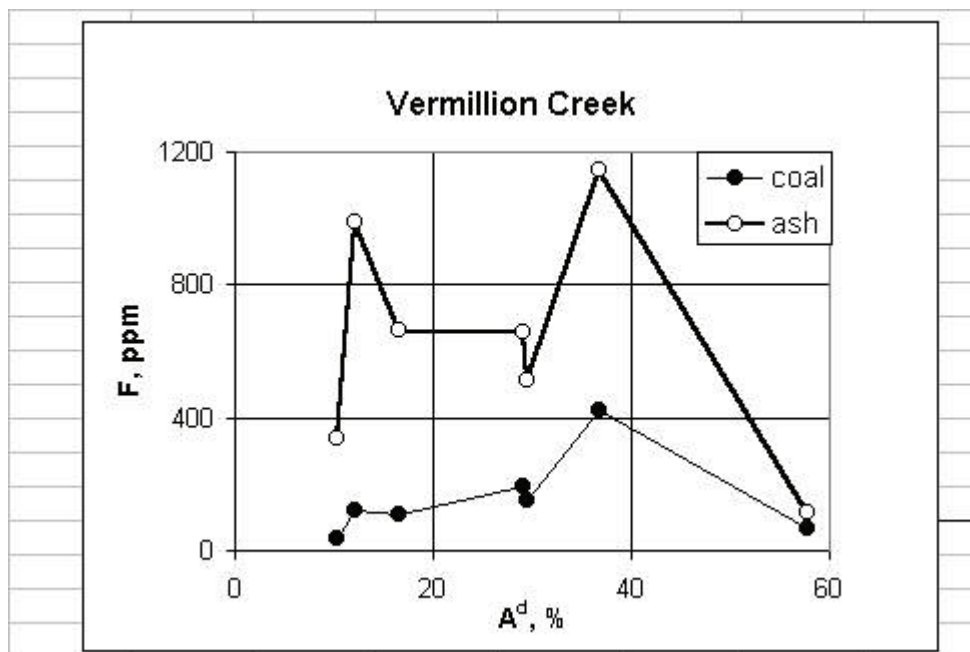
Plotted from the data of Hatch (1987).

Figure 6. Plot of F contents in coal and ash (calculated) of the Vermillion Creek coals.

7.2. Content of Phosphorus

In coals with enhanced P content, a positive F–P correlation may occur, first noted by Crossley (1946) for British coals. Crossley even assumed that F-content could be predicted by the easier-to-determine P-content. However, the latter issue was later disputed by Bethell (1962), who emphasized that, in many coals, the correlation between F and P is not significant. For example, although in high-P Queensland coals high P-content (3.45 %) is accompanied by the F-enrichment (7360 ppm), the P/F ratio is 7.9 (far more than in fluorapatite). In other P-bearing Australian coals P/F ranges from 2.06 (New South Wales) to 10.2 (South Australia) (Durie and Schafer, 1964). It is worth noting also, a P/F ratio deviation from fluorapatite may be due to the presence of F-deficient phosphate, for example, Al- or Fe (also Sr, Ba, REE)-phosphate known in some coals.

7.3. Position of a Bench within Coal Bed Column

In an East German brown coal deposit, F is enriched in coaly-clay partings, as well as in coaly clays of the coal bed roofs and floors (Dässler et al., 1973). In the subbituminous Highvale Mine coals (Alberta, Canada), some F-anomalies are noted: 116–142 ppm against of background of 31–97 ppm. The anomalies are related to high-ash coals and/or to the upper part of the parting (in one coal bed) (Gentzis and Goodarzi, 1995, p. 62).

Such pictures are very similar to vertical distribution of P. As it is well known, phosphorus moved from the buried peat-bed to the nearest alkali barriers, where it was fixed in phosphate (and Al-phosphate) form (Yudovich et al., 1985, p. 127–129). The same process may be assumed for fluorine. Low coalphile coefficient of F (its minor "coal affinity") may be, like P, partly due to F output from the peat beds during diagenesis.

8. GENETIC PROBLEMS

The distribution of F in coal is poorly studied; this forces to use some analogies and suggestions concerning F genesis in coal.

8.1. Does F have an Organic Affinity?

There are no known experimental data about F capture by peat. However, a "F – organics" correlation is found in surface waters due to *soluble* F-organic compounds formation. Could *insoluble* F-organics compounds also be present? At least, the co-precipitation of F with organic-mineral gels in podzol soil illuvial horizons were found (Perel'man, 1972, p. 206–207). Could a similar process can explain a F-enrichment in high-ash coals? As was above noted, F, like P, may be mobile in diagenesis; possibly accounting for the F accumulation in partings and high-ash coals.

8.2. May F be Facies Controlled?

As was shown above (see Sect. 2), an important geochemical feature of F is its "marine-affinity" ("thalassophile" property): an average F concentration in sea water is 1–2 orders-of-magnitude higher than in river water (in humid zone environments) (Perel'man, 1972). Therefore, like boron and sulfur, fluorine contents in coal may be influenced by peat-forming facies: to be higher in paralic (marine influenced) than in limnic (intracontinental) environments. At least, the data about enhanced F-contents in paralic Donbas coals (Gulyaeva and Itkina, 1962) do not contradict this suggestion.

In south Greece, some relatively high F contents (132–258 ppm) are found in Pleistocene (Megalopolis, Peloponnes) and Pliocene (Peloponnes, Kalavrita) lignites. This may indicate the near-sea peat-forming facies (Foscolos et al., 1989).[6]

---

[6] An alternative explanation is epigenetic one: influence of the F-bearing ground waters derived from evaporites.

8.3. May F be Volcanic Controlled?

Theoretically, F entering volcanic exhalation may result in syngenetic F-enrichment in nearby peatbogs. For example, high F-contents in Guizhou Permian coals seem to be directly related with Emeishang basalt flow (Zheng et al., 1999). Moreover, the authors think that F was mainly captured by the peat-forming plants from air, i.e. F in coal may be attested here as primary F_{bio} form!

In general, all these syngenetic mechanisms appear to be probable but data deficiency makes them only hypothetical.

8.4. Epigenetic F-Enrichment

In the Warrior basin, zones of enhanced F (and As) contents are controlled by two cross faults of the Appalachian folded belt and are displayed above the basement uplifts. Coal mineralization is similar to the hydrothermal vein Au-Sb-Cu-mineralization that occured in the southern Appalachians. In contrast to Mississippi Valley Type mineralization resulting from descending brine movement, this mineralization is clearly influenced by the burial metamorphism. As seen from the vitrinite reflectance picture, a heat flow maximum (perhaps, related to the hot fluids input into the coal-bearing strata) was situated on the eastern margin of the Southern Appalachian coal-bearing basin, near the Blue Creek anticline (Goldhaber et al., 1997).

9. BEHAVIOR OF F IN COAL COMBUSTION

During a coal burning in electric power plants (EPP), volatile HF is formed and escapes the combustion in flue gases. A part of evaporated F may be captured by fly ash collected on ESPs (electrostatic precepitators); this part is greatly influenced by CaO content in fly ash which may bond F as CaF2 compound.

9.1. Pulverized Coal Combustion

In Novo-Irkutsk EPP, Jurassic Azeisk brown coals with near-Clarke F contents are combusted. In ash wastes, F is distributed as follows (Boiko and Suturin, 1994, p. 106):

precombustion chamber slag	300 ppm F
fly ash, three ESP fields	0–630 ppm F
ash disposal	440 ppm F

Therefore, F is enriched in fly ash but no more than twofold.

In the Mojave EPP (near Bullhead, Arizona), there is alkali fly ash disposal containing 70 ppm F. Fluorine distributes over the ash size fractions (µm) as follows:

72 ppm (>250 μm) → 66 ppm (250–105 μm) → 68 ppm (105–53 μm) → 83 ppm (<53 μm)

Therefore, in these alkali fly ash, F is not substantionally fractionated (Phung et al.,, 1979).

9.2. Cyclone Burning

In cyclone burning (with known minor yield of fly ash), F is also fully evaporated as HF and only partly captured by fly ash. This is logical because T is here much higher. The laboratory ash from Ruhr bituminous coals contains 600–900 ppm F, and their cyclone fly ash contains some more, up to 1100 ppm. In this-low-Ca ash, F enters silicate spheres, although its form was not established. However, in the cyclone burning of high-Ca Rhine brown coals, ¾ of initial F pass into the slag, and up to 2200 ppm F – into fly ash. A general trend is noted of evaporation of F controlled by flue gas temperature (Beising and Kirsch, 1974).

9.3. Semicoking

A redox medium of the burning and pyrolysis is of value. For example, in the Irkutsk basin coal burning with average F content of 800 ppm, up to 90 % from initial F volatilize and only 100–200 ppm F retained in ash. However, in semicoking (i.e., in more reducing medium), almost all F retains in semicoke and begins to evaporate only at T >1000 oC. After coal and coaly argillite semicokes were calcined up to 1200 oC, 25 % and 40 % initial F were retained (Khankhareev et al., 2002, p. 398).

10. TECHNOLOGICAL INJURIOUS ACTION

Fluorine in coal is an unwanted admixture. It complicates coal burning and processing due to corrosion of the scrubber ceramic fills and silica deposition on the cold sides of the installations heated by flue gases. According Crossley (1946), refractory crubbers were corroded even at slightly enhanced F contents of 120–140 ppm [against <40 ppm F as British coals background (Wandless, 1957)]. Wong et al., (1994, p. 86) noted:

"One of the major concerns for a coal-fired power plant equipped with a FGD system is corrosion in the duct work and the tail-end of the air preheater. Corrosion of refractory materials in contact with flue gases has been attributed to the small amounts of fluorine present in the coal and scrubber sorbent. The metal surfaces (Ti metal, carbon steel, and stainless steel) of the duct work and air preheater have already been abraded by the mass flow of fly ash particles which are mainly composed of small, abrasive silicate glasses. This roughness on the surface provides a very good opportunity for corrosive gases such as HF, HCl and H_2SO_4, which are present in the stream of flue gases, to diffuse into the surfaces and attack the metals".

11. ENVIRONMENTAL TOPICS

Atmospheric F emission may create some environmental problems at coal industrial and domestic burning because of fluorine toxicity.

11.1. Toxicity

In coal burning, high toxic compounds, such as CaF_2, SiF_4 and Na_2SiF_6 may be formed. In the air of populated areas, their permissible limit (calculated on F) has to be no more than 0.005–0.03 mg/m^3. In drinking water, permissible F concentration must be no more than 2 mg/L – that is near the F content in sea water (if more, fluorosis may be caused) (Perel'man, 1972, p. 210).

According the Russian sanitary standards (Belyaev et al., 1993) F concentrations must be no more than (all figures calculated on F):

the air of the populated areas (gaseous Hf and SiF4)
simultaneous concentration   0.02 mg/m^3
average daily norm   0.005 mg/m^3

well soluble compounds (NaF et al.)
simultaneous concentration   0.03 mg/m^3
average daily norm   0.01 mg/m^3

weakly soluble inorganic fluorides (AlF_3, CaF_2, et al.)
simultaneous concentration   0. 2 mg/m^3
average daily norm   0.03 mg/m^3
drinking water (F and F in compounds)   1.5 mg/l

In one Chinese village in 1986 a fluorosis event was described, the result of burning of F-bearing coal (170–1026 ppm F) for stove heating and coking (Dai et al., 1986). Further publications. (Zheng et al., 1999) highlighted a serious problem; extremely high endemic fluorosis levels (dental and skeleton disability) in south and south-east China. Endemic fluorosis were noted in an area of 14 provinces populated with 30 million people, and more than half of them were ill.

Special study (Zheng et al., 1999) showed that F-contents in the environment was not higher than in other provinces. The point was that, the rice drying performed in open, without flues home stoves heated by coal. The burned coals contained up to 2000 ppm F and the rice captured F from air. For example, after three-day-drying, in the rice with a moisture value of 21 % was 6.1 ppm F. After 210-day-drying, the moisture decreased up to 12.4 %, and F content increased up to 130 ppm. The same duration of the drying but using wood-burning stove, at similar initial moisture of 13.7 %, resulted in F content of the rice only 2.5 ppm. The indoors air with coal-burning contained up to 143.5 μg/m^3 F (Zheng et al., 1999).

11.2. Atmospheric Emission

Feed coals imported into Netherlands from Australia and USA have, on average, 11 % ash and 80 ppm F (or 727 ppm on an ash basis). Over 16 analyses series for all Dutch EPPs with pulverized coal combustion, the following F distribution was observed (Meij, 1994):

727 (feed coal ash) $\Rightarrow$ 55 (bottom ash) $\Rightarrow$ 127 (fly ash from four rows of EPS, with median diameter from 22 down to 3 μm) $\Rightarrow$ 1090 (emitted finest fly ash, three fractions with median diameter from 3 down to <0.3 μm).

Therefore, F is depleted in bottom ash and sharply enriched in finest fly ash – an indication of the evaporation followed by the condensation, with partial solid-phase emission. Further, in flue gas clean up by wet scrubbers, F emission may be two-fold decreased (Meij, 1994).

As it exemplified by the German coals combustion (Brumsack et al., 1984), solid-phase F emission is influenced by coal rank. In brown coal burning, enrichment ratio (F content in finest emitted fraction of fly ash / F content in collected fly ash) is far lesser than in bituminous coals burning: 4.6 vs. 12–14[7]:

	collected fly ash	emitted fly ash
brown coals	249 ppm F	1144 ppm F
bituminous coals	165–196 ppm F	2307–2548 ppm F

These data imply that mode of F occurrences in brown and bituminous German coals are appreciably different.

11.3. Fluorine Poisoning of Surface Waters

In 11 Bulgarian ash disposal ponds, F content reaches up to 13.3 mg/L (Bobov Dol EPP); this two orders of magnitude more than F background in surface waters (Bowen, 1966), and more than 25 times – the European Council permissible concentration, 0.5 mg/l (Vassilev and Vassileva, 1992).

Typical F-content range in British fly ash disposals is from zero to 200 ppm. Experimental leaching of the fly ash showed F contents ranged from 0.2 to 2.3 mg/L (Sear et al., 2003). These figures are higher than permissible water concentrations.

11. 4. Threshold of F Toxicity" in Coal

According Russian official norms, the "coal threshold of toxicity" is 500 ppm F (Zharov et al., 1996, p. 15), but Kizilstein et al., (1989) note that the figure *"has no scientific basis"*. That is correct; for example, in the eastern Germany, were bees mortality was described in the

---

[7] Two figures mean two burning regimes: dry and wet bottom.

vicinity of the EPP burning the coals containing no more than 178 ppm F (Dässler et, al., 1973). It is evident that F-emission depends on not only F-content but also on F mode of occurrence and the combustion temperature. Therefore, the F threshold yet has to be determined, for reasons of these considerations.

12. COAL CLEANING AND FLUE GAS CLEAN UP

As F has low coal affinity ("coalphile index"), the mineral site of F is dominant in coal, mostly as Fclay. Only in high-P coals, one can predict an appreciable contribution of phosphatic fluorine, Fphosph, whereas a Forg contribution is, in general, minor. All this means that routine coal cleaning could be an effective method for decreasing the F content. For example, in the Upper Freeport coal seam, clay matter is main F contributor; industrial coal cleaning could decrease F content up to 50 %. In the lab cleaning, F content was decreased even on 78 % (Finkelman, 1993).

As was seen from the Dutch data (Meij, 1994), the wet scrubber flue gas desulfuration (FGD) leads to appreciable lowered F emission. Similar results were obtained in Kentucky EPPs, where a blend of high-sulfur coals of the Illinois basin was burned (Wong et al., 1994; Hower et al., 1997). The feed coals contained on average 3.7 % S and 12.6 % ash. The solid FGD wastes (after vacuum filtration) are composed mostly by $CaSO_3$ with 47.35 % CaO. The final wastes (named as "Poz-o-tec") are the blend of $CaSO_3+CaSO_4$, fly ash and some $CaCO_3$ remainders. They contain (on average) 6.58 % Fe_2O_3 (magnetite), 24.36 % SiO_2, 8.58 % Al_2O_3, 27.10 % CaO, and 31.50 % SO_3. Their appreciable part is represented by new-formed ettringite, $Ca_6Al_2(SO_4)_3(OH_2)$ 26 H_2O, filling the pores between the fly ash silicatic glass spheres. In the technological chain, F is distributed as follows [8]:

94 ppm (feed coal ash) $\Rightarrow$ 124 (fly ash) $\Rightarrow$ 85 (bottom ash) $\Rightarrow$ 898 (FGD wastes) $\Rightarrow$ 501 (final wastes)

Therefore, F in ash wastes relatively enriches in fly ash, and in FGD wastes is sharply enriched. Such F accumulation results from, perhaps, interaction F + CaO (with fluorite formation?)

13. CONCLUSION

1. The World average F content in coals (coal Clarke of F) for the hard and brown coals are, respectively, 82±6 and 90±7 ppm. On an ash basis, these contents are greatly increased and are 580±20 and 630±50 ppm, respectively. As an average, F content in ash is 605 ppm (lower than the Clarke value for sedimentary rocks, 650 ppm). F is, on average, *not a coalphile element.*

---

[8] Our averaging based on four analyses performed during 4-months-long monitoring; all the figures are on dry matter [Hower et al., 1997].

2. Nevertheless, some coals are known to have a F content one order-of-magnitude more than the coal Clarke level. In general, these are either high-ash or high-phosphorus coals, with both the features often combined. This (and some others) features show some similarity between F and P geochemistry in coal. In particular, F, like P, seems to be depleted from the buried peat during diagenesis toward hosting rocks.

3. No less than three F-forms (modes of occurrence) may be present in coal: phosphatic (F_{phosph}), silicatic (mostly F_{clay}), and organic (F_{org}). It can be suggested that F_{clay} dominates in high-ash coals, F_{phosph} in high-P coals, and in ordinary coals with moderate ash yield and near-Clarke P and F contents, F_{org} may be dominant. There is no information concerning chemical species of the F_{org} form. However, by an analogy with P, it seems to exist as an F compound with Ca_{org}, not with organics itself.

4. It is yet not clear, if F is in authigenic CaF_2 and what could be a contribution of such a form to total F content. It seems not to be excluded that such form may have genetic relation with F_{org} (diagenetic or catagenetic transformation, $F_{org} \Rightarrow F_{min}$?) [See (Yudovich, 1978) for details].

5. There are no clear relationships concerning F enrichment in coals. Plausible hypothesis is that F might be syngenetically enriched in coals (a) in paralic (near-marine) coals, and (b) in coals formed with a volcanic activity background. On the other hand, some F anomalies (like that in some Alabama coals) may have resulted from epigenetic hydrothermal F-input, during (or after) coal metamorphism.

ACKNOWLEDGMENTS

REFERENCES

Beising, R. and Kirsch, H. 1974. Das Verhalten des Spurenelementes Fluor aus fossilen Brennstoffen bei der Verbrennung. *VGB Kraftwerkstechnik* 54 (4), 268–286.

Belyaev, M.P., Gneushev, M.I., Glotov, Ya, K., and Shamov, O.I. 1993. Reference Book on the Permissible Concentrations hazardous contaminants in the foodstuffs and environment. Moscow, Gosstansdart [State Standard Publ. House], 120 pp.

Bethell, F.V. 1962. The distribution and origin of minor elements in coal. *Brit. Coal Util. Res. Ass. Monthly Bull.* 26 (№ 12), 401–429.

Boiko, S.M. and Suturin, A.N. 1994. Geochemistry of Azeisk coalfield industrial ashes and their utilization problems. Geol. i geofiz. [*Geology and Geophysics*], 35 (2), 100–108.

Bethell, F.V. 1962. The distribution and origin of minor elements in coal. *Brit. Coal Util. Res. Ass. Monthly Bull.* 26 (№ 12), 401–429.

Bouška, V. and Pešek, J. 1999. Quality parameters of lignite of the North Bohemian Basin in the Czech Republic in comparison with the world average lignite. *Int. J. Coal Geol.* 40, 211–235.

Bowen, H.J.M. *Trace Elements in Biochemistry*. – London – N. Y.: Academic Press, 241 pp.

Bradford, H.R. 1957. Fluorine in Western coals. *Mining Eng.* 9 (1), 78–79.

Bragg, L.J., Oman, J.K., Tewalt, S.J., Oman, C.L., Rega, N.H., Washington, P.M., and Finkelman R.B. 1998. Coal quality (COALQUAL) database – version 2.0: U.S. Geological Survey Open File Report 97-134, unpaginated CD-ROM.

Brumsack, H., Heinrichs, H. and Lange, H. 1984. West German coal power plants as sources of potentially toxic emissions. *Environ. Technol. Lett.* 5, 7–22.

Bykadorov, V.S., Vyalov, V.I., Podkamenny, A.A., and Shibanov, V.I. 2002. Ulughem Basin and other basins of the Tyva Republik. Ugol'naya baza Rossii. T. III. Ugol'nye basseiny i mestorozdeniya Vostochnoi Sibiri. Yuznaya chast'. Moscow, Geoinformmark, 270–363. [Russian Coal Base. Vol. III: East Siberian Coal Basins and Deposits. Southern Part.].

Crossley, H.E. 1946. The inorganic constituents of coal; occurrence and industrial significance. Inst. Fuel, London, *Bull.* 1946, Dec., 57–60, 67.

Dai, G., Wang, Z., Tao, Y., Zhang, Z., Zhang, D., Zhang, G., and Wang, G. 1986. Investigation of fluorosis caused by burning coal. Zhonghua Yufangyixue Zazhi 20, 217 219.

Dässler, H.G., Börtitz, S., Auermann, E., Czerwinski, C., and Tongmann, F., 1973. Über den Fluorgehalte von Braunkohlen der DDR. Z. *Angew. Geol.* 19(9), 447–449.

Durie, R.A. and Schafer, H.N.S. 1964. The inorganic constituents in Australian coals. IV. Phosphorus and fluorine – their probable mode of occurrence. *Fuel*, 43 (1), 31–41.

Evtukhovich, I.L. and Lukashev, O.V. 2001. Geochemistry of Fluorine in Hypergene Zone of Belorussia. Belorussian University, Minsk, 210 pp.

Finkelman, R.B. 1993. Hazardous trace elements in coal: Can we rely on modes of occurrence information to predict their removal? Proceedings of the Tenth International Pittsburgh Coal Conference (Ed. S.H. Chiang), Pittsburgh., 311–313.

Finkelman, R.B. 1980. Modes of occurrence of trace elements in coal. Ph.D. Thesis. Dept. Chem., University of Maryland, College Park, 302 pp.

Finkelman, R.B., Bostick, N.H. and Dulong, F.T. 1992. Influence of an igneous intrusion on the element distribution of a bituminous coal from Pitkin County, Colorado. Ninth Ann. Meet. The Soc. Org. Petrology (University Park, PA, July 23–24). *Abstr. Progr.,* 112–114.

Foscolos, A.E., Goodarzi, F., Koukouzas, C.N., and Hatziyiannis, G., 1989. Reconnaissance study of mineral matter and trace elements in Greek lignites. *Chem. Geol.* 76, 107–130.

Gentzis, T. and Goodarzi, F. 1995. Geochemistry of subbituminous coals from the Highvale Mine, Alberta, Canada. *Energy Sources*, 17(1), 57 91.

Godbeer, W.C. 1987. Results for fluorine in coals and other reference materials. *Geostand. Newslett.* 11 (2), 143–145.

Godbeer, W.C. and Swaine, D.J. 1987. Fluorine in Australian coals. *Fuel*, 66 (6), 794–798.

Goldhaber, M.B., Hatch, J.R., Pashin, J.C., Offield, T.W., and Finkelman, R.B. 1997. Anomalous arsenic and fluorine concentrations in Carboniferous coal, Black Warrior Basin, Alabama: Evidence for fluid expulsion during Alleghanian thrusting. *Geol. Soc. Amer. Abstracts with Programs*, A-51.

Grieve, D.A. and Goodarzi, F. 1993. Trace elements in coal samples from active mines in the Foreland Belt, British Columbia, Canada. *Int. J. Coal Geol.* 24 (1-4), 259–280.

Gulyaeva, L.A. and Itkina, E.S. 1962. Halogens, vanadium, nickel and copper in coals. Geokhimiya [*Geochemistry*] 4, 345–355.

Hatch, J.R. 1987. Element geochemistry. Geological Investigations of the Vermillion Creek Coal Bed in the Eocene Niland Tongue of the Wasatch Formation, Sweetwater County, Wyoming. (Ed. H.W.Roehler, L.Martin). U.S. Geol. Surv. Profess. Pap., No. 1314-G 7, 121–131.

Hower, J.C., Graham, U.M., Wong, A.S., Robertson, J.D., Haeberlin, B.O., Thomas, G.A., and Schram, W.H. 1997. Influence of flue-gas desulfuration systems on coal combustion by-product quality at Kentucky power stations burning high-sulfur coal. *Waste Management*, 17(8), 523–533.

Huang, W., Che, Y. and Tang, D. 2003. Study of trace elements in coal and mining wastes and its significance in China. *J.Coal. Sci. Eng.* (China), 2003, vol. 9, No.2, p. 43–47.

Huggins, F.E. and Huffman, G.P. 1995. Chlorine in coal: an XAFS spectroscopic investigation. *Fuel*, 74 (4), 556–559.

Iordanidis, A. 2002. Geochemical aspects of Amynteon lignites, Northern Greece. *Fuel*, 81, 1723–1732.

Ivanov, S.N. 1962. Physical-chemical Regime of Phosphates in Peats and Sod-podzol Soils. Minsk: Selkhozgiz [Agricultural Publ. House], 251 pp.

Ivanov, V.V. 1994. Environmental Geochemistry of Elements: Reference Book, 2. Main p-Elements. – Moscow: Nedra ["Entrails" Publ. House], 303 pp.

Ketris, M.P. and Yudovich, Ya. E. 2002. Calculation procedure of the coal Clarkes. Lithogenes i geochimiya osadochnykh formatsii Timan-Ural'skogo regiona. Syktyvkar, 111–117. (Tr. In-ta geol. Komi nauch. tsentra UrO Ross. Acad. nauk, vyp. 111). [*Proc. Inst. Geol. Komi Sci. Center*, issue. 111].

Khankhareev, S.K., Admakin, L.A., Suslova, M.G., Krivonos, A.N., Dorokhova, A.V., and Pukhova, A.S. 2002. Irkutsk basin and For-Baikal coal fields. Ugol'naya baza Rossii. T. III. Ugol'nye basseiny i mestorozdeniya Vostochnoi Sibiri. Yuznaya chast'. Moscow: Geoinformmark, 363–475. [Russian Coal Base. Vol. III: East Siberian Coal Basins and Deposits. Southern Part.].

Khrustaleva, G.K., Andrianova, T.P., Medvedeva, G.A., Kvochkina, L.V., and Ulanov, N.N., 2001. Geological Aspects of Coal Conversion to Liquid Fuels: A Review. Geoinformmark, 55 pp.

Kizilstein, L.Ya. 2002. Ecogeochemistry of trace elements in coals. Rostov-na Donu [Rostov-on the Don river]. SK NZ VSh [North-Caucasus Sci. Center of High School], 296 pp.

Kizilstein, L. Ya., Shpitsgluz, A.L., Peretyat'ko, A.G., and Levchenko, S.V. 1989. Estimation of the dangerous level of the toxic element contents in coal and prediction of the air condition near the EPPs, on the geological exploration data . 27th Int. Gol. Congr. Soviet Geol. Rep. Vol. 17, sect. 17: Engineering Geology and Geologic Environment. Moscow: VIMS, VNIGRIUGOL', 154–163.

Kler, V.R. 1988. Minor element concentrations in the coals and coal-bearing formations, in V.R.Kler, V.F.Nenakhova, F.Ya.Saprykin, M.Ya.Shpirt, L.I.Rokhlin, A.F.Kulachkova, R.I.Iovchev. Metallogeny and geochemistry of coal-bearing and oil shale-bearing strata of the USSR: The regularities of the element concentrations and methods of their study. Moscow, Nauka ("Science" Publ. House), 67–142.

Kopp, O.C., Barrett, H.E., Dorsey, A.E., Miller, B.W., Rees, S.O., and Scales, A.S. 1989. Trace elements in coal – keys the past, problems for the future? (Abstr.). *J. Coal Qual.* 8 (3–4), 121.

Kowalevsky, A.L. 1991. Biogeochemistry of Plants. Novosibirsk: Nauka [Science Publ. House], 293 pp.

Kowalevsky, A.L. and Prokopchuk, C.I. 1999. Biolithes in plants and their role in the geochemistry of the hypergene zone. Geochimicheskie bar'yery v zone gipergeneza. Mezhdunar. A.I. Perel'man's symp. (Moskwa: 25–29 Okt. 1999). Tes. dokl. [Geochemical Barriers in Hypergene Zone. Int. Symp. in A.I. Perel'man Memory: Moscow: October 25–29, 1999], 101–104.

Kunstmann, F.H., Harris, J.F., Bodenstein, L.B., and Van den Berg, A.M. 1963. The Occurrence of Boron and Fluorine in South African Coals and Their Behavior During Combustion. *Fuel Res. Inst. S. Afr. Bull.* 63, 45 pp.

Lessing, R. 1934. Fluorine in coal. *Fuel*, 13 (11), 347–348.

Martínez-Tarazona, M.R., Suarez-Fernandez, G.P. and Cardin, J.M. 1994. Fluorine in Australian coals. *Fuel*, 73 (7), 1209–1213.

McIntyre, N.S., Martin, R.R., Chauvin, W.J., Winder, C.G., Brown, J.R., and MacPhee, J.A. 1985. Studies of elemental distributions within discrete coal macerals. Use of secondary ion mass spectrometry and X-ray photoelectron spectroscopy. *Fuel*, 64 (12), 1705–1712.

Medvedev Ya,.V., Sedykh, A.K. and Chelpanov, V.A., 1997. Khankaisky coal basin. Ugol'naya baza Rossii. T. I. Kn. 1. [Russian Coal Base. Vol. V (1)]. – Moscow: Geoinformmark, 174–220.

Meij, R. 1994. Trace element behavior in coal-fired power plants. *Fuel Process. Technol.,* 39, 199–217.

Oman, C.L., Finkelman, R.B., Halili, N., and Goldhaber, M.B. 1995. Anomalous trace element concentrations in coal from the Warrior Basin, Alabama. *Geol. Soc. Amer. Abstr. Progr.* 27, No. 2, 78.

Osokin, P.V. 1993. On trace elements distribution in North Mongolia and South Transbaikal coals. Litol. i polezn. iskopaemye *Lithology and Mineral Resources,* 2, 113–119.

Pachadzhanov, D.N. 1981. Geochemistry of Varycolored Strata, Tadzhik Depression. – Moscow: Nauka ["Science" Publ. House], 244 pp.

Perel'man, A.I. 1972. Elemental Geochemistry in Hypergene Zone. Moscow: Nedra [Entrails Publ. House], 288 pp. Phosphorus and fluorine in Australian coals, 1963. Coal Res. C.S.I.R.O. 21, 2.

Phung, H.T., Lund, L.J., Page, A.L., and Bradford, G.R. 1979. Trace elements in fly ash and their release in water and treated soils. *J. Environ. Quality*, 8, 171–175.

Ren, D., Zhao, F., Wang, Y., and Yang, S. 1999. Distribution of minor and trace elements in Chinese coals. *International Journal of Coal Geology*, 40, 109–118.

Sear, L.K.A., Weatherley, A.J. and Dawson, A. 2003. The environmental impact of using fly ash – the UK producers perspective. Int. Ash. Utiliz. Sympos. (Lexington, KY: 20–22 Oct., 2003). CD-rom Proc., 13 pp. Sedykh, 1997, c. 173

Sedykh, A.K. 1997. Uglovsk coal basin. Ugol'naya baza Rossii. T. V. Kn. 1. [Russian Coal Base. Vol. V (1)]. Moscow: *Geoinformmark*, 115–174.

Seredin, V.V. and Shpirt, M.Y. 1995. Metalliferous coals: a new potential source of valuable trace elements as by-products. Coal Science. (Eds. J.A. Pajares, J.M.D. Tascón). Amsterdam, Elsevier, 1649–1652. (8th ICCS Proc. Vol. II).

Seredin, V.V., Evstigneeva, T.L. and Generalov, M.E. 1997. Au-PGE mineralization in Cenozoic coal-bearing strata of the Pavlovka deposit, Russian Far East: Mineralogical evidence for a hydrothermal origin. Mineral Deposits: Research and Exploration. (Ed. H.Papunen). Rotterdam, Balkema, 107–110. (Proc. 4th Biennial SGA Meet. Turku: 11–13 Aug., 1997).

Seredin, V.V., Shpirt, M.Y. and Vassianovich, A. 1999. REE contents and distribution in humic matter of REE-rich coals. Mineral Deposits: Processes to Processing. (Eds. C.J.Stanley et al.). Rotterdam: Balkema, 267–269. (Proc. 5th Biennial SGA Meet. & 10th Quadr. IAGOD Meet. London: 22–25 Aug. 1999).

Shishkina, O.V., Pavlova, G.A. and Bykova, V.S. 1969. Geochemistry of Halogens in Sea and Ocean Sediments and Their Pore Waters. Moscow: Nauka *Science Publ. House*, 117 pp.

Swaine, D.J. 1990. Trace Elements in Coal. – London: Butterworths, 278 pp.

Trukhin Yu, P. 2003. Geochemistry of Recent Hydrothermal Processes and Geotechnology Prospects. Moscow: Nauka [Science Publ. House], 376 pp.

Vassilev, S.V. and Vassileva, B. 1992. Element composition of waste waters from thermo-electric power plants. C. r. *Acad. Bulg. Sci.* 45 (7), 49–52.

Vyazova, N.G., Kryukova, B.N., Kurbatova, A.I., and Andrulaitis, L.D., 1989. Distribution of fluorine in Siberian coalfields. Geokhimiya *Geochemistry*, 5, 744–747.

Wandless, A.M. 1957. British coal seams: a review of their properties with suggestions for research. *J. Inst. Fuel.* 30, 541–552.

Wong, A.S. 1994. Proton-induced Gamma-ray and X-ray Emission and Their Analytical Applications to Coal Resource Development. Ph.D. Dissertation, University of Kentucky, 00 pp.

Wong, A.S., Hower, J.C., Robertson, J.D., Haeberlin, B.O., Thomas, G.A., and Schram W.H. 1994. Fluorine partitioning in flue-gas desulfurization: examples from coal-fired power plants in Kentucky. *J.Coal Qual.* 13 (3–4), 81–87.

Wong, A.S. and Robertson, J.D., 1993. Multi-elemental analysis of coal and its by-products by simultaneous proton-induced gamma-ray/X-ray emission analysis. *J. Coal Qual.* 12, 146–150.

Yudovich, Ya E. 1978. Geochemistry of Fossil Coals. Leningrad, Nauka ["Science" Pub. House], 262 pp.

Yudovich Ya, E. and Ketris, M.P. 2002. Inorganic Matter of Coals. Ekaterinburg: URO RAN Ural Division of the Russian Acad. Sci., 422 pp.

Yudovich, Ya E., Ketris, M.P. and Merts, A.V. 1985. Trace Elements in Fossil Coals. – Leningrad, Nauka "Science" Pub. House, 239 pp.

Zhang, J., Ren, D.Y, Zhu, Y.M., Chou, C.L., Zeng, R., and Zheng, B. 2004. Mineral matter and potentially hazardous trace elements in coals from Qianxi Fault Depression Area in Southwestern Guizhou, *China. Int. J. Coal Geol.* 57, 49–61.

Zharov Yu,.N., Meytov, E.S., Sharova, I.G., et al., (compilers), 1996. Valuable and toxic elements in Russian Row coals. A reference book. Moscow: Nedra (Entrails Publ. House), 239 pp.

Zheng, B., Ding, Z., Huang, R., Zhu, J., Yu, X., Wang, A., Zhou, D., Mao, D., and Su, H., 1999. Issues of health and decease relating to coal use in southwestern China. Int. *International Journal of Coal Geology,* 40, 119–132.

Chapter 4

NOTE ON RHENIUM IN COAL

Ya. E. Yudovich[*] and M.P. Ketris

Institute of Geology, Komi Scientific Center,
Ural Division of the Russian Academy of Sciences
167023 Syktyvkar, Morozova st., 100, ap. 49. Russia

ABSTRACT

Rhenium is very rare element with Clarke value (average content in the Earth's crust) about 0.001 ppm (= 1 ppb). Geochemistry of Re in coal is poorly known up to now because of analytical problems. Special analytical methods are needed for reliable Re determination in coal. Some coals are known, with Re contents 2–3 orders-of-magnitude higher than Re Clarke value in the Earth's crust, in the range from 0.n ppm up to few ppm.

In Re-bearing coals, it is no doubt that Re_{org} form exists. Perhaps, Re is sorbed on coal organics by weak, ion-exchange bonds. This is accounted for by the Re leachability from coals by surface and ground waters. Some analogues with Re state in black shales indicate that some part of Re may be present in bituminous components of coal (liptinite). The other authigenic Re form may be its sulfide, ReS_2. However, Re sites in coal (modes of occurrence) is now only hypothetic; microprobe study is needed for more knowledge.

There are at least three genetic types of Re-concentrations in coal: Uzbek, Spanish and Kazakh. In *Uzbek* type, Re is probably syngenetic. Its accumulation is due to enhanced Re contents in source rocks. Rhenium leached from terrigenic material may further be captured on reducing peatbog barrier – in organic or sulfide form. In *Spanish* type Re is also mostly syngenetic. Its accumulation is due to considerable contribution of the bituminous organics (like black shale) having extremely high affinity to Re. In *Kazakh* type Re is close associated with U and its companions, in the infiltration epigenetic deposits of the "*bed oxidation*" type. Re dissolved in oxidized waters as

[*] Corresponding author. Y.E.Yudovich
E-mail address: yudovich@geo.komisc.ru

perrhenate ion ReO_4^-, may be captured in brown-coal beds on the reducing barrier, in organic or sulfide forms.

Recently Re-bearing fumaroles were described in the Kurily Islands. Therefore, some Re accumulations may occur in peatbogs of the volcanic areas, or in young lignites – in orogenic depressions with synchronous volcanism. Such Re accumulations may be associated with In, Ge, Mo, Bi and some other elements enriching the volcanic exhalations.

Because Re is very valuable metal, Re-bearing coals may serve as Re industrial resource. The most promising are epigenetic uranium-coal deposits. In addition, some intermountain trough brown-coal fields must be studied for Re, if these coals are associated with volcanics.

Keywords: Rhenium; Coal; Geochemistry; Coal combustion.

Rhenium is ultra-rare chemical element having the Clarke value (mean content in Earth's crust) no more than 0.001 ppm = 1 ppb. All the studies on Re in coal are connected with Russian geochemical school that is noted also in Swaine's (1990) outline.

RHENIUM IN COALS OF THE FORMER USSR: UZBEKISTAN, RUSSIA AND UKRAINE

First note about Re contents in coals within the range of 0.084–0.328 ppm appeared in Russian literature in 1961 (Kuznetsova and Saukov, 1961). In sulfide-rich Jurassic dull lignites of Angren coalfield (Uzbekistan), Re content of 0.08 ppm was found, and in bright low-ash coals – as much as 0.29 ppm (Razenkova and Kuznetsova, 1963). Other samples of the same deposit showed 0.17 ppm (Baranov, 1966) and 0.2–0.4 ppm (Kler and Nenakhova, 1981, p. 49). Later, Baranov (1966) found 0.39 ppm Re in the Sakhalin Island coal, and Yurowsky (1968) published the data on Re content in Donets basin (Donbas) coals. In 18 samples representing high-volatile bituminous coals from 13 Donbas mines, Re contents were in the range from 0.2–0.8 ppm. In cleaned coal (with A^d, ash yield, of 8 %) from Privol'nyanskaya Yuzhnaya mine, Re content was as much as 4 ppm (Yurowsky, 1968).

There are some data indicated Re content in some Russian brown coals as much as 20 ppm (Ratynsky, Spirt, Krasnobaeva, 1980). Moreover, in so-called *infiltration uranium-coal deposits*, Re contents can (?) reach so extremely values as 200–400 ppm (Kler, 1987, p. 93)[1]. Some data also appeared about Re presence in coal sulfides and vitrains (Maksimova and Shmariovich, 1982; Ratynsky, Spirt, Krasnobaeva, 1980; Spirt, Ratynsky, Zharov, Zekel, 1984).

---

[1] Some doubts are cast upon these data; anyhow, maximum Re content cited in (Maksimova and Shmariovich, 1982), is one order of magnitude lower – 52 ppm.

AN ESTIMATION OF COAL CLARKE VALUE OF RE

Because of all analyses published represent only Re-bearing coals with enhanced Re-contents, it is impossible to evaluate Re coal Clarke value some correctly. Therefore, coal Clarke of Re can be calculated only conditionally true. For example, some "background" Re content in the former USSR coals was estimated by Kler (1987) as 0.06 ppm. He based from Re/Mo ratio, 1: 100, in sulfide deposits. However, Kler noted: *"this Re-content level is true if the Re/Mo ratio holds for low-Re coals"* (Kler, 1987, p. 94).

If such estimation is true, coal Clarke value for Re is one order of magnitude higher than Earth's crust Clarke value. If so, we must attest Re as *coalphile element* (about coalphile coefficients, or "coal affinity index", see, for example, Russian monograph (Yudovich and Ketris, 2002) or some papers in English, such as (Yudovich and Ketris, 2004).

Rhenium average distribution trough coal density fractions (for former USSR coals) also support the coalphile nature of Re. The normalized Re contents in high-ash (>1.7 g/cm^3) and low-ash (<1.7 g/cm^3) fractions are in the range of 0.75–1.0 and 1.0–2.9 correspondingly; in ash of the low-ash fractions – from 1.8 up 6.6, and high-ash-fraction Re contribution was from 50 up 63 % from gross Re content in coal (Spirt et al., 1990, p. 189). Therefore, the highest Re concentration coefficient in ash is as high as 6.6.

In Jurassic Nazar-Ailok anthracites (Tadzhikistan), Re contents in low-ash ($A^d = 3.2$ %) and high-ash ($A^d = 17.9$ %) coals are close, 2.1 and 3.3 ppm. This indicate that Re-forms (Re_{min} and Re_{org}) are commensurable (Valiev, Gofen, Pachadzhanov, 1993).

In latest years some Re-analyses by INAA appeared; they show that coals have Re contents at least no less than hosting rocks. For example, four ash of north Ontario (Canada) Lower Cretaceous lignites show Re contents <1, <1, 3 and 5 ppb, that are higher that in hosting rocks (<1 ppb) (Kronberg et al., 1987).

SPANISH RE-BEARING "LIGNITES"

In 1960–1970, special study of Paleogene Spanish "lignites" were performed (Gracia, Martin, 1968; Martin, Garcia-Rosell, 1970, 1971; Martin, Gracia, 1970). In lignite-bearing sandstones of Granada (Arenas-del-Rey) and carbonates of Ebro depression, geochemistry of U and Re was studied.

In lignites from sandstones, where U and Re are syngenetic, average Re contents (ash basis, $A^d = 45$ %) is in the range of 0.24–2.28 ppm, up to 1.08 ppm. *In lignites from presumably carbonate strata,* Re content in ash reaches up to 9 ppm. More detailed study performed on the Tres Amigos mine (Martin, Gracia, 1970) showed that Re is concentrated near the lignite beds roofs, and laterally enriches some bed parts through of few meters long. For example, at average Re content in the Lower bed of 0.35 ppm, the content of 0.94 ppm was found near the roof, and 0.06 ppm – near the bed bottom. This may indicate epigenetic Re input into the lignite bed from the roof.

It must be noted that Spanish "lignites" probably have much bituminous (aquagenic) matter, and by this reason, may be close to the oil shales. This may be indicated by their association with carbonate rocks and very high ash yield in many beds, that is known as very characteristic for oil shales. If it is the case, the Re-enrichment becomes more understandable

https://telegram.me/Geologybooks

because Re is "an element No. 1" for oil shales; it is known to be sharp Re enrichments in oils and bitumen (Yudovich and Ketris, 1994, p. 170–176). These (preliminary) suggestions indicate that some Re-enrichments may be found in coals with sapropelic admixtures, and, may be also – in lipto-biolithic coal varieties (Yudovich, Ketris, Merts, 1985). It is of note, some extraordinaire Re content was found in one sample of vascular plant – 1500 ppm (?!) in ash (Shacklette, 1965).

RHENIUM IN INFILTRATION URANIUM-COAL DEPOSITS

In Mid Asian, besides Angren and Nazar-Ailok coals, Re is found in so called *infiltration uranium-coal deposits*, in association with U, Mo, Se, Ag, Zn, Ge, Co, Pb and some other elements (Maksimova and Shmariovich, 1982).

In one of such deposits[2], for which three drillholes sketchy[3] column are published, epigenetic "ore-controlling" zonality is clearly seen. It is most fully presented in the No. 1 drillhole, where it embraces entire coal bed with hosting rocks (Maksimova and Shmariovich, 1982, p. 73, fig. 2). There are three zones (from above) having some more small subzones.

1. **Oxidation zone.** It includes continental, strong limonitized sand-gravel layers, covered the coal bed with erosion contact. Contents of U and its companions are on the Clarke levels.
2. **Transitional zone.** It includes upper part of the coal bed, and in his pinching-out places – entire coal bed. Two subzones are distinguished: upper (I) with co-existed Fe-oxides and pyrite and lower (II) with sharp pyrite predominance. In upper subzone, U-ore mineralization is near absence, in lower – is weak U-ore mineralization
3. **Reduced (ore-bearing) zone.** It also includes subzones: upper (III) and lower (IV). In the uppermost part of III subzone, the richest U-ores are, in its lower part the ores are poor. The IV subzone is a primary aureole beneath ore body. The U contents are there no more than 0.00n %, and only sometimes its companions show geochemical anomalies.

Coal bed underlayed by the weathering crust of the basement rocks. In places where coal bed is pinching-out, the U-ore partly extends to also the weathering crust.

As is seen from the Table 1, maximum Re contents, reaching up to 52 ppm, are in the rich U-ore zone (subzone III).

---

[2] As one can think, it may be Low-Ili deposit in Kazakhstan, where U-ore is localized in upper part of 4-m-thick coal bed

[3] out of scale

Table 1. Re contents in the epigenetic zonality column, on Low-Ili (?)
uranium-coal deposit

Rocks	Number of analyses	Re contents, ppm	
		range	average
Oxidation zone			
Sandstone	5	<0.005	–
Transitional zone			
Coal (subzone II)	11	0.0068–0.8	0.02
Coal(subzone II)	39	0.34–28	4.2
Reduced zone, III subzone			
Coal (rich ore)	38	0.01–52	9.5
Coal (poor ore)	37	<0.005–13	2.5
Clay – bottom of the splitting coal bed (poor ore)	2	2.7–13	7.8

Compiled from the data of Maksimova and Shmariovich (1982, p. 74).

Mode of Re Occurrence in Coal

Since pioneer studies by Kuznetsova and Saukov (1961) and Razenkova and Kuznetsova (1963), it became known that, in Angren mostly fusain brown coals, Re distribution strongly differs from Mo distribution, although both the elements were suggested earlier as full geochemical analogues. So, Re did not concentrated in sulfides (where Mo was enriched), and bonded with coal organics much weaker than Mo. Perhaps, this bond was ion-exchangeable, because of most Re (up to 62 % in bright, and up to 96 % – in dull coals) was leached by water (Kuznetsova and Saukov, 1961 Razenkova and Kuznetsova, 1963). Experiments with ion-exchange resins showed that Re can partly bind with carboxyl and much weaker – with hydroxyl functionality. However, both the processes are much weaker appeared than for Mo (Kuznetsova and Saukov, 1961).

Further study on epigenetic uranium-coal deposits showed that coal serve as reducing barrier for perrhenate ion (ReO_4^-); Re is concentrated, probably, in sulfide form – in lower part of "transitional" zone, and in upper part of "reduced" (ore) zone. Assuming the Re concentration range in connate waters as $1.8 \cdot 10^{-8}$–$1.9 \cdot 10^{-6}$ g/L (10^{-10}–10^{-8} mol/kg H_2O), one can calculate Eh of Re-sulfide precipitation, in the redox equation "perrhenate – sulfide":

$$ReO_4^- \ (L\ ) + 2S^o\ (S) + 8H^+ + 7e \rightarrow ReS_2\ (S) + 4H_2O$$

The calculations result in:

Eh = (+167 – +150) mV for pH = 6,
Eh = (+32 – +15) mV   for pH = 8

"Therefore… a Re reduction up to sulfide form must appear… in general at low values of redox-potential… Calculated area for the Re precipitation from connate waters as ReS_2 lies beneath equilibrium line between areas of Se (as Se^o) and Mo (as MoS_2) precipitations, localizing inside the wide U-precipitation band… The Re precipitation … may occur at Eh-

values needed for U solid phase formation, and does not need so strong redox potential lowering as it occurs for Mo-mineralization formation… One can think that known in geology close association Re with Mo-sulfides is due to not the coincidence of the thermodynamic reduction conditions for both the elements but rather unlimited ReS_2 and MoS_2 isomorphism in ores" (Maksimova and Shmariovich, 1982, p. 77).

It is of note, however, some contradiction. If Re was precipitated in sulfide form, it would be concentrated in pyrites but this is not the case. Therefore, though above conclusive proofs, they do not give clear answer: how is Re mode of occurrence in U-ores? That is why, Maksimova and Shmariovich said ambivalent: *"The absence of direct Re-Mo correlation and Re-accumulations in Fe-disulfides may indicate either for either ReS_2, or Re bonding with organics. (*Maksimova and Shmariovich, 1982, p. 78).

All the indirect data argued for the weak Re bonding with coal organics: Re permanently presents in mine waters; in circulating water of the coal-cleaning plants (Donbas, Ukraine); in connate waters of coal-bearing strata (Angren, Uzbekistan). For example, Re contents in the Donbas circulating waters reach up to 0.6 ppm, and Re was also found in water condensates by underground gasification of the Angren coals (Kler, 1987, p. 94)).

BEHAVIOR OF RE IN COAL COMBUSTION

In Russian power plants, in mostly stoker combustion, Re output in gas phase from high-temperature furnace zone, with slag-removal coefficient 0.8 is 96–98 % (Shpirt et al., 1990, p. 193). Therefore, Re has extremely high volatility. This implays that, after its condensation from gas phase, it must enrich the fly ash, that is of industrial interest. According to Russian official norm (Valuable…, 1986, p. 14), minimal Re contents being of industrial interest, is 0.1 ppm (coal basis) and 0.5 ppm (ash basis). Therefore, some coals (and, very probable, their fly ashes) have Re contents that may be extracted by coal utilization.

DISCUSSION AND CONCLUSION

1. Geochemistry of Re in coal is poor known up to day because of analytical problems. Special analytical methods are needed for reliable Re determination in coal.
2. Some coals are known, with Re contents 2–3 orders-of-magnitude higher than Re Clarke value in the Earth's crust, in the range from 0.n ppm up to few ppm.
3. In the Re-bearing coals, it is no doubt that Re_{org} form exists. Perhaps, Re is sorbed on coal organics by weak, ion-exchange bonds. This is accounted for Re leachability from coals by surface and ground waters. Some analogues with Re state in black shales indicate that some part of Re may be present in bituminous components of coal (liptinite). The other authigenic Re form may be its sulfide, ReS_2. However, Re sites in coal (modes of occurrence) is now only hypothetic; microprobe study is needed for more knowledge.
4. There are at least three genetic types of Re-concentrations in coal: Uzbek, Spanish and Kazakh:

    i.   ***In Uzbek type*** (Angren Ge-bearing brown coal deposit), Re is probably syngenetic. Its accumulation is due to enhanced Re contents in source rocks. Rhenium leached from terrigenic material may further be captured on reducing peatbog barrier – in organic or sulfide form.

    ii.   ***In Spanish type*** (Arenas del Rey and some others lignites) Re is also mostly syngenetic. Its accumulation is due to considerable contribution of the bituminous organics (like black shale) having extremely high affinity to Re.

    iii.   ***In Kazakh type*** Re is close associated with U and its companions, in the infiltration epigenetic deposits of the "*bed oxidation*" type. Re dissolved in oxidized waters as perrhenate ion ReO_4^-, may be captured in brown-coal beds on the reduction barrier, in organic or sulfide forms.

5.   Recently Re-bearing fumaroles were described in the Kurily Islands (Shaderman and Kremenetski, 2000). Therefore, some Re accumulations may occur in peatbogs of the volcanic areas, or in young lignites – in orogenic depressions with synchronous volcanism. Such Re accumulations may be associated with In, Ge, Mo, Bi and some other elements enriching the volcanic exhalations.

6.   Because Re is very valuable metal, Re-bearing coals may serve as Re industrial resource. The most promising are epigenetic uranium-coal deposits. In addition, some intermountain trough brown-coal fields must be studied for Re, if these coals are associated with volcanics.

ACKNOWLEDGMENTS

REFERENCES

Gracia, I. and Martin A. 1968. Volatilization of rhenium during combustion or gasification of rhenium-enriched lignites. *Ensayos Invest.* 3 (10), 3–8.

Kler, V.R. 1987. Lead, zink, molybdenum, rhenium, copper, cadmium. In: V.R. Kler, G.A. Volkova, E.M. Gurvich, A.G. Dvornikov, Yu.N. Zharov, D.V. Kler, V.F. Nenakhova, F. Ya. Saprykin, M. Ya. Shpirt. Metallogeny and Geochemistry of Coal-bearing and Oil Shale-bearing Strata of the USSR: Elemental Geochemistry. Nauka Moscow ("Science" Publ. House), 77–97.

Kler, V.R. and Nenakhova, V.F. 1981. Paragenetic complexes of mineral resources of the oil-shale- and coal-bearing strata. Nauka, Moscow ["Science" Publ. House], 175 pp.

Kronberg, B.I., Murray, F.H., Fyfe, W.S., Winder, C.G., Brown, J.R., and Powell, M. 1987. Geochemistry and petrography of the Mattagami Formation lignites (Northern Ontario). Coal Science and Chemistry. (Ed. A.Volborth). Elsevier, Amsterdam, 245–263.

Kuznetsova, V.V. and Saukov, A.A. 1961. On probable Re and Mo modes of occurrence in Mid-Asian coals. Geokhimia [*Geochemistry*] 9, 750–756.

Maksimova, M.F. and Shmariovich, E.M. 1982. Rhenium in infiltration uranium-coal deposits. Geol. rudnykh mestorozhdenii [*Geology of ore deposits*] 24 (3), 71–78.

Martín, A. and García-Rossell, L. 1971. Uranio y renio en rocas sedimentarias. II. Cuenca miocena de Granada. *Bol. geol. y minero* 82 (1), 65–69.

Martín, A. and García-Rossell, L. 1971 Uranio y renio en rocas sedimentarias. III. Lignitos de la depresión del Ebro. Bol. geol. y minero 82 (2), 62–69.

Martín, A. and Gracia, I. 1970. Distribution de renio dentro de las capas de lignito. Bol. Real. Soc. esp. hist. natur. *Sec. geol.* 68 (1–2), 111–117.

Ratynski, V.M., Shpirt, M. Ya and Krasnobaeva, N.V. 1980. On rhenium in coals. Dokl. AN SSSR [*Trans. Acad. Sci. USSR*] 251(6), 1489–1492.

Razenkova, N.I. and Kuznetsova, V.V. 1963. On study of the Mo and Re modes of occurrences in coals by means of electrodialysis. Tr. IMGRE [*Proc. Inst. Mineralogy, Geochemistry and Crystallography of Rare Elements*] 18, 20–24.

Shacklette, H.T. 1965. Elements Content of Bryophytes. U.S. Geol. Surv. Bull. 1198-D, 21 pp.

Shaderman, F.I. and Kremenenetski, A.A. 2000. Geochemistry of rare elements in recent metalliferous gas-and-vapor systems. 31th Intern. Geol. Congr. (Rio de Janeiro: Aug. 6–17, 2000) – CD-ROM.

Shpirt, M. Ya, Ratynsky, V.M., Zharov, V.M., and Zekel, L.A. 1984. Study of trace elements modes of occurrence and their behavior in coal processing. In: Razvitie uglekhimii za 50 let [Coal Chemistry Development During 50 Years]. Nedra, Moscow ["Entrails" Publ. House], 224–235.

Shpirt, M. Ya, Kler, V.R. and Pertsikov, I.Z. 1990. Inorganic Components in Solid Fuels. Khimiya, Moscow [*"Chemistry" Publ. House*], 240 pp.

Swaine, D.J. 1990. Trace Elements in Coal. London: Butterworths, 278 pp.

Valiev, Yu Ya, Gofen, G.I. and Pachadzhanov, D.N. 1993. Trace elements in the Jurassic anthracites of the Nazar-Ailok deposit (Central Tadzhikistan). Geokhimia [*Geochemistry*] 2, 243–251.

Valuable and Toxic Elements in Russian Run-of-Mine Coals. A Reference Book. 1996. (Yu N. Zharov, E.S. Meytov, I.G. Sharova, et al., compilers). Nedra, Moscow ("Entrails" Publ. House), 239 pp.

Yudovich, Ya E. and Ketris, M.P. 2002. Inorganic Matter of Coals. URO RAN, Ekaterinburg [*Ural Division of the Russian Acad. Sci.*], 422 pp.

Yudovich, Ya E. and Ketris, M.P. 1994. Trace Elements in Black Shales. Nauka, Ekaterinburg [*"Science" Pub. House*], 304 pp.

Yudovich, Ya E., Ketris, M.P. and Merts, A.V. 1985. Trace Elements in Fossil Coals. Nauka, Leningrad ["Science" Pub. House], 239 pp.

Yurowsky, A.Z. 1968. Mineral Components of Solid Fuels. Nedra, Moscow ["Entrails" Pub. House], 214 pp.

Chapter 5

State of the Art of the Prediction Methods of Ground Movements (Subsidence and Sinkhole) for the Mines in France

Marwan Al Heib

Laboratoire Inires-ecole des Mines de Nancy, France

1. Introduction

The ground movements due to the presence of underground voids, man-made (mines and underground cavities, saps, tunnels etc.) or natural (karstic cavities), can induce variable consequences on the surface (building and infrastructures) and on the safety of the people. The risk of ground movements relate to several countries in the world. Underground work is usually divided into two classes according to duration of activity: temporary activities like mines, or permanent like civil engineering projects (underground tunnels and spaces).

A site is designed to be stable and under control during only extraction period. The temporary character of the exploitations is justified by the mining period and site capacity. Such a definition is conceivable when the surface ground is neither urbanized nor in process of urbanization.

The exploitation of all iron mines - Lorraine (France) was stopped in 1997 and the last uranium mine was closed in 2001. Potashes mine (Alsace – France) ceased in 2003 and the last coalmine stopped in 2004. Today, only active mining industry in Metropolitan France comes out from the extraction of salt, using dissolution and room and pillar mining method.

The majority of the (quarries) underground mines (gypsum, limestone, etc., are also abandoned since long time. It thus remains very little of underground workings in activity.

On the other hand, current mining maps attest the importance of the underground activities during the past period. Today the management of abandoned underground mines obliges us to have tools for predicting movements induced by the degradations of underground structures (pillar and roof) leading to collapse and subsidence.

2. MINING METHODS

Surface subsidence occurs due to mining operations. Two families of mining methods are distinguished (Figure 1):

- Total exploitation where the ore is completely extracted and a treatment of the voids is assured. The void is replaced by a backfill (sands), or caved by the fractured layers of overburden. This method is called total exploitation by caving.
- Partial exploitation covering a broad range of methods: like the room and pillar method, the open stops, the marl-pits, etc. The partial exploitation is limited to exploitations at shallow depths. The limiting depth depends on the dimensions of the pillars and the resistance of the ore. The method of the reduced small islands is a mixed method, the exploited zones are completely extracted but are left separated from each other by pillars, and this method reduces the consequences on the surface. The exploitation of salt layers is also carried out by dissolution. Classification suggested makes it possible to identify two types of exploitation, which present behaviors basically different from the customary long-term stable ones.
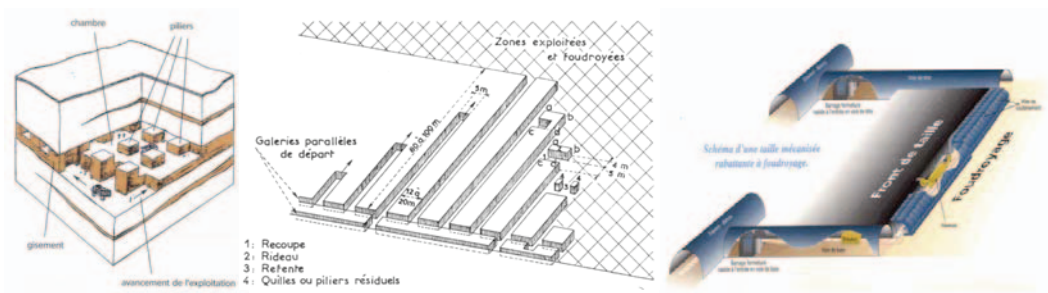
a-room and pillar   b-room and pillar with caving   c-longwall panel

Figure 1. Mining methods: partial and total mined area

3. MOVEMENT TYPES RELATING TO UNDERGROUND WORKINGS

The type of surface movement, the amplitude, the extension of the movements and finally the level of risk, depend on several factors: geometry and localization of the underground voids, in particular depth, the nature of the overburden, the presence of water and mining method.

These movements are divided moreover into two families: slow and progressive subsidence and brutal localized collapse (sinkhole) or generalized (discontinue subsidence). Figure 2 presents the two types of movements according to the depth of the exploitation.
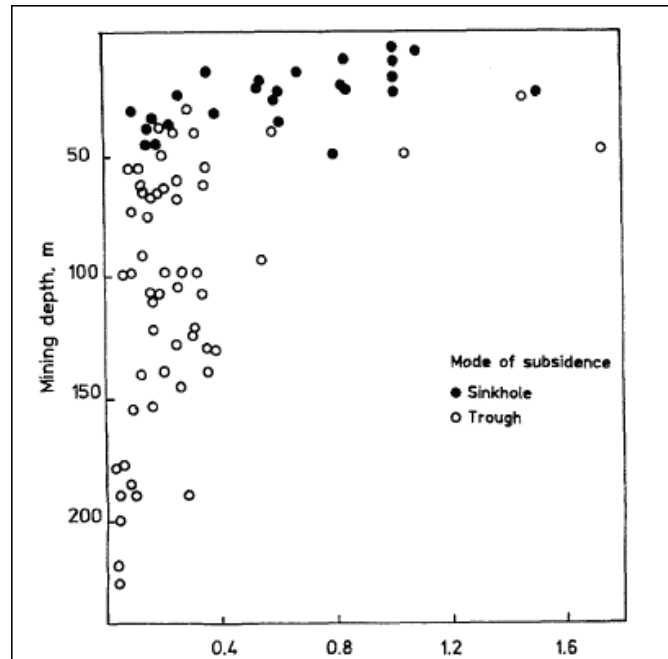
Figure 2. Types of movement (subsidence - trough or sinkhole) according to depth (Sheorey et al., 2000)

Subsidence is the settlement of the soil without failure and discontinuities on the surface (Figure 3). The ground movement is linked with the re-distribution of tresses around underground cavities resulting from the extraction or the disappearance (dissolution, combustion, and even pumping) of ore. These movements, of which the character is generally slow, progressive, and flexible, take the form of a topographic depression on the surface, without important breakable rupture, taking a form of settlement trough. These movements can relate to the total exploitations (removal of total ore) or partial major in the event of collapse of underground work. One distinguishes two types of brutal movements: localized collapse (sinkhole) relates to isolated cavities or crossroads from partial exploitations at a shallow depth and generalized collapses concerns a large room and pillar area.

Figure 3. Examples of movements (subsidence and sinkhole) induced by underground mines

Localized collapse (sinkhole, Figure 3): sinkhole can occur during the extraction of the anthropic cavities (mines, careers, well and tunnels) if yielding ground conditions are presents (a fault or a heterogeneous zone for example). A localized collapse is characterized by the sudden appearance on the surface of a crater of collapse whose horizontal extension generally varies few meters with a few tens meters in diameter. They can appear long time after the abandoned of the mines (several centuries).

Generalized collapse, which is rarer than local collapse, can comparatively assign major partial exploitations to localized collapse. The nature of overburden and the characteristics of the exploitation (proportion of extraction) play an important part in the initialization of collapse. The formation of a generalized collapse also requires a sufficient horizontal extension of work compared to the depth. They appear on the surface and form often discontinuous basins marked by important cracks.

These movements can occur during mine activities and after the closing of mine (Szwedzicki, 2001). The surface movements after the abandoned work are due, in this case, to the ageing or the creep of the rock, the submergence of the underground voids after their abandoned and to the dynamic actions inducing of the vibrations (traffic, mine blasting, military blasting, etc.) in the cavities with very low depth (Szwedzicki, 2001). The underground structures grow to unstable situation and the environmental factors contribute to a differed rupture of the overburden until finding a new durable stable configuration.

4. SUBSIDENCE PREDICTION

4.1. Movement description

The deformation undergone by the grounds of surface following a progressive subsidence breaks up classically into a vertical movement (V) of the ground, called subsidence (S), and a horizontal movement in the plane (U) (Piguet and Wojtkowiak, 2001).

The effects on the surface of subsidence (U and V) are felt apart from the balance of the underground voids. The angle formed with the vertical and the line that connects the edge of the basin at the edge of the underground voids is called the angle of influence (γ).The existence of a dip and faults influences directly the shape of curves and the values of the draw angles. The angle of break (θ) corresponds to the maximum extension strain and the curvature of grounds (Figure 4). The value of the angle of break is largely lower than the angle of influence.

In addition to vertical and horizontal displacements, the subsidence trough can be characterized in each point by the tilt, curvature, and horizontal strains (in compression and extension). Figure 4 presents the profiles associated with each component with depression (horizontal and vertical displacements, horizontal deformation, slope and curvature), schematically for a horizontal exploitation of critical width (W_C).
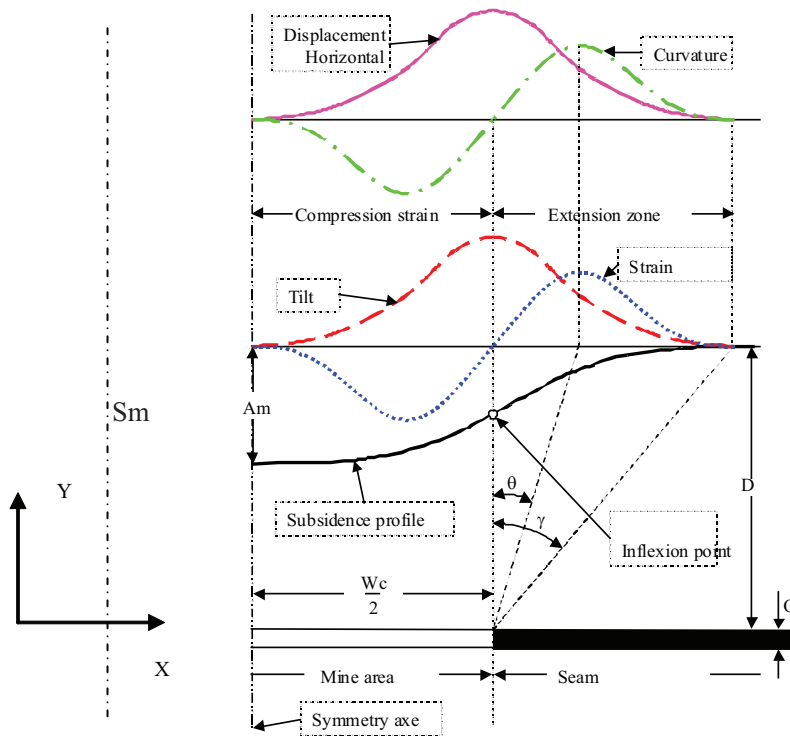
(O: layer open, D, depth, Wc: Width of panel, Sm: maximal subsidence, γ and θ: draw angle and failure angle, U et V horizontal and vertical displacements following X et Y)

Figure 4. Vertical, horizontal, horizontal deformation (strain), tilt and curvature profiles of an undermined rock-mass in flat seam for a critical area of extraction.

4.2. Different stages of the subsidence

For an active exploitation, the feedback available on various French and European fields indicates that the near total of subsidence occurs in the days that follow the extraction. For an abandoned exploitation (by the room and pillar method), subsidence intervenes when the phenomenon of failure of the pillars is initiated within the mining work, under the possible effect of a starting factor (modification of the state of stress or the environmental parameters for example). The subsidence of a point of surface is function of the rate of advance underground work and the creep of the rock. Final subsidence (S_f) for an underground working is the sum of three successive movements (Figure 5-a):

- Phase I, known as initial subsidence, corresponds to the period during which the exploited zone broken down at the bottom penetrates in the influence cone of the observed point (Figure 5-b). In the case of the abandoned mines, several years can correspond to this phase. The influence cone, for a point, is defined by the angle of influence (γ) and the depth (D) of the mine. The subsidence of this phase generally accounts for 10 to 15% of final subsidence;

Starting point
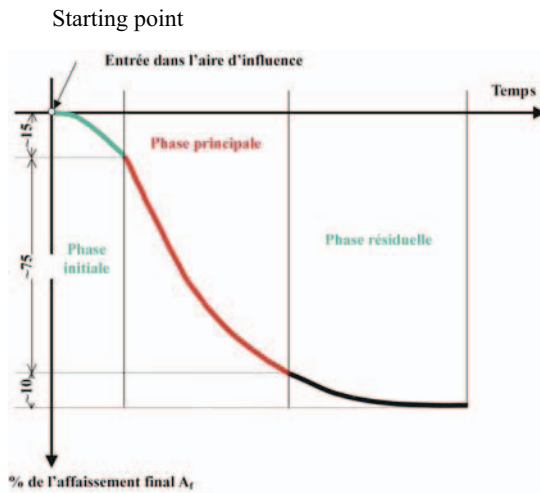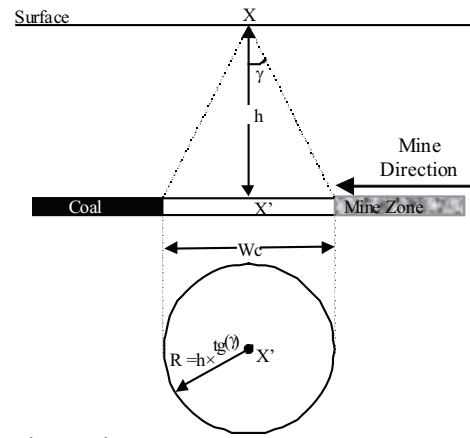
Figure 5-a

Figure 5-b

Figure 5. Influence zone of a point located on the surface over an exploitation area - Typical evolution of a subsidence profile according to the time

- Phase II, known as the principal or the accelerated subsidence phase, it corresponds to the period of subsidence during which the face of the exploited or broken down zone moves away from the vertical of the point, until it left the cone of influence of this point. The values resulting from the bibliography show that depression during this phase, is close to 80 to 90% of the final amplitude of subsidence. It develops classically over a period varying from a few days to several months according to the progress of the work or the rate of failure of the pillars. It is thus the most critical phase during which an attentive follow-up of the evolution of the structures present on the surface can prove to be necessary;

- Phase III, known as residual subsidence (or differed, or delayed) constitutes the final phase of depression. Dependent on time, it continues after the exploitation exceeds the cone of influence of the point considered. Residual subsidence represents only small part of the final total subsidence. After this phase, subsidence value does not move any more. One speaks about stabilized movements.

Table 1 presents examples of residual subsidence values in various countries for coal and iron mines. It is noted that the amplitude of residual subsidence is lower than 10% (except Indian mines, worked at a shallow depth) of total subsidence and its duration lower than 7 years for all the observed coal and iron mines.

Beyond this date, it is difficult to distinguish the natural movements from those induced by exploitation (Al Heib et *al.*, 2005). For the salt mines, the duration of residual depression is perhaps more important.

Table 1. Amplitude and duration of residual subsidence for different coalfields

Case	Mining conditions	Residual subsidence
King dome (Many basins)	Long-wall Plastic over burden	Some months to 1 year for 5 to 6 % of total subsidence
King dome (Durham Coalfield)	Two long-wall mines Strength and competent overburden	6 years for total subsidence The residual subsidence varies between 6.8% and 9%
West Germany	Many long-wall with caving	5 years for the total residual phase but 75% of residual subsidence obtained after 1 year
Australia	Long-wall with caving	3 months
India	Long-wall green land	10 to 20 months; residual subsidence 10 to 30% of total subsidence.
India – Raniganj – west Bengal	Short long-wall with pillars – shallow depth (50 m)	Stabilization of subsidence after 2 years
United Stats	Long-wall excavated layers.	2 to 4 months Residual subsidence is 5 to 10 % of total subsidence
	long-wall	12 % of total subsidence 18 months
Basin d'Illinois	long-wall	7 years for total subsidence
Nord-Pas-de-Calais Albi – Carmaux	Plastic overburden Many seams	99% of total subsidence obtained after 18 months to two years
French coalmines Provence, Lorraine And Blanzy	Competent overburden Many seams	99% of total subsidence obtained after 2 months to 3 years
Iron mines – France – Rencourt (1998)	Room and pillar and sub critical zone	15 % during 6 years after collapse (1998 – 2004)
Iron mines – France – Moutier (1997)	Room and pillar	5 % during 1 year after collapse

4.3. Subsidence prediction methods

The basic aim of all prediction methods is to produce an acceptable accurate assessment of mining subsidence and in some cases, its associated effects on surface structures and ground conditions (Whittaker and Reddish, 1989). The first prediction methods for ground movements started; there is more than 100 years. Chrzanowski *et al*., (1998) provided an outline of the history of the ground movements. It is often carried out using empirical

methods or semi-empirical (Bahuguna *et al.*, 1993, and sometimes numerical (Al Heib, 1993, Aissaoui, 1999 and Abbass Fayad, 2002, Aksoy *et al.,* 2003). Several national and international conferences covering the subject took place in the world[1].

Several prediction methods are exposed in the literature. The empirical methods need the experience feedback to predict the future movements on the surface.

The influence functions are based on superposition of movements for surface points. It is based on the theory that there is an area of influence around a point due to the extraction of small elements within the sphere of influence of that surface point.

The profile function methods predict profiles in two directions across an excavation. They generally used the geometry of the excavation along with equations or tables of data to predict a longitudinal or transversal profile for subsidence and strain (horizontal deformation). The methods of the abacuses make it possible to constitute the profile function (Whittaker and Reddish, 1989, Kratzsch, 1983, Wagner and Schümann, 1991, Peng, 1992).

The numerical methods are also employed (Alejano an *et al.,* 1999, Coulthard and Dutton, 1988, McNabb, 1987, Gilbride *et al.,* 2005). In spite of their potential, the success of numerical methods is less to predict the movements on the surface, whereas than empirical methods. They are very powerful to understand, analyze and determine the mechanisms of movements (Piguet, 1983, Al Heib, 1993, Karmis and Agioutantis, 1999).

The advantage of empirical methods compared to the numerical methods is their capacity to predict the movements with a high degree of accuracy for the concerned basin. On the other hand, the numerical methods are more universal, but they require a thorough knowledge of the grounds and their behavior than the empirical methods. We lastly developed hybrid methods using the advantages of the empirical and numerical methods (Al Heib *et al.,* 2001, Aksoy *et al.,* 2003). Among the empirical methods, allowing predicting maximum subsidence, Proust and the NCB (National Coal Board) methods are the most ones used in France, those methods called also abacuses method (charts). These methods are primarily geometrical; the geometry of the subsidence trough is linked to the geometry of the exploitation.

The method of Proust proposes the following relation to predict maximum depression in the center of a panel:

Sm = O * f1* f2 * G

With: O: opening of the cavity or the worked seam; f1: factor which depends on the control mode of the roof, which varies between 0.25 (pneumatic filling) to 0.9 (caving or integral removal of pit props); f2: factor of depth, grows initially according to the depth then stabilizing themselves or decreasing. For the coalmines of Nord and Pas-de-Calais (France), the factor f2 varies between 0.7 and 0.8 for work with depths lower than 500 m and equal to 1 for depths higher than 500 m, which is also the case of the English coalmines (NCB, 1975). For Lorraine coalmines, one considers that the factor f2 is equal to 1 for depths ranging between 300 and 600 m and 0.8 for depths higher than 600 m. Figure 6 presents the Indian coalmines experience at very low depth, ranging between 50 and 250 m, where subsidence grows almost linearly according to the depth. This evolution of the factor f2 is explained by

---

[1] International Society for Mine Surveying (IMS) organizes for example since 1969 of the conferences devoted to the sets of themes of movements of grounds.

the consolidation phenomenon of the caving grounds under the weight, growing with the depth of mine. Beyond the threshold, this phenomenon is counterbalanced by arching phenomena and by the fact that the conditions of appearance of sub-critical situations become increasingly frequent with great depths; G factor of dimensions of the exploitation, G varies according to the width and the length of the cavity compared to the depth.
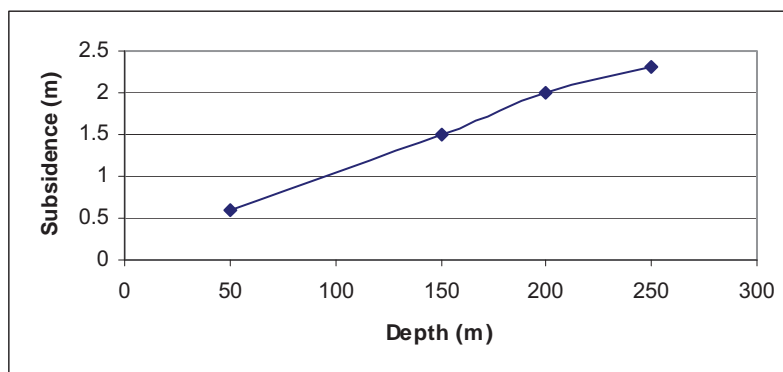
Figure 6. Variation of depression according to the depth for an exploitation supercritical (Singh and Yadav, 1995)

Using maximum subsidence located in the center of the cavity, one determines the profile of the basin using the empirical relations or the abacuses (charts). The method of the abacuses of NCB (NCB, 1975) consists in establishing an empirical curve connecting maximum subsidence to the center of the cavity to the opening and the ratio width/depth (cf. figure 5). This curve can be established only starting from measurements. The subsidence trough is drawn using the influence functions or standard profiles (Aissaoui, 1999). The method of the abacuses can be adopted to predict a progressive depression due to exploitation in activity or abandoned. The prediction of subsidence is often checked thanks to a follow-up of the ground by topometric measurements.

The prediction of the deformation is more difficult because the absence of direct measurements. Nevertheless, the continuous mediums theory enables us to calculate these deformations by deriving the curves from vertical (v) and horizontal (U) displacements if these last are known: the horizontal deformation (strain): $\varepsilon = \dfrac{\partial u}{\partial x}$, the tilt $P = \dfrac{\partial v}{\partial x}$ and the curvature $\rho = \dfrac{\partial^2 v}{\partial^2 x}$.

The empirical relations were established by experience feedback and from the rare measurements to calculate their value according to measured subsidence. Deck (Deck, 2002) listed more than 30 empirical relations to estimate depression, the horizontal deformation, the slope and the curvature. The following empirical relations are often proposed to consider the maximum horizontal (deformation) strain (Wagner and Schümann, 1991, Sheorey and *al.* 2000) $\varepsilon_{max}= \alpha Sm/D$ and the maximum tilt $P_{max}= \beta\,Sm/D$ where Sm is maximum subsidence in the center of the panel and D the depth. Parameter α varies between 0.5 and 1 and β varies

between 1 and 4. These values allow the dimensioning of the works and the exposed structures and the evaluation of the structures damage.

The empirical methods allow the prediction of total and residual subsidence of abandoned mines subject to potential subsidence. This prediction is necessary to determine the amplitude and the extension of the subsidence of the already subsided zones. It is also useful to estimate the amplitude and the duration of residual subsidence and to predict the characteristics of progressive subsidence due to a failure of the pillars of the partial exploitations. We will describe the relations established by feedback experience for the exploitations of French coal and iron mines. The coalmines are deeper (>400 m) than iron mines (<200 m).

4.4. The case of French coalmines

The exploitation of coalmines in France was stopped in 2004. There are no more movements induced by the production run. The establishment of administration stop folders includes the estimation of the movements previously induced by the exploitation and calculation of the amplitude and the extension of residual subsidence.

In the coal basins of Nord and Pas-de-Calais and Lorraine, the method of Proust was used (Proust, 1964) to estimate the subsidence for exploitations by caving and backfilling for a depth higher than 500 m. In Provence coalmine (southern of France), the method of NCB was employed thanks to an empirical profile function (figure 7) established by Arcamone (1980) and checked by Aissaoui (1999). The prediction obtained with this curve is generally in conformity with *in-situ* measurements.

% S/O

W/D

Figure 7. Curves of the forecast of subsidence in the center of the panels according to the geometrical parameters (Width, Depth, Open or Thickness of extraction area), Provence coalmines.

In Lorraine, one often used the method of Proust with factors (f1, f2) given according to the experience. Using many measurements available on the Vernejoul field, we compared the prediction model of Proust with *in-situ* measurements using high precision leveling techniques for 12 configurations in the Lorraine basin (Field of Vernejoul – La Houve). Figure 8 presents a geological cut of the grounds above the exploited coal seams of the field of Vernejoul (La Houve). The overburden is rather resistant and consists of sandstone and conglomerates surmounted of 200 m Vosgean sandstone. The mining method is long-wall with caving, panel width is about 200 m and the length is variable. The depth of the exploitation varies between 450 m and 1000 m.
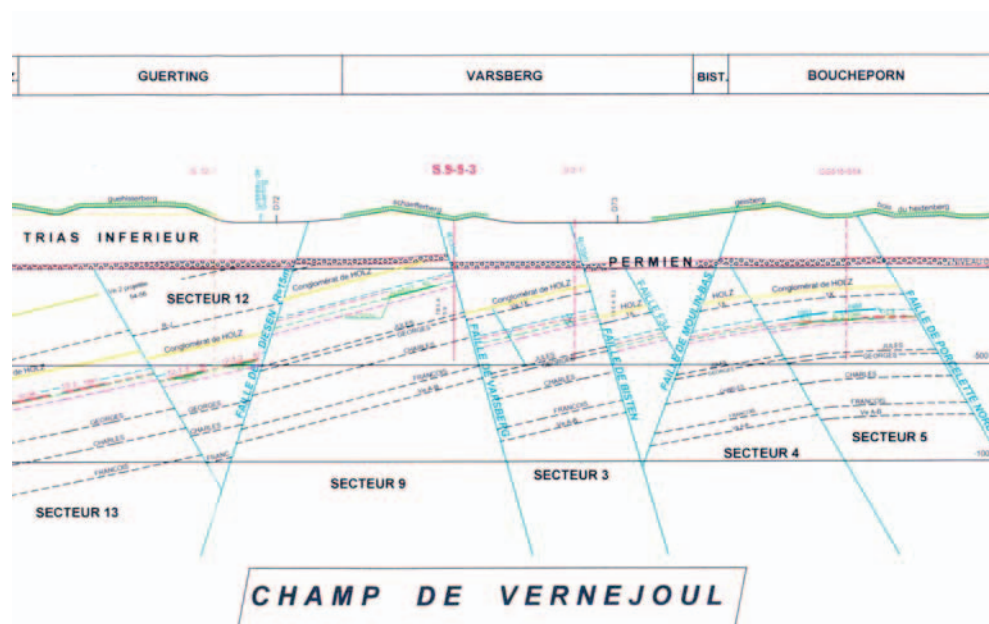
Figure 8. Simplified geological cut of the Lorraine coal basin

Appendix A and B presents the geometrical characteristics and maximum subsidence at the center of the studied panels. Dimensions of the panels are sub-critical, lower than 0.8 times the depth. We presented on Figure 9 (width/depth) and (subsidence/thickness) the ratios of the whole of the cases as well as the curve of Proust. *In-situ* measurements showed clearly that the method of Proust over-estimates the amplitude of maximum subsidence for sub-critical panels; the difference between measurements and the prediction subsidence is about 35%.

We consider that the empirical profile established for the field of Vernejoul (La Houve) allows a precise estimation of the maximum subsidence at center of an exploited zone. It takes into account of the geological and mining environment of the exploitation. A prediction profile of the maximum subsidence, even after the stoppage of the works, is interesting for the management of closure mines. The influence angles (draw) vary between 15° and 40°. The measured average angle is of 32°. If it is considered that maximum subsidence is obtained for a critical width, with 1.4 times the depth, one can determine an angle of influence of 35°. This angle is slightly higher than the measured average angle. An angle of 35° is generally retained

to delimit the zone of influence of the exploitation of the coal basins; this angle varies according to the dip of the worked seam (Huayang et *al.*, 2002).
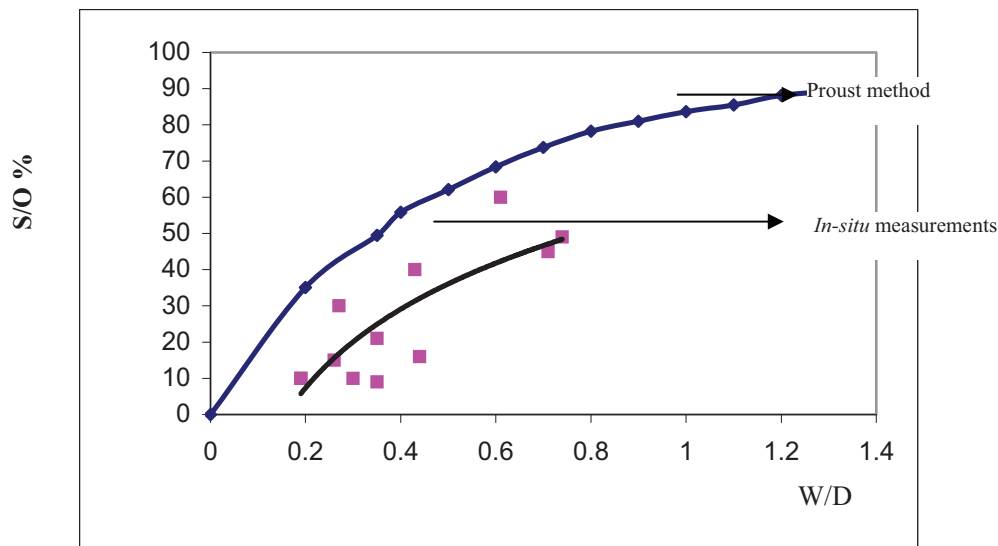
Figure 9. Curves of maximum subsidence (S) in the center of the extraction area, according to the width (W) and the depth (D) of exploited panel - La Houve – Lorraine coalmine.

4.5. Lorraine iron mines (France) experience

The French iron mines are not worked any more since 1997. The Lorraine iron basin, one of important in France, is localized in the North-East. The iron formation has a thickness from 30 to 50 m and small dip (Figure 10). The depth grows in the west to reach 300 m. Several mining methods were employed such as given up room and pillar, total exploitation by removal of pit props, reduced small islands. The overburden corresponds to a succession of marl and limestone of variable thickness.

Several collapses took place, of which majority, after the abandoned of the exploitation (El Shayeb and *al.* 2001, Deck, 2002, Fairhurst and *al.* 2003). In this context, we analyzed 18 cases resulting from the exploitations of the iron mines - Lorraine. They correspond to 11 cases where movements induced at the time of the exploitation by removal of pit props (total mining method), 6 cases where movements measured after a progressive collapse and 1 case, which movements measured after a brutal collapse.

For each case, we have the characteristics of the subsidence trough and the underground voids (appendix 2). The depth varies between 120 and 250 m. We present for each case the couple of data (width/depth and subsidence (extraction ratio* thickness)). An equivalent thickness was been calculated from extraction ratio. For Joeuf case (n°1), we have measurements for several dimensions of the exploited panels. From the data, we plotted two curves: the first curve corresponds to a partial exploitation with only one worked seam and the second curve corresponds to two worked seams separated by a bed thickness lower than 7 m. We thus have two curves to predict the maximum subsidence of the iron mines -

Lorraine, for exploitation in only one layer or two layers (figure 11). The cases of subsidence due to a progressive collapse were projected on figure 11. The ratio "width /depth" varies between 0.8 and 1.6, corresponding supercritical width; the maximum subsidence varies little. The points corresponding to the progressive collapse are perfectly comparable with the cases of total exploitation method.
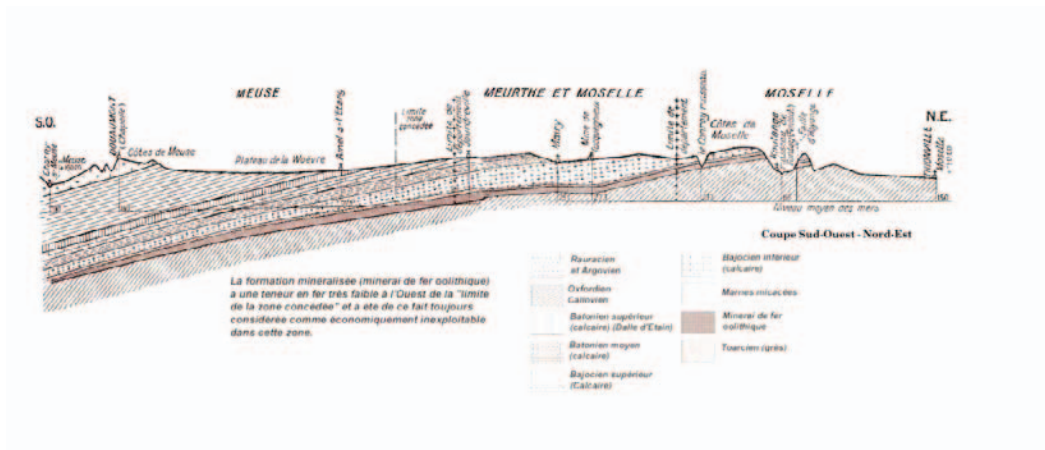
Figure 10. Geological cut NE-SO simplified of the Lorraine iron-bearing basin.

The only analyzed case of a brutal collapse shows induced subsidence is identical to case of removal seam in only one layer thus these curves are applicable for the prediction of the surface movements of progressive subsidence hazard. One can note that the subsidence curve starts for a width of underground panel equal or higher than 0.4 D. maximum subsidence is observed for a width/depth ratio equal to 1, the average angle of influence corresponds to 25° (Wc=2*tan γ*D, Wc is the critical width). The comparison between the curves (figure 9) shows that the subsidence due to iron mines, for sub-critical width, is less than subsidence of coalmines. For critical and supercritical widths, the difference is less important. The difference is probably due to the nature of grounds and the depth of the exploitation.
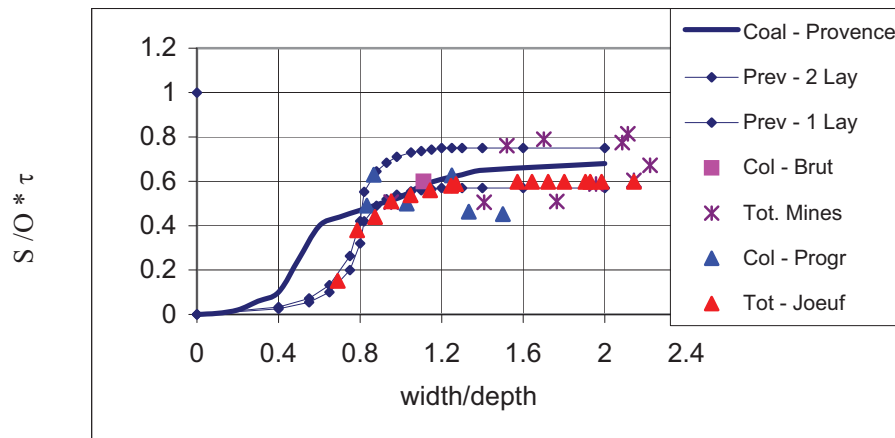
S: Subsidence at the center of the basin and O: thickness of the layer, τ: ratio of extraction.

Figure 11. Curves of forecast of subsidence for the iron mines - case of exploitations in first layer and second layer.

The angle of influence (draw angle) was given from measurements of subsidence by calculating the distance between the edge of the exploitation and a point having a very low movement (<5 cm), taking into account the precision of topometric measurements. This angle varies according to the border of the mining zone. Three situations were distinguished (Table 2):

- Green limit: case where the exploitation is limited by a virgin zone or a barrier pillar (sufficiently large pillar, higher than 0.4 times depth). The angle of influence varies between 0 and 10° with an average value around 6°;
- Few galleries: case where the exploitation is limited by a few galleries. The angle of influence varies between 6 and 29°. The angles of influence increase with the proportion of extraction of the surrounding zones. The average value is of 16°;
- Extraction area: case where the exploitation is limited by a mined area on a critical or supercritical surface. The angle of influence varies between 23 and 40°. The average angle is of 30°. The important angles are explained by the resumption of depression above the pit props removal zones at the time of the exploitation of a close zone.

The average angle of influence of the iron mines (25°) is less important than that of the coalmines (35°). This difference is due to the mining method, the nature of grounds and the depth. The prediction of maximum subsidence, due to potential collapse of room and pillar mined area of the Lorraine iron basin, is from now possible. An equivalent thickness of the worked seam is calculated proportional to extraction ratio. Concerning tilt prediction, the parameter β, allows calculating the tilt, were also given from *in-situ* measurements (Al Heib et *al.*, 2005). The value of the parameter (β) of the maximum slope (Pmax), in edge of a few mined area or a virgin zone, is equal to 5 on the other hand, for a zone near a depilated zone, it is equal to 3.

Table 2. Angles of influence in the Lorraine iron-bearing basin according to the environment of the exploitation

	Green limits	Few galleries	Extraction area
Average	6°	16°	30°
Limit values	[0°-10°]	[6°-29°]	[23°-40°]

Concerning stain prediction, in absence of measurements of direct horizontal (deformation) strain, the parameter (α) of horizontal strain is considered equal to 1.5, which corresponds to the maximum value of the parameter of Lorraine coalmines. The indicated parameters on are used in the Lorraine iron basin in order to establish risk maps of ground movements of the old and abandoned exploitations (Josien, 2006).

5. SINKHOLE PHENOMENA

A located collapse concerning an isolated cavity or a crossroads from limited dimensions, is often called a sinkhole. Localized collapse (sinkhole) is associated with abandoned exploitations or natural cavities at shallow depth (Figures 2 and 3). The sinkhole instability results from the increase of a failure initiated within an underground excavation (gallery, room, isolated cavity…). The vault initiated by the rupture of the roof of the excavation is not stabilized mechanically in the absence of massive layer within overburden; it is propagated gradually towards surface (Figure 12). If space available within the goaf is sufficient so that the blown in and abounded materials can accumulate there without blocking the phenomenon by "auto-filling." The vault can reach the surface of the ground. If the development of a rise of vault is a very slow phenomenon, which can take several years or decades, the appearance of the sinkhole on the surface is done, as for it, in a sudden way, which makes the phenomenon potentially dangerous for the people and the facilities that located in its influence. The appearance of this type of disorder on the surface relates to only major work. The experience feedbacks carried out on several fields thus showed that, except geological specificity or of exploitation, beyond of about fifty meters of depth (and sometimes less), the old mining vacuums were not likely any more to cause this phenomenon on the surface.
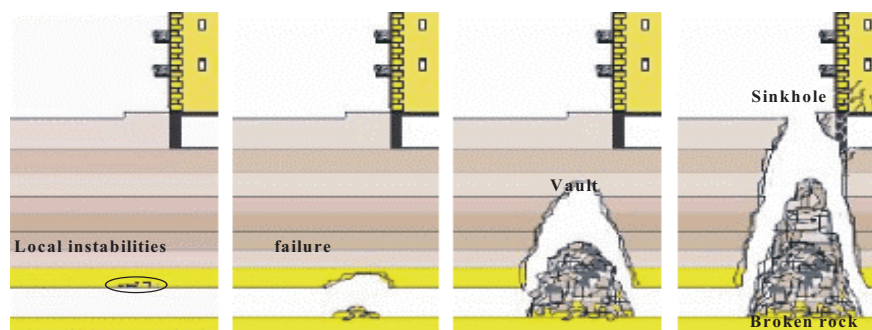
Figure 12. Various stages of the sinkhole formation from the roof of an underground cavity to the surface.

5.1 Sinkhole prediction using empirical methods

The prediction of the formation of a sinkhole is more difficult than that of a progressive subsidence, taking into account the mechanism brought into play which does not result in measurable signs on the surface (Josien, 1999, Debasis and Choi, 2006). The hazard of sinkhole is determined according to the cavity depth. The maximum depth so that a sinkhole emerges on the surface, according to the experience feedback (figure 1), is 50 m (and sometimes less), (Kalendra and Bharat, 1997). In the Paris basin, one considers the depth ratio/height of the cavity, the sinkhole risk is possible if the ratio is lower or equal to 15 (Vachat, 1982). Piggot and Enyon, (1977) consider that there is no risk for a ratio higher than 10. Stathan and Treharne (1991) note that 90% of the sinkholes appear when the ratio depth/height is lower than 6. Figure 13 presents the distribution of the sinkholes according to the depth of the limestone and gypsum mines on Paris area. The rare cases exceeding a ratio of 15 correspond to the presence of a great thickness of fill soil or an exceptional height. These simple empirical rules do not make a difference between bulking grounds (cohesive soil) and the overburden ground contains sand and waste soil. The height of the bulking of beds is an important factor and plays a main role to predict the risk of sinkhole. Another approach is often proposed (Whittaker and Reddish, 1989, Didier and Salmon, 2004), based on the filling of the underground voids thanks to the expansion of the grounds of overburden (figure 14). The sinkhole emerges on the surface if the volume of bulking volume of ground (3 of figure 11) is lower than the sum of the initial volume of the void (1 and 2) and of the ground of covering (3).

$$V (3) * K < V (1) + (V2) + (V3) \text{ with } K: \text{ bulking factor}$$
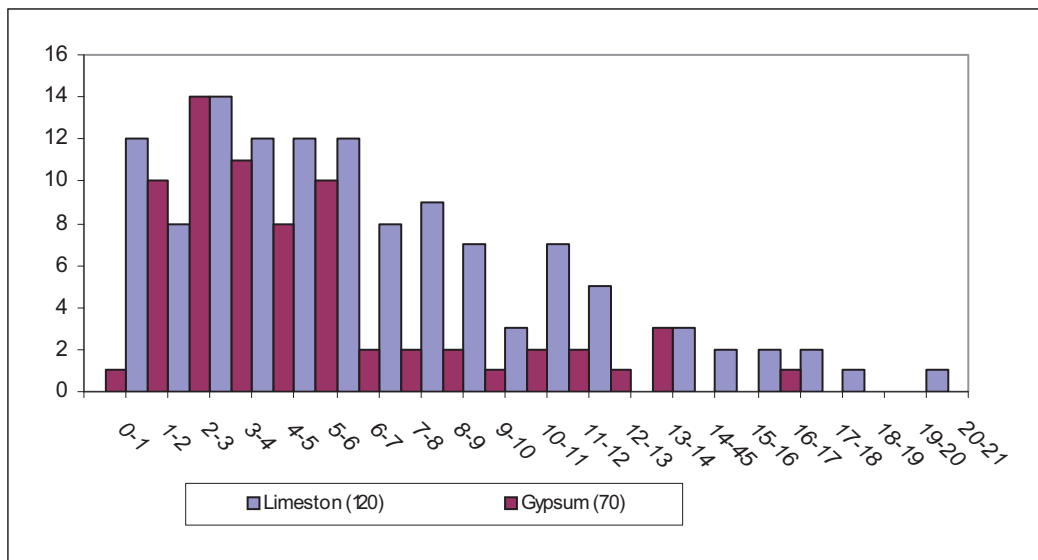
Figure 13. Histogram of ratios depth D to height of galleries (H) affected by sinkhole emerged on the surface for limestone and gypsum mines - Paris (given by Inspection Générale des Carrières, accidents covered the period from 1977 to 2000).

In this case, the geometrical parameters of the cavity (width, height, length) and the characteristics of overburden layers (bulking factor (K), angle of repose of caved rock within mine rooms adjoining collapse area (zone 2), etc.) are taken into account. This approach is useful; nevertheless, it requires the precise knowledge of parameters quoted above. The uncertainty of the prediction depends on the precision of the data. Several researchers propose to take into account uncertainty in the prediction of the increase of subsidence thanks to probabilistic models (Didier and Salmon, 2004, Cauvin *et al.*, 2005).

1: gallery volume ;
2: broken rock with a slop angle
3: overburden volume
4: surface soil
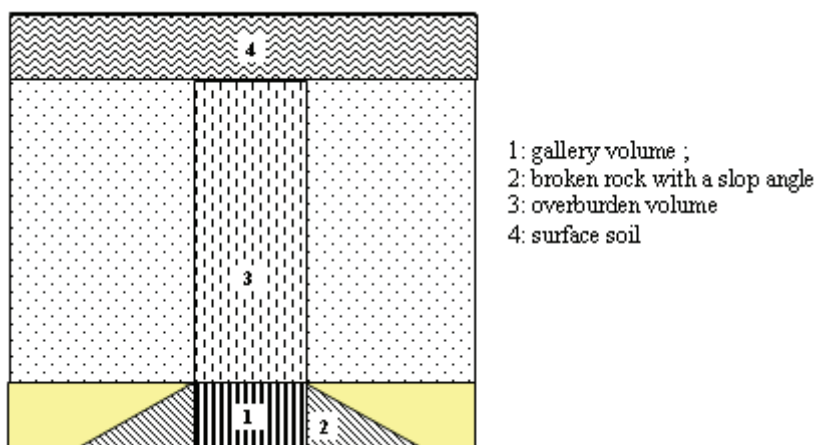
Figure 14. Balance volumes for the increase of subsidence above an underground gallery

5.2. Prediction sinkhole using analytical methods.

The analytical methods are employed more and more to appreciate the behavior of the ground of covering compared to a succession of the beams (Fgure 15). The method of elastic, thin beams makes it possible to often simulate each layer of the roof by a beam on supports, infinitely rigid, simple completely embedded or sometimes partially embedded. The influence of the horizontal stress is often not taken into account. The calculated stresses are compared with the tensile strength of the beam (Mandel, 1959; Fine, 1993; Ennour, 1993; Swift and Reddish, 2002).

The rupture is initiated in the medium for a beam on simple supports. On the other hand, it is initiated at the ends for a fixed beam. This method requires the precise geology knowledge to identify the characteristics of the various layers of overburden (fracturing, thickness and breaking strength, etc). These parameters are essential to determine the risk of sinkhole formation. This method is generally applied to the first layer of the roof. To improve this method and to make it more faithful to *in-situ* inspections, we proposed to calculate stresses by taking into account the stiffness of supports (the nature of the worked seam), layers thickness allowing to distinguish a thick beam from a thin beam, and especially of the distribution of the stresses according to the behavior post-rupture of the rock. The data necessary are geometrical and geotechnical (Abass Fayad *et.al.,* Heib, 2005). The height of the unconsolidated area is determined by successive iterations (Abbass Fayad *et.al.,* Al Heib, 2005). With each stage, one determines the part of layer of the roof whose requests (traction,

shearing and compression) exceed the limits of resistances of the rock. Part of the overburden concerned with the rupture abounds then to fill the voids.
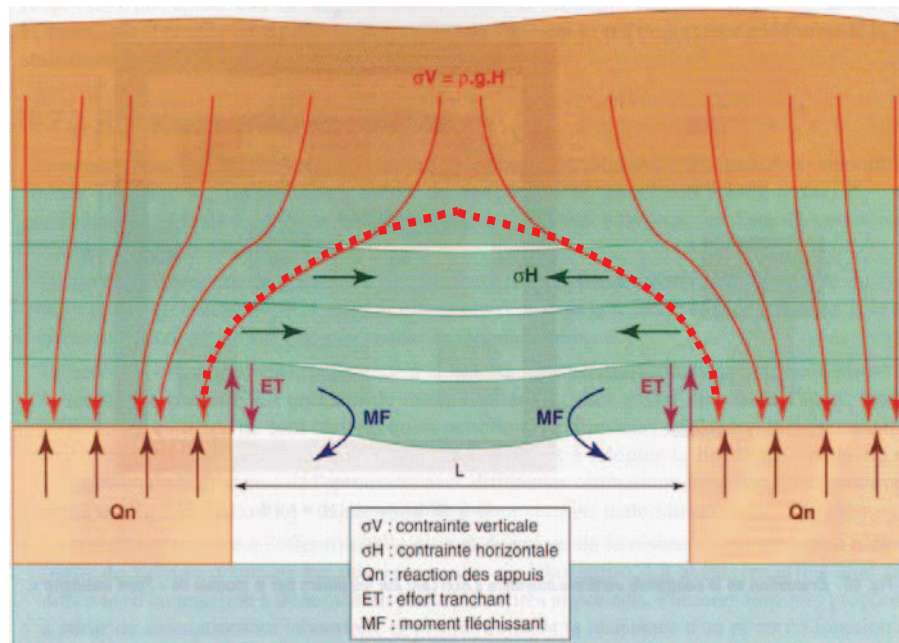
Figure 15. Bending beam model for a laminated roof of underground cavity.

Using the approach of the plastic beams, we simulated the case of a gallery isolated to 8 m of depth under a laminated overburden. Figure 16 presents the increase of subsidence, the shape of the vault and the filled part. The result obtained depends on the geometrical parameters of the layers (thickness) and their mechanical characteristics.
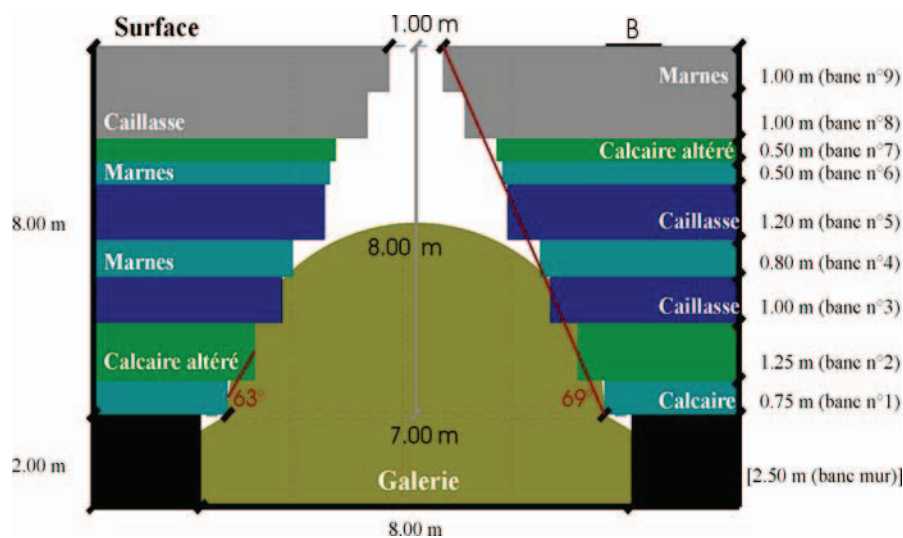
Figure 16. Simulation of the increase of subsidence using the analytical approach in elastoplastic beams.

The modeling of an underground cavity by a continuous medium (finite elements and boundary elements methods) provides the extension of the plastic or damaged zones, without however determining the characteristics of the vault and the real amplitude of the movements on the surface. Numerical modeling using the distinct elements method (code UDEC) was used to determine the evolution of the vault of sinkhole until surface (Figure 17). The adopted methodology is as follows (Abbass Fayad *et al.,* 2004): the plastic zones crossing completely the section are replaced by discontinuities. Successive calculations taking into account the new geometry and discontinuities are undertaken until the disappearance of the plastic zones or the impossibility of the creation of the new fractures. The stability of roof layers was studied until obtaining the balance of stresses. The final result is the shape of the sinkhole vault emerging or not on the surface (Figure 17).

A-numerical calculation: initial state of the plastic points

B-replacement of alignments of the plastic points by fractures

C-successive calculations and formation of the vault
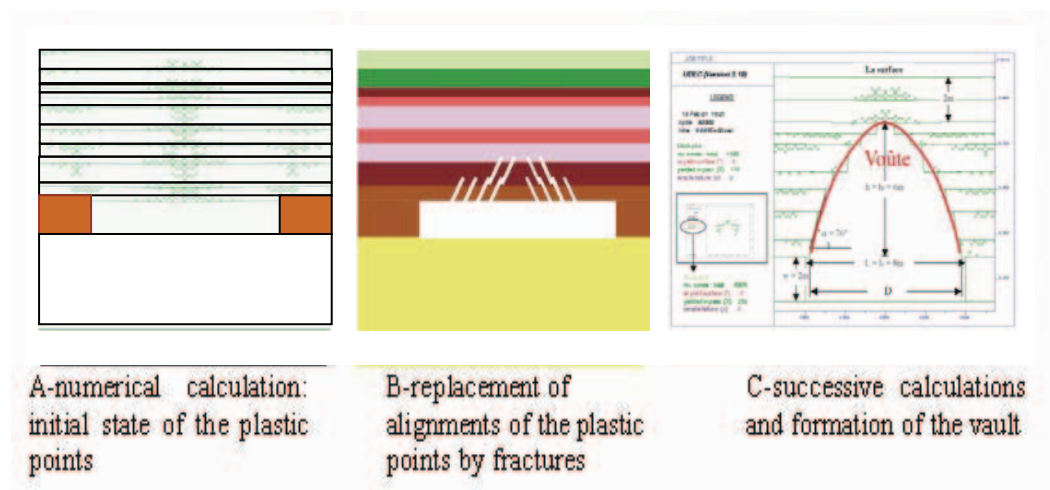
Figure 17. Modeling the progression of a sinkhole using the distinct element method (Abbass Fayad *et al*., 2004).

Compared to the methods quoted before, the numerical methods are more general using for geometrical and geological underground configurations. Nevertheless the number of data necessary depends on the sophistication of the adopted model.

The discontinuous methods thus have an advantage for the prediction of appearance of a subsidence (Abbass Fayad et al.,. 2004). Several more or less strong assumptions are necessary to the application of the Distinct Element method (DEM): geometry of the overburden layers induced fracturing and a pre-cutting of the initially continuous medium in blocks of varied size imposed before calculation. The determining of discontinuities parameters (normal and tangential stiffness) is difficult for a particular case. Nevertheless, this type of calculations makes it possible to study the mechanisms of subsidence and sinkhole, the shape of the vault according to the nature of the grounds and to calculate the coincidence factor according to dimensions of the blocks, etc.

The different discontinuous medium approach was recently proposed. The soil is simulated by a granular medium characterized by dimensions of the particles (circular or an assembly of the circular particles), the porosity of the medium and the type of contacts (linear, standard Hertz Mindlin, cohesion-tension), a code was developed by Itasca above theoretical approach is PFC (Flow Particles Code). The data needed for the model are on a

microscopic scale. The simulation of laboratory tests is necessary to obtain the characteristics of rock mass. The fundamental difference between the two approaches of discontinuous medium lies in the creation of fractures. In PFC2D, the contacts between the particles break and are created according to the state of stresses calculated to each cycle. The results of this modeling make it possible to determine the form of sinkhole and the value of the bulking factor (Sabri, 2002; Gilbride et al., 2005; Caudron, 2007). Figure 18 presents numerical modeling example of sinkhole formation above a circular cavity (6 m in diameter at 9 m depth) using PFC code. The particles are rigid and the contacts are of Mohr-Coulomb type (with an angle of friction of 45°). One distinguishes on the surface the formation of a subsidence (sinkhole) corresponding to 3.3 m depth. The width of the subsidence trough, on the surface, is 25 m. An empirical model would have predicted the formation of subsidence because the depth of the cavity is lower than 50 m; the depth /opening ratio is equal to 1.5, without another precision.
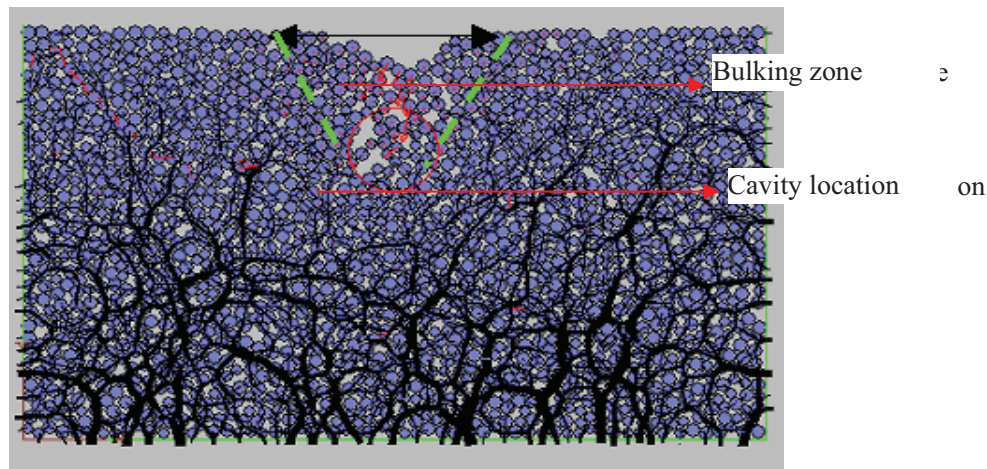
Figure 18. Formation of a subsidence on the surface of an extension of 25 m a 3.3 depth m cavity - Model carried out with PFC2D.

In spite of the results of the numerical models presented above, the prediction of the increase of subsidence using these models remains delicate, taking into account the imposed assumptions and the many data necessary to the model. Numerical modeling requires, each time, an adjustment of the mechanical macro parameters (cohesion, friction, stiffness, and dimensions of the particles). The same conclusion is given by Gilbride *et al.,* (2005) for modeling the generalized collapse by using PFC3D. They note that the approach is not yet mature. A calculation required more than 20 days with the most powerful computers and the choice of the microscopic parameters was difficult.

5.3. Physical modeling

The physical modeling of the natural phenomena is the oldest technique. It makes it possible to carry out observations and to reproduce the phenomena without mobilizing means of calculation and data processing. Compared to the problem arising here, its virtue is the

observation of the mechanisms of rupture and the impact of the movements on the structures on the surface. It is a question of a complementary tool of research to establish a methodology of prediction the formation of the subsidence. By using equivalent materials, it is imperative to respect similarities laws in order to obtain useable results. In partnership with the INERIS, the researchers of the INSA of Lyon, physical modeling is employed to study the sinkhole and subsidence formation above cavities at a shallow depth (Caudron *et al.,* 2006). Figure 19 presents the physical model made up of the steel rollers of diameters (4, 5 and 6 mm), called rollers of Schneebeli. The rollers simulate a ground, the introduction of cohesion made it possible to simulate the presence of a coherent layer on the roof of the cavity. This model makes it possible to create the cavity using a mechanical device. The results are analyzed using software to analyze image processing. Physical models allow observing the various mechanisms of the subsidence and localized collapse (figure 19). We also have the characterization of the trough formed on the surface. Several tested realized allowed to establish a model of prediction of subsidence trough using the relation of Peck (figure 19). Subsidence can be calculated in relation to the volume of the cavity and geometric parameters of cavity (Peck, 1969).

$$S(x) = S_{max} \ e^{\left(\frac{-x^2}{e^{2i^2}}\right)} = \frac{0.667 \ V_{cavity}}{2.5i} e^{\left(\frac{-x^2}{2i^2}\right)}$$

Where S_{max} maximal subsidence at the center of the cavity, i is the localization of the point of inflection of subsidence trough (cf. figure 4). The obtained subsidence profile corresponds to a subsidence characterized by a slope 4 to 5 times more important than that of a subsidence trough associated with a mining area. Actual physical modeling is limited by the problem of scale (1/40), the nature of material used (steel to model the ground) and the reproduction of a subsidence instead of a sinkhole. The development of the physical models, a larger scale, and consisted of more natural materials (ground) will probably make it possible to obtain more realistic results opposite the mechanisms of collapses and their consequence on the surface.
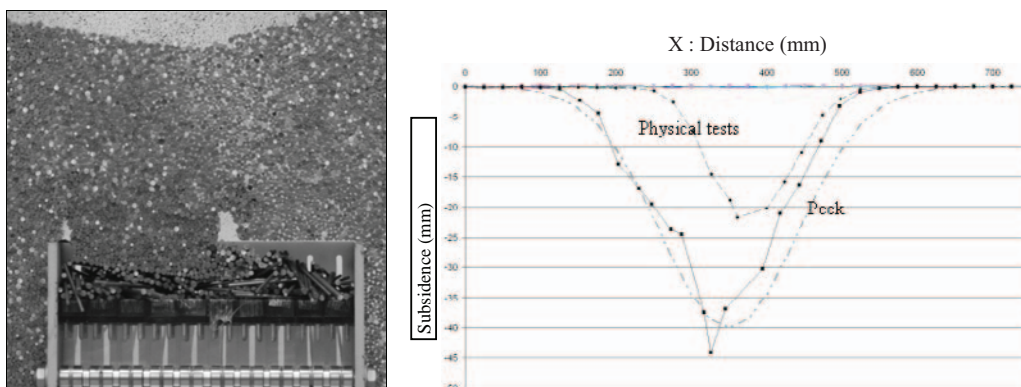
Figure 19. Physical model - mechanism of the subsidence formation and induced subsidence profiles from physical model tests (1: intermediate phase, 2 : final phase) and peck approach (1969).

Conclusion

An overview of subsidence prediction practices was summarized in this paper. The modeling and the prediction of the induced movements (subsidence and sinkhole) by the underground mine works during their mining or after their closure, are realizable by using empirical, analytical and numerical methods. The prediction of the characteristics of the risk movements of grounds must thus be based on the measurements carried out during mining or collapse generating subsidence and sinkhole. The back analysis is an useful tool to predict future subsidence from active and closure mines. We discussed the most used models to predict movements in France. Based on the measurements, we proposed curves for coal and iron mines exploited in France during last decades. These models are probably applicable in other areas of the world having close characteristics of ground and mine. The prediction of subsidence can also be done using empirical rules and analytical models. A mixed approach is proposed, making it possible to associate the advantages of the two approaches. The numerical methods (finite elements and distinct elements) as well as the physical models remain tools of research making it possible to understand the mechanisms of subsidence and sinkhole and to study the complex cases. On the other hand, the numerical models do not allow, up today, a real prediction of the movements of grounds from an operational way.

REFERENCES

Abbass Fayad, A. (2004). Etude de stabilité de fontis au toit des carrières souterraines et traitements apportés aux conséquences induites en surface, PhD, 18 june 2004.

Abbass Fayad, A., Al Heib, M., et Didier, C. (2004). Modélisation numérique de la formation d'un fontis à l'aide du code de calcul UDEC: Influence de stratification, de ses joints et de la couche exploitée. Colloque International de Géotechnique, Beyrouth, Liban. 19 - 22 mai, 2004.

Abbass Fayad, Al Heib M. (2005). Une nouvelle méthode de prédiction de fontis grâce à une modélisation par poutres plastiques. Revue européenne de génie civil. Vol. n°9-10/2005; PP 1067-1093.

Aissaoui K. (1999). Amélioration de la prévision des affaissements dans les mines à l'aide des approches empiriques, numériques et analytiques. Thèse INPL, Ecole des Mines de Nancy, 242 p.

Alejano L.R., Pamirez-Oyanguren P. Taboada J., (1999). FDM predictive methodology for subsidence due to flat and inclined coal seam mining. *International Journal of Rock Mechanics ans Mining Sciences* 36 (1999) 475-491.

Al Heib M. (1993). Les nouvelles méthodes de modélisation numériques et le volume d'influence des exploitations minières en conditions complexes, Thèse de l'INPL 338 p ;

Al Heib M., Linkov A.M., Zoubkov V.V. (2001). On numerical modeling of subsidence induced by mining. Proceedings of the ISRM Regional Symposium EUROCK 2001. Espoo/FINLAND. 4-7 June 2001 pp. 795-799

Al Heib M., Josien J. P. El Shayeb Y (2003). Paramètres d'affaissement pour la hiérarchisation des zones à risque dans le bassin ferrifère lorrain. Conférence de l'après mines 2003, Nancy, France.

Al Heib M., Nicolas M., Noirel J.F., Wojtkowiak F. (2005). Analyse de l'affaissement résiduel après l'arrêt de l'exploitation des mines de charbon. Exemple du bassin houiller de Lorraine – secteur de Morsbach. Nancy-France- Post-Mining 2005.

Aksoy C.O., Kose H., Onargan T., Y. Koca, Heasley K. (2003). Estimation of limit angle using displacement discontinuity analysis in the Soma coal field, Western Turkey. *International Journal of Rock Mechanics and Mining Sciences,* 41 (2004) 547-556.

Arcamone J. (1980). Méthodologie d'étude des affaissements miniers en exploitation totale ou partielle. Thèse Docteur-Ingénieur, INPL – Ecole des Mines de Nancy.

Cauvin M. Verdel Th. Salmon R. (2005). Modeling uncertainties in pillar stability analysis. Post-mining 2005 November 2005.

Bahuguna p.p., Bhawani Singh, Srivastava A.M.C. and Saxena N.C. (1993). Semi-empirical method for calculation of maximum subsidence in coalmines. *Geotechnical and Geological Engineering*, 1993, 11, 249-261.

Caudron M. (2007). Etude expérimentale et numérique de l'Interaction sol-structure lors de l'occurrence d'un fontis. INSA Lyon.

Caudron M. Emariault F. Al Heib M. (2006). Modélisation numérique de l'interaction sol-structure lors du phénomène de fontis. JNGG Lyon 2006.

Coulthard, M.A and Dutton, A,J (1988). Numerical modelling of subsidence induced by underground coal mining. Key questions in Rock Mechanics, 29, 529-536.

Deck O. (2002). Propositions pour une méthodologie d'évaluation de la vulnérabilité du bâti. Thèse, Présentée à l'Institut National Polytechnique de Lorraine.

Didier C. Salmon R., (2004). Evaluation du risque d'apparition d'un fontis en surface : un modèle volumétrique probabiliste. JNGG 2004, Lille. pp. 451-462.

El Shayeb Y., S. Kouniali, J.P. Josien and Y. Gueniffey, (2001). Towards the determination of surface collapse type over abandoned mines in the Lorraine iron basin. Proceeding of the ISRM regional Symposium Eurock 2001. Espoo/Finland. 4-7 June 2001, pp. 819-824.

Ennour S. (1993). Modélisation des galeries de grande largeur en terrain stratifié. Thèse Docteur-Ingénieur, INPL – Ecole des Mines de Nancy.

Fairhust, C., Piguet, J.P., Van der Merwe, N. (2003). Examen de la procedure GEODERIS d'évaluation des risques pour évaluer les conséquences potentielles des affaissements de surface dans le bassin ferrifère lorrain. Rapport d'expertise internationale, mai 2003.28 p.

Fine, J. (1993). Le soutènement des galeries minières. pp. 27-42. Ed. Centre de géotechnique et d'exploitation du sous-sol. Fontainebleau.

Gilbride, L.J., Free, K.S., et Kehrman, R. (2005). Modeling bolck cave subsidence at the Molcorp, Inc., Questa Mine, A case Study. The 40th US Symposium on Rock Mechanics (USRMS); 25-29 Juin.

Josien, J. P. (1999). Carrières souterraines abandonnées. Risque et prévention. Diagnostic et caractérisations des aléas. Bulletin de l'Association Internationale de Géologie de l'Ingénieur n°51, pp.95-111.

Josien, J. P. (2006). Quantification du risque en géotechnique, démarche développée dans les plans de prévention des risques miniers. Journées Nationales de Géotechnique et de Géologie de l'Ingénieur, Lyon.

Huayang, D., Jinzhuang, W., Meifeng, C., Lixin, W., Zengzhang, G. (2002). Seam dip angle based mining subsidence model and its application. *International Journal of Rock Mechanics and Mining Sciences*, 39 (2002) 11-123.

Kalendra, B. S. et Bhart, N.D. (1997). Sinkhole subsidence due to mining. Geotechnical and geological Engineering, 1997, 15, 327-341.

Karmis, M., Agioutantis, Z. (1999). Discussion on the paper, FDM predictive methodology for subsidence due to flat and inclined coal seam mining. *International Journal of Rock Mechanics and Mining Sciences* 36 (1999) 475-491.

Kratzsch, H. (1983). Mining Subsidence Engineering, Springer-Verlag.

McNabb, K.B. (1987). Three dimensional numerical modelling of surface subsidence induced by underground mining. Div. Geomech. CSIRO, Mt. Waverly, Australia, Tech. Rep., 146, 20 pp.

Mandel (1966). Cours de mécanique des milieux continus. Mécanique des solides, tome II. Edition Paris, France: Gauthier-Villars éditeur, 1966. pp. 497-505.

NCB. (1975). Subsidence engineer's Handbook. National Coal Board, London 111p.

Houillères du Bassin de Lorraine. (1983). Affaissements miniers. 84 P, document interne.

Peck, R. B. (1969). Deep excavation and tunnelling in soft ground. Proceeding of the 7th International Conference of soil Mechanics, Mexico, stat of the art.

Piguet, J. P. et Wojtkowiak, F. (2001). Affaissements et déformations au-dessus des exploitations minières : Mécaniques et évolution dans le temps. Mines et Carrières - Industrie Minérale, juin 2001.

Piggot, R.J., and Eynon, P. (1977). Ground Movements Arising from the presence of shallow abandoned mine workings" in large ground movements and structures, J.D. Greddes ed., Wiley and Sons N.Y.

Proust, A. (1964). Etude sur les affaissements miniers dans le bassin du Nord et du Pas-de Calais. Revue de l'Industrie Minérale, Juin-Juillet 1964, 46 n° 6 et 7, 68.

Sabri, M. (2002). Modélisation de cavités souterraines à faible profondeur à l'aide du code de calcul PFC2D. Ecole des Mines de Nancy.

Saxena, N.C., Singh, B. (1980). Investigation into the safety of the railway line against ground movement due to extraction of thick seams in idea. in proceeding of Symposium on Rock mechanics, université du Missouri. Pp 345-355.

Sheorey, P.R., Loui, J.P., Singh, K.B., Sinkh, S.K. (2000). Ground subsidence observations and modified influence function method for complete subsidence prediction. *Int. J. of Rock Mechanics and Mining Sciences*, 37 (2000), 801-818.

Stathan, I., Et Treharne, G. (1991). Subsidence due to abandoned mining in the South Wales coalfield, UK: Causes and mechanisms and environmental risk assessments, proceedings of the 4th International Symposium on Land Subsidence, IAHS publication N0 200, pp. 143-52.

Sigh R.P., and Yadav, R N. (1995). Prediction of subsidence due to coal mining in Raniganj coalfield, West Bengal, India. Engineering Geology, 39 (1995), 103-111.

Szwedzicki, T. (2001). Geotechnical precursors to large-scale ground collapse in mines. *International Journal of Rock Mechanics and Mining Sciences,* 38 (2001), 957-965.

Swift, G.M., and Reddish. (2002). Stability problems associated with an abandoned ironstone mine. Bull Eng Geol Env, (2002) 61, 227-239.

Vachat, J. C.(1982). Les désordres survenant dans les carrières de la région parisienne. Mémoire diplôme Ingénieur CNAM, Paris, 1982.

Wagner and Schümann. (1991). Surface effects of total coal seam extraction by underground mining methods. J.S.Af . Inst. Main. Metall. Vol. 91 N.7, Juillet 1991 pp. 221-231.

Whittaker, B.N., et Reddish, D.J. (1989). Subsidence, Occurrence, Prediction and Control. Ed Elsevier., Amsterdam.

Appendix A. Subsidence caracteristics –Lorraine Basin –La Houve coalmine

Sector	depth (m)	Width (m)	Length (m)	Thickness (m)	Seam n°	Max. Subsidence (m)	length/depth	Subsidence/ thichness
4	525	225	400	8.2	3	3.28	0.43	0.4
5	450	200	400	5.65	2	0.88	0.44	0.16
9-3	425	300		5.5	2	2.5	0.71	0.45
9-1	450	275	600	8.25	3	4.95	0.61	0.6
11	725	200	750	3.83	1	0.5	0.27	0.13
12	800	150	1200	2.6	1	0.19	0.10	0.1
12	800	150	1200	5.9	2	0.6	0.19	0.1
13	950	700	1000	3.3	1	1.63	0.74	0.49
A-2 bis	575	175	300	5.4	2	0.54	0.3	0.1
A-3	650	225	400	5.3	2	1.09	0.35	0.21
A-3	650	225	400	2.6	1	0.22	0.35	0.09
A-2	575	150	500	5.4	2	0.67	0.26	0.15

Appendix B. Subsidence characterization of iron mines – Lorraine

N°	Concession	Site / Mine	Layer	O (m)	H (m)	Lp (m)	□ (%)	Phenomen Type	Sm (m)	Tilt maximal (%)	ε_h mm/m	Influence angle (°)
1	Joeuf	Joeuf	Grise	7	126	87 to 270	85%	Total mine	3.6	11%(V)	43.30	4,5 to 6,50 (V)
2	De Wendel (156)	Moyeuvre	Grise	3.5	135	186 – 300	85%	Total mine	2.0	6.0% (T)	10.90	6 à 13° (T)
3	Moutiers	Moutiers	Grise + Rouge	3.2	125	190	85%	Total mine en second layer (grise)	2.07	2.60% (D)	16	29° (D)
4	Joudreville	Joudreville	Grise	6.5	210	200	85%	Total mine	2.80	2.94% (DE)	12.7	40° (DE)
5	Hettange-Grande	Hettange-Grande	Grise	7.2	175		85%	Total mine	2.81	4.80% (DE)		
6	François	Pierreuse	Grise + Brune	4.1	187	390	85%	Total mine en second layer (Brune)	2.7	1.6 % (DE) / 5.5 %(V)		23° (DE) / 10° (V)
7	Montrouge	CD15	Grise + Brune	3.35	147	500	85%	Total mine en second layer	2.25	3.73% (V, T) / 1.8% (V, T)		8 to 15° (V, T)
8	Auboué - Moineville	Cité de Gorcy	Jaune (S2 & S3) + grise	4	142	200 (N) / 300 (S)	85%	Total mine en second layer (grise)	1.72 (N) / 2.77 (S)	4% (T) / 5% (T)		10 to 20°(effo)
9	Piennes	Piennes	Grise	6	230	450	85%	Total mine	3	3.9%(T, DE) / 2.95 (DE)		21° (T, DE) / 29° (DE)
10	St Pierremont	St Pierremont	Grise	6	170	300	85%	Total mine	2.6	3 % (DE)		9° (T) / 26° (DE)
11	Droitaumont	Jarny	Grise	5	200	1 100	53%	Progressif collapse	1.2	3.3% (T)		
12	Aumetz	Errouville	Brune	3.8	180	240	50%	Progressif collapse	0.88	0.80% (T)		
13	Auboué - Moineville	Cité de Coinville	Grise	5	175	180	40%	Progressif collapse	1.0	3.48 %(T) / 0,1 % (DE)		40°*
14	Auboué - Moineville	Rue de Metz	Rouge + grise	6	150	130	45%	Progressif collapse (grise)	1.70	2.5% (T)		40°*
15	Auboué - Moineville	Moutiers haut	Grise	4	120	150	55%	Progressif collapse	1.38	1.2% (T) / 0.6 % (DE)		
16	Roncourt	Cité St-Joseph	Grise	2.5	150	125	53%	Progressif collapse	0.65	1.0% (T) / 0.5 %(DE)		26 (T) / 38 (DE)
17	Ste Marie aux Chênes	Ida	S2	5	153	170	65%	Brutal collapse	1.95	4.4 % (V) / 2.5 % (V) / 3.4 %(DE) / 9% (DE)		5° (V) / 0° (V) / 15° (DE) / 0° (DE)
18	Rochonvillers	Rochonvillers	Grise	3.5	190		62 %	Brutal collapse	-			

O : Mine thickness; H : depth ; Lp : width of panel ;   : extraction ratio
 Sm : maximal Subsidence;   h : horizontal strain
 T : galleries ; DE : goef or extraction area ; V : green field

Chapter 6

ASSESSMENT OF TOTAL NITROGEN EMISSIONS FROM COAL COMBUSTION IN CHINA

K. L. Luo[1]*, H. J. Li, C.L.Chou[2], X. M. Zhang[1], and Y. S. Dong[1]

[1]Institute of Geographical Sciences and Natural Resources Research,
Chinese Academy of Sciences, 11A Datun Road Anwai, Beijing, 100101, P.R.China.
[2]Illinois State Geological Survey (Emeritus), Champaign, IL 61820, U.S.A.

ABSTRACT

About 400 coal samples from coal mines and 100 fly ash and cinder samples from power stations were collected to study the amount of total annual nitrogen emissions as well as emission ratio from steam coal combustion in China. The results shows that by burning 1t coal (nitrogen content is about 1.14%) in the high-temperature power stations emit about 11.35kg nitrogen into the atmosphere, in the mid-low temperature the fluid bed furnace, chain-grate furnace and boil furnace emit about 12.28kg, 6.45kg and 6.72kg nitrogen, respectively. The nitrogen emission ratio of coal combustion in the high-temperature power stations is about 99.56%, in the mid-low temperature the nitrogen emission ratios of coal combustion of the fluid bed furnace, chain-grate furnace and boil furnace are about 91.64%, 65.16% and 73.82% respectively. The annual total nitrogen emissions from steam coal combustion into the atmosphere in China is estimated to be 18.20 Mt now.

Key words: Coal Nitrogen, total Nitrogen emission, coal combustion

Nitrogen is a main element in coal. Nitrogen oxides are emitted during coal combustion. The total amount of emissions of nitrogen from the coal combustion in China is not certain. Coal is the basic power source in China and about 2.0 Gt of coal is used annual in China now(Wei et al., 2006). Although the nitrogen oxides emissions from fossils fuels combustion

---

* Tel: +86-10-64856503. Fax: +86-10-64851844. Box: 9717 or 9719 E-mail: Luokl@igsnrr.ac.cn

have been studied for a long time, but most studies are about measuring the NOx emissions. No study on the total nitrogen emissions from coal combustion has been conducted.

Nitrogen in coal may generate NOx and N2 etc. during combustion. Because nitrogen oxides (NOx) are main air pollutants (Zhao and Zhao,1996; Zhao et al., 2000), which cause acid rain and smogs in cities and are harmful to people's health (Stephen 2001; Ramanathan 1998), so there are many studies about emissions and control of NOx from steam boilers at power stations (Bartok 1969; Fine 1974; Fujii and Takagi 1974). In China the scientists have done a lot of work on the formation of NOx (Zhao et al., 2000; You et al.,2001), influence factors (Zhong et al., 1998; Huang et al., 2001; Feng et al., 1997), emissions characteristics (Yang et al., 2000; Hou et al., 1997; Xu et al., 1998), the retention of nitrogen during coal combustion (Baxter et al., 1996; Zhao et al., 2002; Liu et al., 2002; Wojtowicz et al., 1994) and N2O emissions from coal combustion (Zhao et al., 1996). All those work is very important, but there is no study on total nitrogen emissions from coal combustion in China. No matter what the forms of nitrogen are emitted duirng coal combustion, they can increase the nitrogen concentration in the environment, especially in the atmosphere.

In this paper, we first establish a new method to account for the total nitrogen emissions during coal combustion as follows.

Nitrogen in coal is apt to vaporize. When the coal is burnt, part of nitrogen remains in the cinders and part is released along with coal dust, among which some part of nitrogen is trapped with the fly ash in dust catchers, the remaining nitrogen is released into the atmosphere. The portion of nitrogen in flyashes and cinders is supposedly less important than that released to the atmosphere, then the latter may be considered the total nitrogen emissions from coal combustion.

1. SAMPLES AND ANALYSES

1.1 Getting representative samples

The samples of coals, fly ashes and cinders were collected from coal mines and power stations as well as industrial boilers by our research group for 6 years and nearly 500 samples were analyzed. All data and samples in this paper are original.

The Permo-Carboniferous coal is widely distributed and it constitutes the largest reserve in China. It includes mainly bituminous coal and a small quantity of anthracite, and it is the main steam coal for power generation (Chen and Zhang 1993; Dai et al., 1997; Luo et al., 2002). Some of the coal samples and all the fly ash and cinder samples were collected from the studied power stations, some of the coal samples were collected from the coal mines in the North China Plate, which are mainly steam coal in China.

The spatial distribution of Chinese coals is quite uneven, with much more resources in the northern and western China and less in the southern and eastern China. Coal deposits to the north of the Kunlun-Qinling Mountains (Figure 1) account for about 90% of all Chinese coal reserves, within which, coal in the North China Plate and northwestern China accounts for about 84%, and Mesozoic lignite in northeastern China only amounts to 4% (Chen and Zhang 1993; Dai et al., 1997; Luo et al., 2002; Luo et al., 2002; Chen 2001; Ye 2001; Zeng 2001). Coal in southwestern China accounts for 10% of total coal reserves in China (Chen

and Zhang 1993; Dai et al., 1997; Luo et al., 2002; Luo et al., 2002; Chen 2001; Ye 2001; Zeng 2001). The nitrogen content of these coals varies from 0.5%-1.5%, about 1.14% on the average on the basis of our research from 1982 to 2002.
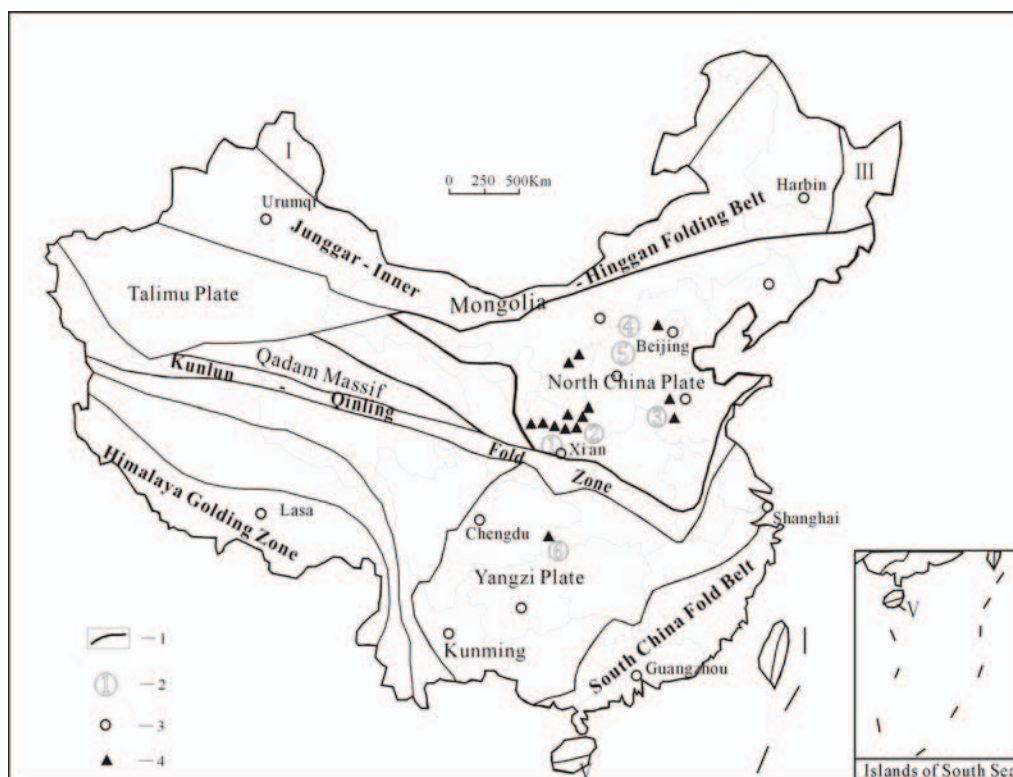
Figure 1. Coal basins and geotectonic units of China and sampling location

1- Geotectonic Boundary (Ma and Deng, 1998); 2- Power Station, ①- The Baqiao power station, ②- The Pucheng power station and the Wangcun power station, ③- The Shiheng power station, ④- The Taiyuan 2nd Power Station, ⑤-The Xishan power station, ⑥- The Nantong power station; 3 - The cities in China; 4- coal sample location.

In China there are 500 Mt coal burnt for power stations and 500 Mt coal burnt for industrial, heating in the winter and cooking. About 60% of the coal burnt for power station is burnt in coal-fired utility boilers at high temperature and 40% is burnt at mid-low temperature (950℃). For the coal burnt at low temperature, about 50% is burnt in fluidized-bed boilers and other 50% is burnt in furnace boilers. The coal burnt for industrial boilers and heating in the winter is about 80% burnt in chain-grate furnace and 20% burnt in boil furnace. In China, more than more than 95% coals were used for the power stations, industrial boilers and heating furnaces in the winter. In order to study the amount of nitrogen emissions from coal combustion in China, we collect the coal samples burnt at high temperature and middle-low temperature at power stations, industrial boilers and coal stoves for heating in the winter, the method of sample collection is in accordance with the Chinese standard for collecting whole-seam samples (GB482-79) (Han 1996). The nitrogen emissions and emission ratios from coal

combustion were evaluated. A quantitative method for the evaluation of nitrogen emissions and a formula for calculation are proposed.

1.2 Selection of sample localities

Large high-temperature power stations such as the Baqiao Power Station in Xi'an, Shaanxi Province, the Pucheng Power Station in Shaanxi Province, the Taiyuan Second Power Station in Shanxi Province and the Shiheng Power Station in Shandong Province were selected. At the same time, three small power plants with low combustion temperature, including the Wangcun power station (fluidized-bed furnace) in Shaanxi Province, the Xishan heating stove (chain-grate furnace) in Shanxi Province and the Nantong power station (boil furnace) in Sichuan Province were also included in this study (Figure. 1).

1.3 Sample analyses

Most of the coal samples and all the fly ash and cinder samples were analyzed at the Geological Testing Center of Academy of Coal Sciences and Coal Testing Center of Shanxi Quality Testing Center. Nitrogen in coal was determined by the Kjeldahl method. Some samples were analyzed at the Institute of Geographical Science and Natural Resource Research, Chinese Academy of Sciences by the same method. The proximate and ultimate analyses of coals and ashes were performed at the Laboratory of the Chenghe Mining Bureau of Shaanxi Province. For quality control of chemical analyses, a standard reference material of coal (GBW11122 from Chinese Standard Sample Study Center, Chinese Academy of Measurement Sciences) was analyzed with each batch of the samples. The relative standard deviation was ± 10% and the detection limit was 10^{-3}.

2. PHYSICAL AND CHEMICAL CHARACTERISTICS OF PERMO-CARBONIFEROUS COAL IN THE NORTH CHINA PLATE AND NORTHWESTERN CHINA

Many industrial and elemental studies on Permo-Carboniferous and Jurassic coal in China have been carried out by many coalfield teams and coal mining bureaus of the former Chinese Ministry of Coal Industry. The ash content of most Permo-Carboniferous coal in northern and northwestern China is in the range of 15 - 30% (about 20% on average), and the carbon content varies from 50% to 80% (about 65% on average). The results of industrial and elemental analyses of Permo-Carboniferous coal from the Chenghe Coal Mine, the Pingyin Coal Mine and the Xishan Coal Mine are listed in Table 1 to 4.

Table 1. Proximate and ultimate analyses of No. 5 (C₂) raw coal from Chenghe Coal Mine

Mad (%)	Ad (%)	Vd (%)	St, d (%)	Qgr, d /MJ • kg⁻¹	Cdaf (/%)	Hdaf (%)	Ndaf (%)	Odaf (%)
1.04	23.5	18.5	2.05	27.55	89.19	4.21	1.30	3.06

Mad, moisture in the air dried sample; Ad, ash in the air dried sample; Vd, volatile matter on dry basis; St, d, total sulfur on dry basis; Qgr,d, gross calorific value on dry basis; Cadf, Hadf, Nadf and Oadf, Content of C, H, N and O on the dry and ash-free basis.

Table 2. Proximate ultimate analyses of No. 5 clean coal from the Chenghe Coal Mine

Mad (%)	Ad (%)	Vd (%)	St, d (%)	Qgr,d /MJ • kg⁻¹	Cdaf (/%)	Hdaf (%)	Ndaf (%)	Odaf (%)
0.89	7.44	16.64	1.56	29.00	89.65	4.54	1.34	2.20

See Table 1 for abbreviations of the units

Table 3. Proximate and ultimate analyses of No. 5 raw coal in the Pingyin Coal Mine

M_f (%)	Mad (%)	Ad (%)	Vd (%)	St, d (%)	Qgr, d /MJ • kg⁻¹	Cdaf (/%)	Hdaf (%)	Ndaf (%)	Odaf (%)
2.00	2.25	21.55	34.06	2.01	26.75	88.6	4.20	1.14	3.80

Mf , moisture lost during air drying. See Table 1 for abbreviations of other units

Table 4. Proximate and ultimate analyses of No. 8 raw coal from the Xishan Coal Mine

Mad (%)	Ad (%)	Vd (%)	St, d (%)	Qgr, d /MJ • kg⁻¹	Cdaf (/%)	Hdaf (%)	Ndaf (%)	Odaf (%)
11.02	14.66	13.34	1.96	30.21	89.92	3.89	1.13	3.11

See Table 1 for abbreviations of the units

3. EVALUATION OF NITROGEN EMISSIONS FROM COAL COMBUSTION

The quantity of fly ash and cinder and their nitrogen content are closely related to coal combustion temperature and other combustion conditions. For example, the Pucheng Power Station with high-temperature boiler and well controlled combustion conditions produced fly ash that was off-white in color. The fly ash and cinder have similar composition (mainly $SiO2$ and $Al2O3$) and burnt completely. Their carbon and nitrogen contents were very low. The fly ash and the cinder account for 90% and 10% of all ashes produced, respectively.

There is a little difference between the quantities of fly ash and cinder when coal is burnt at low temperature and under poor combustion conditions. The fly ashes and cinders generally account for 60% and 40% of total solid residues, respectively (the chain-grate furnace), and those of fluidized-bed and boiler furnaces generally account for 70% and 30% of total solid residues, respectively. For example, the same kind of coal (No. 5 lean coal of Late Carboniferous at the Chenghe and Pubai Coal Mining Bureaus, with nitrogen content of about 1.31%) was mainly used in both the Wangcun and the Pucheng Power Stations. At the Pucheng Power Station, the carbon and nitrogen content in fly ashes are about 0.4% and 0.01%, respectively (Table 5), and those at the Wangcun Power Station are about 7% and 0.21%, respectively (Table 6). Such differences are attributed to the the fact that coals in the high-temperature boilers are more completely combusted.

Under better coal combustion conditions, there is less carbon residue in coal ashes and also less nitrogen remained in fly ashes and cinders. The fly ashes and cinders have little difference in nitrogen content. If coal combustion conditions are less favorable, such as in chain-grate furnace, the carbon content in coal ashes tends to be higher and there is an obvious difference of nitrogen content in the fly ashes and cinders, the nitrogen content in fly ashes is higher than that in cinders. All the above conclusions are based on our analyses of raw coals, fly ashes, cinders.

3.1 Nitrogen emissions from coal combustion at high-temperature power stations

To estimate element emissions from coal combustion, we used to multiply a coefficient or directly subtract the element content in each ton of coal ash from that in each ton of coal.

In fact, the ash content of coal is defined as the amount of residues after complete combustion. For example, suppose the ash content of the coal is 20%, which means 0.2 t of residues remain after 1 t of coal is completely burnt. Therefore, if we evaluate nitrogen emissions from 1 t of coal combustion, we should subtract the amount of nitrogen in fly ashes and cinders, namely the nitrogen content in 0.2 t of residues after coal combustion, from the nitrogen content of 1 t of raw coal. Nitrogen emissions from coal combustion (D) may be calculated by $D = A - (B+C) \times E$, where A, B and C are the nitrogen concentrations in coal, cinders and fly ashes, respectively, and E is the ash content of coal.

The Baqiao and Pucheng Power Stations are about 10 km and 150 km away from Xi'an City (in Shaanxi Province), respectively. The Shiheng Power Station is about 120 km away from Ji'nan City in Shandong Province, and the Taiyuan 2nd Power Station is about 10 km away from Taiyuan City in Shanxi Province. Like most of the large power stations in China, coal-fired utility boilers were used in these power stations, with hearth temperatures reaching 1200℃-1500℃. The bituminous coal used in those power stations mainly came from Permo-Carboniferous coal seams - Nos. 2, 3, 5, 8, 9, 10 and 11 of the Chenghe Coal Mine, the Pubai Coal Mine, the Xishan Coal Mine and the Pingyin Coal Mine ― the typical coal of the North China Plate and northwestern China. Their nitrogen content is in the range of 0.38 - 1.97% with an average of about 1.14%. In addition, both the carbon content of fly ash and that of the cinder from the Pucheng Power Station and the Baqiao Power Station are about 0.4%. The nitrogen content of coal, fly ash, cinder of these power stations is listed in table 5.

Table 5. Nitrogen emissions from combustion of each ton of coal at high temperature power stations

Sample location	Coal seam	Combustion mode	Ash content (%)	Nitrogen in coal (%)			Nitrogen in fly ashes (%)	Nitrogen in cinders (%)	Nitrogen to atmosphere (kg ·t⁻¹)	Nitrogen emission rate (%)
				Min.	Ave.	Max.				
Baqiao power station	No. 11	Coal-fired utility boiler	22.83	0.69	1.03	1.68	0.02	0.03	10.25	99.53
Baqiao power station	5	Coal-fired utility boiler	20.01	0.77	1.34	1.97	0.03	0.04	13.34	99.54
Pucheng power station	5	Coal-fired utility boiler	22.23	0.76	1.31	1.43	0.01	0.01	13.08	99.83
Shiheng power station	5	Coal-fired utility boiler	23.12	0.84	1.01	1.25	0.02	0.04	10.05	99.50
Taiyuan power station	8	Coal-fired utility boiler	20.16	0.38	1.01	1.26	0.03	0.03	10.04	99.40
Average	—	—	21.67	0.69	1.14	1.52	0.02	0.03	11.35	99.56

The combustion temperature is high in boilers of large power stations, so coal is nearly completely combusted and the amount of fly ashes and cinders is approximately equal to the ash content of coal.

For large power stations under good combustion conditions and high combustion temperature, we can get nitrogen emissions from combustion of one ton of coal (D) using the following formula:

$$D = A - (B \times 10\% + C \times 90\%) \times E$$

The nitrogen emission ratio (V) is $V = D/A \times 100\%$.

For example, the Pucheng Power Station mainly used the No. 5 Coal of Late Carboniferous, with a nitrogen content of about 1.31%, and with carbon and nitrogen contents in fly ashes of about 0.4% and 0.01%, respectively. Because the carbon left in the ash is very little, we suppose that coal was completely combusted, so nitrogen emissions from 1 t coal combustion (D) at the high temperature,

$$D = 13.1 \text{ kg} - (0.1 \text{ kg} \times 10\% + 0.1 \text{ kg} \times 90\%) \times 0.2223$$

Because the amount of (0. 1kg×10%+0.1kg×90%) is the nitrogen left in 1 t ash, but 1 t No.5 coal can not left 1 t ash after complete combustion, they only left 0.2223 t ash. So when we evaluate the amount of nitrogen emission from 1 t of coal combustion at high temperature, we should subtract the amount of nitrogen in fly ashes and cinders. Namely the nitrogen content in 0.2223 t of residues after coal combustion should be subtracted from the nitrogen content of 1 t of coal.

(D) = 13.1kg - (0. 1kg × 10% + 0.1kg × 90%) × 0.2223 = 13.08kg.

The nitrogen emission ratio V = 13.08 kg/13.1 kg × 100% = 99.83%

3.2 Nitrogen emissions from coal combustion at the mid-low temperature

Generally speaking, the combustion temperature at the mid-low temperature power stations, industrial boilers and heating furnaces varies from 900℃ to 1000℃, but different stoves have different combustion conditions. The combustion conditions of the fluidized-bed boilers are better than those of the boil furnaces, and much better than those of chain-grate furnaces.

So the coal is burnt incompletely at mid-low temperature, about 0.2% - 20% of coal remains in fly ashes and cinders. Our analyses show that carbon content of the fly ashes and cinders are 0.2% - 25% respectively in mid-low temperature burners. Therefore, for the mid-low temperature burners, the total amount of fly ashes and cinders is more than the ash content in coal, which should be equal to the ash content in coal plus the coal remained in the fly ashes and cinders (Table 6).

Table 6 Nitrogen emissions from combustion of one ton of coal at mid-low temperature (about 950°C)

Sample location	Coal No.	Combustion mode	Ash content in coal (%)	Coal remained in fly ashes (%)	Coal remained in cinders (%)	Nitrogen in coal (%)			Nitrogen in fly ashes (%)	Nitrogen in cinders (%)	Nitrogen to the atmosphere (kg·t⁻¹)	Nitrogen emission rate (%)
						Min.	Ave.	Max.				
Wangcun in Shaanxi	No. 5	Fluidized-bed boiler	22.05	7	0.78	0.77	1.34	1.97	0.21	0.16	12.28	91.64
Xishan power station	No. 8	Chain-grate furnace	26.17	25	18	0.38	0.99	2.36	0.41	0.58	6.45	65.16
Nantong in Sichuan	No. 6	Boil furnace	23.96	23.96	0.29	0.72	0.91	1.3	0.45	0.13	6.72	73.82

For chain-grate furnaces, we can calculate the nitrogen emissions from coal combustion (D) using the following formula:

$$D = A - (B × 40\% + C × 60\%) × E - A × L$$

Where L is used to express the percent of coal remained in fly ashes and cinders. So $L = L_1 × 40\% + L_2 × 60\%$, L_1 and L_2 are the coal remained in the cinders and fly ashes respectively.

For the fluidized-bed furnace and boil furnace, we can calculate the nitrogen emissions from coal combustion (D) using the following formula:

$$D = A - (B \times 30\% + C \times 70\%) \times E - A \times L$$

Where $L = L_1 \times 30\% + L_2 \times 70\%$ and it is about 0.2% - 25% for mid-low temperature stove. L_2 is small (As show in table 6), if necessary we can think the coal remained in the fly ash as the coal remained in the fly ash and the cinder.

The amount of nitrogen remained in cinders mainly depends on the mode and conditions of coal combustion. Under poor combustion conditions, there is more coal residue in the ash, and more nitrogen remains in the fly ash and cinders too. For example, the combustion conditions of the fluidized-bed boilers are better than those of chain-grate furnaces, so that the fly ash and cinders of the fluidized-bed boilers have lower nitrogen content.

Table 5 and Table 6 show nitrogen emissions from combustion of one ton of coal at high temperature power stations and the mid-low temperature boilers. For coal with an average nitrogen content of 1.14%, high-temperature boilers have nitrogen emissions of 11.35 kg. The values for fluidized-bed boilers, chain-grate boilers, and boil furnace are 12.28 kg, 6.45 kg, and 6.72 kg, respectively. The total nitrogen emission rate at high-temperature power stations is about 99.56%, and the values for fluidized-bed boilers, chain-grate furnaces, and boil furnaces are about 91.64%, 65.16% and 73.82%, respectively. The higher combustion temperature the more complete of coal combustion, and more nitrogen in coal is released.

4. CONCLUSIONS

Nitrogen in coal is predominantly emitted to the atmosphere during combustion, but part of nitrogen remains in coal residues. The higher combustion temperature the more nitrogen is emitted to the atmosphere.

Coal accounts for about 70% of total energy consumption in China and this situation will continue for a long time in the future. About 2.0 Gt of coal is used annual in China now(Wei et al., 2006), among which about 1000 Mt of coal is burnt for power station (Wei et al., 2006；Statistical Yearbook of Shaanxi 2001; Statistical Yearbook of Shandong 2001; Statistical Yearbook of Guizhou 2001; Statistical Yearbook of Shanxi 2001; Statistical Yearbook of Inner Mongolia 2001), within which about 60% is burnt at high temperature power stations and about 40% is burnt at mid-low temperature power stations (20, 21, 24). Other 1000 Mt coal burnt for industrial, heating in the winter and cooking. The average nitrogen content of Chinese coal is about 1.14%, so the annual total nitrogen emissions from the power stations to the atmosphere is roughly about $99.56\% \times (1000 \times 1.14\% \times 60\%)$Mt + $73.82\% \times (1000 \times 1.14\% \times 40\% \times 50\%)$Mt + $91.64\% \times (1000 \times 1.14\% \times 40\% \times 50\%)$Mt, namely about 10.58Mt in China; the annual total nitrogen emissions from industrial boilers and heating stoves to the atmosphere are roughly about $65.16\% \times (1000 \times 1.14\% \times 80\%)$Mt+$73.82\% \times (1000 \times 1.14\% \times 20\%)$ Mt, about 7.62Mt. So the annual total nitrogen emissions from steam coal combustion into the atmosphere in China is estimated to be 18.20 Mt now. According to the international statistical caliber China has 114.5 Gt coals that can be mined by today's technologies, if all these coal are burned in the future 200 years, the total nitrogen emission from coal combustion is 1041.95Mt, this is a very big value and it should not be overlooked.

ACKNOWLEDGMENTS

REFERENCES

Bartok. (1969). *Systems Study of Control Methods for Stationary Sources*. Esso Research and Engineering Co., Linden, N.J.GR2-Nos.69pp.

Baxter, L.L., Mitchell, R.E., Fletcher, T.H. (1996). Nitrogen release during coal combustion. *Energy and Fuels*, 10, 188.

Chen, P. (2001). *Properties, Classify and Using of China Coal*. Beijing, China: Chemistry Industry Press, 25pp (In Chinese).

Chen, W.M., Zhang, Z.S. (1993). *Coal Chemistry*. Beijing, China: Coal Industry Press, 1-16pp (In Chinese).

Dai, H.W., Li, R., Li, L.Z. (1997). On the adjustment of varieties, quality and mix of steam coal products in China. *China Coal*, 23(9), 12 (In Chinese, with English abstract).

Feng, B., Yuan, J.W., Lin, Z.J., Liu, D.C. (1997). An analysis of the influence of coal contents on emission of nitrogen oxides. *Journal of Huazhong University of Science and Technology*, 25, 106-108 (In Chinese, with English abstract).

Fine. (1974). Nitrogen in coal as a source of NO. *Fuel*, 52 (2), 120.

Fujii Ogasawara, Takagi. (1974). Evaluation of various factors affecting NO formation and control. *Fuel,* 53 (2), 198.

Han DX. (1996). *Coal Petrology of China*. Xuzhou: China University of Mining and Technology Press, 276-279pp (In Chinese, summary in English).

Hou, D.Q., Yu, D.T., Zhu, J. (1997). Experimental investigation of nitrogen release characteristics in coal combustion process. *Power System Engineering*, 13 (6), 45-50 (In Chinese, with English abstract).

Huang, W., Xiong, W.L., Gong, B.Y., Cao, H.C., Xiao, L.S. (2001). Experimental research on performance of NO_X emission for pulverized-coal boiler furnace. *Power System Engineering*, 17 (6), 354-357 (In Chinese, with English abstract).

Li, Y.H., Li, S.G., Feng, Z.X., Li, Z.Z. (2001). *Experimental study on the formation of NO_X of brown and brown-blending coal combustion*. Proceedings of the CSEE 8, 34-35 (In Chinese, with English abstract).

Liu, J.Z., Cao, X.Y., Zhou, J.H., Zhao, X. (2002). Characteristics of NO_x emission and removal for coal-fired utility boiler. *Journal of Fuel Chemistry and Technology*, 30 (1), 6-10 (In Chinese, with English abstract).

Luo, K.L., Wang, D.H., Wang, L.Z., Feng, F.J., Li, R.B. (2002). Lead emission amount from coal combustion and its environment effect in Xi'an City. *Environmental Science*, 23, 123 (In Chinese, with English abstract).

Luo, K.L., Xu, L.R., Li, R.B., Xiang, L.H. (2002). Fluorine emission from combustion of steam coal of North China Plate and Northwest China. *Chinese Science Bulletin*, 47, 1347.

Ma, L.F., Deng, X.Z. (1998). *China Geological Map Explanation*. Beijing: Geological Press, 2pp (In Chinese).

Ramanathan, V. (1998). Esso research and engineering Co. *Science*, 240, 294.

Statistical Yearbook of Guizhou. (2001). Beijing, China: China Statistical Press, 97pp (In Chinese).

Statistical Yearbook of Inner Mongolia. (2001). Beijing,m China: China Statistical Press,233pp (In Chinese).

Statistical Yearbook of Shaanxi. (2001). Beijing, China: China Statistical Press, 180pp (In Chinese).

Statistical Yearbook of Shandong. (2001). Beijing, China: China Statistical Press, 89pp (In Chinese).

Statistical Yearbook of Shanxi. (2001). Beijing, China: China Statistical Press, 147pp (In Chinese).

Stephen, H.S. (2001). Earth systems engineering and management. *Nature*, 409, 417.

The Survey of the World Energy. (1998). The world Energy Committee.

Wei, Y.M., Fan, Y., Han, Z.Y., Wu,Gang. (2006). China Energy Report (2006). *Strategy and Policy Research*, Science Press (2006), p. 12.

Xu, X.F., Gu, Y.D., Chen, S.Y. (1998). Study on emission of SO_2 and NO during coal combustion. *Journal of Fuel Chemistry and Technology*, 26 (4), 356-361 (In Chinese, with English abstract).

Yang, W.L., Liu, Y.Q., Sun, J.D. (2000). NO_X release characteristics of four power coal in combustion. *Power System Engineering*, 17 (5), 313-314 (In Chinese, with English abstract).

Ye, D.W. (2001). Some suggestion for the development of steam coal preparation and processing. *Coal Preparation Technology*, 5, 1 (In Chinese).

You, X.F., Liu, S.Y., Wu, Z.M., Ren, J., Xie, K.C. (2001). Study on nitrogen and sulfur distribution and functional forms during coal pyrolysis. *Coal Conversion*, 24, 4(In Chinese, with English abstract).

Zeng, Y. (2001). Special coal types in Western China and their exploitation and utilization. *Journal of China Coal Society*, 64(4), 337 (In Chinese, with English abstract).

Zhao, R.L., Zhao, H.T. (1996). Inspection and evaluation of N_2O emission from coal combustion in China. *Environmental Science*, 17 (4), 11-13 (In Chinese, with English abstract).

Zhao, Y., Ma, S.S., Li, Y.Zh., Zhao, J.H., Fu, Y.C. (2002). *The experimental investigation of desulfurization and denitriefication from flue gas by absorbed based on fly ash*. Proceeding of the CSEE 22 (3), 108-112 (In Chinese, with English abstract).

Zhao, Z.B., Chen, H.P., Li, B.Q. (2000). The production and reduction mechanism of N_2O in fluid bed furnace in coal combustion. *Coal Chemical Industry*, 2, 29 (In Chinese, with English abstract).

Zhong, B.J., Yang, J., Fu, W.B. (1998). Influence of coal volatiles compositions on NO_X and SO_2 emissions. *Journal of Combustion Science and Technology*, 4(4), 363-368(In Chinese, with English abstract).

Chapter 7

ELEMENT CONTENT OF LOWER PALEOZOIC STONE-LIKE COAL IN DABA AREA IN SOUTH QINLING MOUNTAIN, CHINA

Luo Kunli[1]*

Institute of Geographical Sciences and Natural Resources Research,
Chinese Academy of Sciences,
11A Datun Road Anwai, Beijing, 100101, P.R.China.

ABSTRACT

In the Lower Paleozoic strata in South Qinling Mountain in the middle of China, there are lots of thin beds of stone-like coal applied here to burnable black shale which is near 40% ash, very heavy and hard, looks like stone, generally called stone coal, enwrapped in lumpish trachytic or interbedded in the fault zones in the axis of folds of the Lower Paleozoic strata. The stone-like coal has higher stages of coal development and it generally is high - stage anthracite coal. About 260 samples of stone-like coal were collected from southwest China to determine the arsenic (As), selenium (Se), mercury (Hg), fluorine (F) content and other element content, and study their distribution pattern sources in this area. The stone-like coal is very rich in sulfur and heavy metals. The sulfur content is about 1.5 to 3%, mercury from 0.3 mg/kg to 2.6 mg/kg, arsenic from 15 to 534 mg/kg, mostly from 50 mg/kg to 150 mg/kg, much high than the average arsenic content of Chinese coals 4.5 mg/kg and the average world coal of 6.1 mg/kg. Selenium ranged from 10 mg/kg to 42 mg/kg, cadmium from 0.2 mg/kg to 36 mg/kg. Fluorine content is from 600 to 3400 mg/kg. There is Se, F, Hg, Cd content enrichment in the stone-like coal, too, and higher than in average the content of Chinese coals and the average of world coal, and higher than the typical Permo-Carboniferous or later coal deposits.

Use of the stone-like coal towarm and cook by local residents has caused serious health problems --endemic fluorosis and arsenic poisoning - in this area.

---

* Tel: +86-10-64856503. Fax: +86-10-64851844. Box: 9717 or 9719 E-mail: Luokl@igsnrr.ac.cn

INTRODUCTION

Lower Paleozoic stone-like coal in the Daba area has large reserves and distributing areas, and very commonly has been a source of energy and heat for thousands of years (mainly domestic coal) in the Daba area of South Qinling Mountain (mainly in South of Shaanxi Province). Locally, however, they are called "stone-like coal" since they are harder and heavier than humic coals . There are large reserves, over 1000 million tons, and most of them are very good in quality, like the good quality of humic coal of the Permo-Carboniferous system and later ages. The stone-like coal beds are generally 1 to 2 m thick, and are very easy to mine.

But it is unusual that before the higher plants occurend on the Earth, there are so many organic, materials. Where did they come from? As we know, in the early Paleozoic time, there were still no higher plants, which is the main substance of the coal, termed humic coal, mainly forming in the Permo-Carboniferous system and later ages. And, what is the composition of the stone-like coal? What is the difference between the stone-like coal and the general coal - humic coal - of the Permo-Carboniferous system and later ages?

The Daba area of South Qinling Mountain is located in the South of Shaanxi Province, in Central China (Fig.1). The Daba area is mountainous with steep hill slopes and deep ravines. Rainfall is heavy, with the annual precipitation 750-1500 mm. The Daba mountain is an intensive denudation area caused by arid conditions most of the year. However, it is heavily dissected by many streams and rivers fed by seasonal rains which have eroded the landscape over time. Major outcrops of Early Paleozoic strata of mainly carbonates, siliceous-carbonic shale, and detrital rock are interbedded and intruded by basic volcanics (diabase, trachy-diabase), and by igneous rock (trachyte, volcanic megaphenocrysts). Due to the influence of recurrent faulting and folding, strata sets within the outcrop are repetitive. Lower Paleozoic stone-like coal is the most widespread stone-like coal in the Daba Mountain area. Lower Paleozoic strata are mainly distribution strata and well developed in the Daba area. The lowest Cambrian beds are mainly composed of siliceous shale, siliceous carbonic slate (Lujiaping Formation), and limestone (Jianzhuba Group).

The mountains in the Daba area are very big and deep, and with steep hill slopes and deep ravines. There is no Carboniferous and Permian distribution developed, both of them are mainly humic coal-forming strata in China, and the Daba area also does not have enough highways just very simple roads between the Village and the good quality humic coals from mining in other place cannot be easily transported here. The stone-like coal is mainly fuel in this region. Many families there have to use the local Lower Paleozoic stone-like coal as fuel.

ANALYTICAL METHODS

Samples were analyzed by $HCl+HNO_3$ dissolution then arsenic and mercury were determined by the hydride generation atomic fluorescence spectrometric (HG-AFS). The common elements in the coal, stone-like coal and black shale were analyzed by the American

Baird ICP-2070 apparatus. They were also analyzed by AAF-800 for arsenic, selenium, cadmium and mercury by Lu Yilun in the laboratory of the Institute of Geographical Sciences and Natural Resources, Chinese Academy of Sciences.
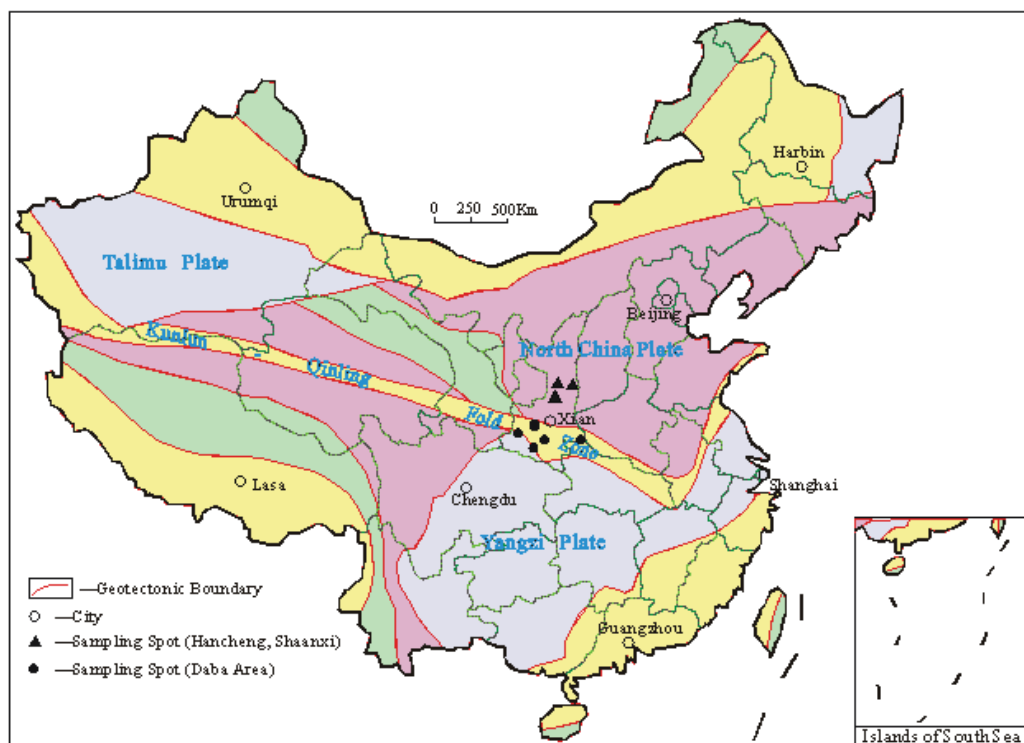
Figure 1.

The proximate analyses of black shale and stone-like coal (GB 212-91) and the ultimate analyses of the coal and ash were performed at the Geological Testing Center of the Coal Academy of the Academy of Sciences, and the Coal Testing Center of the Shaanxi Quality Testing Center, the laboratory of the Chenghe Mine bureaus. The reporting limit and relative error is 10^{-3} and 10% respectively. Total sulfur and forms of sulfur in coal (GB/T-214-1996, GB/T-215-1996) were equated to ISO 157-1975.

The samples of Permo-Carboniferous humic coal were collected from the Hancheng coal mine, Shaanxi, as typical of the Permo-Carboniferous coals of the North China Plate (Figure.1).

STUDY AREA

Qinling Mountain is the eastern part of Kunlun-Qinling Geotectonic Belt (Fig.1), and it is the current boundary between north China and south China. Qinling Mountain is also the geological boundary between the North China Plate and the Yangzi Plate (Ma et al,1998).

The Daba area of South Qinling Mountain is located in southern Shaanxi Province and adjacent part of Chongqi city and Henan Province, in central China (Fig.1). The Daba area is

mountainous with steep slopes and deep ravines. The mountains are denuded by arid conditions most of the year, but the seasonal rainfall is heavy, with the annual precipitation 750-1500 mm..

1. THE ELEMENT COMPOSITION OF STONE-LIKE COAL

Stone-like coals, as its name implies, looks like stone,and applies here to a burnable siliceous black shale- carbon-rich siliceous rock that generally has more than 40% ash and is very heavy and hard. (Table 1).

The Stone-like coal is different with the Carboniferous - Permian coal's gangue, which also have more ash, and some of them are burnable black shale too. The stone-like coal have much more siliceous content in the ash (table 1) than the Carboniferous - Permian gangue. The stone-like coal have more proportion of SiO_2 content in the ash (table 1), the SiO_2: Al2O3 commonly are 5-16:1, and have a high content of CaO and MgO too; the ash in the Carboniferous - Permian coal's gangue (Table 2) have a nearly 1:1 proportion of SiO_2: Al_2O_3, and have a low content of CaO and MgO. Because there are more content of siliceous content in the stone-like coal, so they are harder than the gangue.

The Stone-like coal is different with the common black shale, which including carbonate rock, argillaceous rock, and also including black siliceous rock and have more than 1% of organic carbon but they can not burring.

The Stone-like coal is different with the generlly black shale too, they are always corresponding with the metamorphic rock, they are always have more siliceous content and less Al_2O_3 content in the ash, and more than 20% of organic carbon and much sulfide as well as other havey meatal.

Table 1. The common element content in Early Paleozoic stone-like coal in Daba area, south Shaanxi (%)

Age	Position of their occurance	Ash %	S(%)	SiO2(%)	Na2O(%)	Al2O3(%)	Fe2O3	CaO(%)	MgO(%)	K2O(%)
$\in_3$	fault JGD	26.37/26.41	1.60/1.61	15.27	0.155	1.850	1.322	5.462	1.456	0.956
(7)	fold BXLM	40.20/40.23	2.0/2.20	25.18	0.104	3.726	2.256	3.105	2.148	2.066
S	In igneous HP	41.63/41.37	1.90		0.120	3.479	2.013	2.685	1.949	2.016
S	In igneous HP	41	1.90	24.63	0.102	3.561	1.881	2.839	1.799	1.999
O	JG2	31.20/31.27	1.5	17.45	0.107	2.726	1.576	1.667	0.881	1.401
S	In igneous AB	57.42/57.37	0.7	36.50	0.429	5.651	2.820	3.570	1.298	1.809
$\in_3$	BXLX	76.64/76.62	2.90/3.0	41.96	0.118	10.07	3.306	3.693	3.792	5.365
$\in_1$	L2(58)	41.48/42.91	3.4/5.6	30.70	0.053	4.68	2.88	2.74	1.63	1.51

Table 2. The common element content in the Carboniferous coal and coal gangue in Hancheng Coal Mine, north Shaanxi (%)

Gangue Field No.	SiO2	Fe2O3	Al2O3	CaO	MgO	K2O	Na2O	TiO2
T11g	38.46	0.51	32.8	0.09	0.039	0.221	0.051	1.62
X8#	38.18	0.34	32.06	0.215	0.122	0.471	0.117	1.93
X4#	28.31	1.49	21.24	0.426	0.157	0.569	0.102	0.85
H2#	33.99	1.35	19.48	0.122	0.45	2.86	0.307	1.14
X8g	41.82	1.62	19.67	0.044	0.231	1.96	0.383	1.01
H2#b	52.55	2.49	20.57	0.103	0.898	3.22	0.276	0.978
H2#	29.29	0.369	20.32	0.076	0.334	3.38	0.673	1.04
H11#g	31.82	0.27	35.52	0.036	0.344	0.254	0.086	0.396
coal								
H11#	7.18	0.32	5.76	0.159	0.049	0.274	0.067	0.046
H3#	2.12	0.25	1.5	0.745	0.043	0.253	0.064	0.053
H2#	2.88	1.05	2.15	6.74	0.477	0.317	0.055	0.11
P5#	11.42	1.39	8.37	1.36	0.106	0.494	0.106	0.479
H5#	13.61	0.194	13.59	0.12	0.041	0.722	0.362	0.443
T11#	7.18	2.67	6.81	0.615	0.028	0.667	0.358	0.812
H3#	5.41	0.47	3.88	0.332	0.049	0.216	0.049	0.258
X9#	3.37	1.37	6.77	0.391	0.03	0.145	0.051	0.123
H3#	1.54	0.045	1.37	0.215	0.293	0.802	0.399	0.061
X8#	1.03	0.27	0.797	0.09	0.012	0.231	0.048	0.016
X4#	8.3	2.65	20.48	0.086	0.096	0.267	0.055	1.75
A11#	6.69	1.32	6.97	0.143	0.039	0.775	0.403	0.348

Perhaps stone-like coal should be termed burnable siliceous black shale. Stone-like coal is more than 20% organic carbon and even more ash, and the ash has a siliceous component.

The black shale and stone-like coal found in the Daba area is rich in sulfur and other heavy metals (Table 3). Their heavy metals content is much higher than the Permo-Carboniferous and late ages of coal and coal gangue (Table 4).

Sulfur content is about 2% in stone-like coal of Silurian age, upwards to 2-7% in the lowermost Cambrian black shale and stone-like coal, mercury from about 0.24 mg/kg to 1.446 mg/kg, some samples reach 2.6 mg/kg; arsenic from 16 in the upper Cambrian fault stone-like coal, up to 64-78 mg/kg in Silurian age, to 224 mg/ kg to 516 mg/kg in Lower Cambrian; selenium from about 5 mg/kg in fault stone-like coal of middle-upper Cambrian, upwards to 22 mg/kg on average in the lowermost Cambrian stone-like coal; Cadmium from 0.2mg/kg to 36 mg/kg; Carbon from 5% in lowermost Cambrian black shale to 45% in the lowermost Cambrian stone-like coal.

Table 3. The trace element content in the some Early Paleozoic stone-like coal in Daba area, south Qinling Mountain (ug/g)

Age	Position of their Occurrence	Cu	Zn	Mn	Sr	Ba	P	Co	Ni	Cr	Pb	Ti	Li	As	F	Hg	Se
ε_2	fault JGD	137.6	1304	125.1	200.5	2366	1351	3.135	341.1	184.9	12.96	821.9	8.742	15.36	221.404	0.259	41
ε_3	fold,near igneous,bxlm	182.7	835.9	162.1	121.3	1327	1988	1.157	430.2	260.0	28.81	1773	23.18	34.08	1390.098	0.337	
S	In igneous HP	227.8	1051	144.6	143.3	1145	1994	5.785	415.7	305.9	34.58	1798	25.79	64.99		0.237	12.1
S	In igneous HP	231.4	1001	136.8	139.0	1143	1960	1.315	431.9	226.0	38.89	1675	20.43	78.72	1526.407	0.220	
ε_2	fault JG2	159.3	1479	148.0	252.1	3498	1756	6.046	453.2	222.7	23.74	1542	8.698	53.35	452.947	0.185	
ε_3	In fold,far igneous,Dh									269.4	56.81	2085		9.62	529.2	0.245	4.7
S	In igneous AB	166.0	960.0	952.4	413.6	3284	2004	4.734	382.9	196.5	36.73	1996	20.51	54.64	834.100	0.237	
ε_3	BXLX	1647	1594	110.2	118.6	1320	4555	5.257	927.2	698.4	49.70	5374	96.86	106.8	3167.981	1.445	
ε_1	L2(58)	214.9	921.3		225.4	8220		12.62	449.5	266.8				224.69	642.30	1.085	32.05

Table 4. The trace element content in Carboniferous coal and coal gangue in Hancheng Coal Mine, north Shaanxi (ug/g)

Gague Field No.	Hg	Se	As	P	Mn	Cu	Zn	Sr	Ba	Pb	Cr	Co	Ni	V	B	Cd
T11g	0.211	0.813	0.715	561.9	10.93	5.48	10.11	25.13	10.94	38.99	58.74	38.15	31.9	98.78	11.27	未捡出
X8#	0.347	13.529	0.601	1034	14.41	45.5	73.11	71.35	142.6	40.7	72.36	19.07	16.1	57.09	15.23	0.252
X4#	0.302	5	2.032	1048	58.94	36.8	36.7	448.5	166.7	46.69	61.09	29.11	22.2	60.87	4.52	0.192
H2#	0.207	4.78	2.212	1023	22.11	67.5	21.05	131.6	442.6	29.45	60	34.13	33.2	155.9	55.97	0.246
X8g	0.137	1.884	2.917	4471	45.18	35	20.26	275.9	130.9	29.53	72.56	7.06	24.3	102.9	73.08	0.166
H2#b	0.026	0.855	2.203	637.1	70.75	53.1	82.78	127.9	544.3	29.77	95.72	26.14	33.5	125.7	65.04	0.436
H2#	0.175	3.188	1.335	6792	12.56	54	24.45	137.4	466.2	36.63	52.04	8.52	22.2	142.2	97.18	0.108
H11#g Coal	0.067	2.057	2.67	324.2	19.74	25.9	210.2	73.78	217.7	44.29	3.75	5.04	38.6	52.19	78.82	0.148
H11#	0.703	4.103	0.824	223.6	11	4.92	12.52	59.53	29.75	1.45	34.31	10.04	13.1	19.59	104.2	0.044
H3#	0.889	0.271	0.78	357.7	54.09	63.1	11.38	71.27	17.46	5.27	53.57	25.1	39.8	17.21	1	0.166
H2#	0.444	2.176	0.63	315.8	264.6	15.8	36.98	187.3	53.91	11.33	74.24	16.06	22.7	23.2	4.51	0.298
P5#	0.403	3.768	2.575	925	74.77	29.9	13.09	371.2	87.89	20.35	70.49	24.13	19.9	42.43	45.2	0.21
H5#	0.222	4.783	0.858	273.9	3.18	58	12.57	94.45	60.26	22.75	53.47	32.64	15.9	25.67	44.01	0.09
T11#	0.166	8.406	2.816	762.9	25.22	100	25.84	59.48	18.05	27.69	71.6	28.37	19.6	92.58	36.14	0.08
H3#	0.1	3.043	0.858	391.2	27.51	24.6	27.31	47.47	27.46	13.25	85.4	17.11	33.9	41.21	32.85	未捡出
X9#	0.396	5.263	4.235	701.4	20.62	43.1	1.14	147.2	20.67	26.42	101.4	16.1	14.5	24.33	19.99	0.176
H3#upper	0.163	0.754	1.373	109.9	4.13	28.2	18.16	94.56	29.67	5.11	25.78	32.64	19.1	22.13	0.17	0.4
X8#	0.144	1.188	1.288	698.6	10.74	36.8	713.4	41.4	15.95	7.42	90.08	6.71	13.8	15.85	8.95	0.354
X4#	0.484	4.13	1.259	578.5	8.08	93.3	203.8	450.4	97.7	44.45	42.22	5.37	19.4	52.45	19.88	0.09
A11#	0.463	10.108	2.086	695.8	9.56	51.6	9.08	92.16	17.09	27.05	43.92	26.95	15.6	29.86	36.12	0.176

2. THE RANK OF LOWER PALEOZOIC STONE-LIKE COAL

Industrial and elemental analyses of Lower Paleozoic stone-like coal in South Qinling Mountain are shown in Tables 2 and 3. The ash content of most Lower Paleozoic stone-like coal varies from 15% to 60% (about 40% on average), and the carbon content varies from 20% to 80% (about 40% on average).

There are three types of stone-like coal in the Daba area as follows:

Natural coke: There are two kinds of natural coke in the Daba area, south Qinling Maintain, one is fault coke, which generally occurs between the stone-like coal and surrounding rock. I think it is the black shale which lost its volatile material and the minerals material by high pressure during the tectonic in the late Triassic when the North China Plate collided with the Yangzi Plate. Another one is melting distillation coke which generally occurs between the stone-like coal and igneous rock, it is the black shale loss their volatile material and the minerals material by high temperature during the lava enwraped the black shale or carbonate rocks Natural coke is not a big resource and is generally very thin and always occurs as a very thin bedded (mostly about ten CM) interbedded in the stone-like coal and wall rock always between the stone-like coal and surrounding rock.

Good-quality stone-like - coal Sand - like coal: They occur mostly in the compressional structure belt, in the fault zones and the axes of folds in the southern part of the Daba area where is a deep fault, Daba deep fault, the boundary of Yangzi Plate and Qinling Mountain. They formed during the high pressure during the tectonic.

Stone-like coal - mainly in the Sulurian igneous rocks.

Poor-quality stone-like coal, which are mainly the lower Cambrian black shale far from fault.

Table 4. Proximate analysis and ultimate analysis of good-quality stone-like coal of lowermost Cambrian in Ziyang, south of Qinling Mountain

Sample No.	Mad /%	Aad /%	Vad /%	St, d /%	Q_{DWf} (kcal./kg)	Cad /%	As mg/kg	Se mg/kg	Hg mg/kg
An58	1. 25	42.91	3. 71	4.16	4510	52.11	224.69	32.05	1.09

Note: Mad = Moisture in the air dried sample; Aad = Ash in the air dried sample; Vad = Volatile in the air dried basis; St, d = Total sulfur of dry basis; Q_{DWf} = Net calorific value at constant volume ; Cad = Content of carbon in the air dried sample

Table 5. Proximate analysis and ultimate analysis of the black shale (poor-quality stone-like coal) of lowermost Cambrian in Ziyang, south of Qinling Mountain

Analysis item	Mad /%	Aad /%	Vad /%	St, d /%	Q_{DWf} (kcal./kg)	Cad /%	As Mg/kg	Se Mg/kg	Hg Mg/kg
A17y	1.95	61.25	7. 38	7.16	1700	16.65	266	37.3	2.35

Note: as above

https://telegram.me/Geologybooks

Table 6. Proximate analysis and ultimate analysis of Good-quality stone-like coal of lowermost Cambrian in Xichuan Coal Mine, south Qinling Mountain.(belongs to the Yangzi Plate

Analysis item	Mad /%	Ad /%	Vd /%	St, d /%	Q_{DWf} (kcal./kg)	Cad /%	As Mg/kg	Se Mg/kg	Hg Mg/kg
Index	1.12	46.12	5.0	5.8	4010	42.10	168.2	120.1	0.97

Note: as above

Table 7. Proximate analysis and ultimate analysis of stone-like coal of Sulurian in Haoping Coal Mine, south Qinling Mountain

Sample No.	Mad /%	Ad /%	Vd /%	St, d /%	Q_{DWf} (kcal./kg)	Cad /%	As Mg/kg	Se Mg/kg	Hg Mg/kg
An17	0.98	48.12	2.9	1.9	4060	40.23	122.47	19.56	0.57

Table 8. Proximate analysis and ultimate analysis of Nature coke of Sulurian in Haoping Coal Mine, south Qinling Mountain

Sample No.	Mad /%	Ad /%	Vd /%	St, d /%	Q_{DWf} (kcal./kg)	Cad /%	As Mg/kg	Se Mg/kg	Hg Mg/kg
An 1	0.11	17.69	2.02	0.56	7410	black lead	8.39	1.10	1.99

Table 9. Proximate analysis and ultimate analysis of Nature coke of upper Cambrian in the fault in Tiefu Daba area, south of Qinling Mountain

Sample No.	Mad /%	Aad /%	Vad /%	St, d /%	Q_{DWf} (kcal./kg)	Cad /%	As Mg/kg	Se Mg/kg	Hg Mg/kg
An10	0.58	17.73	2. 38	0.4	7200	73.11	15.84	3.34	1.946

Table 10. Proximate analysis and ultimate analysis of the stone-like coal of middle Cambrian-Ordovician in the Fold or fault in Daba area, south of Qinling Mountain

Sample No.	Mad /%	Aad /%	Vad /%	St, d /%	Q_{DWf} (kcal./kg)	Cad /%	As Mg/kg	Se Mg/kg	Hg Mg/kg
An8	1.45	54.93	3. 891	1.6	2200	25.11	236	36.3	1.946

Note: as above

All stone-like coal in the Daba area is a very high rank of anthracite. Even though the ash content is high, it is a low volatile coal and so very good for home use. Anthracite is the hardest and most energy valuable rank of coal.

COMPARISON OF THE COMPOSITION OF THE BLACK SHALE AND STONE-LIKE COAL OF DABA WITH PERMO-CARBONIFEROUS COAL IN CHINA

The coal evolved from higher plants in the Permo-Carboniferous system and in later ages was termed humic coal. Humic coals are the most widely distributed coals both in China and elsewhere in the world. Permo-Carboniferous coal, mainly including bituminous coal but with some anthracite, is the main resource of steam coal and of coal for household use in China. The Permo-Carboniferous coals account for nearly 58% of all Chinese coals, occurring mainly in North China and Northwest China. Longtan Formation (Late Permian) coals account for about 10%, mainly in Southwest China (Yunnan and Guizhou Provinces). Jurassic coals account for about 39% of Chinese coals (mainly in Northwest China) and the other coals (mainly Triassic, Cretaceous and Tertiary coals) about 5% (Chen et al., 1993). These are all humic coals and most of them formed in continental or marine-margin swampland.

The ash content of most Permo-Carboniferous coal varies from 15% to 30% averaging about 20%, and the carbon content varies from 50% to 80% averaging about 60%. Tables 11 and 12 show the results of industrial and elemental analyses of Permo-Carboniferous coal from Hancheng Coal Mine, north Shaanxi province, a typical coal of the North China Plate.

Table 11. Proximate and ultimate analysis of #2 (early Permian) coal in Hancheng Coal Mine, North China Plate

Analysis item	Mad[a] %	Ad [b]/%	Vd [c] /%	St,d [d]/%	Q_{DWf} (kcal./kg)	Cad [f]/%	Had [g] /%	Nad [h] /%	Oad [i] /%	As Mg/kg	Se Mg/kg	Hg Mg/kg
Index	0.72	20.12	17.43	1.21	6006	66.04	3.33	1.02	2.10	1.2	2.3	0.11

Note: a) Mad=Moisture in the air dried sample; b) Ad=Ash in the air dried sample; c) Vd=Volatile matter of dry basis; d) St, d=Total sulfur of dry basis; e) QDWf== Net calorific value at constant volume; f) Cad, g) Had, h) Nad,i) Oad=Content of C, H,N, O in the air dried sample.

Table 12. Proximate and ultimate analysis of # 5 (late Carboniferous) coal in Hancheng Coal Mine, North China Plate

Analysis item	Mad /%	Ad /%	Vd /%	St, d /%	Q_{DWf} (kcal./kg)	Cad /%	Had /%	Nad /%	Oad /%	As Mg/kg	Se Mg/kg	Hg Mg/kg
Index	0.98	18.76.79	19.04	1.58	6531	69.10	4.20	0.68	3.05	1.02	2.1	0.21

Note: as above

Based on the above tables, the most lower Paleozoic stone-like coal in the Daba area has lower caloric content, lower carbon content and the sulfur content is higher than the humic coal of Permo-Carboniferous coal in North China. The Lower Cambrian black shale and stone-like coal are higher in sulfur, selenium, arsenic and mercury.

3. DISTRIBUTION PATTERN AND OCCURRENCE POSITION OF EARLY PALEOZOIC STONE-LIKE COAL IN THE DABA AREA, SOUTH SHAANXI

Major outcrops of Early Paleozoic strata at South Qinling Mountain consist mainly of carbonates, siliceous-carbonaceous shale, and detrital rocks which are interbedded and intruded by basic volcanics (diabase, trachy-diabase), and by igneous rocks (trachyte, volcanic megaphenocrysts). Due to recurrent faulting and folding, strata sets within the outcrop are repetitive.

Cambrian and Ordovician strata are the most widespread strata in the Daba Mountain area (Figure.2). The Lower Cambrian beds are mainly composed of siliceous shale or siliceous carbonaceous slate (Lujiaping Formation, lowest Cambrian and upper Neoproterozic) and stone-like coal; the middle Cambrian to Ordovician strata are mainly composed of limestone, dolomite and marl, which are interbedded and intrudeds a lot beds of basic igneous rocks (diabase, trachy-diabase). Silinum strata in here are mainly composed of black shale or carbonaceous slate, in the Northern part of Daba are interbedded and intruded by igneous rocks (trachyte, volcanic megaphenocrysts). Three-measured sections in the Daba area of south Qinling Mountain are discussed below. These may be the main souce of Lower Paleozica strata stone-like coal in Daba area.
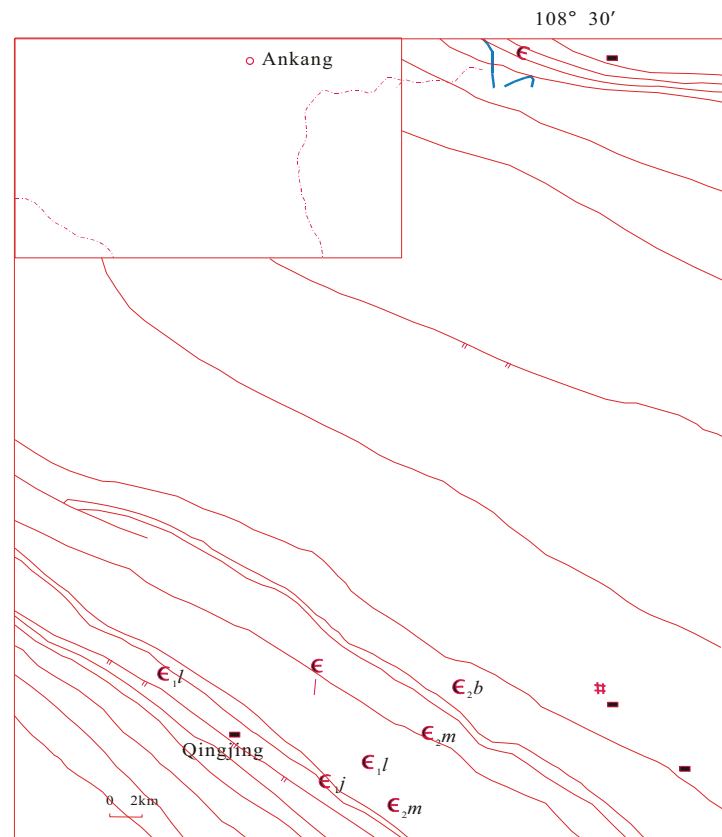
Figure 2. Geological map and section position in the Daba area.

3.1. Lower and Middle Cambrian Section in Lujiaping, South of the Ziyang County (Figure 1.), Shaanxi Province, Daba Area of South Qinling Mountain

This section is the typical section of the Lujiaping Formation. Several geological teams have measured here; Qing (1983) was the first to find the Lower Cambrian small shelly fossils in this section. Earlier researchers did not deal with the geochemistry of this section.

Superjacent strata: Mabaguan Formation, Middle Cambrian

23.	gray, thick bedded marl	36 m
22.	litter fault with stone-like coal	4 m
21.	greenish-gray, thick bedded marl	67 m
20.	greenish-gray, medium-thick bedded mud marl and calcareous slate	
19.	greenish-gray, medium-thick bedded mud marl and calcareous slate	78 m

---------------conformity---------------

Jianzhuba Formation, upper part of Lower Cambrian($Є_{1j}$)

18.	dark gray, banded crystalline limestone interbedded with carbonaceous laminae.	16.7 m
17.	gray, thin-medium bedded crystalline limestone	10.8 m
16.	dark gray-black, carbonaceous and siliceous schist	9.6 m
15.	litter fault with stone-like coal	0.4 m
14.	dark gray, siliceous carbonaceous schist interbedded with several layers of thin-bedded stone-like coal	18.2 m
13.	dark gray, thin-medium bedded, carbonaceous micritic limestone	4.8 m
12.	dark gray, thin-medium bedded, crystalline limestone, the trilobite *Kootenia* is present	76.8 m

--------------- conformity --------------

Lujiaping Formation, Lower Cambrian($Є_1l$) and upper Neoproterozic (Upper PreЄ)

11.	light gray-green (after weathering), sericitized schist and silty slate. in the upper part of this bed, fragments of trilobites and brachiopods	66.1 m
10.	dark green slate	20 m
9.	dark gray, siliceous carbonaceous slate	3 m
8.	black, pyrite nodule-bearing siliceous schist and carbonaceous slate	6.8 m
7	greenish-gray, massive diabase	21.2m
6	black, thin-bedded silicalite {IS THIS CHERT?}, interbedded with witherite {IS THIS THE BaCO3 }and black siliceous slate and carbonaceous slate	36.1 m
5.	thick-bedded black siliceous schist and carbonaceous slate	20.4 m
4.	thin-bedded black siliceous schist and carbonaceous slate interbedded width witherite	20.1 m
3.	this bed contain 4 gyres of thick-bedded black chert think about interbedded siliceous schist and carbonaceous slate interbedded with stone-like coal (about 20m), low part is one 16 m thick-bedded black chert	6-40m) 223.6 m

2. thick-bedded psephitic {I'D USE "RUDITIC"} dolomite interbedded with siliceous conglomeration conglomerate, phosphatic dolomite and phosphorite; contains small shelly fossils: Archaeooides sp. (似古蛋), Protohertina sp.(原赫兹刺) 23m; middle part contains small shelly fossils Chancelloria sp.(开腔骨针) 18m; lower part contains small shelly fossls: Hyolithidae(软舌螺科钙质骨针) 25 m

1. thick-bedded psephitic {I'D USE "RUDITIC"} dolomite interbedded with siliceous conglomeration conglomerate, phosphatic dolomite and phosphorite; contains small shelly fossils

---------------conformity?---------------

thick-bedded dolomite

---------------conformity---------------

Yaolinghe group gray-green conglomerate slate 千枚岩
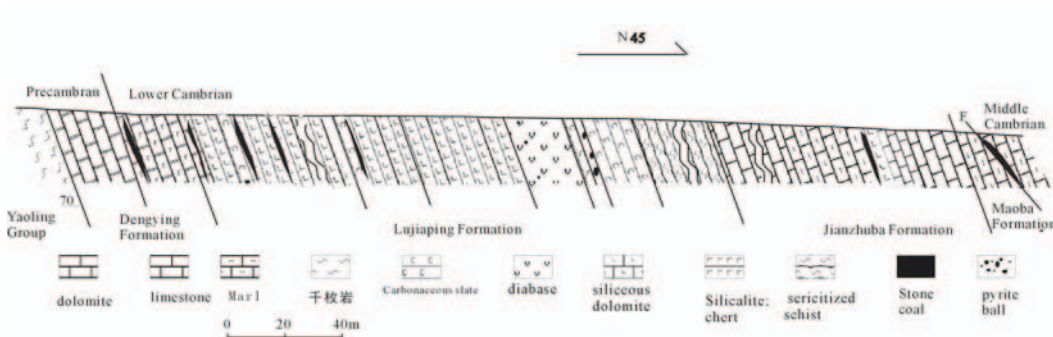
Figure 3. section of the Lujiaping Formation in the Lujiaping, south of the Ziyang County (Fig.1), Shaanxi Province, Daba area of South Qinling Mountain

3.2. Middle to Upper Cambrian to Ordovician Stone-Like Coal Section in the Daba Area of South Qinling Moutain, South of Pingli Connty, Shaanxi

Middle to Upper Cambrian to Ordovician mainly marl or limestone and dolomite. There is very good-quality stone-like coal in the Middle to Upper Cambrian to Ordovician strata in the Daba area of South Qinling Mountain which occurs mostly corresponding to the structure belt, in such features as fault zones, the axes of folds.

Ordovician

16. greenish-gray, thin bedded mud marl and calcareous slate
25. zonal limestone and lime dolomite
23. gray, thin bedded limestone and mud dolomite   46 m

--------------fault with stone-like coal --------------

22.	litter fault with stone-like coal	4 m
21.	greenish-gray, thin bedded marl	33 m
20.	19 greenish-gray, medium-thick bedded mud marl and calcareous slate	38.2 m

--------------fault with stone-like coal --------------

Baxian Formation, Upper Cambrian(C_{3b})

18.	dark gray, banded crystalline limestone interbedded with carbonaceous laminae	16.7 m
17.	gray, thin-medium bedded crystalline limestone	10.8 m
16.	dark gray-black, limestone	19.4 m
15.	litter fault with stone-like coal	0.4 m
14.	dark gray, siliceous carbonaceous schist interbedded with several layers of thin-bedded stone-like coal	18.2 m
13.	dark gray, thin-medium bedded, carbonaceous micritic limestone	4.8 m
12.	dark gray, thin-medium bedded, crystalline limestone	46.1 m

--------------axes of fold with stone-like coal --------------

Baguamiao Formation, upper part of Middle Cambrian(C_{2b}) and Maobaguan Formation (C_{2m})

11.	light gray medium-thick bedded mud marl and limestone	69 m
10.	dark green thin bed marl	28 m
9.	gray thin bedded mud dolomite and limestone	31m
8.	bedded mud marl and limestone.	8m
7.	greenish-gray, thin- bedded mud marl	21.2m
6.	thin-bedded limestone and dolomite	18.2 m
5.	thick-bedded limestone and dolomite	86.8 m
4.	thin-bedded carbonate slate and marl interbedded with thin-bedded limestone and dolomite	20.1 m
3.	thin-bedded mud marl.	

3.3. Silurian Stone-Like Coal in the Daba Area

There is abundant stone-like coal of Mid-Lower Silurian in Haoping Town (which is to the southeast of Naore Village) and Xianghe, Ankang County (which is to the east of Daba area). Silurian stone-like coal reserves account for 70% of all stone-like coal resources in the Daba area, South of Qinling Mountain.

Silurian stone-like coal in the Daba area, South of Qinling Mountain occurs in one form in the igneous rock.. All Silurian stone-like coal in Daba area is enveloped in trachytic pyroclastic rock or neighboring the igneous rock, not outcrop orebody, and occurs mostly in sack-like, lenticle or lotus root-like in Haoping, as in other areas of the Daba Mountain. There is top-quality stone-like coal in Haoping, Ziyang County and Xianghe, Ankang County, which have great reserves, even more than millions of tons elsewhere. Single coal orebody is generally 3~4 m high, 1~5 m thick, from several to tens of meters long, and it has a much

smaller thickness and volume than other strata because of its discontinuous layers. So stone-like coal has little influence on the surface environment despite its high selenium content(8, 9, 10), and there is no typical selenosis in stone-like coal distribution region in Haoping, Ziyang County and Xianghe, Ankang County.

Now take an example of stone-like coal section of Daguiping Formation, Silurian in Haoping Town. The section lies on the side of highroad in Haoping stone-like coal mine, measured along the highroad.

Distribution of Silurian stone coal in Daba Mountain
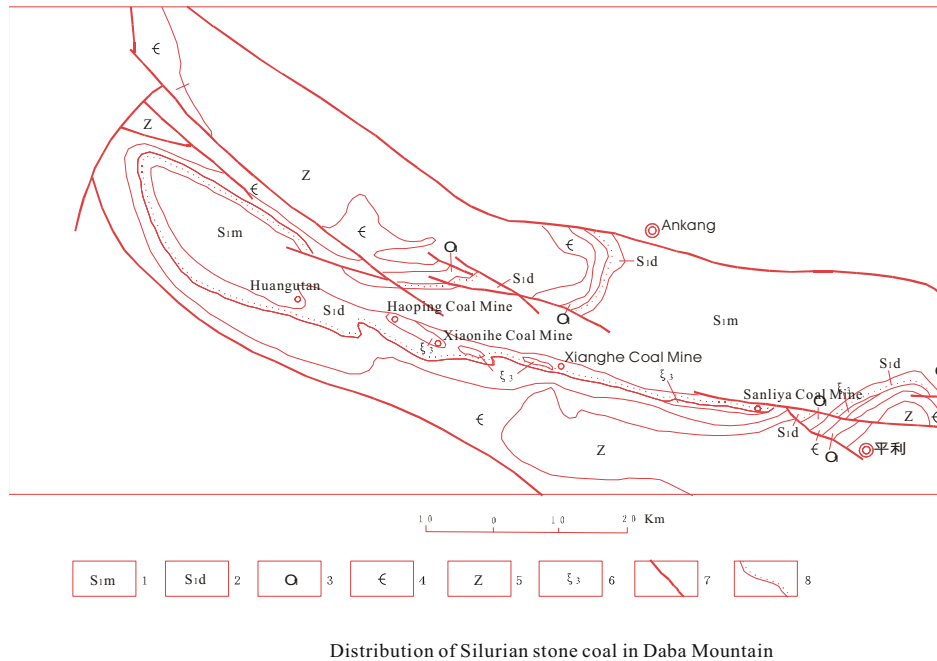
1. Meiziya Formation, Silurian ; 2.Daguiping Formation, Silurian ; 3.Lower Ordovician ; 4.Cambrian ; 5.Later Proterzioic ; 6.trachyte ar

Figure 4. Superjacent stratum: the upper portion of Daguiping Formation, Mid-Lower Silurian

9.   black-gray, silty siliceous and carbonaceous slate (sage green slate
     in the upper portion)   82 m
8.   brownish-red-gray, almond-shaped structure, trachytic pyroclastic rock   218.2 m

---------------fault ---------------
7   black-gray, almond-shaped structure, trachytic volcanic tufflava with
     5 beds stone-like coal   206.6 m

---------------fault ---------------
6.   fault crash zone   13.2 m
5.   lumpish trachytic enwrap with 4 beds stone-like coal   103.4 m
4.   lumpish trachytic pyroclastic rock   312.6 m
3.   black-gray, silty siliceous and carbonaceous slate   108 m

2. brownish-red-gray, trachytic pyroclastic rock enwrap with 4 beds
    stone-like coal   236.7 m
1. brownish-red-gray, trachytic pyroclastic rock enwrap with 4 beds
    stone-like coal   334.1 m
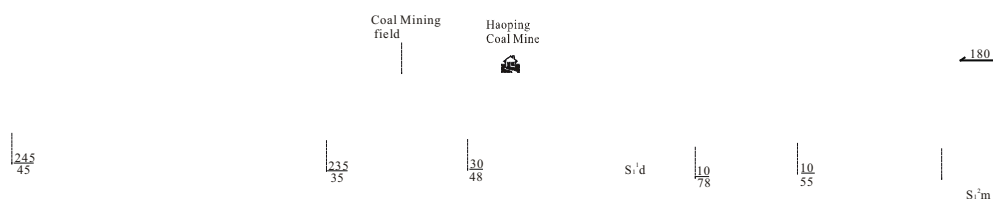
Figure 5.

4. OCCURRENCE OF EARLY PALEOZOIC STONE-LIKE COAL IN DABA AREA, SOUTH SHAANXI

The stone-like coal in the Daba area, South of Qinling Mountain occurrence has three forms: in the contact zone of black shales and igneous rock; among igneous rock, and in fault zone or axid of folds.

Good-quality stone-like coal in the Lower Paleozoic strata of South Qinling Mountain occurs mostly corresponding to the structure belt, in such features as fault zones, the axes of folds, or corresponding with igneous rocks. The shape of the stone-like coal ore bed generally occurs in sack-like bodies, lenses, or nodular lens-like bodies. But most of the stone-like coal in the lower part of the Lower Cambrian position, but not continuous layers. Except for the stone-like coal ore bed near the fault, the stone-like coal of lower Cambrian in the Daba area is mostly poor quality stone-like coal and the carbon content is generally about 20%. But the black shale in the lower part of the Lower Cambrian which has a carbon content of about 5-20% generally occurs as stratigraphically continuous layers.

The Silurian stone-like coal, which has great reserves, accounts for nearly 70% of stone - -like coals in the Daba area, other age stone-like coals account for nearly 30%. Areas in the Daba area such as the Haoping coal mine(HP) in Ziyang county, the Bashan in Ankang county (AB) and Xianghe(XH) Ankang County, all contain the Silurian stone-like coal, whose reserves are estimated to be even more than millions of tons. Single coal orebody is generally 3~4 m high, 1~5 m thick, from several to tens of meters long, and it is the first important stone-like coal in the Daba Mountain.

The biggest stone-like coal mine is at Haoping (Silurian in age) (Edit Committee on Ziyang County Annals 1989; Luo and others 1995c), located about 20 km north of Ziyang

Contuny town (Fig.1); it has large reserves and its coal is very commonly used in the Daba area. There also are a lot of small stone-like coal mines everywhere in the Daba area.

Most of the stone-like coal of the Silurian period in the Daba area is enveloped in trachytic pyroclastic rock or neighboring trachytic pyroclastic rock in the fault and the axis of anticline or syncline, not an outcrop in a continuous orebed, and occurs mostly in sack-like, lenticle or lotus root-like in Haoping, as it is in other areas of the Daba Mountain. There is top-quality stone-like coal in Haoping, Ziyang County and Xianghe, Ankang County, which have great reserves, even more than millions of tons somewhere. A single coal orebody is generally 3~4 m high, 1~5 m thick, from several to tens of meters long, and it is the first important stone-like coal in the Daba Mountain and has the greatest reserves of all.

The rocks of Upper Cambrian and Ordovician strata in Daba area mainly limestone and dolomite as well as marl. Stone-like coal occurs in the Upper Cambrian and Ordovician strata mostly corresponding the structure belt, in the fault zones, or the axes of folds.The sulfur and heavy metal in the Upper Cambrian and Ordovician stone-like coal is more low than the Lower Cambrian stone-like coal, and the F and As is lower than the content both of Silurian and Lower Cambrian stone-like coal in Daba area, South Qinling Mountain.

Even most of the stone-like coal in the lower part of the Lower Cambrian can be found in a strata position, but they still not occur as stratigraphically continuous layers, most are in sack-like bodies, lenses, or nodular lens-like bodies, too. These are of poor quality and the carbon content is generally about 20%, only near the big extrusion. Fault, mainly near the famous deep fault -Daba Mountain, which is the boundary fault of Yangzi Plate and Qinling Mountain. That area has very good -quality stone-like coal from the Lower Cambrian.

Most stone-like coal of the Cambrian and Ordovician in the Daba area is present to the zoster of a fault and the axis of anticline or syncline, not the outcrop of a continuous orebed too, and occurs mostly in sack-like, lenticle or lotus root-like which depend on the shape of zoster of the fault and the axis of anticline or syncline. There is top-quality stone-like coal in Tiefu and Gaotan, Ziyang County, and Zhenba County, which have great reserves too, even though not biger than stone-like coal of Silurian, also there is more than millions of tons in the Tiefu and Gaotan, south Ziyang County. Single coal ore body is generally 3~4 m high, 1~5 m thick, from several to hundreds of meters long, and it has a high quality coal in the Daba area. Except for the lower Cambrian stone-like coal and black shale, the content of S, As, Se, and F in the middle Cambrian to the Ordovician is generally lower than the lower Cambrian stone-like coal and black shale as well as the stone of the Silurian.

CONCLUSIONS

The Lower Paleozoic stone-like coal in the Daba area is the burnable siliceous black shale, which has more than 20% of organic carbon and more ash, and its ash have more siliceous components, very high content of F ,As, Se, Cd, and Hg.

The Stone-like coal used in the Daba Area has caused a lot of human health problems. In the Haoping Coal Mine, 80% of the people suffer from Fluorine- poisoning and arsenic-poisoning. The Fluorine- poisoning and arsenic- poisoning in this area were confirmed as coming from burning "fluorine and arsenic-rich stone-like coal". There are Fluorine-poisoning and arsenic- poisoning problems reported in the Haoping town and other places in

the Daba area where the citizens use more stone-like coal for warmth and cooking..Where does the arseic and fluorine in stone-like coal come from? How can we control them?
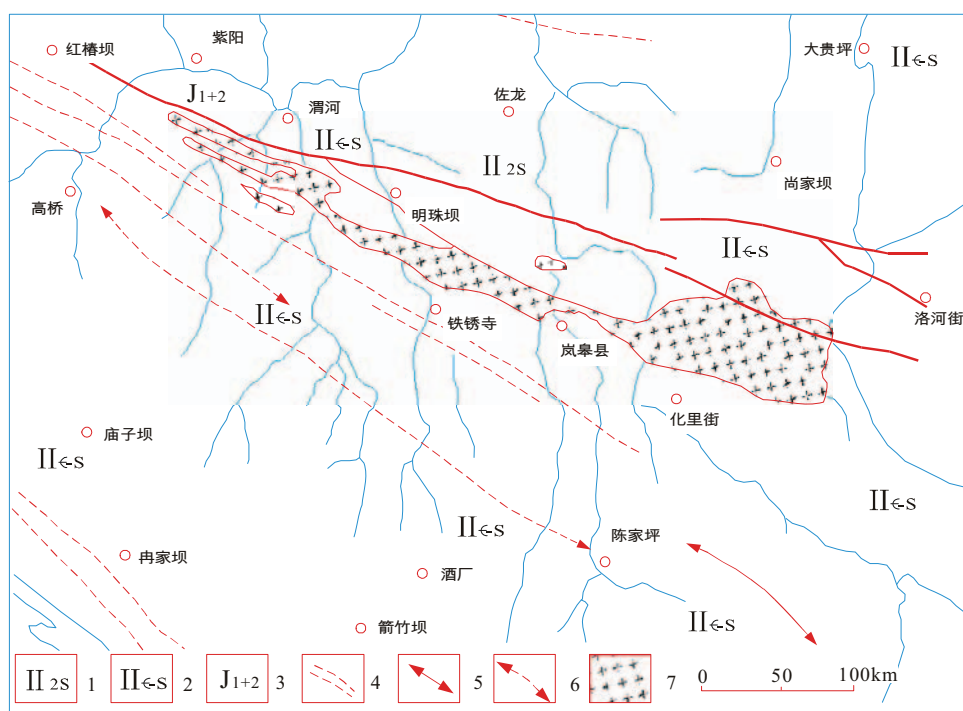
REFERENCES

Berry, W.B.N., Wilde, P. (1978). Progressive ventilation of the oceans—an explanation for the distribution of the lower Paleozoic black shale's: *American Journal of Science*, 278, 257-275.

Chen, P. (2001). *Properties, classify and use of China Coal*. Chemistry Industry Press, Beijing, China, pp.25. (In Chinese).

Chen, W.M., Zhang, Z.S. (1993). *Coal Chemistry*. Coal Industry Press. Beijing, pp.1-16. (In Chinese).

Deyi, Ren., Fenghua, Zhao,Yunquan, Wang., and Shaojin, Y. (1999). Distributions of minor and trace elements in Chinese coals. *International Journal of Coal Geology*, v.40, pp.109-118 (In Chinese).

Edit Committee on Ziyang County Annals. (1989). *Ziyang County Annals*. Sanqing Press, Xian, China, pp.650-652 (in Chinese).

Jenkins, R.J.F., Hasenhohr, P. (1989). *Trilobites and their trails in a black shale: Early Cambrian of the Fleurieu Peninsula, South Australia*. Trans. Roy. Soc. South Australia, 113 (4), 195-203.

Leggett, J.K. (1980). British lower Paleozoic black shales and their palaeo-oceanographic significance. *Journal of the Geological Society of London*, 137, 139-156.

Liu, Y.J., Cao, L., Li, Z.L., Wang, H., Chu, T., and Zhang, J.(1984). *Element Geochemistry*. Science Press,Beijing, China. pp.407-414 (in Chinese).

Li, J.Y., Ren, S.X., and Chen, D.Z. (1982). Study on Relation between Selenium in Shaanxi Environment and Big-condyle Illness. *Acta Scientiae Circumstantiae*, v.2 (2), pp.91-100 (in Chinese).

Luo, Kunli., Wang, Wuyi., Pan, Yuntang., and Tan, Jian. (2001) Selenium Content and Distributing Pattern of Paleozoic strata in South Qinling Mountain, Shaanxi. *Geological Review*, v.47(2), 211-217 (in Chinese).

Luo, Kunli., and Jiang, Jisheng. (1995a). Distributing Pattern of Selenium of Lower Cambrian in Ziyang and Langao County, Shaanxi, China. Jour. *Geology-geochemistry*, v.1, 64-68 (in Chinese).

Luo, Kunli., Chen, Demei., and Ge, Lingmei. (1994). *Accompanied and Associated Ores in the Paleozoic Black Shale and Coal of Shaanxi Province, China*. Xi.an: Northwest University Press, Xian, China (in Chinese).

Luo, Kunli., and Qiu, Xiaoping. (1995b). Analysis on selenium-rich crops in Ankang district, Shaanxi—the case of Ziyang County. *Natural Resource*, v.2, pp.68-72 (in Chinese).

Luo, Kunli. (2003). The age of rock distribution in the selenosis region, south Shaanxi province. *Geological Review*, v.49(4), 383-388 (in Chinese).

Luo, Kunli., Tan, Jian'an., and Wang, Wuyi. (2002). Chemical mobility of selenium in Early Paleozoic rock and stone-like coal in Daba Mountain, South Qinling. *Acta Scientiae Circumstantiae*, v.22(1), pp.86-91(in Chinese).

Ma, L.F., and Deng, X.Zh.(1998). *China Geological Map Explanation*.Geological Press, Beijing,China. 1998), pp.2.

Martens, D.A., and Suarez, D. L. (1997). Selenium speculation of marine shales, alluvial, and evaporation basin soils of California. *J. Environmental Quality*, v.26, pp. 424-434.

Mei, Z.Q. (1985). Summary on two selenium-rich areas of China. *Chinese Journal of Endemic*,V.4, pp.379-385 (in Chinese).

Swaine, D.J. (1990). *Trace elements in coal*. Butterworths, London, UK, pp.212-246.

Thornton, I., Kinniburgh, D.G., and Pullen, G. (1983). *Geochemical Aspects of Selenium in British Soils and Implications to Animal Health*. Reprinted from Trace Substances In Environment Health-XV-II. A symposium. D. D. Hemphill. Ed., University of Missouri, Columbia.

Wu., R.T. (1996). The developing trend of coal production in China. *China Coal*, v.22(12), pp.11-14 (In Chinese).

Xiang, Liwen., Zhu, Zhao. Ling., and Li, Shanji. (1999). *The Cambrian System of China–in Stratigraphy of China*. Geology Publish House press, Beijing, China, pp.1-95 (in Chinese).

Zhao, Chengyi., Ren, Jinghua., and Xue, Chengze. (1993). Selenium of Soil in Rich Selenium Area—Ziyang. *Acta Pedologica Sinica*, v.30(3), pp.253-259 (in Chinese).

Zhu, L. (1983). Petrography of Early Paleozoic highly Metamorphosed boghead coal and its geological significance. *Geological Review*, v.28(2), 245-261 (in Chineese).

Zhizheng, Ye , Jiang, Chinese Coal Geology (1994) Characteristics,sedimentary environment and origin of the Lower Cambrian stone-like coal in Southern China 6 / 04 P 26-31.

Chapter 8

HEAVY MINERALS AND HIGH-TEMPERATURE MINERALOGY IN COAL

*Junying Zhang**

State Key Laboratory of Coal Combusion
Huazhong University of Science and Technology, Wuhan, 430074 China

ABSTRACT

Minerals are important components in coals. The transformations of mineral matter during coal combustion are a key factor in clean utilization of coal. The mineralogical characteristics in coals and their products have been investigated broadly and there are various tasks to be carried out. Some of these are outlined below.

1. Heavy minerals in coal. Use the low temperature ashing (LTA) and the float-sinking methods to separate heavy minerals in coals, and combine X-ray diffraction (XRD) and scanning electron microscopy with energy dispersive X-ray analysis (SEM-EDX) to describe the mineralogical characteristics of heavy minerals. Reveal the mother-rock properties of the sediment-source region, the coal-forming environments and hydrodynamic conditions.

2. Interaction and redistribution of single minerals during coal combustion. Speculate the complex mineral combination evolution during coal combustion and elucidate the interaction mechanism of various minerals combination through a simple monomineral partitioning mechanism.

3. Relationship between typical minerals (Fe-bearing minerals, Ca-bearing minerals, and Al-bearing minerals) in coal and the formation of particulate matter (PM). The minerals are the main source of PM during coal combustion, however, the detailed relation between the minerals and PM is unknown. Systematic drop tube furnace experiments should be conducted to elucidate the contribution of typical minerals to PM formation during coal combustion.

4. Mineralogy of ash deposits of coal-fired boilers. The vaporization of minerals in coal is the main source of deposition in coal-fired boilers. Combine muti-discipline theories to investigate the mineralogy of slag and fouling, and interpret the formation mechanisms of boiler slagging, fouling and ash deposit.

---

* Email: jyzhang@huist.edu.cn

In summary, the integrated theory of physicochemical transformation and interaction of mineral components during coal combustion should be constructed, which would be helpful to operating the coal combustion equipments safely and controlling the pollution emissions.

Keywords: mineralogy, heavy minerals, PM, Ash deposit, Coal, Coal combustion

1. INTRODUCTION

Mineral matter is an important component in coal. As defined by Gary et al.,(1972), "mineral matter" refers to "the inorganic material in coal" [1]. "Mineral matter" is more specifically defined by Standards Australia as "the sum of the minerals and inorganic matter in and associated with coal" [2]. Most of the problems associated with coal utilization arise out of some ways from the incorporated mineral matter [3, 4], rather than directly from the maceral components [2]. Mineralogy of coal has been widely discussed and summarized. More than 316 minerals have been identified in coals, most of which are accessories or trace minerals [4-6]. Coal geology and geochemistry may be important in the elucidation of coal genesis, in determining the modes of elements occurrence, in the correlation of coal seams, and in the characterization of mineral matter source areas [4]. Vassilev and Menendez have described the physical-chemical characteristics of the heavy concentrated of fly ashes[7].They found that the heavy concentrates which come from the heavy minerals in coal enriched both economically and environmentally important minerals and have a great number of trace elements with higher concentration in comparison with other fractions. However, there are only few studies on the mineralogy of the heavy minerals in coal.

The transformation of minerals during coal combustion is the main source of particulate matter (PM) and ash deposition in boilers. Many scientists have investigated the formation mechanism of PM and ash deposit during coal combustion. The formation of PM was summarized as four formation mechanisms, including mineral coalescence, char fragmentation, excluding mineral fragmentation, and vaporization and subsequent condensation of inorganic matter [8-10]. The relationship between mineral transformation and PM is still not clear. Many of the mechanisms of mineral transformations have been identified and are detailed only by considering the elements, such as iron, calcium, and aluminum, which also have been associated with slagging and fouling [11-13]. Nevertheless, the impacts of their different speciation and contribution in coals and ashes on ash deposition are still not clear.

2. HEAVY MINERALS IN COAL

Systematic understanding of minerals in coal is of importance for revealing the source-rock properties of the sediment-source region, the coal-forming environments and hydrodynamic conditions. Many methods had been used to characterize the mineral matter in coal, and were summarized by Vassilev and Tascon (2003) [14], Huggins (2002)[15], and Ward (2002)[2], respectively. The major minerals identified in coal are quartz, clay minerals (especially kaolinite, illite, and interstratified illite/smectite), plagioclase, feldspars, gypsum, carbonates such as siderite, calcite and dolomite, and sulphide minerals such as pyrite [2, 4].

The other identified minerals are commonly present as minor or accessory phases including phosphate minerals, such as apatite or alumino-phosphates of the crandallite group, titanium minerals, such as anatase, and alumino-carbonates, such as dawsonite [2, 16-19]. Vassilev et al., (1994) listed a number of other minerals found in high-ash coals of Bulgaria, with notes on their modes of occurrence [20]. Many of the more unusual minerals reported in coal were noted only from optical or electron microscope studies; they are not always sufficiently abundant to be identified by XRD analysis of whole coal or isolated mineral fractions [2].

The mineralogical analysis techniques used for coal have also been applied to studying the products of mineral reactions at high temperatures, including fly ashes, slags and other residues derived from coal combustion. The mineralogy, chemical composition, and other physical-chemical characteristics of coal combustion residues have been broadly discussed [7, 21-31]. Vassilev et al. combined different physical separation methods and mineralogical analysis techniques to systematically describe the mineralogy of fly ashes from power plants [7, 25-29]. Amorphous materials such as glasses are a major component in fly ash, and the minerals identified in fly ash mainly include quartz, mullite, calcium oxides, iron oxides, aluminisilicates, and sometimes sulfates. Others minerals are identified as minor or accessories in fly ash.

Mineralogy and phases composition of coal have been studied broadly. However, the research on the heavy minerals in coal is still lacking. Vassilev et al. has described the mineralogy and morphology of the heavy concentrates (HCs) separated from fly ashes [7]. Their phase-mineral composition (in decreasing order of significance) commonly includes aluminosilicate glass, hematite, magnetite, larnite, quartz, periclase, mullite, corundum, lime, char, melilite, rutile, plagioclase, wollastonite, ferrian spinel, and anhydrite. Several accessory minerals of Ba, Ce, Cl, Cr, Cu, F, Fe, La, Mn, P, Pb, Th, Ti, Y, and Zr, are also typical components of HCs. Isolation of the minerals from higher-rank coals without major alteration can be achieved by ashing the coal at low temperature (120–150°C) in an electronically excited oxygen plasma [32, 33], which has been validated by many studies [19, 34-38]. The K1050X oxygen plasma low temperature asher was used to oxidize the organic components in coal and separate the minerals. Then the low temperature ash was collected to conduct sink-float experiments with bromoform ($CHBr_3$ with a density of 2.89 g/cm^3). After the separation, the heavy minerals (sink fraction) were washed and dried in an electrical furnace at 150°C X-ray diffraction (XRD) and scanning electron microscopy with energy dispersive X-ray analysis (SEM-EDX) were used to describe the mineralogical characteristics of heavy minerals. The XRD results show that the sink fraction minerals include siderite, hematite, quartz, kaolinite, and pseudorutile (Fig. 1). It's noticeable that pseudorutile is the first time to be discovered in coal by XRD. It can also be found in the images by SEM-EDX (Figs. 2-3). Some accessory heavy minerals including amphibole (Fig. 2), barite (Fig. 4), zircon (Fig. 5), and bauxite (Fig. 6) are also identified. These accessory heavy minerals are unusually discovered in coal because of their low concentration. Combination of the LTA and float-sinking experiments is a good way to identify the real heavy minerals, which is more helpful to reveal the mother-rock properties of the sediment-source region, the coal-forming environments and hydrodynamic conditions. Systematic separation and analysis of heavy minerals from different coal samples still need to be done in the future.
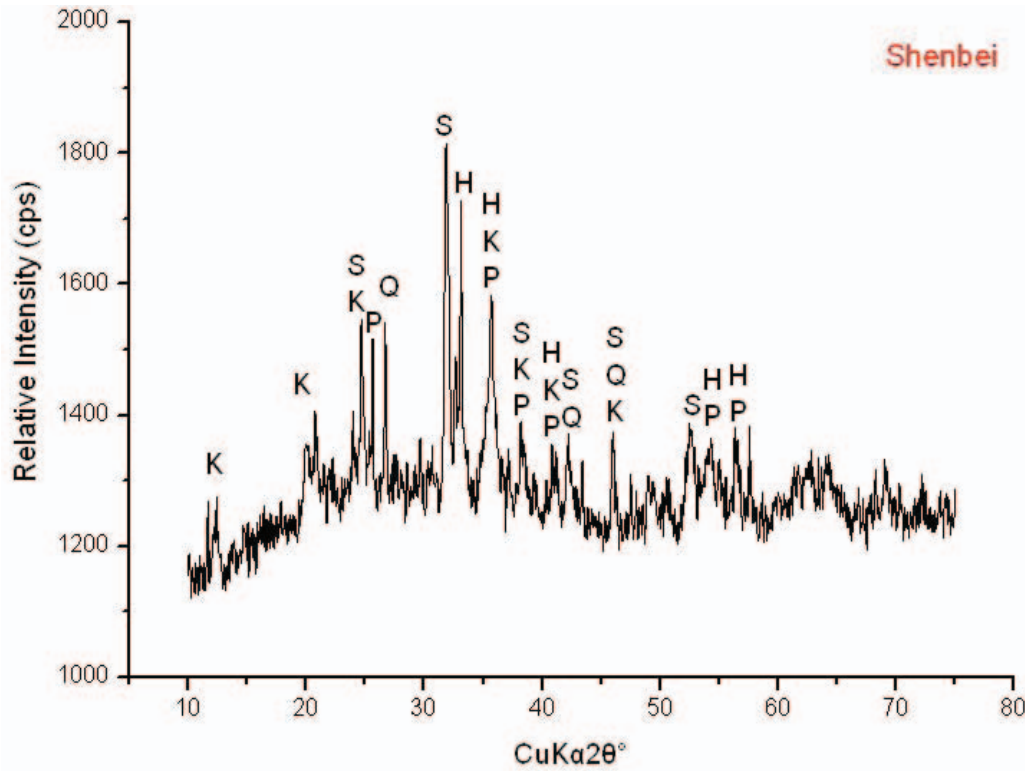
Figure 1. X-ray diffractogram of heavy minerals separated from Shenbei lignite (H:hematite; K: kaolinite; P: pseudorutile; Q:quartz; S:siderite).
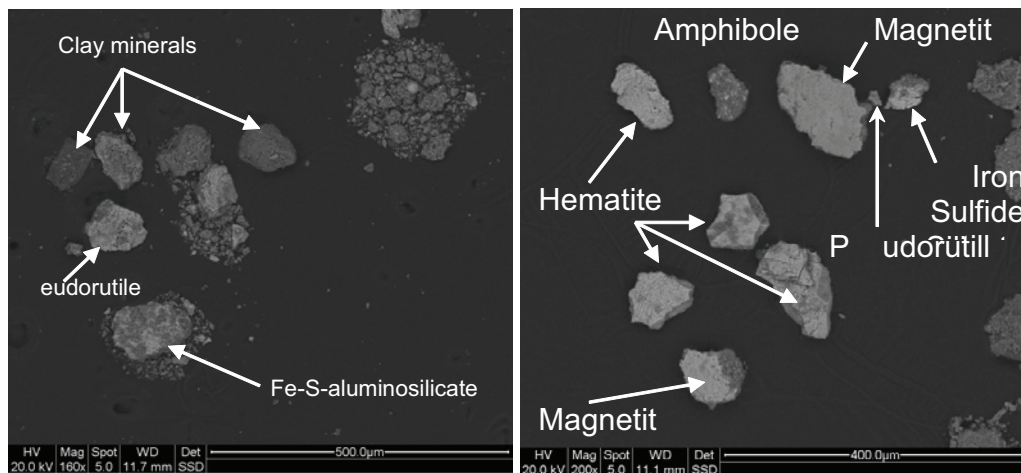
Figure 2. SEM images of heavy minerals.

https://telegram.me/Geologybooks
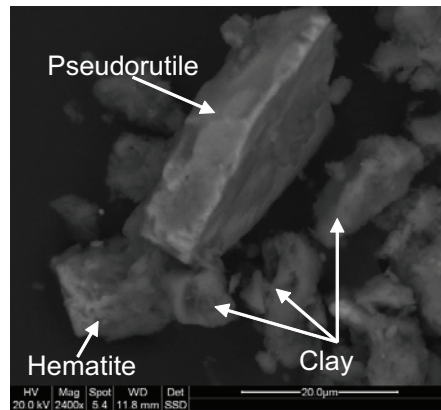
Figure 3. SEM image of iron-bearing minerals in the sink fraction.
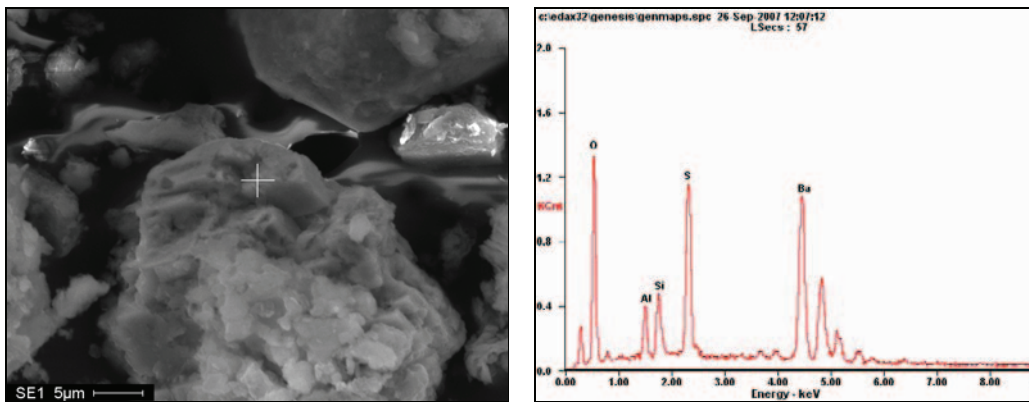
Figure 4. Barite (BaSO$_4$) with few clay minerals on the surface.
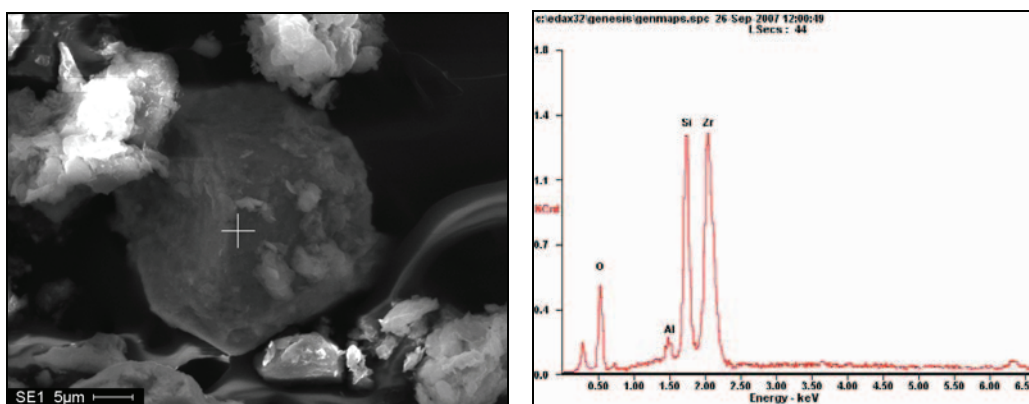
Figure 5. Zircon in the sink fraction.
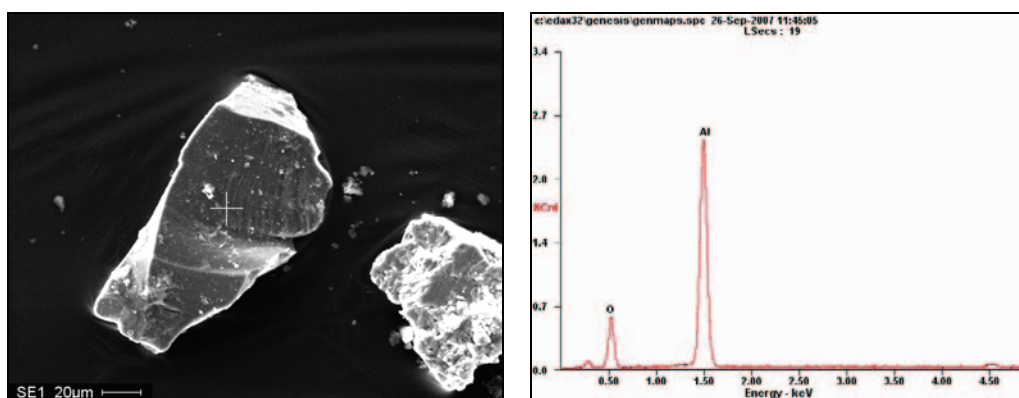
Figure 6. Bauxite in the sink fraction.

3. PARTITIONING AND REDISTRIBUTION OF MONO-MINERALS (FE-, CA-, AL-MINERALS) DURING HEATING FIELDS

The transformation processes of minerals during coal combustion are complex and difficult to clarify. The thermal behavior of minerals commonly found in coal has been examined by mineralogists for years using differential thermal analyzers under air at slow heating rates. A large portion of these investigations were summarized in an extensive survey of thermal behavior of coal minerals by Watt [38]. The transformations experienced by several minerals most commonly found in coal have been summarized by Jackson [39], and Bryers and Walchuk [40]. The results could be used only as a guideline for predicting the thermal behavior, as thermal shocking during combustion in the presence of carbon and other mineral forms will alter some of these transformations and may also defer others until post-combustion deposition on heat-transfer surfaces [38]. However, describing the partitioning of mono-minerals is still a good way to understand the behavior of minerals in coal during heating fields. Many researchers have done valuable work in this field [41-45]. By studying the mineralogy, microstructures and chemical compositions of single fly ash particles from different mono-minerals in coal, it has been possible to propound the mechanisms for their formation (Figs.7-9).

3.1. Iron-bearing minerals

The transformation of typical iron-bearing mineral, pyrite is shown in Fig.7. The excluded pyrite transformation diagram indicates that pyrrhotite oxidation derived from surface inward, as indicated by previous work [44, 46, 47]. This is a result of the oxidation process being controlled by the diffusion of oxygen to the particle surfaces, resulting in an oxide shell and pyrrhotite core [47]. The subsequent oxidation of pyrrhotite produces a FeO melt, crystallization to magnetite occurs, with further oxidation resulting in the formation of hematite, as established by previous work. But at the same time, the FeO fusing with the

aluminosilicates may result in the formation of aluminiosilicate-bearing ferro-oxides, as indicated by the mechanisms diagram. These transformations depend on reaction conditions, temperature and the distributions of minerals in the coal.

Included pyrite minerals within the char will experience a locally reducing environment during the combustion of the char. Oxidation of included pyrrhotite will thus not proceed to any great extent until the completion of char combustion. This delay of the oxidation of included pyrite may account for a significant number of Fe-O-S ash particles. These particles are typically spherical and molten [47]. Under oxidizing conditions these ash particles would be expected to be oxidized, producing ferro-oxides, as the pathway of excluded pyrite. For reducing stoichiometries, however, on completion of char combustion included mineral particles are still subjected to reducing conditions and thus are not likely to be oxidized significantly. During longer residence time these molten ash particles may contact silicates or aluminosilicates as in the branches of the glass formation pathway. During the fusion of the included minerals, it is likely that there exists a distinct difference in the composition of glasses. The fusion of pyrite-derived ash particles with aluminosilicates equivalence will form high-ferriferous aluminosilicates; ferro-aluminosilicates derived from the combination of aluminosilicates with few included pyrite-derived ash particles; the fusion of ferro-oxides and few aluminosilicates form aluminosilicate-bearing ferro-oxides (Fig. 7).
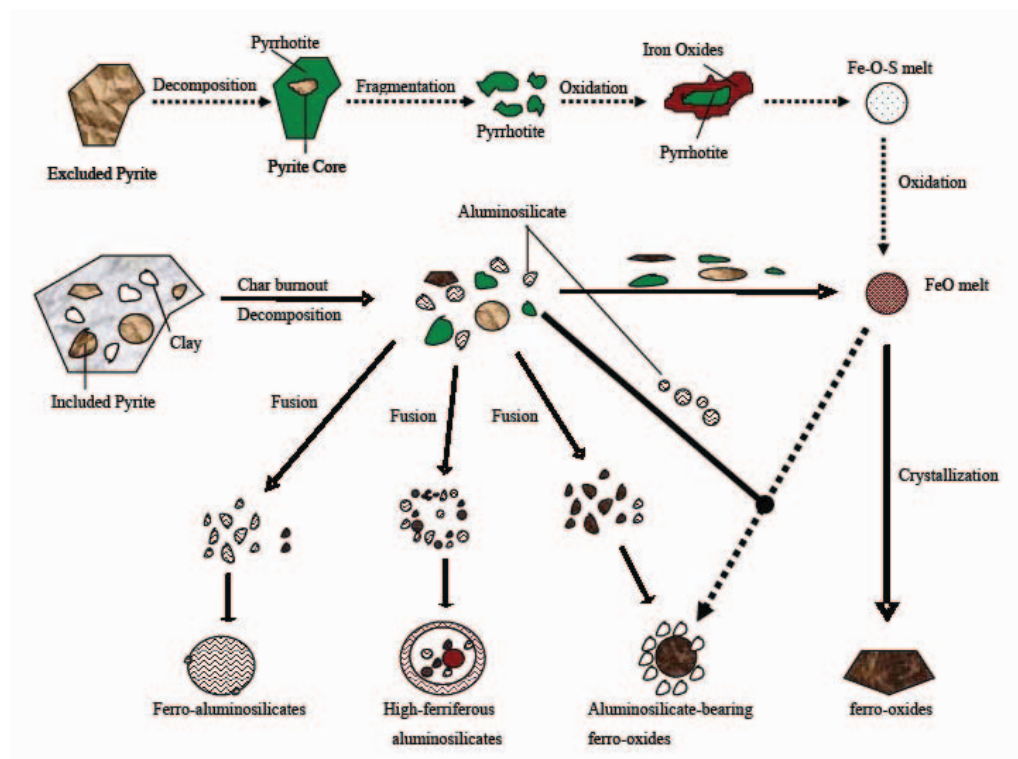
Figure 7. Transformation mechanisms of pyrite during coal combustion.

3.2. Calcium-bearing minerals

According to the chemical composition of high-calcium fly ash particles, the high calcium fly ash has been divided into four types, by knowing their microstructures and mineralogy compositions, a mechanism for their formation has been propounded (Fig. 8). Excluded calcium-bearing minerals transformation diagram indicates that Ca-O clusters are derived from the decomposition of calcium-bearing carbonate and sulfate, as indicated by precious work [48]. The CaO may be given off from the burning coal particles as a CaO fume or may remain within the particles and react with the clay, quartz and other minerals to form molten aluminosilicate slag [49]. The CaO fume apparently reacts with SO_2 to form $CaSO_4$ which is a part of the initial, presumably sticky layer in both superheater and waterwall deposits [50]. Included calcium-bearing minerals are likely to scavenge a portion of fine clay minerals to form calcium aluminosilicates, which have lower melting point, often occurring as molten slag. During the fusion of the included minerals, it is likely that there exists a distinct difference in composition of glasses. The Ca-S-X components may derive from the desulfuration reaction of calcium aluminosilicates or the combination of calcium sulfate and clay minerals (Fig. 8). These transformations depend on reaction conditions, temperature, and the distributions of minerals in coal. The amount of aluminosilicates in raw coals is a key factor affecting the transformation of calcium into fly ashes or boiler deposits. Calcium sulfate is an important source of the initial layer in both super heater and water wall deposits, while calcium aluminosilicates are the main source of the molten slag.
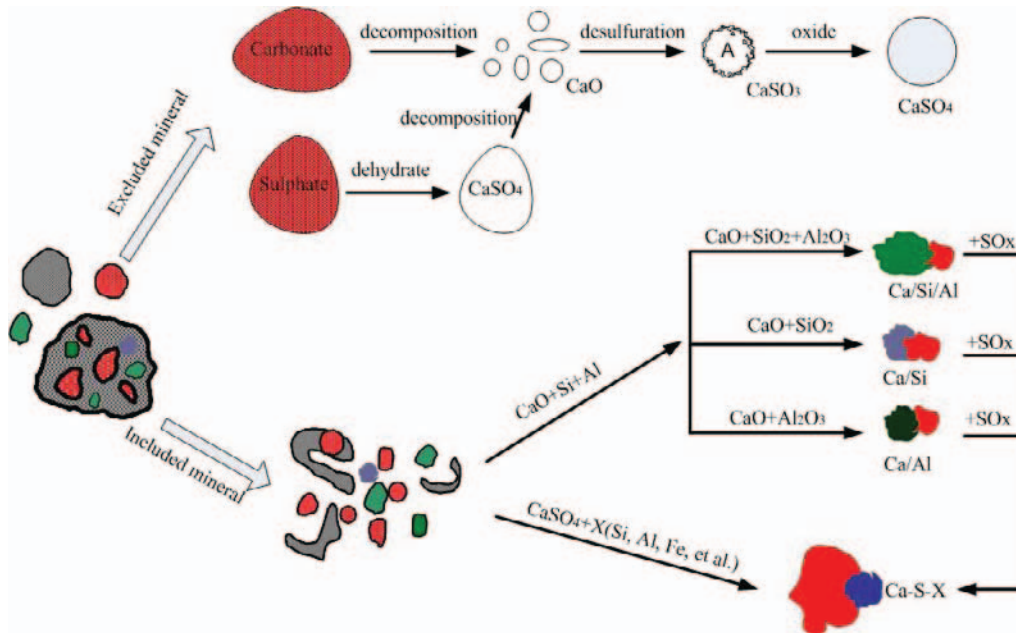
Figure 8. Transformation of calcium-bearing minerals during coal combustion.

3.3   Aluminum-bearing minerals

Boehmite is the main aluminum-bearing minerals in high-aluminum coal [51]. A transformation mechanism of boehmite during coal combustion was propounded after a systematic investigation of high-aluminum coal combustion experiments (Fig. 9). Excluded boehmite dehydrates at ~500 to form γ-Al_2O_3, which first transforms to δ-Al_2O_3 and then to θ-Al_2O_3 before undergoing a reconstructive phase transformation to α-Al_2O_3 [52]. For the included boehmite, the combination of magnesite with boehmite will promote the transformation of θ-Al_2O_3 to α-Al_2O_3, while the zircon will restrain the formation of α-Al_2O_3. The θ to α-phase transformation of alumina for both excluded and included boehmite is achieved through a nucleation and growth process [53, 54]. This process is an important factor for submicron particle formation.
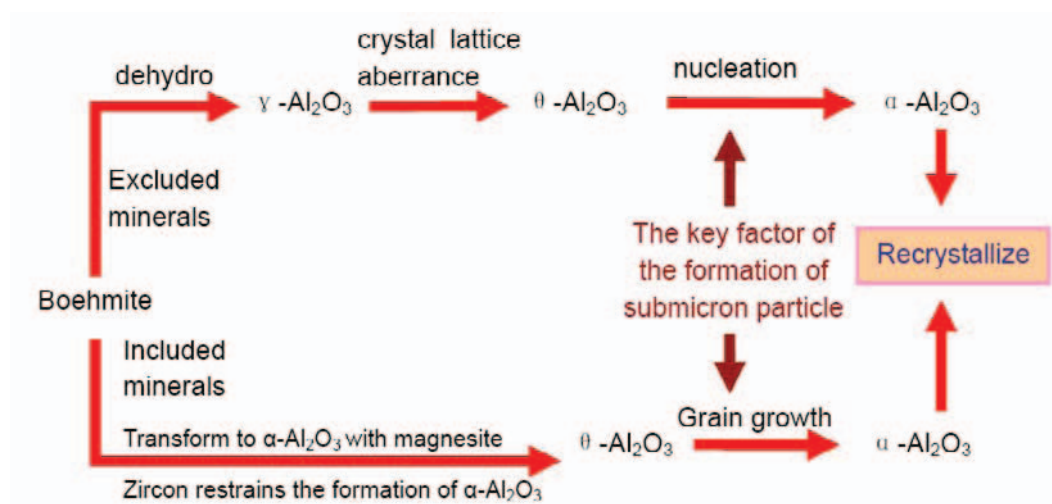
Figure 9. Transformation of boehmite during coal combustion.

The transformation mechanism of minerals has been more clear than before, however, the quantity and kinetic of mineral transformation especially those of included minerals combined with coal particles are still uncertain.

4. RELATION BETWEEN TYPICAL MINERALS AND PM

Minerals are the main source of PM during coal combustion. However, the detailed relation between the minerals and PM is still unclear. During combustion, the mineral matter undergoes a variety of physical and chemical changes which depend on their original modes of occurrence, their time-temperature histories, and interactions among the minerals [55, 56]. Generally speaking, the mineralogy and size distribution of ashes are quite different from those of the minerals particles originally in coal.

Systematic drop tube furnace experiments were conducted to elucidate the contribution of typical minerals to the PM formation during coal combustion. The experiment results indicate

that, illite and pyrite indeed undergo fragmentation, the particle size distribution of two minerals has obvious changes and the mean diameter for volume decreases after experimentation, especially for the illite (Fig.10). The fragmentation of minerals is an important mechanism for PM formation.
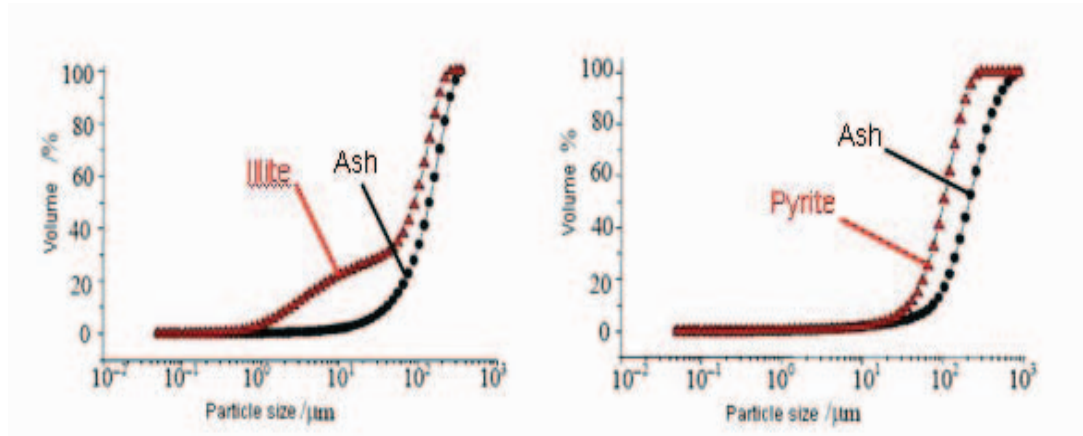
Figure 10. Comparison of particle size distribution of Illite and Pyrite after experiment [57].
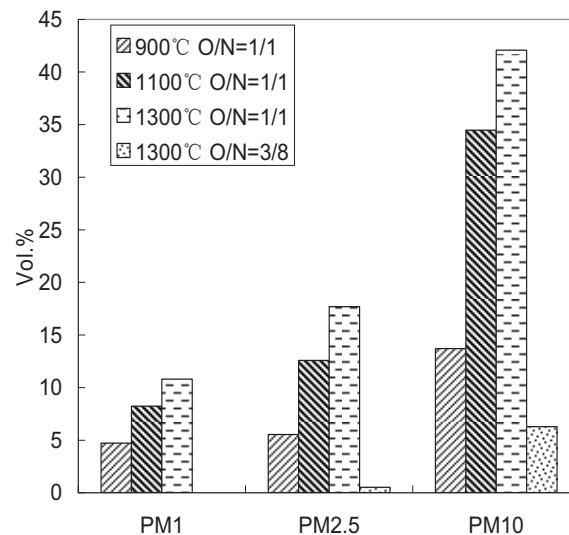
Figure 11. PM emission during high-aluminum coal combustion in different conditions

The emission of PM from typical high aluminum coal combustion has been investigated, as shown in Fig. 11. The emission of PM soars with the increasing of temperature from 900°C to 1100°C. However, the amount of PM increases little after 1100 °C. Oxide concentration is also an important factor in promoting the formation of PM.

The quantitative contribution of minerals to the formation of PM is still uncertain. And the formation mechanisms of PM especially primary particulate matter need to be investigated in detail.

5. MINERALOGY OF ASH DEPOSITION

Mineral matters have been considered as the main source of deposition, almost every mineral may influence the ash deposits. Quartz as condensed vapor, or a sorbent of alkalis, and captured aggregate may contribute to deposition within a given combustor in several different ways [58]. Kaolinite may also capture aggregate or possibly as a sorbent for alkalis in fouling [38]. Pyrite and calcite are typical minerals in coal for their contributions to ash deposits, which have been discussed broadly [44, 49]. Understanding the mineralogy of ash deposition is helpful to reveal the formation mechanisms of slagging, fouling and high temperature corrosion.

5.1. High temperature corrosion

The high temperature corrosion by sulfur of the superheater tubes surface from pulverized coal combustion is a very complex phenomenon as a function of many chemical and physical processes of minerals in coal.

Several typical high-temperature corrosion samples were collected from a coal-fired power plant. Their mineralogy, chemical composition, and microstructure were determined by XRD, X-ray fluorescence spectrometry (XRF), optical microscopy, and FSEM-EDX. Their pore size distribution was analyzed by a nitrogen adsorption specific surface area analyzer [59].

The X-ray diffractograms from different layers of high-temperature corrosion products are shown in Fig.12. The main components of corrosion are iron sulfides and iron oxides, indicating that the corrosion is the typical sulfide corrosion. The iron sulfides content decreases and the aluminosilicate component content increases from inside to outside of corrosion products.
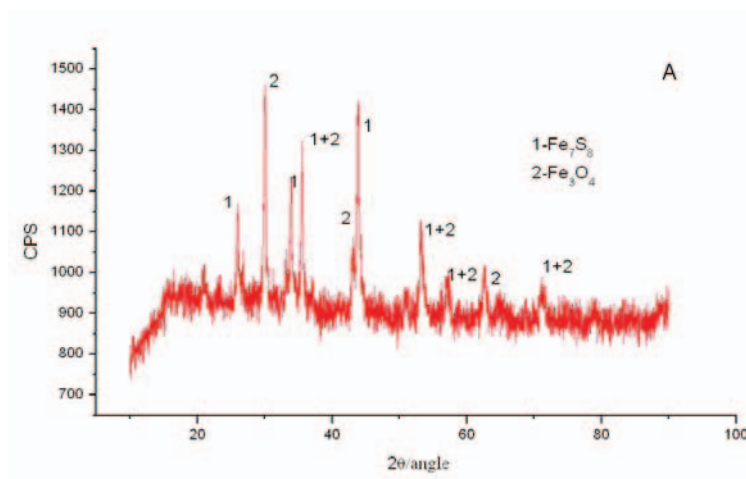
(A) Inner layer of the corrosion

Figure 12. (Continued on next page.)
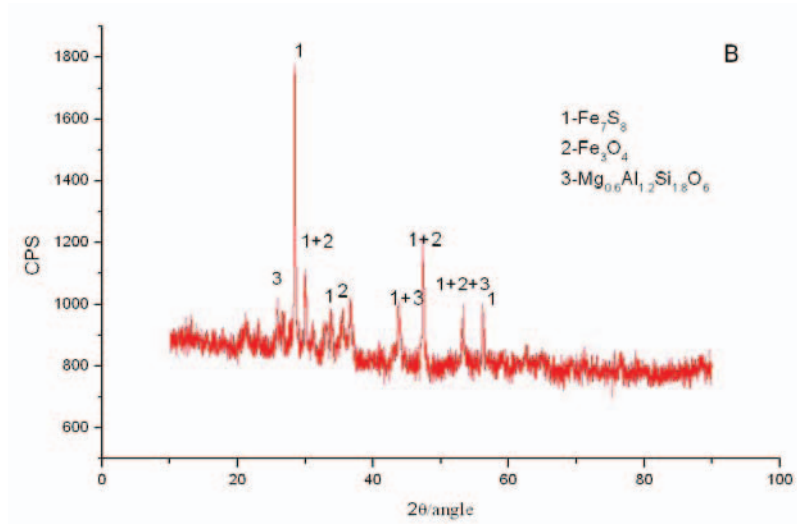
(B) Intermediate layer of the corrosion.
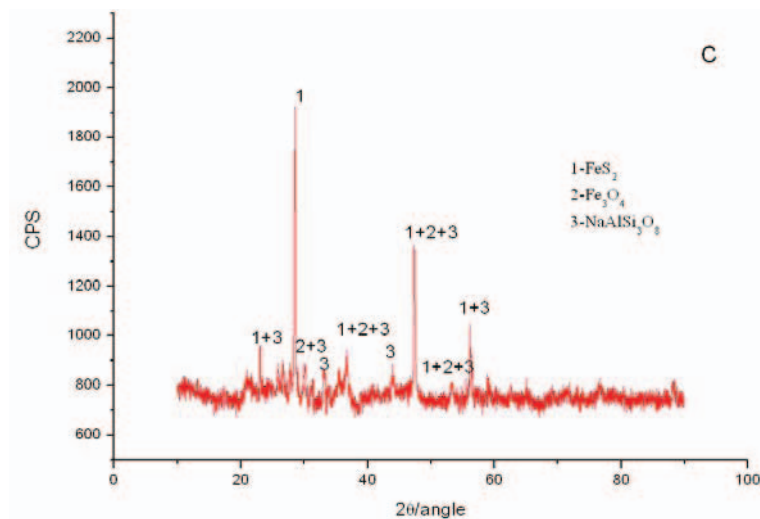
(C) Outer layer of the corrosion.

Figure 12. X-ray diffractograms of the corrosion layer.

Metallography microscope studies reveal that the corrosion product with an obvious hierarchical structure that has compact inner layer and loose porous outer layer (Fig. 13). The inner layer which formed after high temperature crystallization has relatively simple mineral composition and asymmetric distribution. On the contrary, the outer layer has complex mineral composition and symmetrical distribution, and contains a lot of spherical uncrystalloid fly ash particles.

From inner to outer layer of the corrosion, more finestra, especially big ones we found, and the aperture of small finestra is about 500Å while that of big finestra is about 1500Å (Fig. 14). The existence of finestra facilitates the spread of corrosion medium, and makes it possible to infiltrate into inner slag and erode the superheater tubes wall. Though the structure

of the inner corrosion product is compact, it can not stop the infiltration of S^{2-} because of the limitation of crystal lattice.
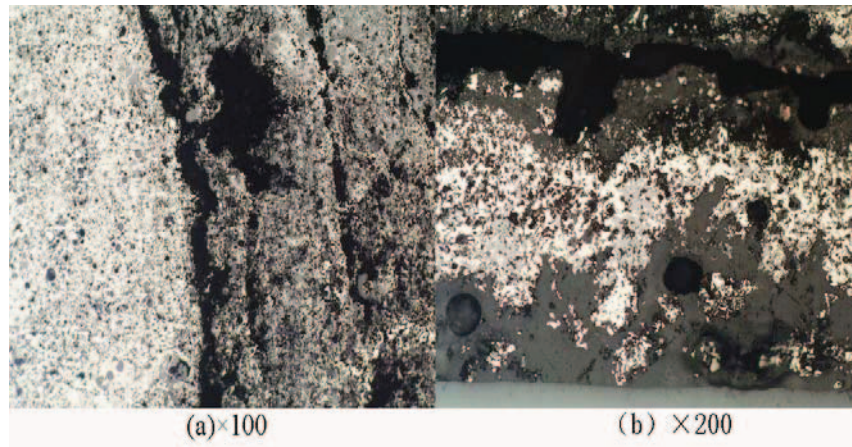
Figure 13. Metallography micrograph of corrosion sample.
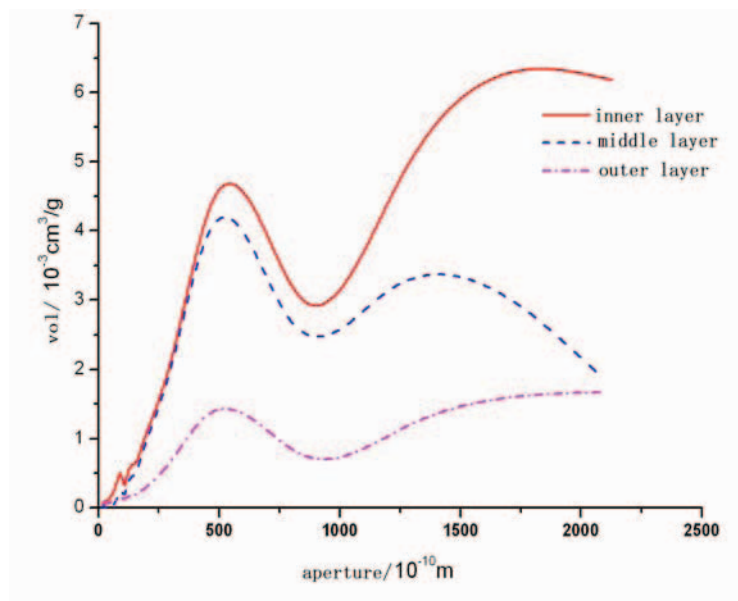
Figure 14. Aperture distribution of the corrosion layer

The distribution of the elements from inner to outer layer of the corrosion was investigated using XRF (Fig. 15). The contents of Fe and S in inner layer of corrosion product are high. From inner to outer layer of the corrosion, the contents of Fe and S decrease, and the contents of Si and Al increase, and other elements have no obvious change, such as Na, Ca, K, and Mg because of low concentration.
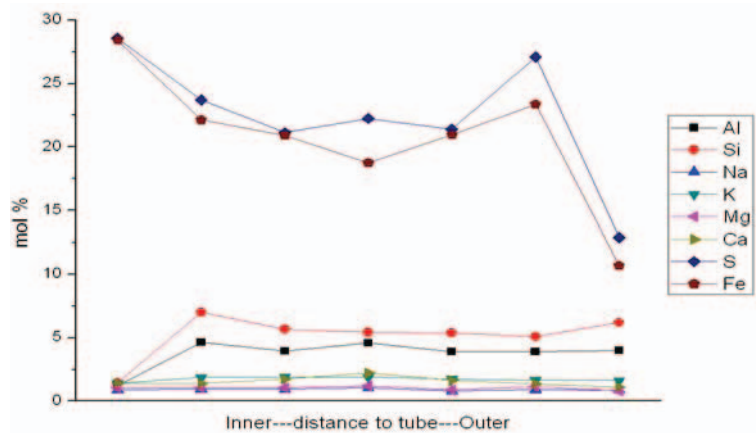
Figure 15. Elements distribution of the corrosion layer.

The sulfide corrosion is a familiar type in superheater tubes corrosion. H_2S derived from pulverized coal combustion reacted with tubes metal, and Fe-sulfides were formed at high temperature. The corrosion rate is in direct proportion to the concentration of H_2S and the sulfur content in coal burned.

5.2. Slagging and Fouling

Slagging is defined as deposition of fly ash on heat-transfer surfaces and refractory in the furnace volume primarily subjected to radiant heat transfer. And fouling is defined as deposition in the heat-recovery section of the steam generator subjected to convective heat exchange by fly ash quenched to a temperature below its predicted melting point, condensation by volatiles [38].
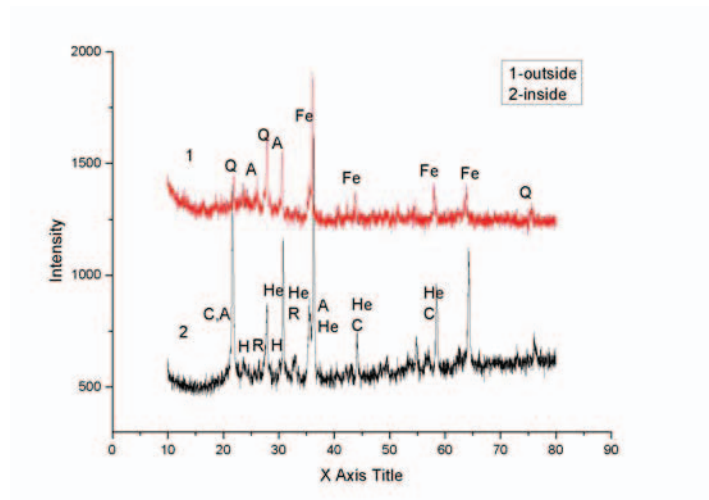
He: hercynite; A: anorthite; Fe: Fe-ringwoodite; Q: quartz; H: hematite; R: rutile; C: cristobalite

Figure 16. X-ray diffractograms of slag.

Analyzed by XRD, the minerals of the high-rank coal slag consist of hercynite, quartz, hematite, anorthite, rutile, and Fe-ringwoodite (Fig.16), originating from pyrite and clay minerals. The iron oxide content decreases from inside to outside of the slag, which may account for the selective deposition of the initial layer.

Observed from the SEM photos, we find the contents of crystal decrease while the glass-phases increase from inner layer to outer layer of slag .The main crystals in the iron-slag are mullite, quartz, rutile, and iron-rich minerals such as hercynite identified by the EDX. The slag microstructure is mass interwoven needles on the iron aluminosilicate glass, hercynite and mullite are the main minerals (Fig. 17).
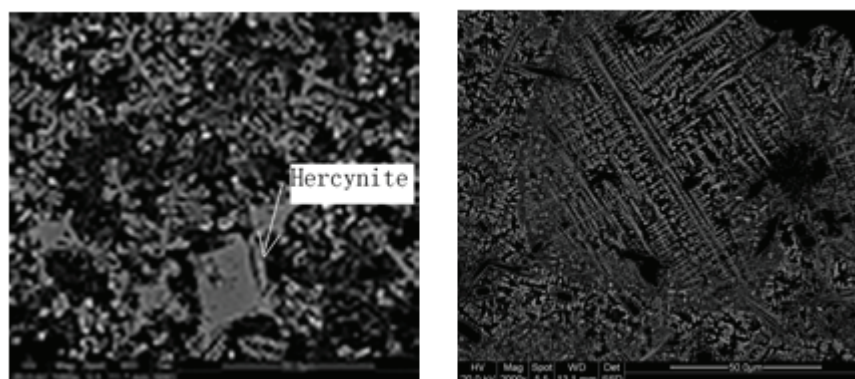
Figure 17. SEM images of slag.

The steps for forming slag with low-rank coals differ slightly from bituminous coal because of the presence of calcium and sodium as organically-bound mineral matter instead of iron. Understanding the mineralogy of ash deposition is helpful to reveal the formation mechanisms of slagging and fouling.

6. SUMMARY

Mineralogy of heavy minerals in coal is almost blank in coal geology. Systematic research on heavy minerals in coals should be valuable for both coal geology and coal utilization.

The transformation of minerals under high temperature during coal utilization is a complex problem. It is difficult to resolve and clarify by combustion theory. Combining coal geology and combustion theory to investigate mineral transformation is a good way with potential prospects.

ACKNOWLEDGMENTS

REFERENCES

[1]   Gary, M., McAfee, R., and Wolf, C. L. (1973). *Glossary of geology*. American Geological Institute: Washington, DC, p 805.

[2]   Ward, C. R. (2002). Analysis and significance of mineral matter in coal seams. *International Journal of Coal Geology,* 50, (1-4), 135-168.

[3]   Gupta, R., Wall, T. F. and Baxter, L. A. (1999). *The Impact of Mineral Impurities in Solid Fuel Combustion*. Plenum: New York, USA, p 768.

[4]   Vassilev, S. V., and Vassileva, C. G. (1996). Occurrence, abundance and origin of minerals in coals and coal ashes. *Fuel Processing Technology,* 48, 85-106.

[5]   Finkelman, R. B. (1981). *Modes of occurrence of trace elements in coal*. No. OFR-81-99, U.S. Geological Survey Open-File Report, p 322.

[6]   Vassilev, S. V., and Vassileva, C. G. (2005). Methods for characterization of composition of fly ashes from coal-fired power stations: A critical overview. *Energy and Fuels,* 19, (3), 1084-1098.

[7]   Vassilev, S. V., and Menendez, R. (2005). Phase-mineral and chemical composition of coal fly ashes as a basis for their multicomponent utilization. 4. Characterization of heavy concentrates and improved fly ash residues. *Fuel,* 84, (7-8), 973-991.

[8]   Buhre, B. J. P., Hinkley, J. T., Gupta, R. P., Nelson, P. F., and Wall, T. F. (2006). Fine ash formation during combustion of pulverised coal-coal property impacts. *Fuel,* 85, (2), 185-193.

[9]   Yan, L., Gupta, R., and Wall, T. (2001). Fragmentation behavior of pyrite and calcite during high-temperature processing and mathematical simulation. *Energy and Fuels,* 15, (2), 389- 394.

[10]   Wigley, F., and Williamson, J. (1998). Modelling fly ash generation for pulverised coal combustion. *Progress in Energy and Combustion Science,* 24, (4), 337-343.

[11]   Reid, W. T. (1984). The relation of mineral composition to slagging, fouling and erosion during and after combustion. *Progress in Energy and Combustion Science,* 10, (2), 159-169.

[12]   Wall, T. F. (1992). Mineral matter transformations and ash deposition in pulverised coal combustion. *Symposium (International) on Combustion,* 24, (1), 1119-1126.

[13]   Gupta, R. P., Wall, T. F., Kajigaya, I., Miyamae, S., and Tsumita, Y. (1998). Computer-controlled scanning electron microscopy of minerals in coal: Implications for ash deposition. *Progress in Energy and Combustion Science,* 24, (6), 523-543.

[14]   Vassilev, S. V., and Tascon, J. M. D. (2003). Methods for Characterization of Inorganic and Mineral Matter in Coal: A Critical Overview. *Energy and Fuels,* 17, 271-281.

[15]   Huggins, F. E. (2002). Overview of analytical methods for inorganic constituents in coal. *International Journal of Coal Geology,* 50, (1-4), 169-214.

[16]   Ward, C. R. (1974). Isolation of mineral matter from Australian bituminous coals using hydrogen peroxide. *Fuel,* 53, (3), 220-221.

[17]   Finkelman, R. B., and Stanton, R. W. (1978). Identification and significance of accessory minerals from a bituminous coal. *Fuel,* 57, (12), 763-768.

[18]   Ward, C. R., Corcoran, J. F., Saxby, J. D., and Read, H. W. (1996). Occurrence of phosphorus minerals in Australian coal seams. *International Journal of Coal Geology,* 30, (3), 185-210.

[19]   Ward, C. R., Taylor, J. C., Matulis, C. E., and Dale, L. S. (2001). Quantification of mineral matter in the Argonne Premium coals using interactive Rietveld-based X-ray diffraction. *International Journal of Coal Geology,* 46, (2-4), 67- 82.

[20]   Vassilev, S. V., Yossifova, M. G., and Vassileva, C. G. (1994). Mineralogy and geochemistry of Bobov Dol coals, Bulgaria. *International Journal of Coal Geology,* 26, (3-4), 185-213.

[21]   Sakurovs, R., French, D., and Grigore, M. (2007). Quantification of mineral matter in commercial cokes and their parent coals. *International Journal of Coal Geology,* 72, (2), 81-88.

[22]   Koukouzas, N., Hamalainen, J., Papanikolaou, D., Tourunen, A., and Jantti, T. (2007). Mineralogical and elemental composition of fly ash from pilot scale fluidised bed combustion of lignite, bituminous coal, wood chips and their blends. *Fuel,* 86, (14), 2186-2193.

[23]   Zhao, Y. C., Zhang, J. Y., Sun, J. M., Bai, X. F., and Zheng, C. G. (2006). Mineralogy, chemical composition, and microstructure of ferrospheres in fly ashes from coal combustion. *Energy and Fuels,* 20, (4), 1490-1497.

[24]   Koukouzas, N. K., Zeng R., Vassilis P., Xu, W., and Kakaras, E. K. (2006). Mineralogy and geochemistry of Greek and Chinese coal fly ash. *Fuel,* 85, 2301-2309.

[25]   Vassilev, S. V., Vassileva, C. G., Karayigit, A. I., Bulut, Y., Alastuey, A., and Querol, X. (2005). Phase-mineral and chemical composition of and fractions separated from composite fly ashes at the Soma power station, Turkey. *International Journal of Coal Geology,* 61, (1-2), 65-85.

[26]   Vassilev, S. V., Vassileva, C. G., Karayigit, A. I., Bulut, Y., Alastuey, A., and Querol, X. (2005). Phase-mineral and chemical composition of composite samples from feed coals, bottom ashes and fly ashes at the Soma power station, Turkey. *International Journal of Coal Geology,* 61, (1-2), 35-63.

[27]   Vassilev, S. V., Menendez, R., Diaz-Somoano, M., and Martinez-Tarazona, M. R. (2004). Phase-mineral and chemical composition of coal fly ashes as a basis for their multicomponent utilization. 2. Characterization of ceramic cenosphere and salt concentrates. *Fuel,* 83, (4-5), 585-603.

[28]   Vassilev, S. V., Menendez, R., Borrego, A. G., Diaz-Somoano, and M., Martinez-Tarazona M.R. (2004). Phase-mineral and chemical composition of coal fly ashes as a basis for their multicomponent utilization. 3. Characterization of magnetic and char concentrates. *Fuel,* 83, (11-12), 1563-1583.

[29]   Vassilev, S. V., Menendez, R., Alvarez, D., Diaz-Somoano, M., Martinez-Tarazona, M. R. (2003). Phase-mineral and chemical composition of coal fly ashes as a basis for their multicomponent utilization. 1. Characterization of feed coals and fly ashes. *Fuel,* 82, (14), 1793-1811.

[30] Sakorafa, V., Michailidis, K., and Burragato, F. (1996). Mineralogy, geochemistry and physical properties of fly ash from the Megalopolis lignite fields, Peloponnese, Southern Greece. *Fuel,* 75, (4), 419- 423.

[31] Martinez-Tarazona, M. R., Spears, and D. A. (1996). The fate of trace elements and bulk minerals in pulverized coal combustion in a power station. *Fuel Processing Technology,* 47, (1), 79-92.

[32] Gluskoter, H. J. (1965). Electronic low temperature ashing of bituminous coal. *Fuel,* 44, 285-291.

[33] Miller, R. N., Yarzab, R. F., and Given, P. H. (1979). Determination of the mineral-matter contents of coals by low-temperature ashing. *Fuel,* 58, (1), 4- 10.

[34] Adolphi, P., and Stoerr, M. (1985). Glow discharge excited low temperature ashing: a new technique for separating mineral matter of coals. *Fuel,* 64, (2), 151- 155.

[35] Allen, R. M., and Carling, R. W., VanderSande, J. B. (1986). Microstructural changes in coal during low temperature ashing. *Fuel,* 65, (3), 321- 326.

[36] Ward, C. R., and Taylor, J. C. (1996). Quantitative mineralogical analysis of coals from the Callide Basin, Queensland, Australia using X-ray diffractometry and normative interpretation. *International Journal of Coal Geology,* 30, (3), 211- 229.

[37] Ward, C. R., Taylor, and J. C., Cohen, A. R. (1999). Quantitative mineralogy of sandstones by X-ray diffractometry and normative analysis. *Journal of Sedimentary Research,* 69, (5), 1050-1062.

[38] Bryers, R. W. (1996). Fireside slagging, fouling, and high-temperature corrosion of heat-transfer surface due to impurities in steam-raising fuels. *Progress in Energy and Combustion Science,* 22, (1), 29-120.

[39] Jackson, J. P. (1979). From mineral matter to deposits in P-F fired boiler. In *Pulverizing Coal Firing-The Effect of Mineral Matter*, Wall, T., Ed. University of Newcastle: pp 136-139.

[40] Bryers, R. W., and Walchuk, O. R. 1985. *Investigation of pyrites as a contributor to slagging in eastern bituminous coals*; Department of Energy: Pittsburgh, Pennsylvania,

[41] Stucki, J. W., Baitinger, W. E., and Roth, C. B. (1976). Analysis of iron-bearing clay minerals by electron spectroscopy for chemical analysis (ESCA). *Clays and Clay Minerals,* 24, (6), 289- 292.

[42] Sarofim, A. F., Howard, J. B., and Padia, A. S. (1977). Physical transformation of the mineral matter in pulverized coal under simulated combustion conditions. *Combustion Science and Technology,* 16, (3-6), 187- 204.

[43] Falcone, S. K., and Schobert, H. H. (1986). Mineral transformations during ashing of selected low-rank coals. *ACS Symposium Series,* 114- 127.

[44] Srinivasachar, S., Helble, J. J., and Boni, A. A. (1990). Mineral behavior during coal combustion. 1. Pyrite transformations. *Progress in Energy and Combustion Science,* 16, (4), 281- 292.

[45] Srinivasachar, S., Helble, J. J., Boni, A. A., Shah, N., Huffman, G. P., and Huggins, F. E. (1990). Mineral behavior during coal combustion. 2. Illite transformations. *Progress in Energy and Combustion Science,* 16, (4), 293- 302.

[46] Srinivasachar, S., and Boni, A. (1989). Kinetic model for pyrite transformations in a combustion environment. *Fuel,* 68, 829-36.

[47]   McLennan, A. R., Bryant, G. W., Stanmore, B. R., and Wall, T. F. (2000). Ash formation mechanisms during pf combustion in reducing conditions. *Energy and Fuels,* 14, (1), 150-159.

[48]   Zhang, L., Sato, and A., Ninomiya, Y. (2002). CCSEM analysis of ash from combustion of coal added with limestone. *Fuel,* 81, (11-12), 1499-1508.

[49]   Huffman, G. P., Huggins, F. E., Shah, N., and Shah, A. (1990). Behavior of basic elements during coal combustion. *Progress in Energy and Combustion Science,* 16, (4), 243-251.

[50]   Huffman, G. P., Huggins, F. E., Levasseur, A. A., Durant, J. F., Lytle, F. W., Greegor, and R. B., Mehtat, A. (1989). Investigation of atomic structures of calcium in ash and deposits produced during the combustion of lignite and bituminous coal. *Fuel,* 68, (2), 238-242.

[51]   Dai, S., Ren, D., Chou, C.L., Li, S., and Jiang, Y. (2006). Mineralogy and geochemistry of the No. 6 Coal (Pennsylvanian) in the Junger Coalfield, Ordos Basin, China. *International Journal of Coal Geology,* 66, (4), 253-270.

[52]   Yen, F. S., Lo, H. S., Wen, H. L., and Yang, R. J. (2003). θ- to α-phase transformation subsystem induced by α-Al_2O_3-seeding in boehmite-derived nano-sized alumina powders. *Journal of Crystal Growth,* 249, (1-2), 283-293.

[53]   Wen, H.L., and Yen, F.S. (2000). Growth characteristics of boehmite-derived ultrafine theta and alpha-alumina particles during phase transformation. *Journal of Crystal Growth,* 208, (1-4), 696-708.

[54]   Kao, H.C., and Wei, W.C. (2000). Kinetics and microstructural evolution of heterogeneous transformation of θ-alumina to α-alumina. *Journal of the American Ceramic Society,* 83, (2), 362-368.

[55]   Ninomiya, Y., Zhang, L., Sato, A., and Dong, Z. (2004). Influence of coal particle size on particulate matter emission and its chemical species produced during coal combustion. *Fuel Processing Technology,* 85, (8-10), 1065- 1088.

[56]   Zhang, L., and Ninomiya, Y. (2006). Emission of suspended PM_{10} from laboratory-scale coal combustion and its correlation with coal mineral properties. *Fuel,* 85, (2), 194-203.

[57]   Liu, X. W., Xu, M. H., Yao, H., Yu, D. X., Gao, X. P., Cao, Q., and Hao, W. (2006). Research on fragmentation behavior of illite and pyrite in coal. *Zhongguo Dianji Gongcheng Xuebao/Proceedings of the Chinese Society of Electrical Engineering,* 26, (21), 88-91.

[58]   Wibberley, L. J., and Wall, T. F. (1982). Alkali-ash reactions and deposit formation in pulverized-coal-fired boilers: the thermodynamic aspects involving silica, sodium, sulphur and chlorine. *Fuel,* 61, (1), 87-92.

[59]   Gao Q., Zhang J., and Qiu J., Zhao Y. (2007). A study of high temperature corrosion characteristics of coal-fired utility boilers. Journal of Engineering for Thermal Energy and Power. 22(3), 292-296

Chapter 9

A QUANTIFICATION METHOD OF WHOLE BULK COAL X-RAY PATTERNS

S. Kalaitzidis[1], S. Papazisimou[1], K.Christanis[1], G.Cressey[2], and E.Valsami-Jones[2]

[1]Department of Geology, University of Patras, GR-265 00 Rio-Patras, Greece
[2]Department of Mineralogy, The Natural History Museum, Cromwell Road, London, SW7 5BD, UK

ABSTRACT

The identification and quantification of minerals contained in coals are very important in a) elucidating the environmental conditions established during peat accumulation in the palaeomires, b) assessing the behavior of coals during combustion for power generation, c) evaluating the potential for various industrial applications, and d) determining the mode of occurrence of potential toxic and hazardous trace elements.

X-ray diffraction (XRD) is the most frequently applied method in determining the mineralogical composition of coal samples. The inherent limitation to the quantitative identification, when bulk sample is used, is the low signal to noise ratio of the diffractogramme due to the interference of the organic matter. In order to increase the sensitivity of X-ray diffraction, 'coal products' obtained after low-temperature (using oxygen-plasma) or high-temperature ashing or even oxidation using chemical agents, are used. Nevertheless, the composition of these 'products' might significantly differ from the original on the bulk coal samples as a result of the treatment.

Quantification of mineral matter based on XRD patterns also exhibits inaccuracies due to certain effects such as the preferred orientation of the mineral grains in the sample holder and the variation in absorption of X-rays by the minerals and the organic matter. Various quantification methods for the study of minerals in coals have been developed, which mainly operate on a semi-quantitative basis. Among the most known and promising quantitative methods are the analyses using an external standard (spike) such as corundum and the Rietveld-based method (integrated intensities of the main

diffractogramme peaks), as well as a combination of Rietveld technique and full pattern fitting.

By using curved position-sensitive detectors (PSD) that enable the rapid (5 min) acquisition of diffraction patterns in the angular range 3-120° 2θ, a quantification method of minerals in bulk low-rank coals was developed. This was worked out in a series of published and unpublished studies, which are reviewed in this communication. The method is based on full mineral pattern fitting techniques, also incorporating the fitting of pure organic phases in order to simulate the whole coalified sample. Fresh to slightly humified (recent) plant material, in the case of peat samples, and heavy-media separated organic material in the case of lignites, have been used as standards after determining their mass absorption coefficients experimentally. The procedure, as well as the advantages and limitations of the method are described in detail.

1. INTRODUCTION

Coal is a highly heterogeneous organic sedimentary rock consisting of both a variety of humified plant-derived organic matter, which underwent coalification, and various inorganic mineral phases; the latter appear either as crystalline to amorphous minerals in various grain sizes. The kind and the contents of organic and inorganic matter significantly vary in coals depending on the different coal-forming environments. This variation might be striking also from place to place within the same coal deposit, depending primarily on the local geological and climatic conditions, which prevailed in the coal-forming palaeoenvironments, namely in the palaeomires (McCabe, 1984; Raymond et al., 1990; Neuzil et al., 1993). Therefore, the assessment of both the qualitative and quantitative features of the mineral matter contained in a coal is a significant tool in interpreting the forming conditions for scientific and exploration purposes, as well as in evaluating the quality of commercially utilized coal. Furthermore, the knowledge of the mineral matter is essential for evaluating the behavior of the peat/coal in several technological applications. For example in the power generation sector it is important to predict the impact on boiler erosion, ash production and slagging effects (e.g. Raask, 1985; Querol et al., 1994; Heikkinen et al., 1998; Gupta et al., 1999) and in other industrial applications such as production of soil improvements, coke production, gasification, in which the kind of mineral matter influences the raw-material handling and the chemical features of the final products.

The heterogeneous nature of coal makes identification difficult, and quantification of the inorganic constituents contained is even more problematic. The application of a single method, capable of evaluating the inorganic matter fully is unlikely. Usually the optimum results are provided by a combination of analytical techniques, including examinations under both optical and scanning electron microscopes (SEM), determinations using X-ray diffraction and geochemical analyses (Vassilev and Tascón, 2003).

Previous studies have demonstrated the importance of X-ray diffraction analysis in the identification of mineral phases occurring in peat (e.g. Bailey and Kosters, 1983; Wüst et al., 2002), as well as in high-rank coals (e.g. Cressey and Cressey, 1988; Querol et al., 1997; Ward et al., 2001). However, the quantification of coal mineral matter using X-ray diffraction is quite problematic due to "inherent" limitations of the technique such as the background level of the signal of the organic matter present in peat/coal, the degree of mineral

crystallinity, variations of X-ray absorption by the different minerals and preferred orientation effects (Ward et al., 2001).

In order to overcome the noisy background signal in a diffraction pattern caused by the organic matter, XRD analyses on the combustion products of peat/coal is often adopted. However, using various ashing techniques, including high- and low-temperature ashing techniques or wet oxidation, new mineral phases usually form or already existing minerals may break down (e.g. Andrejko et al., 1983; Ward, 1986, Kalaitzidis and Christanis, 2004).

Among the best known and accepted quantitative approaches are the external standard (spike) method, in which a standard such as corundum, is added to the sample, and the Rietveld-based method (Rietveld, 1969; Ward and Taylor, 1996). In the former, the quantity of each mineral phase is calculated from the relation of its peak intensity to this of the corundum; nevertheless, this method does not provide satisfactory results if clay minerals dominate in the sample (Ward and Taylor, 1996). In the Rietveld method the whole profile of an X-ray diffraction pattern is taken into account (e.g. Taylor and Matulis, 1991; Mandile and Hutton, 1995; Hutton and Mandile, 1996). According to this method an X-ray diffraction pattern of each mineral contained in a multiphase sample, is produced and fitted to the actual XRD profile by applying iterative least-squares analysis until full matching of the pattern is achieved. The Rietveld technique is the base of the quantification method applied by using SIROQUANT[TM] software, which is a promising technique for the study of organic sediments and sedimentary rocks (Ward and Taylor 1996). In most cases this method is limited to XRD patterns from low-temperature coal ashes or even to XRD patterns of bulk samples after the removal of the pattern attributed to the organic matter using a background subtraction routine (e.g., Ward et al., 2001; Wüst et al., 2002).

In this paper a new, non-destructive (*sensu* non-oxidative) quantification procedure is proposed, which is based on full-pattern fitting technique, by incorporating the fitting of a pure organic phase in order to simulate the coalified organic material, and hence to obtain a whole-sample quantification. For the X-ray diffraction analysis a curved position-sensitive detector (PSD) is used that enables the rapid acquisition of diffraction patterns in the angular range 0-120° *2θ*. Peat and lignite samples from Greek deposits, with various degrees of mineral matter contents are examined. The procedure, as well as the advantages and limitations of the method are described in detail.

The following quantification method is an advance to the method described by Papazisimou et al. (2004), which was applied on lignite samples.

2. THEORETICAL BACKGROUND OF THE QUANTIFICATION METHOD

The diffracted intensity from hkl planes in a single-phase powder sample is expressed by the equation:

$$I_{hkl} = \left(\frac{I_o \, kmLp}{\mu} \right) F_{hkl}^2 V \qquad\qquad 2.1.$$

where I_o: intensity of incident beam, k: *experimental* constant, m: multiplicity of reflection, Lp: Lorentz-polarization factor, μ: linear absorption coefficient of the phase, F_{hkl}: structure factor, and V: volume of diffracting crystals. The same mineral phase A within a multiphase mixture will display diffracted intensity:

$$I_{hkl}^{A} = \left(\frac{I_o kmLp}{\mu'} \right) F_{hkl}^{2} V^{A}$$ 2.2.

where μ': linear absorption coefficient of the total matrix and V^A: volume fraction of the mineral phase A in the mixture.

Using this approach Cressey and Schofield (1995) have shown that for a matrix consisting of several different compounds with similar mass absorption coefficients, the diffracted intensity of each phase is simply proportional to the total weight of this phase in the matrix. However, if the mass absorption coefficients of the different compounds significantly vary, a correction is required taking into consideration the mass absorption coefficient of the whole matrix. In this sense every mineral phase, which can be identified in a diffraction pattern, can be quantified by comparison to the pattern that corresponds to the 100% of the pure mineral phase (standard pattern).

According to Batchelder and Cressey (1998), by applying a correction for absorption and calculating the phase proportions as a normalized ratio, the weight percentage of a mineral phase within a multiphase matrix is simply a function of its measured pattern fit fraction modified by the mass absorption coefficients for each phase:

$$w^i = \frac{w_{app}^i \big/ (\mu/\rho)^i}{\sum_i \left(w_{app}^i \big/ (\mu/\rho)^i \right)}$$ 2.3

where w^i: true weight of mineral phase i within the sample, w_{app}^i: apparent weight of mineral phase i within the sample (pattern fit value), $(\mu/\rho)^i$: mass absorption coefficient of phase i.

The mass absorption coefficient (μ/ρ) for mineral phases is calculated based on the stoichiometry, taking in account the respective (μ/ρ) values of the chemical elements (Int. Union of Crystallography, 1974). Similarly, the (μ/ρ) values of organic phases can be calculated using the concentrations of the elements C, H, N, O and S (e.g. Papazisimou et al., 2004), as these are the main elements compositing the organic compounds, or determined experimentally, as will be presented below.

3. X-RAY DIFFRACTION PROCEDURE

3.1. Sample preparation

Peat samples (87 in total) from three major peatlands in Greece, as well as 13 lignite and sub-bituminous coal and mud samples from the most important coal-bearing basins in Greece have been examined (for details about the origin and the description of the samples refer to Christanis et al., 2007; Kalaitzidis, 2007). The samples and the mineral standards were prepared following the method described by Batchelder and Cressey (1998). The peat and lignite samples were dried at 105°C for 24 h and then gently ground to produce a smooth powder. Powder has also been produced from root tissues of the plant *Cladium maricus*, which is the dominant peat-forming species in Greece, in order to use it as standard for the organic matter. Additionally, density separation was applied on the lignite samples using heavy liquids (e.g. $ZnCl_2$ solution); the light (organic-rich) fraction was ground and used to simulate the coalified organic matter. The powder was loaded into a circular well mount (15 mm in diameter and 1 mm deep). To avoid inducing a high degree of preferred orientation of platy crystals parallel to the top surface, each sample was packed and levelled to the rim of the circular well holder using only the narrow (knife) edge of a small steel spatula until a smooth flat surface was obtained. The packing procedure took less than 1 min per sample.

3.2. X-ray data acquisition

The method utilizes a curved position-sensitive detector (PSD) with an output array consisting of 4096 channels representing an arc of approximately 120° *2θ* (0.03147^o actual channel width). The detector enables diffraction patterns to be acquired rapidly by measuring diffracted intensity at all angles simultaneously around the 120° arc. All the data were collected using an ENRAF-NONIUS PDS 120 (Powder Diffraction System 120) with a curved PSD and a fixed beam-sample-detector geometry. A germanium-111 monochromator was used to select only Cu$K\alpha_1$ radiation from the primary beam and tube-operating conditions were 45 kV and 45 mA. Horizontal and vertical slits between the monochromator and the sample were used to restrict the beam to 0.24 mm X 5.0 mm, respectively, and thus, the irradiated area was constant. Measurements were made in reflection geometry with the powder sample surface at a fixed angle of $\sim5^o$ to the incident beam. The sample was rotated continuously around an axis vertical to its surface. This statistically increases the number of crystallites oriented in diffracting positions. The tilt of the sample surface to the beam was held constant during data acquisition. Data acquisition times of only 5 min were required for all the analyses, to obtain an acceptable signal of the pattern. Unground NIST silicon powder (SRM 640) was used as an external standard for the *2θ* calibration. The detector was connected to a computer and the *2θ* linearization was performed using the ENRAF-GUFI software by applying a least-squares cubic spline function.

This type of arrangement allowed the digital acquisition of patterns that display relatively high signal/noise ratio within a relatively rapid time-span of 5 min. Furthermore, a series of pure mineral standards, from the collection of the Natural History Museum, London, that occur within the studied organic sediments were also analyzed using the same parameters.

3.3. Data processing

Whole X-ray pattern evaluation was performed using ENRAF-GUFI software, according to the procedure described by Cressey and Schofield (1995). Briefly, this consists of sequential pattern-stripping involving three steps:

a)   for each mineral phase identified within the sample, a standard pattern produced from a 100% pure sample of that phase is superimposed upon the multiphase sample.

b)   the standard pattern counts are proportionally reduced, by multiplying by a user-defined fraction (scale-fit which yields the pattern fit value w^i_{app}), in order to achieve the best match (assessed by eye) to that mineral phase within the multiphase sample, taking into account the whole pattern. The fitting process is quite rapid and usually only few iterations are required to approach the optimal fit. The scale-factor for the optimal fit represents the weight fraction of the mineral phase (uncorrected for absorption effects) within the multiphase sample.

c)   stripping the reduced-intensity mineral standard pattern using a subroutine of the software.

This three-step procedure is repeated until all the phases are subtracted and the residual pattern does not reveal the presence of any other phases.

The sample preparation method minimizes any preferred orientation of the mineral grains and the static sample-detector geometry records a close-to-random diffraction pattern. Hence, the diffraction intensities from the different phases present in the mixture are totally proportional to each other, and can be compared directly with the pattern intensities from the single-phase standards. This process provides a rapid quantitative assessment of all the contained mineral phases. Although the order in which the different minerals were removed, does not affect the final quantification, generally it is suggested to strip first the most easily identifiable phases (sharp peaks). In practice the stripping method has a pattern fitting precision of ~1% for the patterns of non-clay minerals and of ~3% for the clay minerals (Cressey and Schofield, 1995).

By knowing the mass absorption coefficients of the identified mineral phases and applying equation (2.3), the weight percentage of each mineral is calculated.

In the cases of inorganic sediments the residual pattern represents noise or amorphous to poor crystalline phases, almost impossible to identify. On the contrary, in the organic sediments the residual pattern represents mainly the organic matter. Hence, a standard pattern is needed to attribute to the peat and lignite organic matter. The subtracting of a scale-fitted organic-matter pattern would reduce the counts of the residual pattern almost to zero, and knowing the mass absorption coefficient for the organic component would enable a full quantification of the multiphase peat/coal sample to be made.

3.4. Obtaining an organic matter pattern

A series of different peat-forming herbaceous-plant tissues at various humification stages were examined using the PSD diffractometer in order to obtain an organic standard pattern

that would stimulate the organic pattern of the examined peat samples. The optimum pattern, i.e. the pattern that satisfied most of the studied Greek peat samples, was retrieved from the roots of *Cladium mariscus* (abbreviated in the following ClR), the pattern of which reveals a broad intensity maximum in the 2θ region of 10-25º, which can be resolved into two intensity features at ~16º and ~20º 2θ (Figure 1).
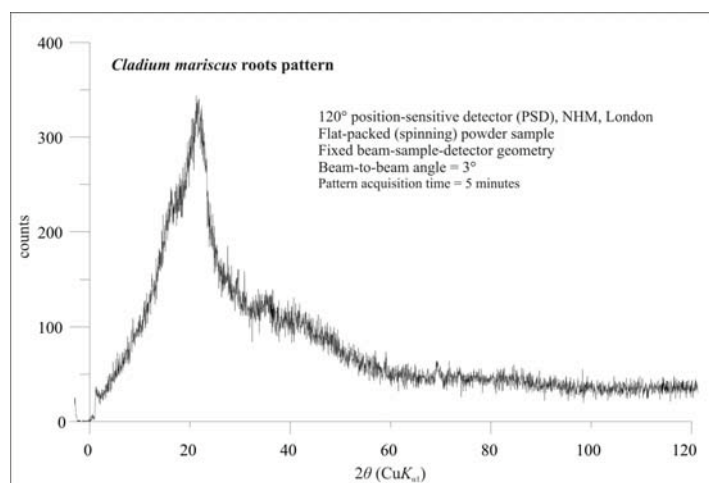
Figure 1. X-ray diffraction pattern of the *Cladium mariscus* roots.

Additionally, the organic matter of the lignite samples was simulated by the organic-rich fraction of density separated (using heavy liquids) Pleistocene Greek lignite (Figure. 2). It was recognized that for samples of the same rank the geometry of the organic fraction in X-ray patterns were similar as also is reported by French et al. (2001).
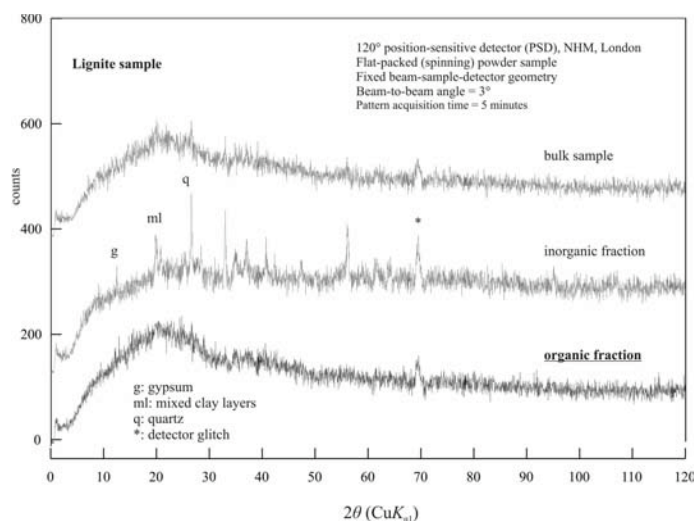
Figure 2. X-ray diffraction patterns of a lignite bulk sample and the respective density separated fractions. The pattern of the organic fraction has been used as standard-pattern for the quantification method.

In most cases by subtracting the organic-pattern produced a flat residual with counts close to zero (Fig. 3). In the final residual pattern minor positive or negative peaks sometimes remain, which arise from preferred orientation or matrix absorption effects, resulting in slight mismatching of the major peaks of the standard patterns. However, since the evaluation process involves the fitting of the whole pattern and not only single peaks, the above effects do not influence significantly the quantification.
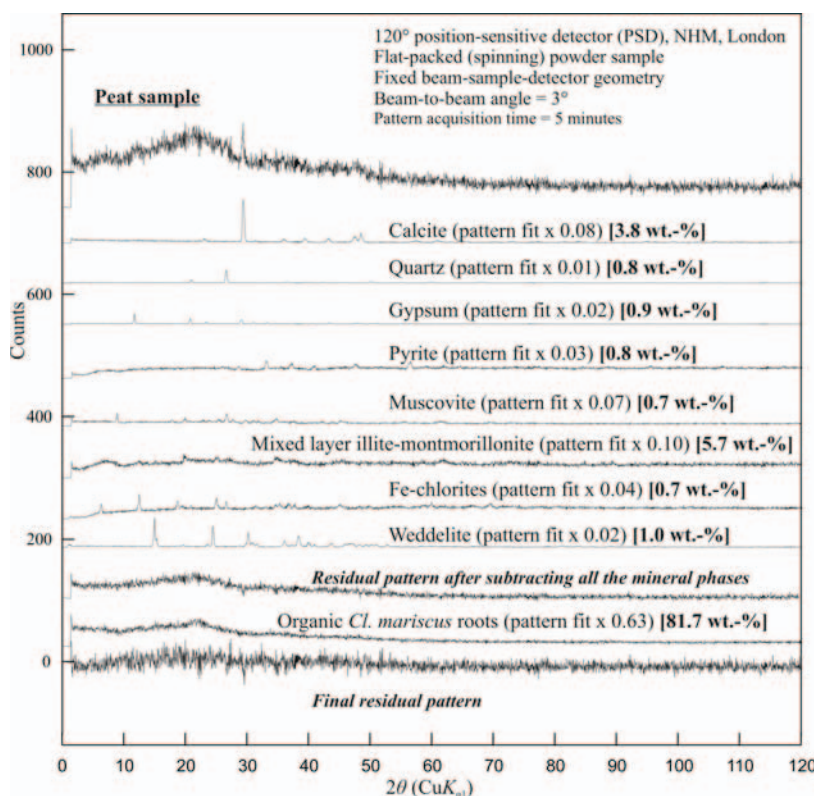
Figure 3. Sequence showing the procedure of whole-pattern matching and stripping from an initial multiphase peat pattern. In brackets the value of the pattern fit and the actual weight percent of each phase.

3.5. Experimental determination of the (μ/ρ) coefficient of the organic matter

As already mentioned, the mass absorption coefficient (μ/ρ) of the organic matter is required for the quantification method. There are two ways to calculate this coefficient: either from the elementary composition or by experimental analysis of a weighed-out binary mixture of the organic matter and a crystalline phase of known absorption value.

From geochemical analysis the compositional formula of the examined *Cladium mariscus* roots (ClR) was determined $C_{51}H_{1.6}N_{1.6}O_{44.2}Ca_{0.7}Al_{0.03}Fe_{0.05}K_{0.4}Mg_{0.1}Na_{0.1}P_{0.1}S_{0.1}Si_{0.2}$ (Kalaitzidis, 2007) and therefore its mass absorption coefficient $[(\mu/\rho)^{CIR}]$ is calculated to be 6.86 cm^2·g^{-1}. Additionally the (μ/ρ) values for the peat and the lignite samples calculated from

the composition in C, H, N, O and S range from 6.5-10.5 and 5.7-13, respectively (Table 1; Papazisimou et al., 2004; Kalaitzidis, 2007; Christanis et al., 2007).

Table 1. Example of the data used for the quantification procedure and the results for one peat (Ph-141) and one lignite (Pel-5) samples

Sample	ash	C	H	O	N	S	(μ/ρ) [a]
	wt.-% (on dry basis)						$cm^2 \cdot g^{-1}$
Ph-141	18.6	46.2	4.9	27.4	1.8	1.1	7.3
Pel-5	34.5	35.8	3.1	21.2	0.6	4.8	12.7

Mineral contents in wt.-% (on dry basis) using experimental $(\mu/\rho)^{org}$ (=21 $cm^2 \cdot g^{-1}$)
(w^i_{app}: pattern fit)

	Calcite	Quartz	MCL[b]	Chlorite	Gypsum	Pyrite	FeO[c]	Wed[d]	Mica	OM[e]	MM[f]
Ph-141	3.8 (0.08)	0.8 (0.01)	5.7 (0.1)	0.7 (0.04)	0.9 (0.02)	0.8 (0.03)		1.0 (0.02)	0.7 (0.07)	81.7 (0.61)	18.3
Pel-5	2.0 (0.04)	1.7 (0.02)	28.8 (0.3)	1.0 (0.04)	5.0 (0.1)	2.0 (0.06)	1.0 (0.06)			58.5 (0.39)	41.5

[a]: (μ/ρ): calculated from C, H, O, N, S contents
[b]: MLC: Mixed clay layers
[c]: FeO: Fe-oxides absorbed to the organic matrix
[d]: Wed: Weddellite
[e]: OM: Organic matter
[f]: MM: mineral matter

For the experimental approach in the peat samples, two mixtures of organic matter and pure halite were prepared according to the method proposed by Batchelder and Cressey (1998). The mixtures were:

1. ClR 55.7 wt.-% plus halite 44.3 wt.-%,
2. ClR 46.3 wt.-% plus halite 53.7 wt.-%.

For the lignite organic matter the mixture was: organic matter (i.e. the light fraction after density separation) 45.1 wt.-% plus halite 54.9 wt.-%. The mass absorption coefficient of the total binary mixture $(\mu/\rho)'$ is provided by the equation:

$$(\mu/\rho)' = w^{NaCl}(\mu/\rho)^{NaCl} + (1 - w^{NaCl})(\mu/\rho)^{org} \qquad (3.1)$$

where w^{NaCl}: the actual weight fraction of halite, $(\mu/\rho)^{NaCl}$: the mass absorption coefficient of halite (78.2 $cm^2 \cdot g^{-1}$) and $(\mu/\rho)^{org}$: the requested coefficient of the organic matter.

The actual weight of halite (w^{NaCl}) within the mixture is proportional to the determined apparent weight (w^{NaCl}_{app}), multiplied by a factor related to the mass absorption coefficients:

$$w^{\text{NaCl}} = w^{\text{NaCl}}{}_{app} \, [(\mu/\rho)'/(\mu/\rho)^{\text{NaCl}}] \tag{3.2}$$

By using the GUFI 5.0 software the halite apparent weight ($w^{\text{NaCl}}{}_{app}$) was determined with high precision (Fig. 4):

For the *Cladium mariscus* mixtures:

Mixture 1: $w^{\text{NaCl}}{}_{app} = 0.75$ (with $w^{\text{NaCl}} = 0.443$)
Mixture 2: $w^{\text{NaCl}}{}_{app} = 0.81$ (with $w^{\text{NaCl}} = 0.537$)

For the lignite organic matter mixture: $w^{\text{NaCl}}{}_{app} = 0.82$ (with $w^{\text{NaCl}} = 0.549$)
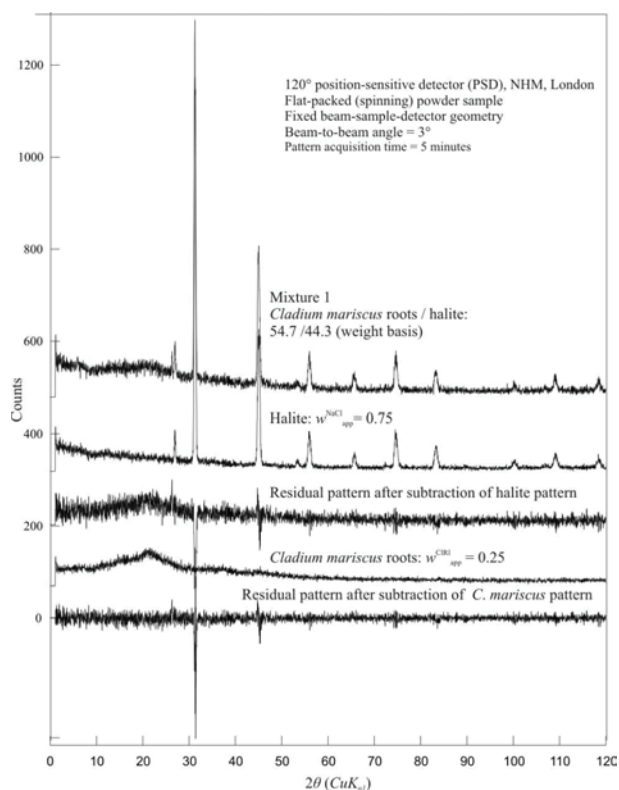
Figure 4. Experimental determination of the mass absorption coefficient $(\mu/\rho)^{\text{CIR}}$ of the organic-matter standard (*Cladium mariscus* roots). The positive/negative peaks in the residual arise from imperfect peak overlap caused by an increased beam penetration depth in the sample of lower absorbance. However, these features do not affect the quantification result obtained by matching peak intensities. The negative residual at 31.7° is caused by a greater degree of preferred orientation of the {100} cleavage fragments at ~15° to the surface in the halite standard. This main peak of halite is not necessary, and therefore not used, for the quantification assessment.

Finally from equations (3.1) and (3.2) the mass absorption coefficient of the organic matter can be calculated:

$$(\mu/\rho)^{org} = \frac{w^{NaCl}(\mu/\rho)^{NaCl}\left(\dfrac{1}{w_{app}^{NaCl}}-1\right)}{1-w^{NaCl}} \tag{3.3}$$

Thus determined, the mass absorption coefficients $[(\mu/\rho)^{ClR}]$ from the two ClR experiments are 20.7 and 21.3 $cm^2 \cdot g^{-1}$, respectively, with a mean value of $(\mu/\rho)^{ClR} = 21$ $cm^2 \cdot g^{-1}$. The mass absorption coefficient determined experimentally for the lignite organic matter is, remarkably, almost the same value $((\mu/\rho)^{org} = 20.9$ $cm^2 \cdot g^{-1})$.

The significant variation from the calculated value based on stoichiometry, denotes that the absorption depends on the structural arrangements and not only on the chemical element proportions. The experimentally determined value was used for the quantification procedure since it verifies better the mineral matter content (Figures. 5 and 6).
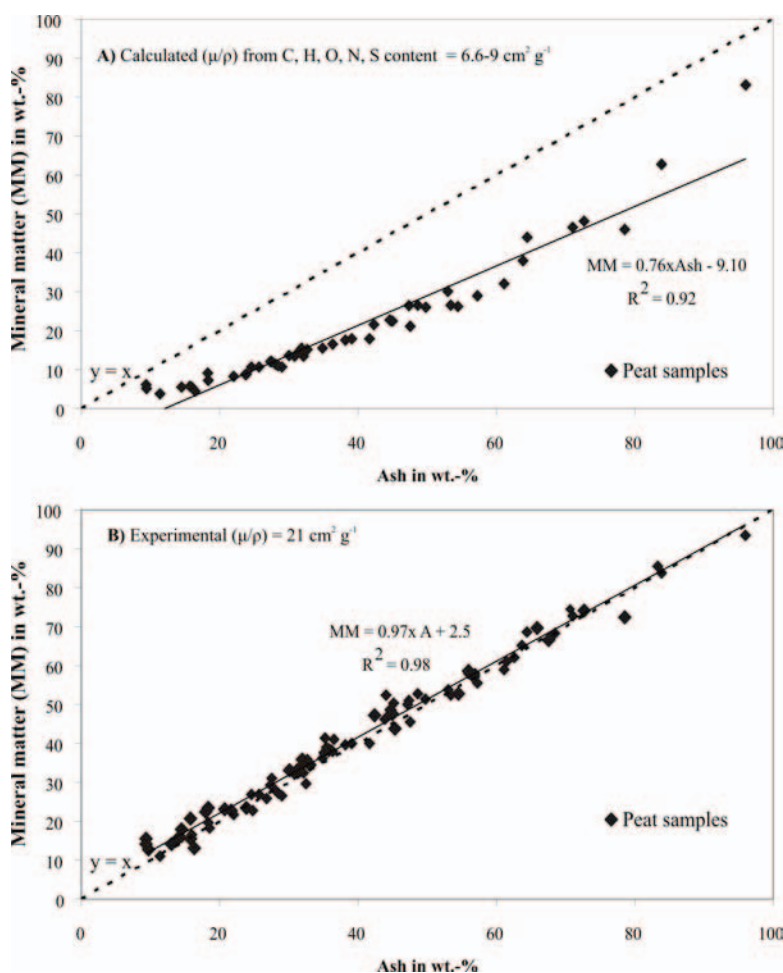
Figure 5. Correlation between mineral matter contents quantified using the PSD procedure and the ash yields (determined after combustion at 550°C) of Greek peat samples: (A) using calculated mass absorption coefficient (μ/ρ) from C, H, O, N, and S contents and (B) determining the (μ/ρ) coefficient experimentally (numerical data from Kalaitzidis, 2007).
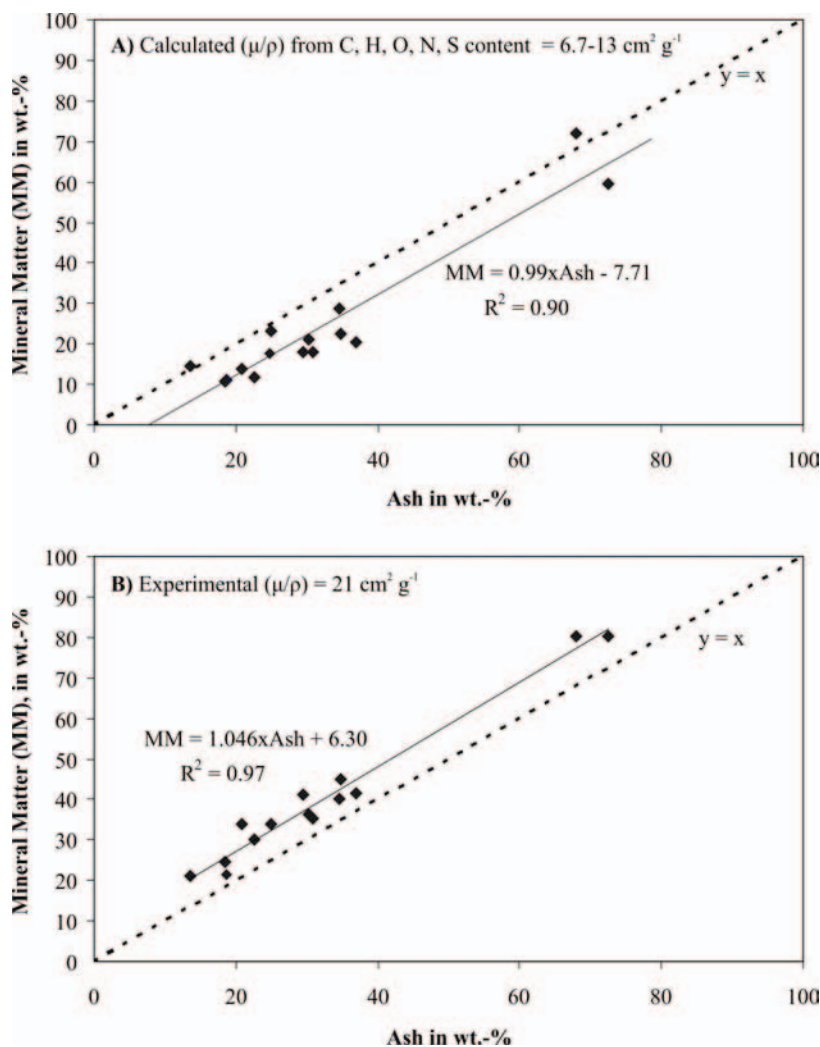
Figure 6. Correlation between mineral matter contents quantified using the PSD procedure and the ash yields (determined after combustion at 750°C) of Greek lignite, sub-bituminous and mud samples: (A) using calculated mass absorption coefficient (μ/ρ) from C, H, O, N, and S contents and B) determining (μ/ρ) experimentally (for the numerical data refer to Christanis et al., 2007).

4. DISCUSSION AND CONCLUSION

The advantages of the PSD pattern-stripping quantification procedure on inorganic sediments are the rapid acquisition of counts and the relatively simple data processing (Batchelder and Cressey, 1998). The difficulty in quantifying the mineral component of coal, peat and other organic sediments using X-ray diffraction techniques, lies in the presence of the organic matter that causes dilution of the signal; additionally, there are no standards in the diffraction software libraries and hence, usually the organic matter is not taken into account (e.g., Ward et al., 2001).

The proposed method overcomes this problem by adopting the fact that the organic matter of coaly sediments can be simulated either by fractionation, and hence obtaining a pure organic fraction, or by using fresh to slightly humified (recent) plant material in the case of peat.

A similar approach is discussed in French et al. (2001), who have used the patterns of organic matter (coaly) samples that have been obtained after acid-demineralization, providing a structure model in SIROQUANT[TM] project. Nevertheless, the introduction of the organic mass absorption coefficient as described in the present paper optimizes the quantification process.

In order to check the reliability of the obtained results, the mineral matter contents calculated from the X-ray diffraction procedure are plotted against the ash yields determined after thermal oxidation of the samples (Figs. 5 and 6). The linear regression analysis shows that there is a very strong correlation ($R^2 \geq 0.9$) between mineral matter contents determined by the proposed procedure and ash yields, verifying the applicability of the technique. Processing the data by applying the mass absorption coefficient $(\mu/\rho)^{org}$ calculated from the C, H, O, N, S contents results to a relative underestimation of the mineral matter contents in relation to the ash yields, as can be seen from Figures 5A and 6A. On the contrary, by applying the experimental $(\mu/\rho)^{org}$ value the linear regression correlation coefficients increase, and further the mineral matter contents are similar or higher than the ash yields (Figs. 5B and 6B). The latter is the frequently observed trend, since during combustion the water and the volatile substances both contained in the minerals, escape and also minerals break down, depending on the combustion temperature (Andrejko et al., 1983; Ward, 1986). Noteworthy to mention that the equations that satisfy the linear regression correlation of the data in the case of the experimentally determined $(\mu/\rho)^{org} = 21$ fit better to the widely used Parr equation (MM = 1.08·Ash + 0.55·S; see Speight, 1994) than in the case of the calculated $(\mu/\rho)^{org}$ coefficient from C, H, O, N, S data (Figs. 5 and 6). Moreover, comparing the different set of samples according to the combustion temperature for ash yield determination it is evident that for the peat the contents of mineral matter are similar to these of ash, since limited modifications occur at 550°C, whereas for the lignite and sub-bituminous coal samples, which were combusted at 750°C, the difference increases, as a consequence of mass loss during thermochemical reactions.

An additional verification of the quantified data is provided through the correlation of the concentrations of major oxides that are either inferred from the PSD quantification or measured by geochemical analysis (ICP-AES). It is concluded that the correlations for SiO_2, Al_2O_3, CaO and Na_2O are very strong (Fig. 7), being equal or even better than these obtained from similar studies using SIROQUANT[TM] software (e.g. Ward et al., 2001; Ward and French, 2004). The observed minor deviations are probably due to the organic affinity of elements, probable inefficient digestion of elements and the not exact correspondence of the normic concentrations of the minerals to the stoichiometry of the actual mineral standards.
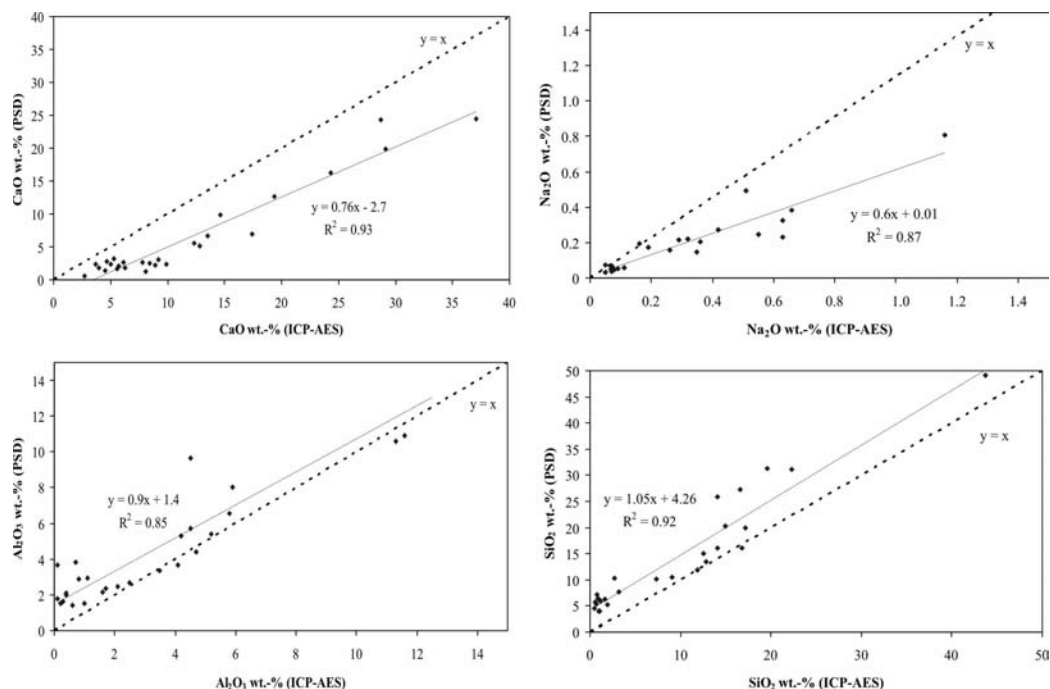
Figure 7. Correlation between oxide contents in peat samples inferred from PSD quantification process and oxide contents directly determined from bulk peat using ICP-AES (for original data refer to Kalaitzidis, 2007).

The main advantage of the proposed X-ray diffraction technique is the rapid acquisition of high signal/noise patterns of coal samples, the minimization of the preferred orientation effect, the ability to reproduce results rapidly and reproducibly, as well as the non-requirement for sophisticated software handling. Concerning the results, it is among the few methods that provide whole-coal mineral matter quantification. The disadvantage might be the difficulty in obtaining an organic matter pattern to satisfy the structure of every sample. Nevertheless, a future task should include the preparation of a data set from the organic-fraction patterns of various coals worldwide, along with the experimental determination of their respective mass absorption coefficients. These should enable the wide application of the quantification method presented here.

ACKNOWLEDGMENTS

REFERENCES

Andrejko, M. J., Feine, F., Cohen, A. D. (1983). In *Testing of peats and organic soils.* Jarrett, P. M.. Ed. ASTM STP 820, ASTM Special Technical Publication: Philadelphia, USA, pp 5-19.

Bailey, A., Kosters, E. C. (1983). In *Mineral matter in peat;* Raymond, R. Jr., Andrejko, M. J., Eds. Los Alamos National Lab. NM: Los Alamos, USA, pp 39-52.

Batchelder, M., Cressey, G. (1998). *Clay Clay Miner.* 46/2, 183-194.

Christanis, K., Lambrakis, N., Valsami-Jones, E., Cressey, G., Kalaitzidis, S., Papazisimou, S., Bouzinos, A., Giannouli, A., Siavalas, G. (2007). *Characterization of the organic and inorganic fractions of peat, lignite and other organic sediments, using modern analytical techniques;* Techn. Report, 3rd EU-Framework Pythagoras Project; University of Patras: Patras, Greece, 62 pp. [in Greek].

Cressey, B. A., Cressey G. (1988). *Int. J. Coal Geol.* 10, 177-191.

Cressey, G., Schofield, P. F. (1995). *Powder Diffr.* 11/1, 35-39.

French, D., Taylor, J., Dale, L., Matulis, C. (2001). In *Proc. 18th Pittsburgh Int. Coal Conference,* University of Pittsburgh, School of Engineering: Newcastle, 7 pp.

Gupta, R., Wall, T. F., Baxter, L. A. (1999). *The impact of mineral matter impurities in solid fuel combustion.* Plenum: New York, USA, 768 pp.

Heikkinen, R., Laitinen, R. S., Patrikainen, T., Tiainen, M., Virtanen, M. (1998). *Fuel Proc. Technol.* 56, 69-80.

Hutton, A. C., Mandile, A. J. (1996). *J. Afr. Earth Sci.* 23/1, 61-72.

International Union of Crystallography. *International tables for X-ray Crystallography, Volume IV*, Ibers, J. A., Hamilton, W. L. Eds. (1974). The Kynoch Press: Birmingham, England, UK.

Kalaitzidis, S. (2007). *Peatification and evolution of peatlands in Greece.* Ph.D. Thesis, Department of Geology, University of Patras: Patras, Greece, 532 pp.

Kalaitzidis, S., Christanis, K. (2004). *Mineral Wealth,* 132, 7-16 [in Greek, with English abstract].

Mandile, A. J., Hutton, A. C. (1995). *Int. J. Coal Geol.* 28, 51-69.

McCabe, P. (1984). In *Sedimentology of coal and coal-bearing sequences.* Rahmani, R. A., Flores, R. M. Eds. Spec. Publ. Int. Ass. Sediment. Blackwell Sc. Publ.: Oxford, England, Vol. 7, pp 13-42.

Neuzil, S., Supardi Cecil, B. C., Kane, J. S., Soedjono, K. (1993). *Geol. Soc. Am., Spec. Paper,* 286, 23-44.

Papazisimou, S., Kalaitzidis, S., Christanis, K., Cressey, G., Valsami-Jones, E. (2004). *Energ Fuels,* 18, 547-559.

Querol, X., Fernández-Turiel, J. L., López-Soler, A. (1994). *Mineral. Mag.* 58, 119-133.

Querol, X., Whateley, J. L., Fernández-Turiel, J. L., Tuncali, E. (1997). *Int. J. Coal Geol.* 33, 255-271.

Raask, E. (1985). *Mineral impurities in coal combustion: behavior, problems, and remedial measures;* Springer Verlag: Berlin, 484 pp.

Raymond, R. Jr., Cladney, E. S., Bish, D. L., Cohen, A. D., Maestas, L. M. (1990). In *Recent advances in coal geochemistry,* Chyi, L. L., Chou, C. L., Eds, *Geol. Soc. Am. Spec. Paper,* 248, 1-12.

Rietveld, H. M. (1969). *J. Appl. Cryst.* 2, 65-71.

Speight, J. G. (1994). *The chemistry and technology of coal.* 2nd ed. Dekker: New York, USA, 642 pp.

Taylor, J.C., Matulis, C. E. (1991). *J. Appl. Crystallogr.* 24, 14-17.

Vassilev, S. V., Tascón, J. M. D. (2003). *Energ Fuels,* 17, 271-281.

Ward, C. R. (1986). *Austral. Coal Geol.* 6, 87-110.

Ward, C. R., French, D. (2004). *Analysis and significance of mineral mater in coal. Short Course Notes*; Proc. 21st Annual Meeting of the Society of Organic Petrology (27 September-01 October), TSOP: Sydney, Australia, 70 pp.

Ward, C. R., Taylor, J. C. (1996). *Int. J. Coal Geol. 30*, 211-229.

Ward, C. R., Taylor, J. C., Matulis, C. E., Dale, L. S. (2001). *Int. J. Coal Geol.* 46, 67-82.

Wüst, R. J., Ward, C. R., Bastin, M. R., Hawke, M. I. (2002). *Int. J. Coal Geol.* 49, 215-249.

Chapter 10

COAL SYSTEM CONCEPT AND ITS APPLICATION EXAMPLE IN FUXIN BASIN

Zhao Zhongxin[1], Wang Hua[2] and Liu Junrong[1]

[1] Jidong Oilfield Company, Petrochina, Tangshan, Hebei, P.R.China
[2] China University of Geosciences, Wuhan, Hubei, P.R.China

ABSTRACT

Although coal geology study evolves slowly, in the 80's and 90's of the last century, there was a great progress in it including a study on peatland, coal petrology, coal geochemistry, coal measures deposits and its sedimentary environment, especially on coalbed gas and environmental protection in relation to combustion recently. This article's aim is to put forward a new study method to solve some problems in coal geology study. Through summarizing the former study, consulting petroleum system's concept and method, and integrating coal geology and systematology, we put forward the concept of coal system. Coal system is an integrated system that includes coalbed, coal measures, depositional facies and all kinds of geological actions relating to coal forming. As a system, Coal system has its own factors, actions, hierarchy and study content. Its basic factors are substance sources (paleobotanic and peat), coal-accumulation environment and underground thermal stream. And its geologic actions include: Peat original and allochthonous accumulation; burying action caused by diastrophism and geothermal metamorphism. The rational collocation of these basic factors and coal-forming actions in dimensional-temporal domain conduce the forming of valuable coalbeds. In hierarchy, a coal system can be divided into substance source subsystem, accumulation subsystem and metamorphism subsystem in temporal domain. In dimensional domain, it may fall into lower class subsystems resembling an upper system. And the study contents include every aspect of coal system factors, actions and hierarchy. At last, we take Fuxin basin as an example to explain how to start a coal system study. Discussion of the problem should be focused on in a study process.

1. INTRODUCTION

Coal geology study includes several aspects, such as study on peatland (Cohen, 1970; Moore and Bellamy, 1974), coal petrology (ICCP, 1963; 1971; 1976), structure analysis of coal-forming basin (MeKee et al., 1975; Wanless et al., 1978; Burchfiel, 1980), coal sedimentology (Rahmani and Flores, 1984; Scott, 1987), coal geochemistry (MacKowsky, 1975; Jenkins, 1978) et al. Recently, research on coal-forming basin as an integrated system is starting to flourish (Potter and Pettijohn, 1977; Conybeare, 1979; Dickinson, 1994, 1997; Li, 1999). And now, the study of coal-generated hydrocarbons is prevailing (Karweil, 1966; Brooks, 1967, 1969, 1970; Stach, 1982) in coal and petroleum geology research.

So far, coal geology study mas mainly seen progress on the subject of peatland and its forming-environment, coal petrology, coal sedimentology, coal geochemistry, coal-forming basin research and coal-generated hydrocarbons; and through this study more and more fruits are gained. But each of these studies is isolated. And there is a new trend that coal geology study need to be more integrated and systematical. Thus, we put forward the concept of the coal system.

2. COAL SYSTEM DEFINITION AND DESCRIPTION

Based on former studies and consulting on the petroleum system concept, coal geology and systematology, we put forward the concept of the coal system.

Petroleum system developed from the Oil System that brought forward by Dow (1972). Through the efforts of Magoon (1994), Perrodon (1992) and Demaison (1991), plentiful theoretic and actual fruits are gained so far. The coal forming mechanism is similar to oil and gas forming. In the forming process, they all underwent several geologic processes, such as source depositing, burying, metamorphism et al. And after oil and gas forming, it underwent a process of migrating, but coal output in the original coal-forming area basically. According to the difference and similarity between coal and oil-gas forming, we combined coal geology and systematology, and put forward the concept of a coal system. The purpose of this concept is to describe the turbulant natural phenomenon and complex geologic action of the coal forming process more systemically and accurately.

According to von Bertalanffy (1984)'s systematology, a system can be divided into a a natural system (substance system, energy system, biology system, zoology system), artificial system (concept system, tool system, manage system, society system et al.) and composite system (the composite of natural and artificial systems).

Coal system is defined as a natural system. It includes coalbed, coal measures, depositional facies and all kinds of geological actions relating to coal forming. Its basic factors and geologic actions are shown in Table 1. The rational collocation of these basic factors and coal-forming actions in temporal and dimensional domain can form the valuable coalbed.

Table 1. Basic factors and coal-forming actions of a coal system

Basic factors	Coal-forming actions
Source (paleobotanic and peat)	Peat original or allochthonous accumulation
Accumulation environment	Burying action caused by diastrophism
Underground thermal stream	Geothermal metamorphism

2.1 A coal system includes three basic factors

2.1.1. Source

Source includes paleobotanic and peat. Paleobotanic are all kinds of higher paleoplants relating to coal forming material, and they are a source of peat. Peat is the preexistence of the coal. The higher plants reliquiae is reconstructed by biochemistry action. Peat is the mixture of the reconstructed material of plant reliquiae and minerals dissolved in water.

2.1.2. Accumulation environment

The plant reliquiae need an environment to translate peat. Through observing the modern peat field, most of the peat is located in the high latitude area of the Northern Hemisphere. In this area, the advantaged peat accumulation environment include lagoon behind shore barrier, brim zone of bay, middle-upper tidal flat, fluvial delta plain, floodplain and yoke lake of sinuous river, alluvial fan plain and inland lake bank et al. (Ralhmani, 1984; Scott, 1987; Diessel, 1992; Cobb, 1993; Galloway, 1996).

2.1.3. Underground thermal stream

Peat translates into coal by diagenesis after being buried. While underground temperature rises gradually, coal ranks become higher because of the rising of coal metamorphism degree. Coal metamorphose action mostly due to temperature rising which accelerate chemistry reaction. Yang (1999) indicates coal-forming metamorphism results from diversiform underground thermal stream source: 1) natural geothermic grads; 2) magma; 3) hot fluid or hot water; 4) high temperature resulting from the deep rupture; 5) Moho surface rise form the abnormity terrestrial heat field. During the period of coal forming, it commonly under goes metamorphism several times, which may produce different rank of coal**.**

2.2 The coal-forming action includes

2.2.1. Peat original and allochthonous accumulation

According to whether the plant reliquiae underwent transition, coal accumulation is divided into original and allochthonous accumulation. We have universally accepted that "most of the valuable coal deposit is original created" for a long time. But recently, the studies on storm allochthonous coal have made great progress (Cohen, 1970; Stach, 1975). Wang (1997) considers most coal is original output coal, but some coal is undoubtedly

allochthonous forming. For example, cannel is composed of peat that is pushed into a lake, and stacked in addled mud.

2.2.2. Burying action caused by diastrophism

After the paleobotanic died, its reliquiae needed to be buried to form peat. Peat preservation and translation into a coalbed needs the lithosphere to descend rapidly and greatly, which leads to peat being buried.

2.2.3. Metamorphism during the coal-forming process

After peat accumulated and was buried, the factor that impels organic matter to transform into coal is heat. Heat comes from terrestrial heat, magma heat, etc. Along with the temperature rising, the elements of H, O and N are reduced gradually. And the element C enriches correspondingly. The aggregate degree of organic molecule increased gradually. In this way, peat can translate into coal or high-rank coal along with temperature rises unceasingly. We call the times that peat translates into coal or coal, translate high-rank coal, critical moments (Figure 1).

Geology epoch 1	Geology epoch 2	Geology epoch 3	Geology epoch 4	Geology epoch 5	Geologic time scale Coal rank
	200	150	100	50 (Ma)	
					Anthracite
					Soft coal
			Critical moment		Lignite
		Critical moment			Peat
	Critical moment				Paleo-plant
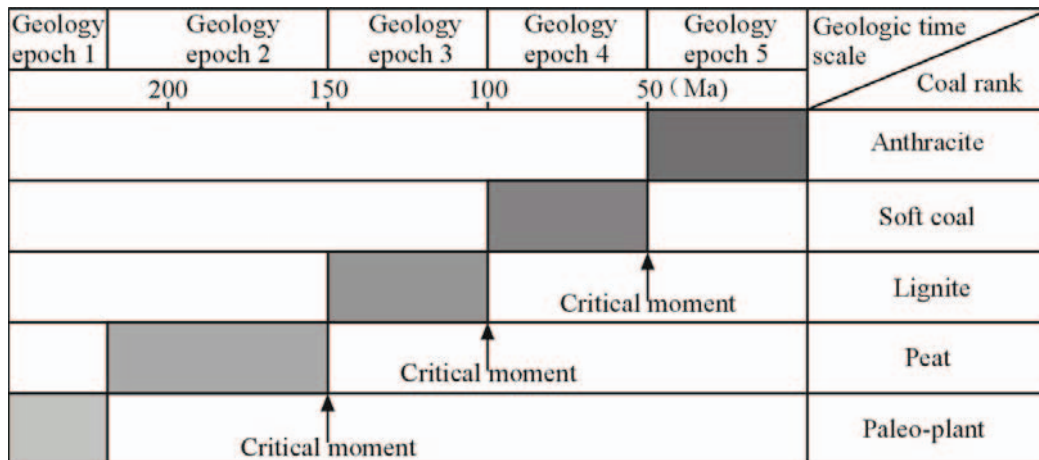
Figure 1. A fictitious events chart of coal system (From Zhao et al., modified, 2002)

The events chart shows the critical moments and the relationship between geologic time and coal rank in a fictitious coal system.

2.3. Coal system hierarchy

Generally, a system hierarchy is a complex relationship between system and subsystem. The subsystem is contained by higher class system and contains a lower class system. When a part of a coal system is studied, it may be looked upon as an integrated subsystem that is contained by a coal system, and the parameter of the subsystem is thought of as its own factors. And the coal system factors are thought as outer factors or adjacent subsystems. According to what was mentioned above, we think a coal system can be divided into two types of subsystems in temporal - dimensional domain.

A coal system can be divided into a source subsystem, a depositional subsystem, and a bury and metamorphose subsystem in temporal domain. In each subsystem, it has its own factors and components. The factors of source subsystem are the type of plant and the geography range of plant growth. Accumulation subsystem includes original or allochthonous accumulation. Burying and metamorphose subsystem contains pressure and temperature et al. (Figure 2).
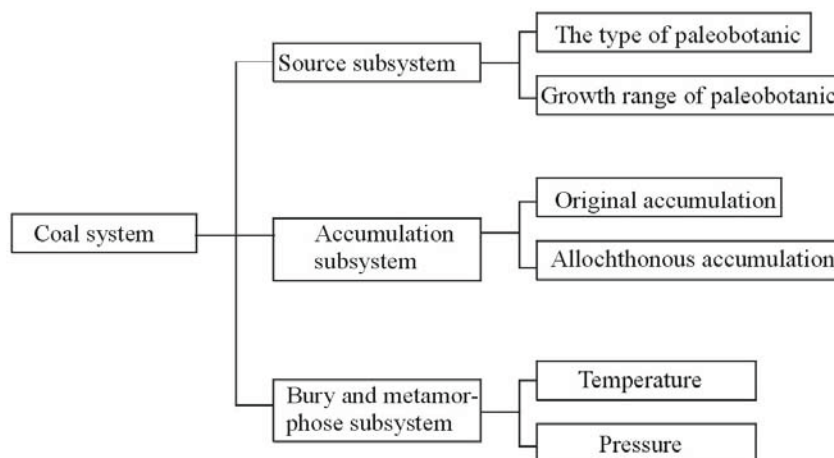
Figure 2. Sketch map showing the coal temporal subsystem (FromZhao et al., modified, 2002).

Each contains a coalbed and its bottom and top rock and coal measures. The forming of coal measures and it contains coalbed and its bottom and top rock result from the sea (lake) level periodically changed (cycle of lithosphere). So a suit of coal measures may be considered as a coal subsystem. Some similar subsystems like it can form a higher system. In general, all coalbed and coal measures formed in an integrated period may be considered as an integrated coal system in a basin. Also it is the highest coal system. Downwards, it is divided into some coal subsystems. These coal subsystems together include its own coalbed, coalbed bottom and top rock and coal measures (Fig.3).
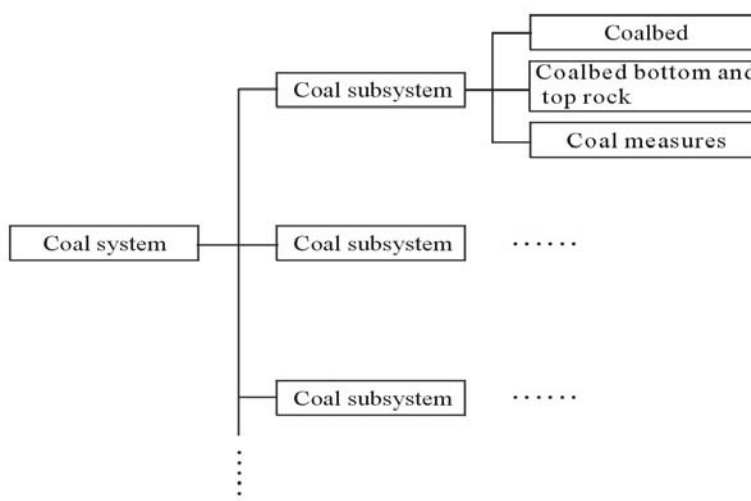
Figure 3. Sketch map showing the coal dimensional subsystem (From Zhao et al., modified, 2002).

2.4. The study content and methods

Coal system studies include factors, coal-forming actions and subsystems analysis. And the appendix studies include coalbed methane and hazardous minor and trace elements, etc. In general, the content of coal system studies include:

1. The study on coal property: micro-element, ash content of coal (sulfur dioxide, quartz, carbonate rock, clay mineral and major abio-component that identify coal type);
2. The study on coal facies (coal/peat lithology facies variety in both vertical and transverse);
3. The study on peat forming environment and sedimentary action of clastic material;
4. The study on clastic deposit among coalbeds;
5. The study on coal measures sedimentary environment and model;
6. The study on characteristics of paleobotanic;
7. The study on characteristics of coal basin tectonic movement;
8. The study on characteristics of coal basin thermal evolution.

The in formation needed for a coal system may is in Table 2.

Table 2. The study content of a coal system

Chart and Table	The needed information	Aim
Chart	The accurate location of coalfield in a coal system	Geography range of a coal system;
Table	List the coalfields name, the age and lithology of coal measures	Identified sedimentary rock and sedimentary structure
Transverse profile	Structure and stratum information	Indicate the coal measures; Determine the coal basin tectonic movement
Events chart	The affection of coal system result from lithosphere movement; indicate the coal evolvement and critical time in each phase	Events chart is a map sum up the coal rank, critical moment, the geological epoch and the relationship among them
Contrast between coalbed	Plant evidence, for example, paleobotanic fossil or isotope data evidence come from difference coalbed	Establish geochemistry, plant and isotope relationship; determine the geography and stratum range; identify the various coal system

We consider that each coal system study should include some part of Table 2 content.

When we start a coal system study, the first mission is to confirm it. The foundation of confirming relates to the knowledge of coal chemistry. We consider all coal measures

including given elements combination as a coal system. And considering the complexity of elements (Jenkins, 1978), we only select several elements for determining the coal system. There are many scientists who gather lots of data about the elements in coal (Mackowsky, 1975; Renton, 1982; Goodarzi, 1995), Such as Ag, As, Ba, Be, Cd, Co, Cl, Cu, Cr, F, Hg, Mn, Mo, Ni, Pb, Se, Sb, Th, Tl, U, V and Zn. And in general, we may study various combination of elements to confirm coal system according to different coalfields, such as ICP-AES, INAA et al.

3. AN EXAMPLE FROM FUXIN BASIN TO EXPLAIN A COAL SYSTEM STUDY

Now, we take Fuxin basin as an example to interpret a coal system study primarily.

3.1. Introduction

Fuxin basin is located in the west of Liaoning province in P. R. China. It is an NNE fault-subsidence basin. Fuxin basin is about 80km from north to south, and about 11-22km from west to east. The area of this basin is about 1500km^2. The depth of basin floor exceeds about 3000m. It is in the located on northeast of the Sino-Korea plate in tectonic setting (Figure 4).
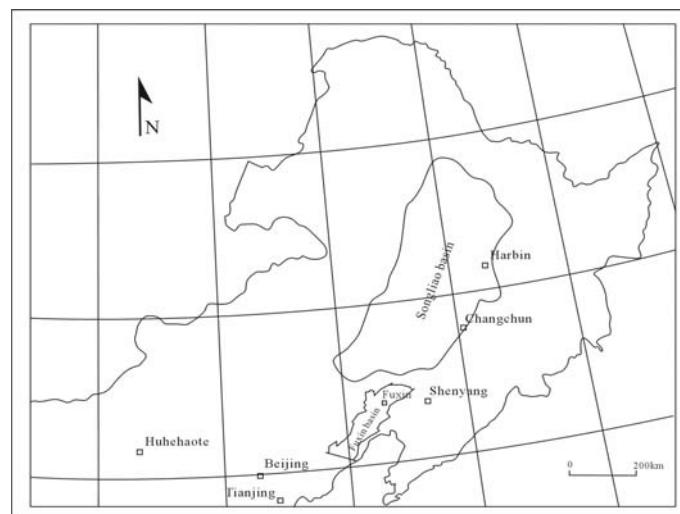
Figure 4. The location of Fuxin Basin (From Li, 1988, modified).

3.2. Geology setting

Fuxin basin floor is composed of metamorphic lava of Great Wall series, it is filled by the late Jurassic—early-middle Cretaceous stratum. From bottom to top, they are Yixian

Formation(J3y), Shahai formation(K1sh), Fuxin formation(K1f) and Sunjiawan formation (K2s). They sediment in the Yanshanian movement period, and are controlled by Yanshanian movement (Table 3).

**Table 3. Stratigraphic division and tectonic evolution of Fuxin basin
(From Gong et al., 1998, modified)**

Stratum			Structure movement		Evolvement	
Group	**Series**	**Formation**				
Mesozoic	Middle-Cretaceous	Sunjiawan	Yanshanian movement	III	**Strike-slip**	
	Down-Cretaceous	Fuxin		II	rift subsidence	Primary Subside
		Shahai				
	Up-Jurassic	Yixian		I		Original Subside

3.3. Coal system study

Because Fuxin basin is a small basin, in the sediment epoch of late Cretaceous, there was a similar depositional environment, uniform stream, analogical source rock sedimentation-organism combination type; Magma hydrothermalism; deep-and-large fault-hydrothermalism; Underground water (Li, 1988). In order to interpret the study of a coal system simply, we assume the coal measure has analogous combination of given elements in the sediment epoch of late Cretaceous of the Fuxin basin. But in a practical study, we need careful geochemistry analysis.

Now, we consider coal and coal measure of Down-Cretaceous sediment in Fuxin basin as an integrated coal system to explain how to conduct a study.

3.3.1. Factors analysis

3.3.1.1. Source

In Figure 6 and Figure10, there is a large area of marsh and swamp in the Fuxin basin. That is the advantageous environment for peat-forming (the coal source). And the alluvial fan, fan delta plain and shallow lake are good for coal-forming paleobotanic growth. In Shahai and Fuxin formations, the mainly paleobotanic are gymnosperm, such as cycad, gingkgo, Coniferae plants (Liu, 1995). They are good peat-forming plants.

3.3.1.2. Paleoenvironment

From ancient times to now, several paleo-environments occurred in the Fuxin basin. There are the half-dry alluvial fan, humid alluvial fan, fan delta and shallow lake, fore fan and inner fan flooded plain, underwater sparry current and turbidite, deep lake and turbidite, fan delta-lake, fore fan flooded billabong, fore fan flooded plain, alluvial fan. And the sedimentary environment of peat accumulation, such as alluvial fan, fan delta, fore fan and inner-fan flooded plain and fore-fan flooded billabong developed in some of these sedimentary environments (Figure 5).
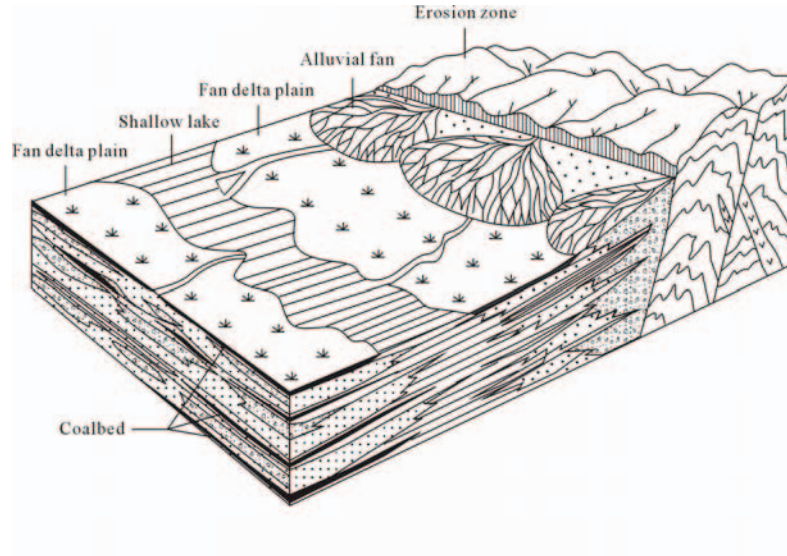
Figure 5. Configuration of the depositional systems and coal-forming model in fan-delta and shore zone in shallow lake margin (From Li, 1988, modified)

3.3.1.3. Thermal stream

In general, we determine the underground thermal state by measuring the Rom% among the coal measures. In the Fuxin basin, we found Rom% mutative gradient is about 0.03%. The relationship between Rom% and deep(D) is linear. And its correlative index $\gamma > 0.9$. Its cause comes from natural geothermic grads. In the Fuxin basin, there are several abnormal metamorphose zones. In these zones, the coalification degree rises markedly. And I think this is owed to magma action (Figure 6).
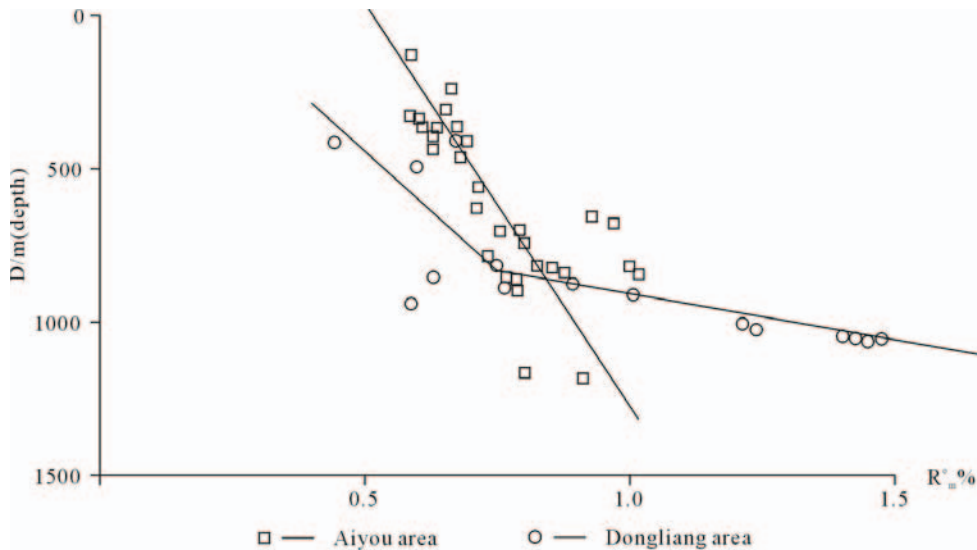
Figure 6. Vitrinite reflectance value showing different trends with the depth (D) in Dongliang-Aiyou area of Fuxin Basin (From Li, 1988, modified)

https://telegram.me/Geologybooks

Figure 6 shows the source of the underground thermal stream of the Fuxin Basin is not single.

3.3.2. Coal-forming action analysis

3.3.2.1. Peat accumulation

In Fuxin basin, peat mostly accumulates in the original paleobotanic growth of location. Figure 7 shows the location of peat accumulation, such as the Delta plain, Alluvial fan, swamp et al. The Fuxin basin is a closed basin. The sediment is limited in the basin. And in the coal petrology study, we don't find the obvious evidence of transit action. But using the microscope, in the coalbed, Liu (1995) found large numbers of half-protonema, clastic desmocollinite and inert material. These show that coal-forming paleobotony reliquiae and peat go through light transit process. And a lot of cracked dispersal cuticle was also identified in this transit. But as a whole, the coal in the Fuxin basin may be considered as output in the original area.

Figure 7. Configuration of depositional systems before the main coalbed of Taishang Member in the Fuxin Basin (From Li, 1988, modified).

3.3.2.2. Structure evolvement

In the Fuxin basin, the structure movement is mainly taken on fault activity. These faults mainly developed in the Yanshanian period. There are 3 series of faults (WE, NE and NNE). These fault activities lead to the lake level rising and descending. It continually forms advantaged environment for plant growth. And because of frequent structure movement, it lead to paleobotanic and peat being buried rapidly (Figure 8).
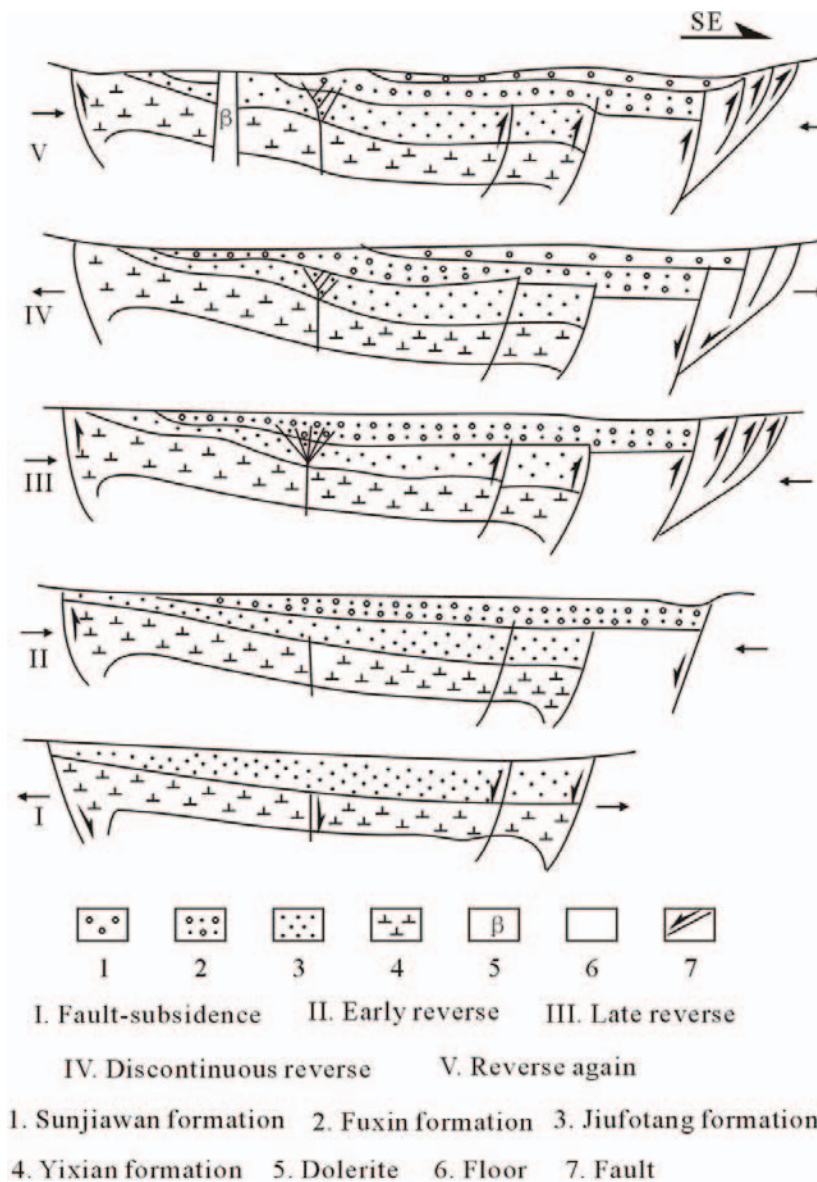
Figure 8. Structure evolvement of the Fuxin basin (From Yun et al., 1995, modified).

3.3.2.3. Metamorphose

The coal metamorphoses result from an underground thermal stream and terrestrial heat (natural geothermic grads). In the northeast of China, there are several basins like Fuxin basin. By analyzing these basins' coalification, Li (1988) considered there are two zones from west to east in this region. In the west zone, most coal is lignite. And in the east zone, the coal is lower and middle metamorphose soft coal. And because of magma activity, several local abnormal zones exist in these two zones. In the Fuxin basin, the coal is mostly lignite. After early-Cretaceous, the magma activity strengthens the coalification degree in some local zones of the Fuxin basin, and leads to the character of the coal changing rapidly, and so brings about some higher coal.

3.3.3. Hierarchy

In the dimensional analysis, each sedimentary act may be considered as a dimensional subsystem. And each sedimentary act results from the water level change or tight structure movement. In each sedimentary act, each factor of dimensional subsystem is contained, such as coalbed, coalbed bottom and top rock and coal measures (Figure 9, 10). In some sedimentary act unit there is no coalbed. But because it has the latent conditions that can form coal, we still consider it as a latent dimensional subsystem.

In the temporal analysis, each paleoenvironment map of sedimentary act can show a temporal subsystem's characteristics, each paleoenvironment map shows temporal subsystem factors, such as paleobotanic, growth range of paleobotanic, location of peat accumulation and the sedimentary time. We can conclude the buried deep, temperature and pressure of each sedimentary act by analyzing the phase of sedimentation.
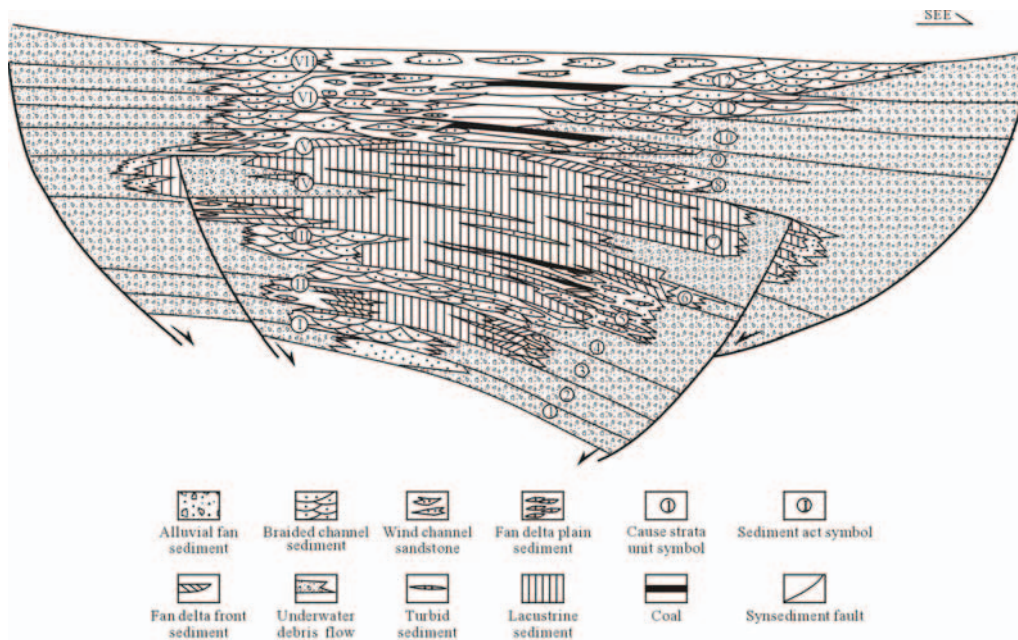
Figure 9. Division of sedimentary act (genetic stratigraphic unit) and dimensional subsystem of profile in the Fuxin basin (From Li, 1988, modified).
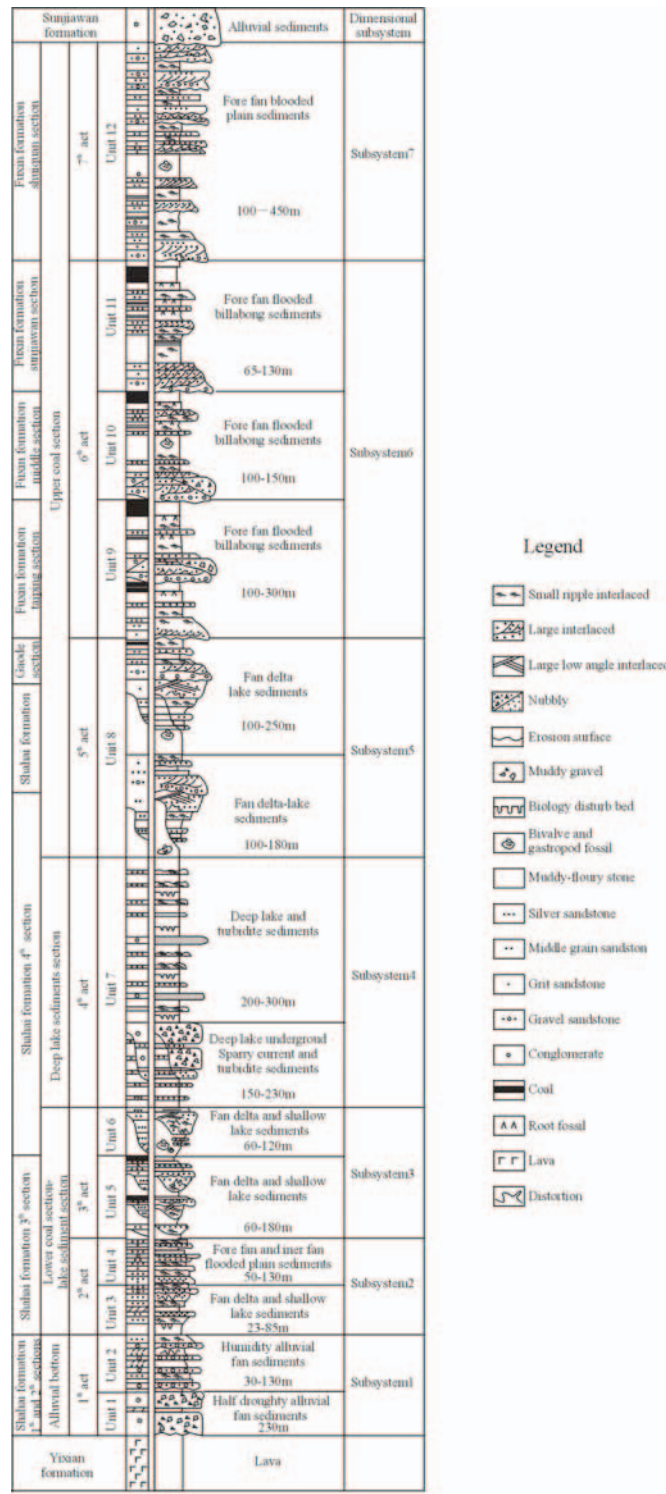
Figure 10. Division of sedimentary act (genetic stratigraphic unit) and dimensional subsystem of depositional succession in the Fuxin basin (From Li, 1988, modified).

4. DISCUSSION

1. The determination of a coal system. In general, the sediment (genetic stratigraphic unit) of a small basin between sediment intervals (in an integrated sedimentary period) can be considered as a coal system approximatively. Because it has an approximate depositional environment, this type of sediment has approximate source, terrestrial heat, paleogeography, accumulation style et al., which will lead to approximate combination of given elements.

2. The study on factors of a coal system can go ahead before determining the coal system. And when studying a coal system, we also can gather all works by former researchers as our materials. The most important thing is that the coal system is an integrated study.

3. Coal-generated hydrocarbon research is an intersection between a coal system and a petroleum system. Its study contents include the former part about a coal system and the tail part about petroleum system. And both coal systems and petroleum systems all belong to an energy system (Figure 11). That is, every geology system is not isolated, it will be contained or contain another.
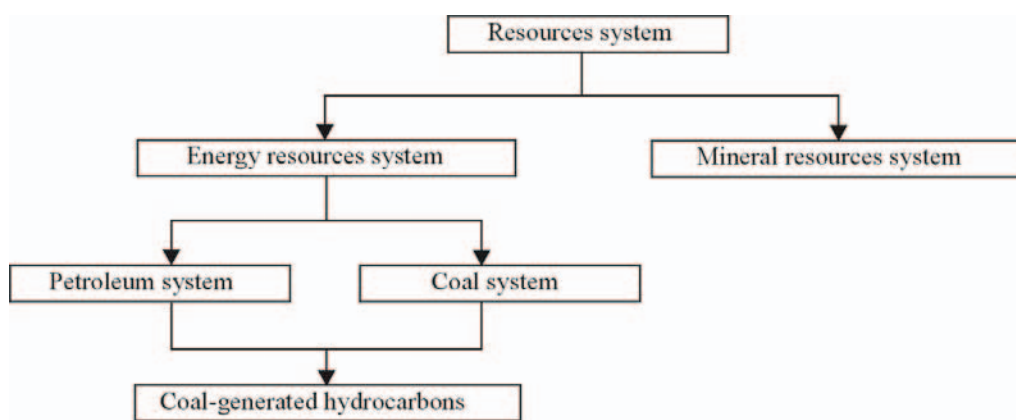
Figure 11. The outline of various geology systems

4. The coal system has not put forward new study content about coal geology, and its aim is to describe a complicated, disordered natural phenomenon and geologic action of the coal forming process accurately and systemically.

5. CONCLUSIONS

A coal system consists of a coalbed, coal measures, depositional facies and all kinds of geologic actions relating to coal forming. Its basic factors are substance sources (paleobotanic and peat), coal-accumulation environment and underground thermal stream. And its geologic actions include: Peat original and allochthonous accumulation; burying action caused by diastrophism and geothermal metamorphism. The rational collocation of these basic factors

and coal-forming actions in temporal and dimensional domain can form the valuable coalbed. A coal system can be divided into substance source subsystem, accumulation subsystem and metamorphism subsystem in temporal domain. In dimensional domain, it may fall into several low class subsystems resembling with a super coal system. And each subsystem has its own factors and study content.

The study content of a coal system includes coal property study; the study on environment of peat forming and its depositional actions; the study on clastic deposit among coalbeds, and the study on coal measures depositional environment and model.

The studies on the Fuxin basin give an example for a coal system. The example is only a primary application about a coal system. In the future, we will continue this study in order to get more useful fruits about coal systems.

The putting forward of a coal system is part of the idea to systematize coal geology study. We hope this paper can attract attention and discussion among those working in geology.

REFERENCE

Brooks, J. D. (1967). The diagenesis of plant lipids during the formation of coal, Petroleum and Natural Gas. Geochim. et Cosmochim. *Acta*, 31, 2389-2397.

Brooks, J. D. (1969). The diagenesis of plant lipids during the formation of coal, Petroleum and Natural Gas. Geochim. et Cosmochim. *Acta*, 33, 1183-1194.

Brooks, J. D. (1970). The use of coals as indicators of the occurrence of oil and gas. *Austral. Petrol. Expor. Ass. J.*, 10, 35-50.

Burchfiel, B. C. et al. (1980). *Continental tectonies. National Academy of Science*, U.S.A.

Cobb, J. C., Cecil, C. B. (1993). *Modern and ancient coal rotating environments*. Geol Soc Spec Pap. 286,1-198.

Cohen, A. D. (1970). An allochthonous peat type from Southern Florida. *Geol. Soc. Am. Bull.*, 81, 2477-2482.

Conybeare, C. E. B. (1979). *Lithostratigraphic analysis of sedimentary basins*. Acadamic Press, Inc., New York, USA.

Demaison, G,. Huizinga, B. J. (1991). *Genetic classification of petroleum system*. AAPG Bulletin. 75(10), 1626-1643.

Diessel, F. K. (1992). *Coal-Bearing Depositional Systems.* Springer-Verlag, Berlin, Germany, 721pp.

Dickinson, W. R. (1994). Basin Geodynamics*. Basin Research*, 5, 195-196.

Dickinson, W. R. (1997). *The Dynamics of Sedimentary Basins*. Washington D.C. USA: National Research Council, 43.

Dow, W. G. (1972). Application of oil correlation and source rock data to exploration in Williston basin(abs.). AAPG Bulletin, v. 56, 615 pp.

Galloway, K. E., Hobday, D. K. (1996).Terrigenous clastic depositional systems, Application to Fossil Fuel and Groundwater Resources. New York, USA: Springer-Verlag, 489.

Goodarzi, F. (1995). *Geology of trace elements in coal*. In: Swaine, D. J., Goodarzi, F., eds. Environmental aspects of trace elements in coal. Dordrecht: Kluwer Academic Publishers, 51-75.

Gong, J., Wen, Z., Dai, C. (1998). Reservoir characteristics and exploratory targets of Fuxin Basin. *Marine Geology and Quaternary geology*. 18 (2), 81-90. (in Chinese with English abstract).

ICCP. (1963). *International Handbook of Coal petrology*. 2nd ed., Centre National la Recherche Scientifique, Paris.

ICCP. (1971). *International Handbook of Coal petrology*. suppl, 2nd ed., Centre National la Recherche Scientifique, Paris.

ICCP. (1976). *International Handbook of Coal petrology*. 2nd . suppl, 2nd ed., Centre National la Recherche Scientifique, Paris.

Jenkins, R. G., Walker, P. L. Jr. (1978). *Analysis of mineral matter in coal*, in "Analytical Methods for Coal and Coal Products" (ed. by C. Karr, Jr.), II, 265-291.

Karweil, J. (1956). Die metamorphse der Kohlen vom Standpunkt der physikalischen Chemie. Deutsh. *Geol. Gesell. Zeitshr*, 107, 132-139.

Liu, B., Jang, J., Liu, J. (1995). A Study of The relationship between the paleobotanic assemblage and the macrolithotype of coal. *Journal of Fuxin Mining Institute* (Natural Science), 14(1), 67-69 (in Chinese with English abstract).

Li, S. (1988). *Fault basin analysis and coal accumulation*. Beijing, China: Geological publishing House. (in Chinese with English abstract).

Li, S. (1999). Basin Analysis and Some New Studies of Coal Geology. *Earth Science Fronties*, 6 (suppl.), 133-138 (in Chinese with English abstract).

Magoon, L., and Dow, W.(1994). *The Petroleum System-From Source to Trap*. AAPG Memoir, Tulsa, Oklahoma, USA: Publicated by AAPG. 60, 3-24.

Moore, P. D., Bellamy, D. J. (1974). *Peatlands*. Elek Science, London, UK.

Mekee, E. D. et al. (1975). *Paleotectonic investigations of the Pennsylvanian System in the United States*. Geological Survey Professional Paper 853, Washington.

Mackowsky, M. T. (1975). *Minerals and elements occurring in coal*, in "Coal Petrology", 121-131.

Potter, P. E., Pettijohn, F. J. (1977). *Paleocurrents and basin Analysis*. Springer-Verlag, New York, USA.

Perrodon, A.(1992). Petroleum systems: models and applications. *Journal of Petroleum Geology*, 15(3), 319-326.

Ralhmani, R. A., Flores, F. R.eds. (1984). Sedimentology of coal and coal-bearing sequences. *Internat Assoc of Sedimentologists Special Paper*, 7, 1-412.

Renton, J. J. (1982). Mineral matter in coal, in "coal structure" (ed. By R. A. Meyers) Academic press, New York, USA, 283-326.

Scott, A, C, ed. (1987). Coal and coal-bearing Strata: recent advances. *Geol Soc Special Publication*, 32, 1-332.

Stach, E., MacKowsky, M. Th., Teichmuller, M., Taylor, G. H., Chandra, D., Teichmuller, R. (1982). *Stach's Textbook of Coal Petrology*.

Stach, E., Mackowsky, M.Th., Teichmuller, M. et al. (1975). *Stach's Textbook of Coal Petrology*. Berlin-Stuttgart: Gebr Borntraeger, 428 pp.

Von Bertalanffy, L. (1984). *General systems theory: foundations, development, applications*. New York, USA: George Braziller.

Wang, H. (1997). *Analyses geologiques du basin houiller stephanien des Cevennes*(France). Edition Jamana, (lann), 254pp.

Wanless, H. R. et al. (1978). Paleoenvironmental maps of Pennsylvanian rocks, Illinois Basin and Nortern Midcontinent Region. *The Geological Society of America*, MC-23.

Yang, Q. (1999). Superimposed metamorphism of Chinese coal. *Earth Science Frontiers*, 6(suppl.), 1-8. (in Chinese with English abstract).

Yun, W., Wang G., Jin, H. (1995). The Reverse Structure Characteristics of Fuxin Basin. China coal geology., 7(3), 7-11 (in Chinese with English abstract).

Zhao, Z., Wang, H., Gan, H., Han, J. (2002). Coal system. *Coal geology and exploration*, 30(2), 12-15 (in Chinese with English abstract).

Chapter 11

ENERGY SOURCES AND COAL RESERVES IN THE CZECH REPUBLIC AT THE BEGINNING OF THE 21ST CENTURY

Jiří Pešek[1]

Charles University, Prague, Faculty of Science,
Albertov 6, 128 43 Praha 2, Czech Republic,

ABSTRACT

Decision of the Czech Government about the increase in proportion of energy production from nuclear sources is the only possible solution in the long-term perspective. In 2005, about 65 % of the electric energy was based on burning coal, mostly lignite, which is actually the worst alternative for the use of this raw material in the new millennium. It is also to be borne in mind that Czech reserves of coal will be exhausted by about 2040, at the latest. Moreover, we burn raw material which even nowadays serves for the manufacture of plastics, pharmaceutical products and other chemicals. Although all large power plants burning coal are desulphurized, they still exhale a number of toxic elements such as As, Be, F, Se and heavy metals. The idea that a part of the electric energy may be generated from alternative sources is correct, but its advocates are usually silent about the very high price of this energy. Currently, only about 3.5 % of electricity is generated from these sources.

INTRODUCTION

The huge increase in electricity production after 1948 obviously resulted in higher extraction of coal reserves, particularly those of lignite. About 65 % of electric energy in our

---

[1] e-mail: ir@natur.cuni.cz

country is still being generated from lignite (Fig. 1). As a matter of fact, this is a certain progress since it was more than 90 % in early 1960s.
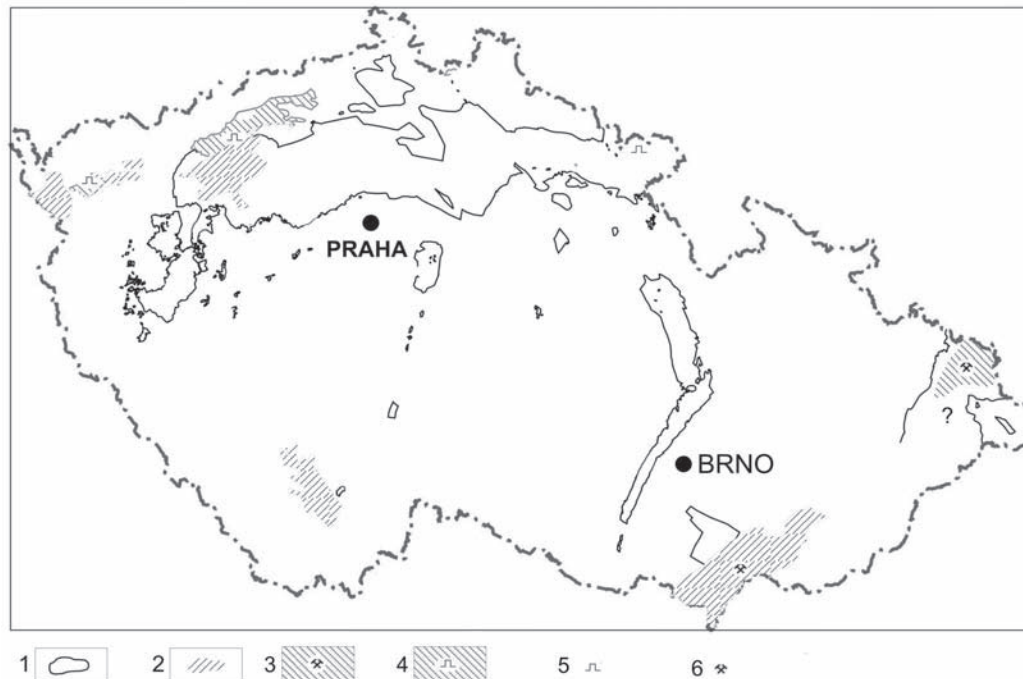
Figure 1. Distribution of bituminous coal and lignite deposits in the Czech Republic:

1 – outline of the Permo-Carboniferous bituminous coal basins, 2 – outline of the Tertiary lignite deposits without or with unimportant mining activity, 3 – coalfield with several active bituminous deep coal mines, 4 – coalfield with several active lignite open-cast mines, 5 – active but local open-cast bituminous coal mine, 6 – active but local deep lignite mine.

Our lignite reserves are limited and estimated to be exhausted within the next 35 years at the latest, according to the raw material policy adopted in January 2004 by the Czech Government. Moreover, combustion of lignite reduces the reserves of the present and particularly of future chemical raw material. Besides that, regardless of desulphuration of all large power plants, we still exhale As, Be, F, Se, heavy metals and other harmful substances into the atmosphere, which have negative impact on the environment. Consequently, it is apparent that gradual replacement of electricity generation from coal by other sources becomes a hot issue.

ELECTRIC ENERGY SOURCES

Sources of electric energy used by the human population to meet their needs, such as heat, light, propelling of engines and devices, transportation and so on, can be distinguished into conventional and un-conventional sources. Their understanding varies in different

countries and at different latitudes. Both categories include renewable and non-renewable sources.

Considering the geographic position of the Czech Republic and its climatic conditions, the conventional non-renewable energy sources include especially coal, oil, natural gas and radioactive minerals. Conventional renewable sources are exemplified by water energy. The sources are understood somewhat differently abroad. Sets of masts with rotating propellers can be seen in Denmark, some parts of California and southern Spain. In these countries, wind energy is considered a conventional and renewable source, much like in Australian bush. Similarly, solar collectors used for heating greenhouses and water for households or swimming pools in California, Australia, Israel and some European countries in the Mediterranean produce energy, which can be also considered conventional and renewable. In the Czech Republic with its long winter nights and overcast sky, only few hours or sunny days would be at disposal for its full use. Therefore, wind and solar energy are still perceived here as unconventional, though renewable, energy sources. Some other energy sources in this category are biomass (straw, hay, waste wood), communal waste, waste heat, landfill material, movement of marine water, geothermal heat and synthesis of nitrogen or deuterium and tritium. In the Czech Republic, we should reject local sources such as communal waste, waste heat or landfill material, much like energy produced by the sea or sources of far future – nitrogen, deuterium and tritium.

ENERGY POTENTIAL OF THE CZECH REPUBLIC

The following sources should be considered for the Czech Republic:

a. **non-renewable sources** – the Czech Republic now covers all demand for bituminous coal and lignite more or less from its own sources. Despite intensive post-WW II exploitation of radioactive minerals, we still have resources of these materials, while the production of oil and natural gas represents less than 5 or 2 %, respectively, of the annual consumption of the country. The principal source for the generation of electric energy in the Czech Republic was, and still is, lignite. Still in 2005 lignite burned in thermal power plants generated almost 65 % of electric energy. The biggest advantage of thermal power plants is their ability to achieve the desired capacity within one hour following, e.g., a year-long period of idleness. Desulphurization units of the flue gases type with a 90-95% efficacy were installed in all our major thermal power plants by the end of 1998; fluid combustion is tested or operated in three power plants. As a result, SO_2 emissions in the Czech territory dropped by 40 % compared to the 1970s. It should be also considered that our thermal power plants (Figure 2) find more or less effective use for about 30-40 % of the materials burned, producing CO_2, NO_x, ash, slag and the so-called energy gypsum.
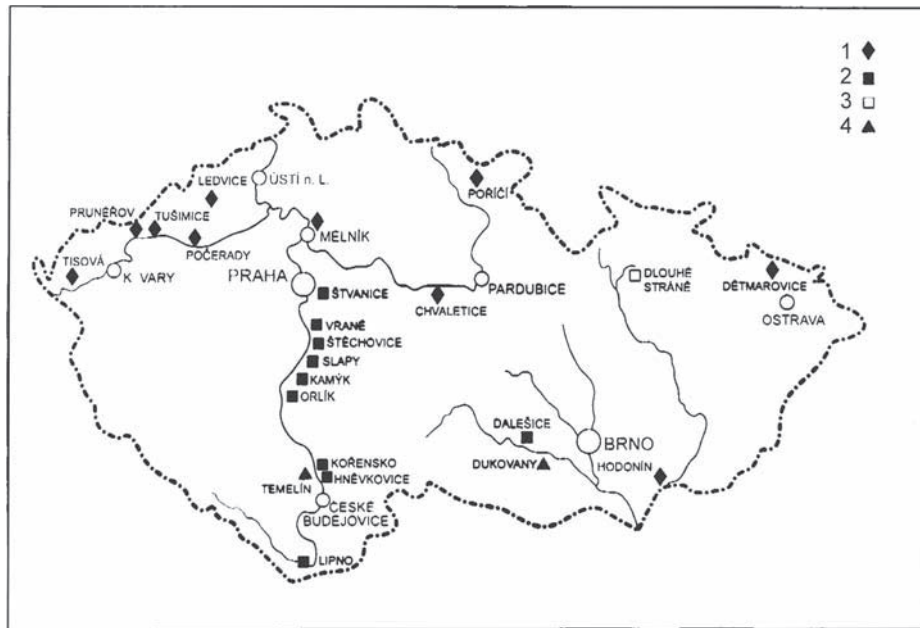
Figure 2. Distribution of major power plants throughout the Czech Republic:
1 – active steem power plant, 2 – active hydroelectric power plant, 3 – hydroelectric power plant under
    construction, 4 – active nuclear power plant.

The second most important energy source of the present is nuclear energy. In 2005
it constituted 31 % of electric energy production in the Czech Republic. This
means that electric energy produced exclusively from nuclear fuel was supplied to
the energy system approximately one and a half working days in a week.

b. **renewable sources** – growing importance of renewable sources in the future follows
from the resolution of the European Union recommending its Member States to
achieve an 8 % proportion of alternative sources in electricity production by 2005. In
the Czech Republic, some 3.5 % of electric energy production is provided from
alternative sources. The Czech government, in its approved document on Energy
Management Policy of 2004, presupposes an increase in the proportion of renewable
sources in the total electric energy consumption by 5–6 % in 2006 and by 8 % in
2010.

According to the calculations of the Czech Energy Agency, an increase to 6 % would
imply 242 billion CZK (1 USD ~ CZK 19).

The plausible alternative sources in the Czech Republic include primarily the production
of electic energy by river water, wind, possibly also solar collectors and maybe even
geothermal energy. The development of these sources is, however, connected with multiple
problems. Yet at the end of WW II, some 11,700 small hydroelectic power plants were in
operation in the former Czechoslovakia. As of January 1, 1999, approximately 1960 turbines
were installed in the Czech Republic. Even after the construction of the "Vltava River
Cascade", hydroelectic power plants provided 2.2 % of our electric energy consumption in
2005. Their output cannot be increased considerably, although their installed (i.e.,

theoretically possible) energy output would allow an almost 14 % share in the electric energy production.
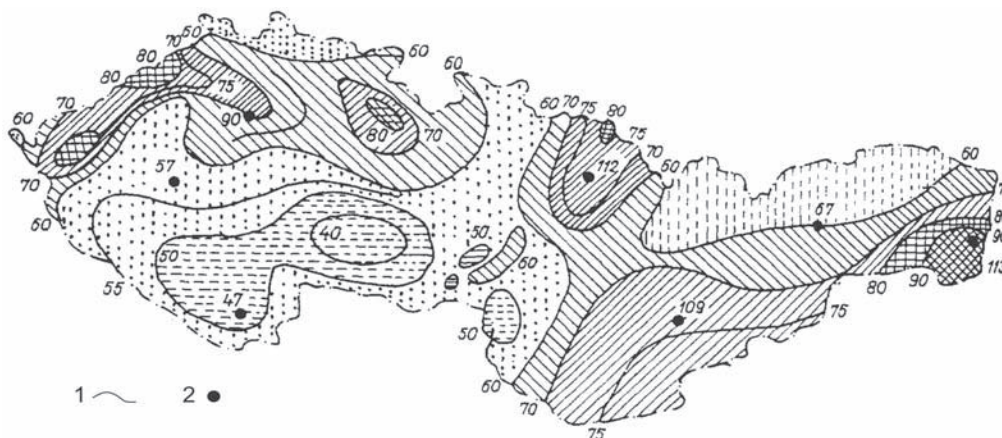
Figure 3. Heat flow of geothermal energy in the territory of the former Czechoslovakia, modified from Balák (1989)
1 – isoline of mVm^{-2}, 2 – borehole.

As concerns wind energy, wind turbines are, however, more appropriate as local sources. In the Czech Republic, they have been installed especially in the Krušné hory Mts. and Jeseníky Mts. Although the wind energy potential is low on most of our territory, effective annual production of some 1.5.109 kWh is estimated, of which about 0.1.109 kWh a year are currently used. A not negligible problem related to wider use of wind turbines is their relatively high price and production cost (Table 1) and about 10% efficiency in our conditions.

Table 1. Specific costs of the production of electric energy depending on the type of electricity power plant. Based on the data in Roubíček & Buchtele (2002)

Type of electric power plant	CZK.kWh^{-1}
Temelín nuclear power plant	1.984
Combined-cycle gas block	1.974
Lignite block	2.054
Bituminous coal block	2.518
Internal combustion turbine for natural gas	6.967
Biomass combustion	5.482
Hydroelectric power plant with 10 MW capacity	3.486
Wind power plant	8.542

The high financial demands are also associated with any larger-scale development and operation of solar devices. It is known that financial problems led to the closure of the giant solar complex in Almaria (U.S.A.), where insolation allows almost 100 % effectivness at

daytime. In Australia, having a sufficient number of sunny days, solar energy is used only for heating home swimming pools or greenhouses. In the Czech Republic, solar energy can be used only as a local source for heating water. Even under such circumstances, however, solar energy would generally provide full coverage of energy consumption only from April to October due to the limited duration of sunshine. In the rest of the year, other sources must be used.

Geothermal energy cannot be viewed as a imporant energy source on the Variscan-consolidated Bohemian Massif. Only some areas in NW and NE Bohemia could be considered.

The use of biomass in the Czech Republic is rather a pipe dream. The problem lies not only in the fact that the small area of the Czech Republic is not suitable for its mass production, but also in the release of harmfull toxic elements and heavy metals into the atmosphere during its combustion, much like during the combustion of fossil fuels.

HISTORY OF COAL MINING IN THE FORMER CZECHOSLOVAKIA AND THE CZECH REPUBLIC AS A RESULT OF ELECTRIC ENERGY PRODUCTION

The unprecedented increase in electric energy production in the former Czechoslovakia since the 1940s was necessarily reflected in coal mining, hence also the relatively rapid – and not always economic – exploitation of its resources. It should be noted that the former Czechoslovakia produced over 90 % of electric power from the combustion of lignite in the early 1960s. This figure dropped to almost 65 % in 2005. The electric energy production in Czechoslovakia of 4.1.109 kWh in 1937 more than doubled by 1950, and was increasing by 6 to 14.109 kWh in each of the consecutive five-year periods. So, 89.109 kWh electric energy were produced in 1989. Between 1992 and 1994 in the Czech Republic (after the Slovak Republic separation) a minor decrease in electric energy output occurred. Its production was 83 .109 kWh in 2004 (Figure 4).

The increase in the electric energy production was definitely followed by an increase in the coal production. Lignite production in 1985 was approx. 5.5 times higher compared to that in 1937; an increase by 370 % was marked in years 1950-1985. It was only in the late 1980s that the activation of nuclear power plants permitted a decrease in the volumes of extracted coal (Dopita & Pešek 1995). The production of bituminous coal increased by some 80 % in 1950-1970 compared to 1937. As the Czech Republic contributed to the world exploitable coal reserves by less than 0.5 %, the extensive coal exploitation also brought about a relatively rapid exhaustion of the Czech coal reserves.

The consumption of coal in the former Czechoslovakia was clearly disproportionately high, which resulted in unnecessary overexploitation of deposits including all consequences. With lignite annual production of around 30 mill. tons in the North Bohemian Lignite Basin, some balance with nature was still persisting in this region. After its increase to almost 75 mill. tons in 1984 and over 20 mill. tons in the Sokolov Basin, emissions of SO2 and NOx into the atmosphere increased due to lignite combustion. Also, severe ecological damage and health problems in the population appeared.
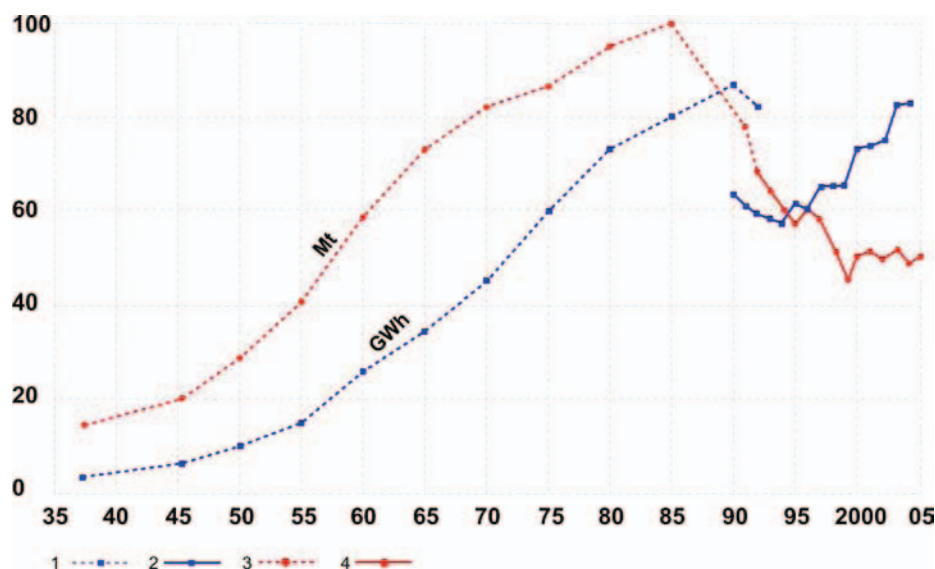
Figure 4. Amount of extracted lignite in Mt and electric energy in GWh generated in the former Czechoslovakia and in the Czech Republic in years 1937-2004 and 1990-2005, respectively

1 – amount of generated electric energy in the former Czechoslovakia, 2 – as above, in the Czech
    Republic, 3 – amount of extracted lignite in the former Czechoslovakia, 4 – as above, in the Czech
    Republic.

Economic development after 1989 accelerated the drop in the demand for bituminous coal and lignite. This was reflected by a decrease in coal production down to the economic and operation limits of some mining companies, but also by closures of mines. Naturally, the state government as well as the local self-administrative bodies were, and still are, striving for reduction of negative effects on the environment related to mining and use of solid fuels. The lignite production was decreasing from 1984, when it reached a maximum of ca. 100 mill. tons, to 45–49 mill. tons in 1999–2005.

In the W part of the North Bohemian Lignite Basin, the lowermost part of the Main Seam with high sulphur contents was abandoned. Extraction of the Josef Seam in the Sokolov Basin was stopped in 1995 due to its high concentrations of sulphur and arsenic. All this is reflected in the present situation of our coal mining, hence also in seeking ways towards modifying its present unfavourable situation as fast and as effective as possible. Besides economic, technical and technological problems, also serious problems in the social area implying political problems should be tackled. The decrease in the demand for coal in the Czech Republic relates not only to the above mentioned reasons but also to the restructuring of our economy, with gradual reduction of metallurgical production and orientation of industry to less energy-demanding productions. It has to be emphasized, however, that the drop in industrial production in the Czech Republic and the former Czechoslovakia has not resulted in a proportional decrease in its energy demands yet. Even now, the energy demands of our production are about 2.3 times higher than those in the EU Member States.

LIFE SPAN OF COAL RESERVES IN THE CZECH REPUBLIC

The life span of coal reserves in the Czech Republic is the key problem to be taken into account in the formulation of our energy management policy. As of January 1, 2006, the measured and inferred reserves of lignite amounted to $5.6.10^9$ tons but extractable reserves amounted to $1.5.10^9$ tons at the currently extracted deposits. In 2004, the Czech Government presumed exhaustion of all available lignite reserves in 2040. Additional $2.2.10^9$ tons of extractable reserves are represented by deposits suggested for exploitation but mostly by deposits in reserve base with unsettled conflicts of interests, and other deposits. If the expected decrease in production is taken into account, e.g. to 40 mill. tons/year, all these reserves would extend the lifetime of their exploitation by approx. 52 years, i.e., almost until 2090.

It is generally estimated that more than 60 % of electric energy in the Czech Republic will be still produced from coal in 2008. According to Synek (1997), this proportion will drop to 30 % by 2030. This estimate, if correct, raises the question as to whether the two new nuclear power plant blocks will be sufficient to meet our energy needs in the first half of this century. It also calls for a re-evaluation of the land-use and ecological limits set out by the Czech Government in 1991 to provide coal to be mined after 2040 (these limits were, however, confirmed by the Energy Management Policy of the Czech Republic approved in January 2004), or for an elaboration of a long-term multi-variant plan indicating what sources will be used to meet our energy needs in the coming decades.

Important is the fact that a thermal power plant produces about 1 mill. tons of slag and ash every year; in contrast, a nuclear power plant of the same capacity produces only 35 tons of burnt fuel. It should be also noted that the lifetime of several thermal power plants of 4000 MWe in total capacity will expire in around 2010, and that the construction of each of the Czech nuclear power plants lasted almost two decades. Analogically, opening of a new mine and its putting into full-capacity operation takes at least 10 years. Should we consider import of coal or electric energy, we would have problems paying for it: in 2003, imports of oil, gas and nuclear fuel at a cost of 70-80 billion CZK contributed by no less than 9 % to the overall negative balance of our foreign trade (State energy policy 2004). In 2000, we paid about 90 billion CZK for all imported minerals (Dvořák & Nouza 2002). Moreover, lignite imports from the neighbouring countries – surely not at low cost – will imply import of 20 % of spoil or more, which will later turn into ash.

NUCLEAR ENERGY MANAGEMENT IN THE CZECH REPUBLIC

Two nuclear power plants (Dukovany and Temelín) operate in the Czech Republic. Our opponents to nuclear energy most often use arguments, which are not totally false but are often taken out of context. This was surely contributed by the accident of the nuclear reactor at Tchernobyl, which supported the general aversion for nuclear power plants. In contrast to the Tchernobyl power plant, pressurized-water reactors were installed in our relatively new nuclear power plant at Temelín. Obviously, the most economic policy would be imports from other countries with a surplus of electric energy at present, but to do this, the Czech Republic would have to find itself in a completely different economic position. Some neighbouring

countries, particularly their mass media and occasionally even individual governmental representatives, were arguing against the completion of the Temelín power plant and its putting into operation. They argumented, among others, by increased radiation levels and ecological impacts on the population of the region, and also by the hitherto untested combination of western and eastern (Westinghouse and Russian) technologies. Long-run measurements in the neighbourhood of the older Dukovany nuclear power plant, however, indicated no increase in natural radioactivity. The arguments about increased incidence of leukaemia in the area turned out to be false. The nuclear power plants, when operated safely, affect the health of the population to a much lesser degree than thermal power plants. The long-lasting activity against the opening of the Temelín nuclear power plant makes me convinced that some of the most important factors in this issue are purely commercial and political interests.

The Temelín nuclear power plant will undoubtedly produce energy at costs comparable or even cheaper to those of our lignite-burning thermal power plants. The produced energy will be competitive on the European market, too, even though its production at Temelín also includes the costs for the removal of the nuclear facility and the radioactive waste disposal, according to the "Atomic Act" of 1994.

One of the arguments against the use of nuclear energy is the problem of the disposal of nuclear fuel, now generally stored in the so-called provisional depots. The technology of storage as well as the potential sites of repositories are known from all countries involved including the Czech Republic and follow very strict regulations. It is known that the sites must be free of fractures, if possible, in an acid rock environment, better resisting the waethering process in the topmost layers of the Earth crust.

Radioactive waste will be kept in hermetic containers made of special steel. Parameters of the containers are governed by law in the Czech Republic, which is in line with the EU standards. In addition, the containers will be lined with bentonite to the thickness of approx. 1 m, to be isolated from air. The present solution of the end of the fuel cycle, adopted in the Czech Republic in 1995, presupposes a final deposition of fuel in a deep-seated repository within 50 years after its provisional storage. It can be expected that the technology of further processing of spent fuel will have been solved by that time, including the restart of the fission reaction, reducing the radiation considerably. The deep-seated repositories should thus accommodate only a negligible part of the fuel now kept in provisional storage. In the Czech Republic, the government gained the possession of all operated radioactive waste repositories on January 1, 2000.

CONCLUSIONS

Reserves of the Czech Republic fossil fuels are markedly limited. The year 2040 will bring (on condition that the land-use and ecological limits in the coal basins in the Krušné hory piedmont area will be observed by the governments to come) an exhaustion of the most important lignite reserves in the country. Alternative sources, such as wind, sun or water, cannot cover – at the given conditions – the most part of our energy consumption, but may contribute to the improvement of the environment. In the Czech Republic, the increase in energy consumption could get partly eliminated by the reduction of energy demands in

industry. This submitted reflection implies the following possible solutions: 1) lifting the land-use and ecological limits accepted by the Czech Government in 1991, or 2) development of our own nuclear energy facilities, or 3) anticipation of the dependence of the Czech Republic on electric energy imports from abroad, or import of coal for our thermal power plants.

REFERENCES

Balák, R. (1989). *Nové zdroje energie*: Polytechnická knižnice SNTL, Praha, CR, pp.1-205 (in Czech).

Dvořák, A., and Nouza, R. (2002).*Ekonomika přírodních zdrojů a surovinová politika*: Vysoká škola ekonomická, Praha, CR, pp. 1-166 (in Czech).

Roubíček, V., Buchtele, J. (2002).*Uhlí, zdroje, procesy, využití:* Montanex, Ostrava, CR, pp. 1-173 (in Czech).

Dopita, M., Pešek, J. (1995). *Uhlí-Rudy-Geol. Průzk.* 201-207 (in Czech).

Synek, E. (1995). *Uhlí-Rudy-Geol. Průzk.* 323-332 (in Czech).

Sine.(2004). *Státní energetická koncepce České republiky*. MS Ministry of trade and industry. Praha, CR (in Czech).

Reviewed by RNDr. Vladimír Prouza, PhD.

Chapter 12

THE APPLICATION OF C7 LIGHT HYDROCARBONS TECHNIQUE TO OIL AND CONDENSATE FROM TYPE III ORGANIC MATTER

Ching-Tse Chang, Li-Hua Lin , and Cheng-Lung Kuo

Exploration and Development Research Institute
CPC Corporation, Taiwan

INTRODUCTION

The chapter describes the C_7 light hydrocarbons technique to oil and condensate from Type III organic matter in Northwestern Taiwan, and discusses the potential of C_7 light hydrocarbons as markers for petroleum exploration. Their bulk geochemical features include the whole oil $\delta^{13}C‰$ values, Pristane/ Phytane ratio and C_7 compounds parameters. With relatively limited coverage of oil samples, this detailed C_7 compounds geochemical study on a large set of condensate and oil samples collected from major fields across the basin has provided significant insights into the biodegradation evaporative fractionation maturation depositional environment and oil system in petroleum generation in northwestern Taiwan.

Geology and Geochemical characteristics
Geology
Geochemical characteristics

Methodology
Sampling and analytic method
Calculation

Application
Toluene/n-Heptane vs. n-Heptane/ Methylcyclohexane and the Evaporative Fractionation of condensate-oil.

2-MH+2,3-DMP vs. 3-MH+2,4-DMP and the petroleum system

Heptane value and Iso-heptane value and maturation of crude oil.

3-Phase diagram of parent (P1), mono-branch (P2) and poly-branch (P3) of heptane isomers and the biodegraded degree of condensate-oil

Triangular relationship diagram of branch (3RP), 5-membered-ring (5RP) and 6-membered-ring (6RP) heptane isomers and the depositional environment of oil.

N2/P3 vs. P2 and P2+N2 vs. P3 to identify the relationship of depositional environment.

GEOLOGY AND GEOCHEMICAL CHARACTERISTICS

Geology

Northwestern Taiwan is the major petroleum province in Taiwan and is believed to contain several trillion cubic feet of gases in place as well as substantial amounts of oil and condensates. The sedimentary basins in the onshore and offshore western Taiwan developed on the passive continental margin in the eastern Asia from the Late Cretaceous to Tertiary. The basins include several fault-bound basins that are separated by rift horsts. The oil and condensate major productions are concentrated in the foothill belt in the onshore Hsinchu–Miaoli region (Fig.1), which is characterized by anticlinal structures parallel to the Central Taiwan Mountain Ranges and striking in a NE-SW direction. The oil reservoirs in the sedimentary basins in the northwestern Taiwan are mainly deltaic-littoral—neritic sandstones in the Upper Oligocene to Upper Miocene strata, but the production has been dominantly from the quartzose sandstones in the Early Miocene Formation. The reservoirs range in depth from 300 to over 5000 meters in the fields. As most of the oils and condensates are produced from the Late Oligocene-Middle Miocene sandstones. The potential source rocks in the available sample collection contain dominantly gas-prone, type III organic matter. Gasoline range hydrocarbons the C_7 compounds, have been widely utilized in petroleum geochemistry studies for determining oil groups derived from the same source rock, prediction of maturity, alteration of the crude oils due to water washing, bio- degradation or evaporative fractionation, Since condensates or light oils have very low concentrations of the C_{15+} fraction and, therefore, biological markers, correlation to source rocks can be problematic. In these cases utilization of light hydrocarbons from source rocks has been useful for correlating source rocks to and condensates to black oils. and the origin of light hydrocarbon in the same oil system and the thermal maturity applicable The oils analyzed in this study are found in terrigeous reservoirs ranging in the age from Pliocene to Oligocene in the onshore Hsinchu to Miaoli region from North- western Taiwan.
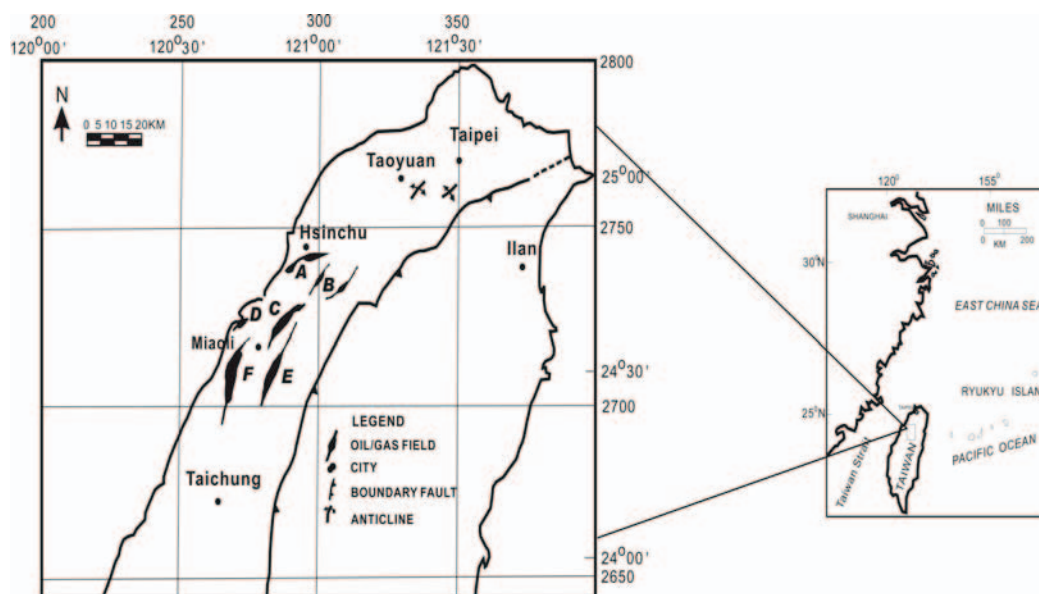
Figure 1. Map of Northwestern Taiwan, showing the location of A, B, C, D, E, F, oil samples.

Geochemical characteristics

The oil and condensate reservoirs of the sedimentary basins in northwestern Taiwan generally are in the deltaic–littoral–neritic sandstones of Upper Oligocene to Upper Miocene strata. Oils and condensates produced from these basins are terrigenous, with a variable $\delta^{13}C‰$ ratio from −30.07 to −27.50‰/PDB, and Pristane / Phytane ratio from 4.79 to 9.22. A large set of condensate and oil samples were collected from major gas fields across the Hsinchu–Miaoli basin, and the Kovat's Index was used to identify C_7 light hydrocarbons in the samples(Fig.2).The isomeric parameters of C_7 included single-branched and multiple-branched heptanes and isomeric pairs, such as nC_7/Methylcyclohexane ratio vs. Toluene/nC_7 ratio, 2-MH+2, 3-DMP vs. 3-MH+2, 4-DMP, n-Heptane ratio vs. iso-Heptane ratio. The ratios for parent (P1), mono-branch (P2) and poly branch (P3) heptane isomers ranged from 37 to 64%, 29 to 45% and 6 to 19%, respectively. The ratios for nC_7/Methylcyclohexane and Toluene/nC_7 ranged from 0.16 to 0.60 and1.52 to 10.58, respectively. The n-Heptane value and iso-Heptane value ranged from 10 to 26 and 0.8 to 1.8 respectively and the iso-alkanes (3RP), cyclopentanes (5RP), cyclohexanes (6RP) ratios ranged from 6 to 29%, 5 to 13% and 53 to 90%, respectively with the 2-MH+2,3-DMP vs. 3-MH+2,4-DMP found to be constant for the linear equation Y=1.1458X−0.0755. The use of this technique as a qualitative tool shows that all the oils from the northwestern Taiwan were mature, free of biodegradation, affected by evaporative fractionation and derived from the same petroleum system. The source rock of the oils should be terrigenous.
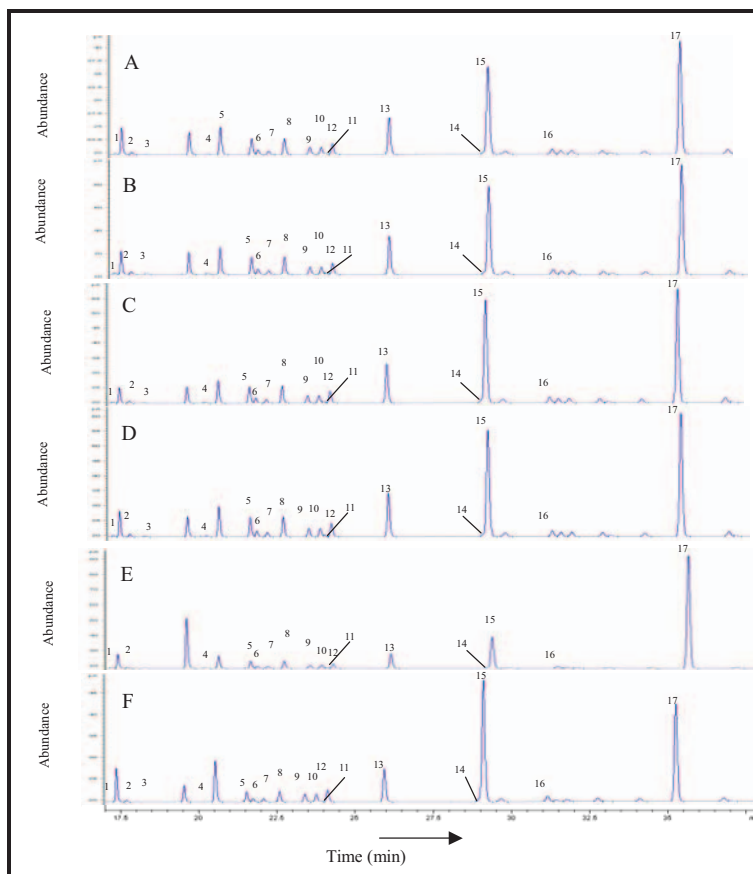
Figure 2. Partial crude oil range gas chromatogram of A, B, C, D, E, F, oil samples and assignment of peaks:
1=2,2-Dimethylpentane(2,2-DMP); 2=2,4-Dimethylpentane(2,4-DMP);
3=2,2,3-Trimethylbutane(2,2,3-TMB); 4=3,3-Dimethylpentane(3,3-DMP);
5=2-Methylhexane(2-MH);6=2,3-Dimethylpentane(2,3-DMP);
7=1,1-Dimethylcyclopentane(1,1-DMCP);8=3-Methylhexane(3-MH);
9=cis-1,3-Dimethylcyclopentane(c1,3-DMCP);
10=trans-1,3-Dimethylcyclopentane(t1,3-DMCP); 11=3-Ethylpentane(3-EP);
12=trans-1,2-Dimethylcyclopentane(t1,2-DMCP); 13=n-Heptane(nC7);
14=cis-1,2-Dimethylcyclopentane(c1,2-DMCP);15=Methylcyclohexane(MCH);
16=Ethylcyclopentane (ECP); 17= Toluene (TOL).

METHODOLOGY

Sampling and analytic method

Oils and condensates were carefully collected at the head of wells in northwestern Taiwan （Figure 3）, at ambient pressure conditions and stored in 5.0 ml glass containers, with a screw-on Teflon lined cap. The samples were collected at temperatures between $20\text{-}35^0$ C, but were immediately refrigerated to below $-6\ ^\circ$C (Figure 4).

The Hewlett-Packard 6890N gas chromatograph was used to analyze the oil samples. The gas chromatograph (GC) was equipped with an auto sampler for injections, a flame ionization detector (FID), and electronic pressure flow controllers to ensure constant flow throughout the oven-heating program. The GC was operated using the following analytical materials and conditions: HP-1 column (100m×250μm I.D.×0.5μm film thickness), injector temperature of 250 $^{\circ}$C, pressure 283KPa, split ratio set to 100:1, and FID temperature of 300 $^{\circ}$C. The GC oven was programmed from 35 $^{\circ}$C with a 13 min initial isotherm, then an initial heating rate program of 10 $^{\circ}$C /min to 45 $^{\circ}$C with a 15 min hold time after which the rate was decreased to 1 $^{\circ}$C /min to a temperature of 60 $^{\circ}$C with a 15 min hold time. The rate was then set to 1.9 $^{\circ}$C /min to a final temperature of 200 $^{\circ}$C with 5 min hold time. Helium carrier gas was used with a minimum purity of 99.999%, and additional filters were used to remove any residual water, oxygen, and hydrocarbons. The injected sample volume was 0.5u1. The crude oil was back flushed after an inject 0.3 min, to remove the heavy component. The assignment of the C_7 compounds was based on comparison to the chromatogram reference provided by the supplier of a commercial mixture of paraffins, naphthenes and aromatic hydrocarbons (AC Gravimetric PIONA Standard).
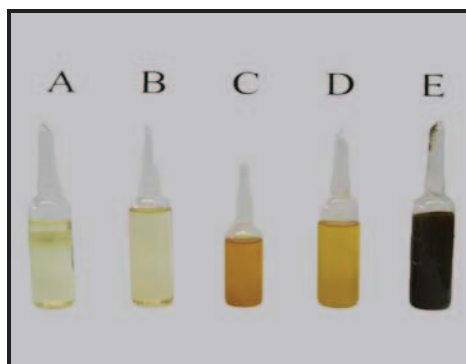
Figure 3. The oil and condensate samples from Taiwan oil fields. （Photo by Dragon Lee）

Figure 4.The samples were collected at temperatures between 20-35^{0}C, and were refrigerated to below –6 $^{\circ}$C. （Photo by Dragon Lee.）

https://telegram.me/Geologybooks

Calculation

The calculation of the percentage of each compound, $\%E_x$ was made, using the following equation
Where:

$$\%E_x = 100 \; \frac{\%\,Wx - \%\,Wxi}{\%\,Wx} \qquad \text{【Eqn 1】}$$

$\%$Wx=wt.$\%$ of the compound X obtained from the initial chromatogram.

$\%$Wxi=wt.$\%$ of the compound X obtained from the initial chromatogram at the time i.

The principle was the following formula:

$$LRIx = 100Z + \left(\frac{100(tRx-tRz)}{tR(Z+1)-tRz} \right) \qquad \text{【Eqn 2】}$$

X = compound of interest
Z = carbon number of n-alkane eluting prior to X
tRx = unadjusted retention time of component of interest (X)
tRz = unadjusted retention time of n-alkane eluting prior to X
tR(Z+1) = unadjusted retention time of n-alkane eluting after X

Using measured weight percentages of each compound determined from the GC analysis on crude oil samples, Detail Hydrocarbon Analyze (DHA) analysis was performed on concentrations of C_7 compounds to statistically evaluate any differences between the oils. DHA is a statistical means for evaluating variance in data sets. Agilent Chemstation software was used to perform DHA analysis and equal weight was given to each C_7 compound in the DHA (ASTM5134).

APPLICATION

To evaluate the crude oil light hydrocarbon C_7 compound data, a very precise analytical methodology was required. Therefore, the reproducibility of the chromatographic method was evaluated by analyses of a commercial mixture of hydrocarbons. The quality criteria were established by analogous chromatographic method. This data（Table 1）was then used to calculate the various light hydrocarbon parameters and some results were obtained.

Table 1. Summary of C$_7$ Hydrocarbon parameters from Northwestern Taiwan oils

Sample No.	Formation	Geological Age	nC	MCH	Tol/nC7	3MH+24 DMP	H+23D MP	Isoheptane value	Heptane value	P	P2%	P3%	3	5	6	P2+N2%	N2/P3	P2	P3
A01	Talu	Early Miocen	049	216	338	38		153	1 87	44	41	15	199	130	671	85	137	578	174
A02	Talu	Early Miocen	037	330	266	296	123	1650		49	39	13	133	111	756	89	179	457	206
A03	Mushan	Early Miocen	037	450	119	123	140	2151		64	30	7	68	64	89	359	209	210	054
A04	Yutengping	Pliocene	046	308	141	147	149	2463		65	29	6	87	76	86	743	202	251	139
A05	Hopai	Middle Mioce	040	273	270	301	124	1798		50	38	12	142	119	740	739	179	467	145
A06	Talu	Early Miocen	041	343	145	152	139	2236		62	31	7	88	79	83	758	194	254	145
A07	Chinshui	Pliocene	046	093	300	339	156	1603		37	45	19	291	176	533	307	117	498	046
B01	Talu	Early Miocen	032	655	046	049		132	1544	45	40	15	101	88	727	144	077	145	
B02	Piling	Early Miocen	029	915	075	080		124	1451	45	39	16	82	68	80	720	139	127	147
C01	Talu	Early Miocen	032	548	129	139	131	1572		46	41	13	108	90	82	373	169	221	062
C02	Talu	Early Miocen	060	139	246	279	178	1930		41	42	17	274	146	58	709	106	411	144
C03	Talu	Early Miocen	041	226	320	361	123	1757		48	40	12	163	133	704	773	177	556	157
C04	Peiliao	Early Miocen	037	258	273	304	120	1790		51	38	11	134	119	747	86	191	478	175
C05	Wuchishan	Oligocene	035	28	272	303	119	1700		50	39	12	135	118	747	16	18	472	025
C06	Wuchishan	Oligocene	039	308	280	312	123	1796		50	38	11	133	113	754	78	16	48	178
C07	Wuchishan	Oligocene	045	395	316	354	159	1751		42	43	14	163	106	731	624	145	548	136
D01	Talu	Early Miocen	047	304	340	38	160	1762		42	43	15	187	119	694	81	138	56	18
D02	Talu	Early Miocen	047	260	279	312	161	2095		51	38	11	152	104	744	625	151	491	625
E01	Mushan	Early Miocen	038	97	176	195	125	1741		50	40	11	70	63	857	380	223	312	08
E02	Wuchishan	Oligocene	038	1090	157	170	124	178		52	38	10	61	56	88	875	230	277	196
E03	Mushan	Early Miocen	021	969	158	161	114	1210		43	42	15	76	75	849	699	18	260	134
E04	Wuchishan	Oligocene	048	725	152	170	143	183		46	43	12	104	80	86	939	196	271	207
E05	Wuchishan	Oligocene	043	768	116	130	131	1752		47	41	11	93	77	81	499	206	207	08
E06	Mushan	Early Miocen	038	1058	082	090	119	1701		48	41	11	71	65	854	440	209	146	071
E07	Wuchishan	Oligocene	039	646	08	093	124	1768		49	39	12	94	80	86	68	18	142	126
F01	Talu	Early Miocen	030	456	237	257	131	148		44	42	14	123	101	775	794	167	405	18
F02	Talu	Early Miocen	044	267	293	329	138	187		48	39	12	156	118	726		167	511	
F03	Talu	Early Miocen	045	270	334	377	146	1910		48	40	12	160	116	724	340	165	58	070
F04	Talu	Early Miocen	045	494	075	073	146	2637		72	23	5	48	50	902	120	215	130	029
F05	Talu	Early Miocen	030	457	234	256	130	1451		44	42	14	125	104	771	198	165	400	051
F06	Talu	Early Miocen	027	419	145	158	132	1459		46	41	14	118	99	78	58	160	248	090
F07	Talu	Early Miocen	048	223	341	38	153	182		43	43	14	202	133	665	82	145	591	202
F08	Talu	Early Miocen	042	277	263	293	133	1936		52	38	11	137	111	752	761	177	461	146
F09	Talu	Early Miocen	049	235	364	415	150	1962		47	40	13	179	121	700	423	147	634	091
F10	Talu	Early Miocen	026	273	174	196				58	32	10	86	126	78	455	316	299	100
F11	Talu	Early Miocen	046	273	290	325	146	2004		50	39	11	149	110	741	417	171	512	074
F12	Talu	Early Miocen	025	299	068	077				58	32	10	82	119	799	325	315	118	057

*data abnormal

Toluene/ n-Heptane vs. n-Heptane/ Methylcyclohexane and the Evaporative Fractionation of condensate-oil

Thompson (1987, 1988) and Larter and Mills (1991) suggested that formation of the gas-condensates can be related to fault activity or erosion, especially in the basins with rapidly deposition sediments in the Tertiary time. Furthermore, aromaticity was also found to increase from the shallow layer to the deep layer. We propose that when the fault cuts through the reservoir saturated with subterranean gas, the pressure drops, and gas and liquid are separated. The hydrocarbons in the gas phase escaped along the fault to accumulate in traps where temperature and pressure were lower. The hydrocarbons in the shallow reservoirs formed gas-saturated oils if a good seal was present. High-temperature and high-pressure experiments conducted by Thompson (1987) and Larter (1991) have demonstrated that the

gas condensates formed by separation of gas and liquid had an increase in saturates and a decrease in aromaticity in the shallow zone while oils in the deep reservoirs had an increase in aromaticity and a decrease in saturates. Since aromatic compounds are less evaporative than saturates, Thompson (1987) called the separation of gas from oil in the subsurface "Evaporative Fractionation".

The analysis of the oils revealed that the value of nC_7/ Methyl-cyclohexane for the region was between 0.16 and 0.60, while Toluene/nC_7 value ranged from 1.52 to 10.58. The graph depicted in Fig 5 demonstrates that the hydrocarbons in the shallow reservoirs were derived from migration of the oils in deep formations consistent with evaporative fractionation.
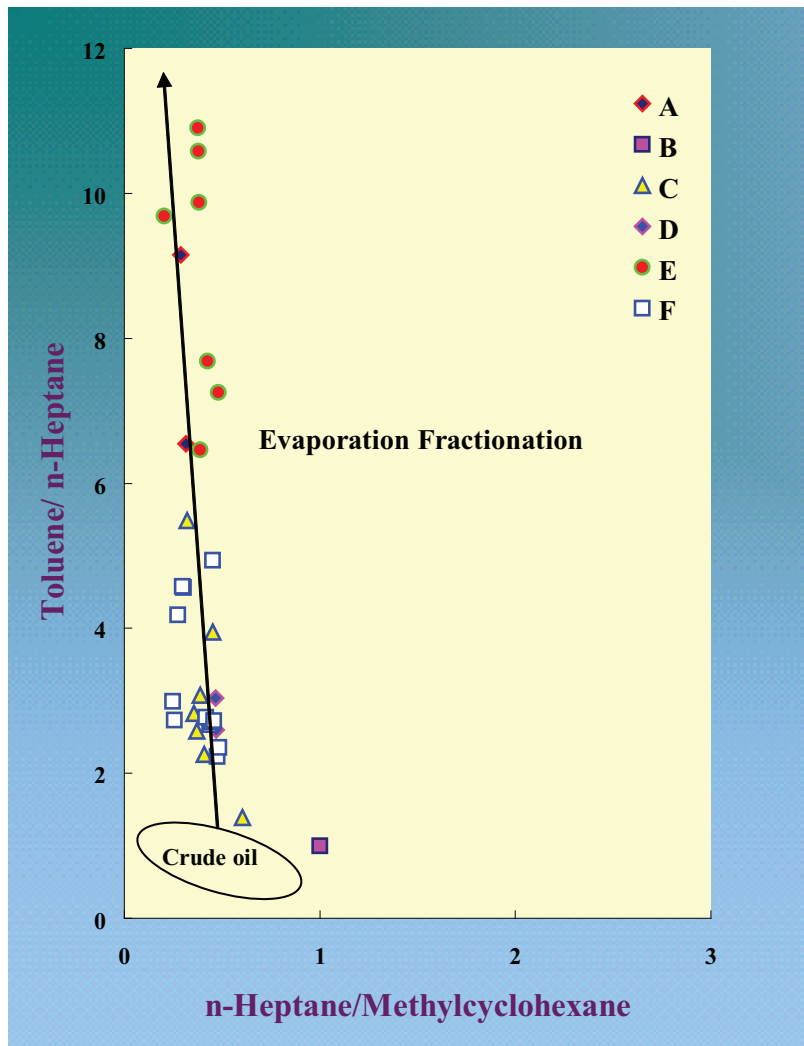
Figure 5. Paraffinicity vs. Aromaticity plot for the Northwestern Taiwan oils (modified from Talukdar and Dow, 1990). It should be Evaporative Fractionation in the figure above.

2-MH+2,3-DMP vs. 3-MH+2,4-DMP and the petroleum system

Mango (1987, 1990b, 1997) determined that four different heptane isomers had fixed roles in different petroleum systems. These 4 heptane isomers are 2-methylhexane (2-MH), 3-methylhexane (3-MH), 2,3-dimethylhexane (2,3-DMP), and 2,4-dimethylhexane (2,4-DMP). He thought that 2-MH and 3-MH were parent compounds present in kerogen, and 2,3-DMP and 2,4-DMP were the daughter compounds derived from the parents. He proposed that kerogen generated parent compounds only and the daughter compounds were formed from parent compounds through reactions catalyzed by metals. In theory, both 2-MH and 3-MH came from the reaction of a 3-member ring intermedaite; 2, 4-DMP was transformed from 2-MH parent compound; and 2, 3-DMP was from 2-MH and 3-MH parents. In different petroleum systems, (2-MH+2, 3-DMP) / (3-MH+2, 4-DMP) would have a different specific value (K1).

The oils analyzed show a very good linear relationship between (2-MH+2, 3-DMP) and (3-MH+2, 4-DMP) the linear equation Y = 1.1458X – 0.0755 and R² = 0.9986.(Fig 6) Since the K1 value, for each of the samples, was 1.1458, the oils, from this region, according to Mango (1987), were derived from the same petroleum system.
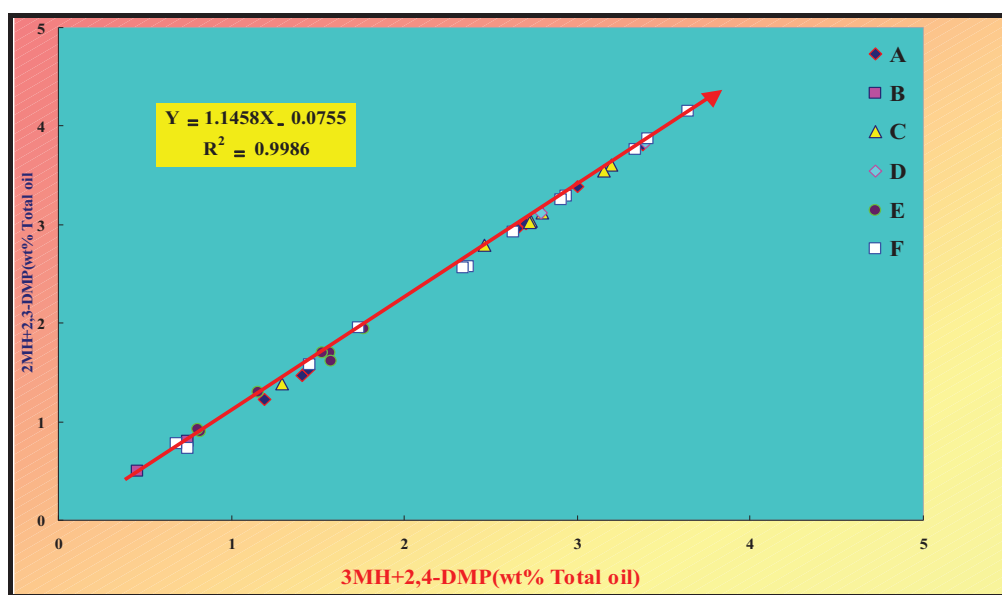
Figure 6. 2-MH+ 2,3-DMP vs. 3-MH+ 2,4-DMP Mango (1987) graphs for Northwestern Taiwan oils and the linear equation Y=1.1458X-0.0755 (with R^2=0.9986).

Heptane value and Iso-heptane value and maturation of crude oil

Four different degrees of crude oil maturation have been identified from the coordinates of C_7 n-heptane values and iso-heptane values (Thompson, 1983). These four degrees were described as normal, mature, supermature, and biodegraded. Through maturation, light hydrocarbon molecules were found to increase. Molecules with different chemical structures were also found to have different increasing rates. The production of chain molecules

required less activation energy than that of ring molecules with the same number of carbon atoms. Therefore, under the same thermal maturation process, chain hydrocarbons had a faster formation rate than ring hydrocarbons. For thermal stability, the isomeric chain compounds were found to be more stable than the ring compounds. Generally, the index numbers of both compounds increase with maturity. The specific values of chain and ring hydrocarbons were used in this study to evalauate the degree of maturation in the crude oils.

The n-heptane and isoheptane values of the Thompson parameters,(Figb 7) for chain and ring molecules, of the oils were approximately between 10 and 26, and between 0.8 and 1.8, respectively. The results indicates that maturation of the oils from the region were between normal and mature. Heptane value and vitrinite reflectance were used to calculate the maturity which was estimated to be over 0.8% Ro (Thompson, 1983).
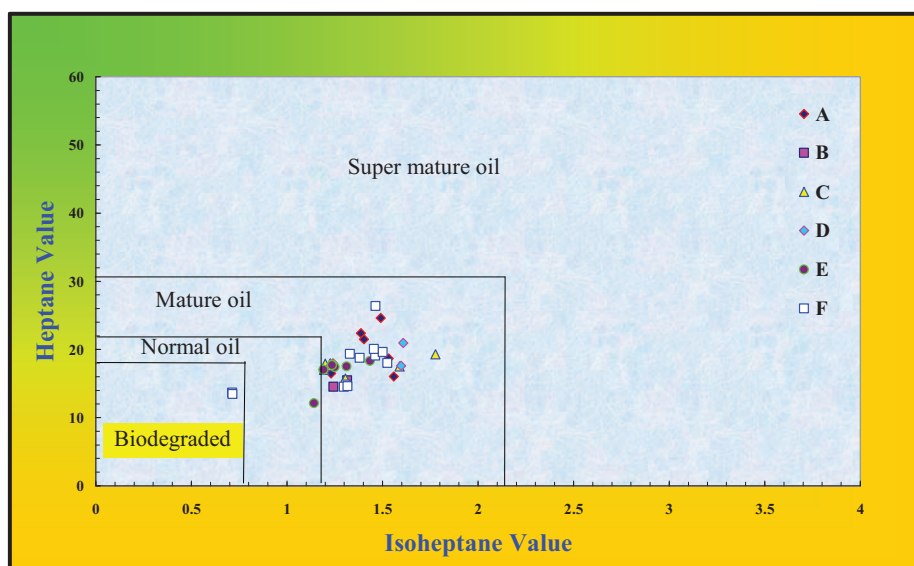
Figure 7. Thompson's (1983) Heptane and Isoheptane Values diagram of the analyzed oils from Northwestern Taiwan showing the oils range from normal to mature in thermal maturity.

3-Phase diagram of parent (P1), mono-branch (P2) and poly-branch (P3) of heptane isomers and the biodegraded degree of condensate-oil

The degree of bio-degradation in crude oil can be identified from the difference in heptane isomers. Generally, n-heptane is more susceptible to biodegradation and the branched compounds less so and hence, biodegraded oils have more branched compounds relative to n-heptane. The chemical relationship between parent and branched heptane isomers were used to evaluate the degree of biodegradation of the oil samples in this study. The parent (P1), mono-branch (P2) and poly-branch (P3) heptane isomers were used to make a triangular diagram, depicted in Fig 6. Each coordinate of the triangular diagram, P1, P2 and P3, were represented by the parent n-heptane, mono-branched heptane alkanes and poly-branched heptane alkanes, respectively. With increasing biodegradation of oils, abundaces of branched compounds (P2, P3) tend to increase relative to the parent compound (P1).

The analysis of the oils, yielded 37% ~ 64% for P1, and about 29% ~ 45% and 6% ~ 19% for P2 and P3, respectively. The relative abundances of the compounds showing in the triangular diagram (Figure 8) indicate that the oils in the region were nearly free from biodegradation and the use of heptane isomers P1, P2, and P3 to evaluate bio-degradation of the oils is feasible, which is consistent with the Thompson's plot shown in Fig 7.
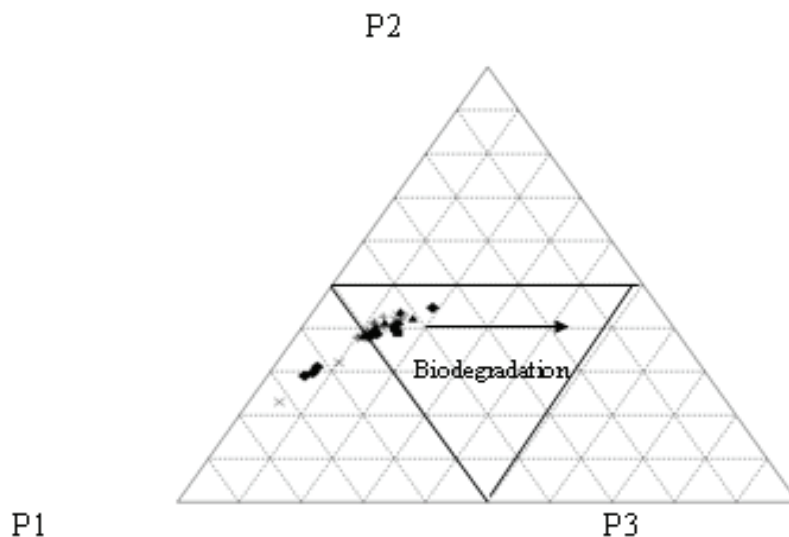
Figure 8. Dow's (1991) Ternary plot of P1 (nC_7), P2 (monobranched C_7 alkanes) and P3 (polybranched C_7 alkanes) showing Northwestern Taiwan oils have suffered little biodegradation.(◆ ： Sample A ; □ : Sample B ; ▲ : Sample C ; ○ : Sample D ; ＋ ： Sample E ; × ： Sample F)
P1: n-heptane
P2: the sum of 2-methylhexane, 3-methylhexane
P3: the sum of 2,2-dimethylpentane, 2,4-dimethylpentane, 2,3-dimethylpentane, 3,3-dimethylpentane, 3-ethylpentane

Triangular relationship diagram of branch (3RP), 5-membered-ring (5RP) and 6-membered-ring (6RP) heptane isomers and the depositional environment of oil

The predominance of heptane isomers in light hydrocarbons can be used to identify the depositional environment of the source rocks of crude oils. Abundant iso-alkanes (3RP) are-found in oils derived from a lacustrine source, while abundant cyclopentanes (5RP) are in oils derived from a marine source and abundant cyclohexanes (6RP) are present in oils derived from a terrigenous source.

The analysis of the oils, showed that the relative abundance of 6RP was 53~90%, which was larger than those of 3RP (6~29%) and 5RP (5~13%). As shown in Figure 9, most oils fall in the position of 6RP indicating that the source rocks, of the oils in the region are terrigenous. These findings are consistent with other gas chromatographic data of the oils "Pristane/ nC_{17} vs. Phytane/ nC_{18}" shown in Fig 10.
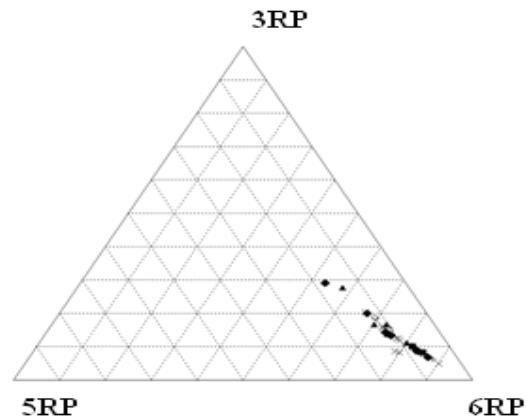
Figure 9. Mango's(1994) Ternary plot of isoalkanes (3-RP) cyclopentanes (5-RP) and cyclohexane (6-RP) of oils from Northwestern Taiwan showing the oils are terrigenous oils. (◆ ： Sample A ； □ ： Sample B ； ▲ ： Sample C ； ○ ： Sample D ； ＋ ： Sample E ； × ： Sample F)
3RP: the sum of 2,2-dimethylhexane, 2,3-dimethylhexane, 2,4-dimethylhexane, 3,3-dimethylhexane, 3,3-dimethylhexane, 3-ethylpentane, 2-methylhexane, 3-methylhexan
5RP: the sum of ethylpentane, cis-1,2-dimethylcyclopentane,trans-1,2-dimethylcyclopentane,1,1-dimethylcyclopentane, cis-1,3-dimethylcyclopentane, trans-1,3- imethylcyclopentane
6RP: the sum of methylcyclohexane, toluene
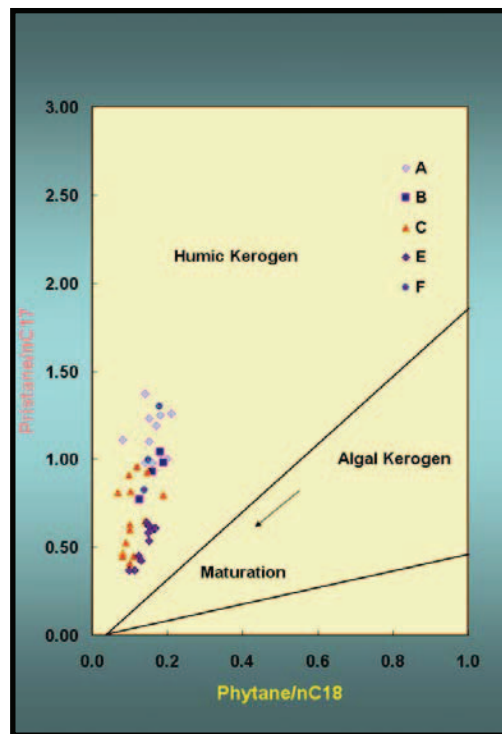
Figure 10. A crossplot of the Phytane/n-C18 ratio vs. the Pristane/n-C17 ratio classifying the depositional environment of Northwestern Taiwan oils as shown in the Cannon (1980) diagram and modified by Lin (1998).
N2/P3 vs. P2 and P2+N2 vs. P3 to identify the relationship of depositional environment (Fig.12)

According to the Mango (1990) diagrams of "N2/P3 vs. P2"(Fig.11A) and "P2+N2 vs. P3" (Fig.11B) shown in figure 11 could be used to identify the deposition environment of a lacustrine or terrigenous sourced crude oil. The two diagrams were found to be particularly useful in identifying the mixed oils.

The "P2+N2 vs. P3" coordinate was used to analyze the oils. A trend line, $Y = 0.028X+b$, was obtained. This result indicats the source rock is terrigenous. The "N2/P3 vs. P2" coordinate was also used to provide a more reliable analysis of the oils, which further demonstrates a terrigenous source for the oils. All the N2/P3 values were larger than 1. This result confirms the "Pristane/Phytane vs. δ^{13}C‰" relationship and demonstrates that all the oils from the region were derived from swamp and terrigenous organic matter.
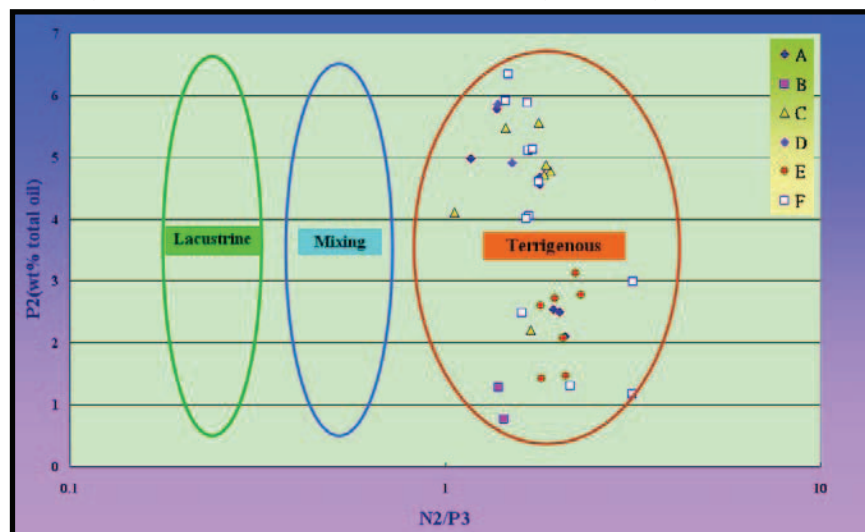
Figure 11A
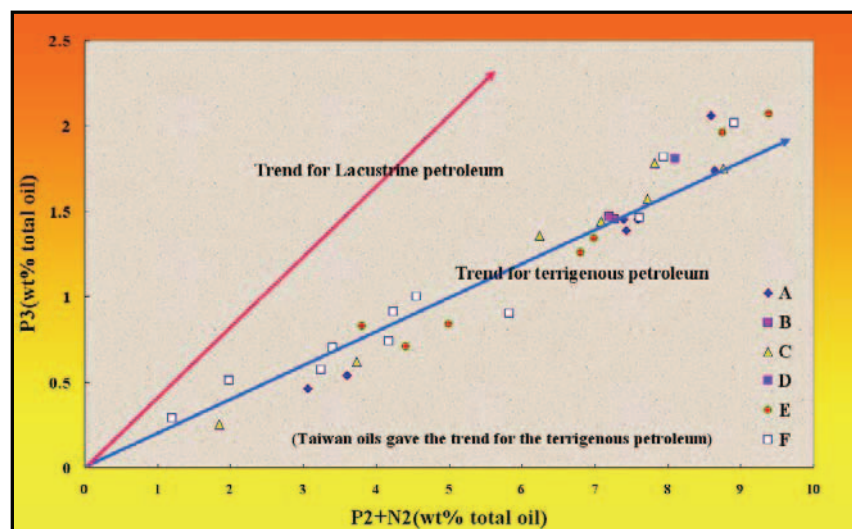
Figure 11B. Mango(1990) crossplots of oils and condensates from Northwestern Taiwan: (A) the upper crossplot N2/P3 vs. P2. (B) the lower crossplot, P2+N2 vs.P2 showing the oils and condensates derived from for terrigenous sources

(◆ : Sample A ; □ : Sample B ; ▲ : Sample C ; ○ : Sample D ; ＋ : Sample E ; × : Sample F)
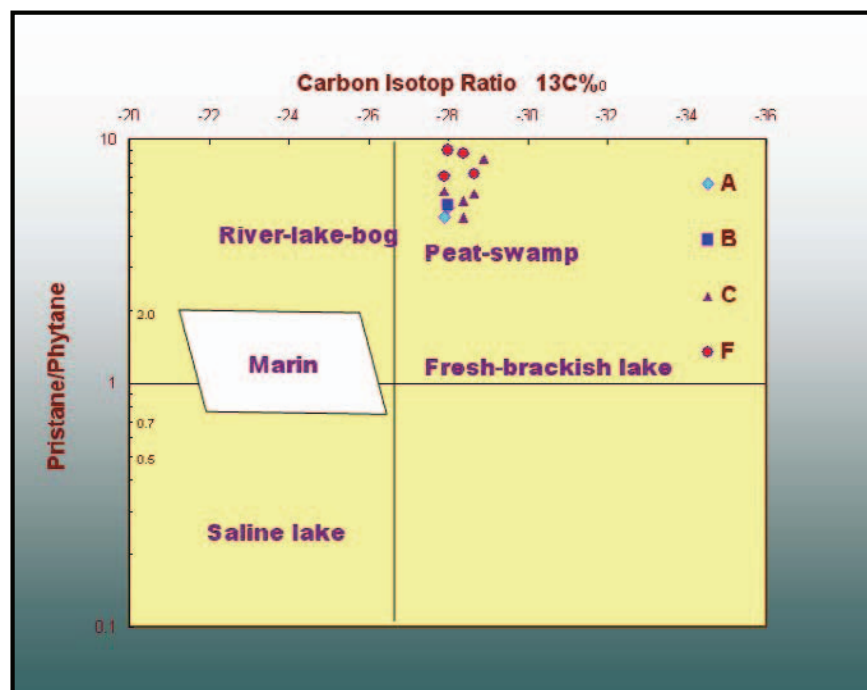
Figure 12. Luo (1988) crossplot of the Pristane/Phytane vs. Carbon Isotope Ratio ($\delta13C^0/_{00}$) indicates the Northwestern Taiwan oils are derived from peat-swap (terrigenous organic matter) oil, modified from Lin (1998).

SUMMARY

A number of statements can be made from this study:

a. The relationship of "Toluene/n-Heptane vs. n-Heptane/ Methylcyclohexane", demonstrates that all the oils from the Northwestern region of Taiwan were affected by evaporative fractionation.

b. The relationship show in the diagram, (2-MH+2,3-DMP) vs. (3-MH+2,4-DMP), indicates that all the oils in the region were derived from the same petroleum system.

c. The diagram of "Heptane value and iso-Heptane value", shows that the oils are mature.

d. The relationship between parent, mono-branched and poly-branched heptane isomers - P1, P2 and P3, indicates that the oils are nearly free of biodegradation.

e. The triangular diagram of branched, 5-membered ring and 6-membered ring heptane isomers, demonstrates that the depositional environment of the source rock of the oils was terrigenous.

f. The plots of (N2/P3 vs. P2) and (P2 + N2 vs. P3) also support that the depositional environment of the source rock of the oils was terrigenous.

REFERENCES

Canipa-Morales, N.K., Galan-Vidal, C.A., Guzman-Vega, M.A., Jarvie, D.M. (2003). Effect of evaporation on C_7 light hydrocarbon parameter. *Organic Geochemistry*, 34, 813-826.

Connan, J., Casson, A.W., (1980). Properties of gas and Petroleum liquids derived from terrestrial kerogen at various maturation level. *Geochimica et Cosmochimica Acta*, 44, 1-23.

Chou, J.T. (1970). A petrographic study of the mesozoic rocks underneath the Western Taiwan. *Petrogeo1 Taiwan*, 7, 209-228.

Chung, H.M., Walters, C.C., Buck, S., Bingham, G. (1998). Mixed signals of the source and thermal maturity for petroleum accumulations from light hydrocarbons, an example of the Beryl field. *Organic Geochemistry*, 29, 381-396.

Cooles, G.P., O'Brien, A.P., Watt, J.J. (1991). Quality control procedure for the gas chromatographic determination of light hydrocarbons in petroleum liquid. *Journal of Chromatography,* 588, 259-264.

Dow, W.G. (1991). *DGSI Total quality geochemistry analytic report for CPC*. (unpublished in Chinese).

Dzou, L.P., Hughes, W. (1993). Geochemistry of oils and condensates, K Field, offshore Taiwan: a case study in migration fraction. *Organic Geochemistry*, 20, 437-462.

Jarvie, D.M., Walker, P.R. (1997). Correlation of oils and source rocks in the Williston Basin using classical correlation tools and thermal extraction very high resolution C7 gas chromatography, 18th International Meeting on Organic Geochemistry, 22-26 September 1997, Maastricht, The Netherlands, *Abstract for oral presentation*, P. 51-52.

Kuo, C.L., Lin, L.H., Shen, J.C., Chang, C.T. (2002). Petroleum phase and potential analyses of source rocks in Northwestern Taiwan. *The Bulletin of Chinese Institute of Mining and Metallurgical Engineers*, 179, 161-124.

Larter, S., Mills, N. (1991). *Phase-control molecular fractionations in migrating petroleum charges*.England, W.A., Fleet, A.J., (eds), Petroleum Migration, Geological Society. Special publication, 59, 137-147.

Lin, L.H., Chou, T.E., Chang, C.T., Kuo, C.L. (2003). The application of thermal-reservoir rocks for oil and gas exploitation and production. *Journal of Petroleum*, 39, 1, 15-30.

Lin, L.H., Kuo, C.L. (1998). *Geochemical characteristics of hydrocarbon in Northwestern* Taiwan. EDRI annual report. (unpublished in Chinese)

Luo, B., Yang, X., Lin, H., Zheng, G.D. (1988). *Characteristics of mesozoic and cenozoic non-marine source rocks in north-west China.* Fleet, A.J., Kelts, K.,Talbot, M.R., Lacustrine petroleum source rocks. Geological Society. Special Publication, 40, 291-298.

Mango, F.D. (1987). An invariance in the isoheptanes of petroleum. *Science*, 237, 514-517.

Mango, F.D. (1990a). The origin of light cycloalkanes in petroleum. *Geochimica et Cosmochimica Acta*, 54, 23-27.

Mango, F.D. (1990b). The origin of light hydrocarbons in petroleum：A kinetic test of the steady –state catalytic hypothesis. *Geochimica et Cosmochimica Acta*, 54, 1315-1323.

Mango, F.D. (1994). The origin of light hydrocarbons in petroleum ring preference in the closure of carbocyclic rings. *Geochimica et Cosmochimica Acta*, 58, 895-901.

Mango, F.D. (1997). The light hydrocarbons in petroleum. A critical review. *Organic Geochemistry*, 26, 417-440.

Manzur, A., Simon, C.G. (2004). Change in the molecular composition of crude oils during their preparation for GC and GC-MS analyses. *Organic Geochemistry*, 35, 137-155.

Obermajer, M., Osadetz, K.G., Fowler, M.G., Snowdon, L.R. (2000). Light hydrocarbon (gasoline range) parameter refinement of biomarker-based oil-oil correlation studies, an example from Williston Basin. *Organic Geochemistry*, 31, 959-976.

Odden, W., Patience, R.L., Van-Graas, G.W. (1998). Application of light hydrocarbons (C4-C13) to oil/source rock correlations: a study of the light hydrocarbons compositions of source rock and test fluids from offshore Mid-Norway. *Organic Geochemistry*, 28, 823-847.

Oung, J.N. (1989). Geochemical study on biomarkers in the oils from Taiwan. *Petroleum Geology of Taiwan*, 24, 180-210.

Peters, K.E., Moldowan, J.M. (1993). The *biomarker guide interpreting molecular fossils in petroleum and ancient sediments*. Prentice hall, New Jersey, 361.

Powell, T.G., Boreham, C.J. (1994). *Terrestrially sourced oils, where do they exist and what are our limits of knowledge?- a geochemical prospective*. Geological Society. Special Publication, 77, 22-29.

Radke, M. (1988). Application of aromatic compounds as maturity indicators in source rocks and crude oils. *Marine and Petroleum Geology*, 5, 224-236.

Talukdar, S.C., Dow, W.G. (1990). Geochemistry of oils provides optimism for deeper exploration in atlantic off Trinidad. *Oil and Gas Journal*, 12, 118-122.

Ten Haven, H.L. (1996). Application and limitations of Mango's light hydrocarbon parameters in petroleum correlation studies. *Organic Geochemistry*, 24, 957-976.

Thompson, K.F.M. (1983). Classification and thermal history of petroleum based on light hydrocarbons. *Organic Geochemistry Cosmochim Acta*, 47, 303-316.

Thompson, K.F.M. (1987). Fractionated aromatic petroleums and the generate on of gas-condensates. *Organic Geochemistry*, 11, 573-590.

Thompson, K.F.M. (1988). Gas-condensate migration and oil fractionation in deltaic systems. *Marin and Petroleum Geology*, 5, 237-246.

Thompson, K.F.M. (1991). Contrasting characteristics attributed to migration observed in petroleum reservoired in clastic and carbonate sequences in the Gulf of Mexico region. *Petroleum Migration Geological Society*. Special Publication, 59, 191-205.

APPENDIX

1. The light hydrocarbon of C$_7$

C$_7$ Hydrocarbon

Peak	Compound	Abbreviation
1	2,2-Dimethylpentane	2,2-DMP
2	2,4-Dimethylpentane	2,4-DMP
3	2,2,3-Trimethylbutane	2,2,3-TMB
4	3,3-Dimethylpentane	3,3-DMP
5	2-Methylhexane	2-MH
6	2,3-Dimethylpentane	2,3-DMP
7	1,1-Dimethylcyclopentane	1,1-DMCP
8	3-Methylhexane	3-MH
9	cis-1,3-Dimethylcyclopentane	c-1,3-DMCP
10	Trans-1,3-Dimethylcyclopentane	t-1,3-DMCP
11	3-Ethylpentane	3-EP
12	Trans-1,2-Dimethylcyclopentane	t-1,2-DMCP
13	n-Heptane	n-C$_7$
14	cis-1,2-Dimethylcyclopentane	c-1,2-DMCP
15	Methylcyclohexane	MCH
16	Ethylcyclopentane	ECP
17	Toluene	TOL

Retention time (min)
(a) Gas chromatogram of a crude oil hydrocarbon mixture. (b) Partial crude oil range gas chromatogram

2. Thompson's Parameters (1983)

Aromaticity=Toluene/ nC_7
Paraffinicity= nC_7/ Methylcyclohexane

Heptane Value =

$$\frac{\text{n-heptane}}{\begin{array}{l}\text{(n heptane+cyclohexane}\\ \text{+2,3-dimethylpentane+1,1-}\\ \text{dimethylcyclopentane+3-}\\ \text{methylhexane+cis-1,3-}\\ \text{dimethylcyclopentane+trans-}\\ \text{1,3-dimethylcyclopentane}\\ \text{+3-ethylpentane)}\end{array}} \times 100$$

【Eqn 3】

$$\text{Isoheptane Value} = \frac{\text{2-methylhexane+3-methylhexane}}{\text{cis-1,3-dimethylcyclopentane+trans-1,3-dimethylcyclopentane+trans-1,2-dimethylcyclopentane}} \quad \text{【Eqn 4】}$$

3. Mango's parameters (1994)

P1 =   n-heptane

P2 =   2-methylhexane+3-methylhexane

P3=   2,2-dimethylpentane+2,4-dimethylpentane+2,3-dimethylpentane+3,3-dimethylpentane+3-ethylpentane

N1=   1-dimethylcyclopentan   +   cis-1,3-dimethylcyclopentane+trans-1,3-dimethylcyclopentane

N2=   1,1-dimethylcyclopentane+cis-1,3-dimethylcyclopentane+trans-1,3-dimethylcyclopentane

RP3=   2,2-dimethylhexane+2,3-dimethylhexane+2,4-dimethylhexane+3,3-dimethylhexane+3,3-dimethylhexane+3-ethylpentane+2-methylhexane+3-methylhexane

RP5=   ethylpentane+cis-1,2-dimethylcyclopentane+trans-1,2-dimethylcyclopentane+1,1-dimethylcyclopentane+cis-1,3-dimethylcyclopentane+trans-1,3- imethylcyclopentane

RP6 =   methylcyclohexane+toluene

4. Biomarkers ratios (Cannon 1980)

$$\text{Pr/C}_{17} = \frac{\text{2,6,10,14-tetramethylpentadecane}}{\text{n-C}_{17}} \quad \text{【Eqn 5】}$$

$$\text{Ph/C}_{18} = \frac{\text{2,6,10,14-tetramethylhexadecane}}{\text{n-C}_{18}} \quad \text{【Eqn 6】}$$

$$\text{Pr/ Ph} = \frac{\text{2,6,10,14-tetramethylpentadecane}}{\text{2,6,10,14-tetramethylhexadecane}} \quad \text{【Eqn 7】}$$

5. Molecular structure of C7 isomers ball stick model. Color code: Carbon, blue; Hydrogen, violet;
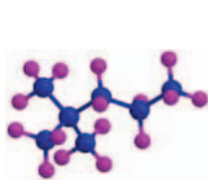
2,2-Dimethylpentane
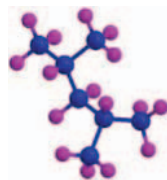
2,4-Dimethylpentane
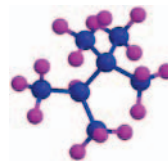
2,2,3-Trimethylbutane
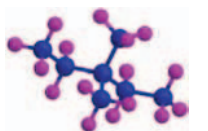
3,3-Dimethylpentane
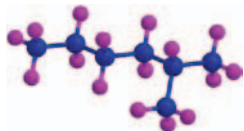
2-Methylhexane
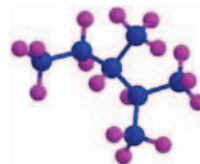
2,3-Dimethylpentane
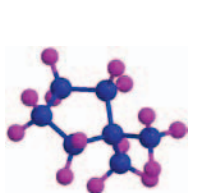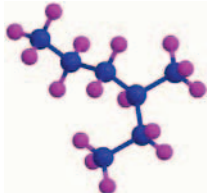
1,1-Dimethylcyclopentane
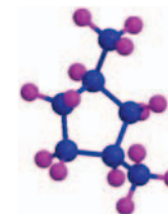
3-Methylhexane

cis-1,3-Dimethylcyclopentane
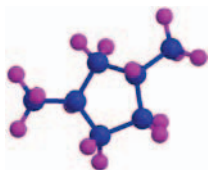
Trans-1,3-Dimethylcyclopentane
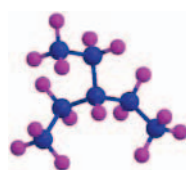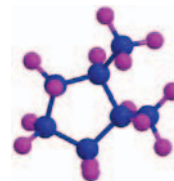
3-Ethylpentane

Trans-1,2-Dimethylcyclopentane
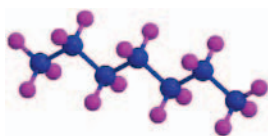
n-Heptane
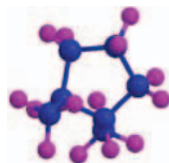
cis-1,2-Dimethylcyclopentane
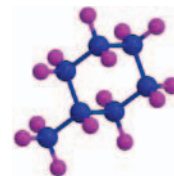
Methylcyclohexane
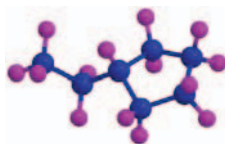
Ethylcyclopentane
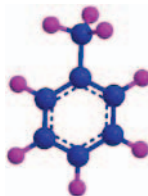
Toluene

INDEX

A

absorption, xi, 167, 168, 170, 172, 174, 175, 176, 177, 178, 179, 180
absorption coefficient, xi, 168, 170, 172, 174, 175, 176, 177, 178, 179, 180
accidents, 104
accounting, 14, 69
accuracy, 43, 47, 96
acid, 28, 55, 116, 179, 209
activated carbon, 33
activation, 7, 39, 206, 220
activation energy, 220
adjustment, 108, 124
administration, 98
administrative, 207
adsorption, 18, 27, 157
Ag, 46, 47, 48, 84, 189
age, 4, 20, 24, 28, 41, 131, 141, 144, 188, 212
ageing, 92
air, 70, 71, 72, 77, 116, 119, 133, 135, 152, 209
air pollutants, 116
Alabama, viii, 54, 59, 75, 76, 78
Alberta, 69, 76
alkali, 55, 60, 69, 70, 71
alkane, 216
alkanes, 213, 220, 221
alluvial, 12, 144, 185, 190
alternative, xii, 69, 201, 204
aluminosilicate(s), 28, 29, 149, 153, 154, 157, 161
aluminum, 148, 155, 156
ambient pressure, 214
ambivalent, 86
ammonium, 54
amorphous, 168, 172
amplitude, 90, 94, 98, 99, 107
Amsterdam, 50, 78, 87, 113
analytical models, 110

analytical techniques, 168, 181
anatase, 149
animals, 55
anion, 45, 46, 61
anthropic, 92
anthropogenic, 2, 14
apatite, 55, 58, 59, 60, 61, 63, 149
apatites, 60
appendix, 100, 188
application, 107, 111, 168, 180, 197, 225
argillite, 71
arid, 55, 128, 130
arithmetic, 4, 6, 7, 11, 13, 14, 19, 20, 22, 28, 43, 57
Arizona, 70
aromatic, 215, 218, 226
aromatic compounds, 218, 226
aromatic hydrocarbons, 215
arsenic, vii, viii, ix, x, 2, 5, 9, 14, 24, 25, 26, 27, 30, 31, 33, 76, 127, 128, 131, 135, 142, 207
arsenic poisoning, x, 127
artificial, 184
ash, viii, ix, x, 11, 12, 14, 17, 18, 20, 21, 22, 24, 27, 32, 33, 39, 40, 41, 42, 45, 47, 49, 53, 54, 56, 57, 58, 59, 60, 61, 62, 63, 64, 67, 68, 69, 70, 71, 73, 74, 75, 78, 82, 83, 86, 115, 116, 118, 119, 120, 121, 122, 123, 125, 127, 129, 130, 131, 133, 134, 135, 142, 147, 148, 149, 152, 153, 154, 157, 158, 160, 161, 162, 163, 164, 165, 168, 175, 177, 178, 179, 188, 203, 208
Asia, 212
Asian, 84, 87
assessment, 95, 168, 172, 176
assignment, 214, 215
assumptions, 107, 108
ASTM, 54, 181
atmosphere, ix, 17, 27, 115, 116, 121, 123, 202, 206
atomic emission spectrometry, 27
attention, 2, 4, 12, 14, 18, 24, 197

E

N

O

T

X-ray diffraction (XRD), x, xi, 147, 149, 157, 161, 167, 169